INVESTIGATING THE ROLE OF THE IMMUNE SYSTEM IN MOUSE MODELS OF BONE LOSS

By

Naiomy-Deliz Rios-Arce

A DISSERTATION

Submitted to
Michigan State University
in partial fulfillment of the requirements
for the degree of

Comparative Medicine and Integrative Biology-Doctor of Philosophy

2019

ABSTRACT

INVESTIGATING THE ROLE OF THE IMMUNE SYSTEM IN MOUSE MODELS OF BONE LOSS

By

Naiomy-Deliz Rios-Arce

The prevalence of osteoporosis is drastically increasing. Osteoporosis is characterized by low bone mineral density, which results in increased bone fragility and fractures. Current therapeutic drugs for osteoporosis are not effective for everyone, they are expensive, and long-term use can have unwanted and detrimental side effects. Therefore, new therapies that mitigate the current side effects are necessary. However, to further develop better treatments against osteoporosis it is imperative that we understand the mechanisms involved in this disease.

In the first part of this thesis, we aimed to understand the role of interleukin 10 (IL-10) in type 1 diabetes (T1D) induced bone loss. Studies have shown that during diabetes there is a significant decrease in IL-10 levels. The role of this cytokine in bone physiology is well known. However, how IL-10 affects bone health during short- and long-term diabetes has not been studied. By using IL-10 deficient mice, we found that in the absence of IL-10, vertebral and femoral trabecular bone loss are significantly exacerbated during T1D, indicating that low levels of IL-10 during T1D can be detrimental to the bone. Interestingly, this effect was only seen at one month after diabetes onset and not at three months, suggesting that during the early stages of diabetes IL-10 is important in modulating bone density. We also identified that these effects were associated with corresponding changes in osteoblast mRNA expression in the bone, suggesting that IL-10 primarily affects bone anabolic events. *In vitro* data shows that the MAPK pathway is involved in IL-10 regulation of osteoblast gene expression in diabetic conditions. These results demonstrate

that IL-10 is required for osteoblast regulation during early diabetes-induced bone loss and that low levels of IL-10 during diabetes could possibly exacerbate bone loss.

In the second part of this thesis, we aimed to understand the role of T and B lymphocytes in *Lactobacillus reuteri* 6475 beneficial effects on bone. Our lab has shown that treatment with *L. reuteri* enhances bone density and prevents bone loss in several animal models. However, the mechanism by which *L. reuteri* increases bone density is not completely understood. This study demonstrates that T and B lymphocytes are required for the beneficial effects of *L. reuteri* on bone density in healthy male mice. We also reveal, in co-culture experiments, that *L. reuteri* regulates T-cell-expression of factors that increase osteoblast gene expression. Together, this study extends our knowledge in understanding the role of *L. reuteri* in regulating bone density and identify the T-lymphocytes as a possible mechanism.

In the third part of this thesis, we aimed to understand the role of T and B lymphocytes on the effects of gut microbiota dysbiosis on bone density. Our lab recently demonstrated that 2-week oral treatment with broad spectrum antibiotics followed by 4-weeks of natural gut microbiota repopulation results in dysbiosis and femoral trabecular bone loss in male mice. By using T and B lymphocyte deficient mice (Rag-KO) we found that lymphocytes are required for dysbiosis-induced bone loss. We also show that post-antibiotic treated wild type and lymphocyte deficient mice express different microbiota profiles, characterized by low levels of Lactobacillales in wild type compared to Rag knockout mice. Furthermore, treatment with *L. reuteri* prevents dysbiosis-induced trabecular bone loss in wild type mice. Taken together, our studies demonstrate the role of T and B lymphocytes in dysbiosis-induced bone loss and identify *L. reuteri* as a possible treatment against bone loss.

To my Mom, Dad, Sisters, & beloved Husband.
I could not have done this without you.
Thank you!

ACKNOWLEDGEMENTS

Completing my Ph.D. would not have been possible without the encouragement, support and guidance of so many people. I extend my sincerest gratitude to everyone who has supported me during this process.

I would like to first express my sincere gratitude to my mentors Drs. Narayanan Parameswaran and Laura McCabe. Thanks for not only allowing me to join your lab, but also for your time, knowledge, mentorship, and most of all patience. Thank you for always having a positive attitude towards unexpected data, for always cheering me up, and helping me with my project. I would also like to thank both of you for supporting my career goals and for allowing me to participate in many professional development programs. Your advice and recommendations have helped me grow not only as a scientist, but also as a person. Thank you for taking a chance with me and for guiding me into becoming the scientist that I am today.

I also appreciate the help provided by the members of my dissertation committee, Drs. Linda Mansfield and Lorraine Sordillo. Thank you for your valuable feedback, expertise, guidance, and insight into my project and for helping me to improve my scientific and critical thinking. I appreciate all the time and dedication that you have devoted to my scientific career.

I would like to extend special thanks to the current and past members of the lab: Regina Irwin, Dr. Fraser Collins, Dr. Michael Steury, Dr. Sandi Raehtz, Jon, Nick, and Jun. Thank you all for making the days in the lab fun and for always helping me with my projects. To Mike, thank you for training me when I first started in the lab. To Regina, thanks for all of your feedback in my cell culture experiments and for making my life in the lab easier. To Fraser, thank you for all the training and for always be willing to help me no matter how far away you are. To Nick, thanks for all the feedback for my dissertation and for listening to my complaints. I also would like to

thank my undergrads Rick, Sid, Kevin, and Andrew. Thanks for being such amazing kids and for always be willing to help me with my projects.

A special thanks to Jon who made my days in the lab better. Thanks for listening to my complaints, for helping me with my projects, and for always cheering me up. I would not have made it through this process without your support and friendship. Thanks for all the Pita Pit lunches! I will always be in debt to you.

I would like to thank all of the members and faculty of the Comparative Medicine and Integrative Biology Program and the Physiology Department at Michigan State University for their support and help throughout my studies. Dr. Vilma Yuzbasiyan-Gurkan and Dimity thanks for always helping me and for your support.

My special gratitude to Drs. William Atchison and Anne Dorrance. Thanks for introducing me to graduate school and for being the first ones to give me the chance to do research here at MSU. Thank you Bill for always willing to help me and for your unconditional support. I am forever thankful for the opportunity that you gave me.

To my friends here at MSU. Ninotchska and David, thanks for being such great friends since the first day that I arrived in Michigan. Your friendship and support have been amazing. Thanks for listening to my complaints and for letting me play with Diego. To the most amazing girl and friend that I know, Janice; thanks for always being there for me and for helping me with everything. Thanks for making my time in Michigan a great one and for always having fun with me. To Siomara and Patricia, thanks for your feedback and for being great friends.

Most importantly none of this would have been possible without my family. To my mom and dad, I can’t explain how thankful I am for all the things you have done and taught me. Thank you for always believing in me, for encouraging me to pursue my dreams, and for inspiring me to always aim higher. Thanks for always supporting my education and for being with me every step

of the process. To my sisters Johe and Joha, thanks for the long phone calls, for making me feel like I was always at home, and for taking care of Gasper and Woody. To my sister Kiki, you have taught me that everything is possible, you are my major inspiration and I will always be grateful for your emotional support and encouragement. To my dogs Woody, Gasper and Yanki, thanks for being my stress relief and for always making sure that I have fun. Yanki, thanks for sitting next to me during my long nights of studying.

Lastly, I would like to thank my husband and his family. Neldyn, it is impossible to explain how grateful I am for your love and affection. Thank you for everything that you have done for me and for moving across the country to be with me. I couldn't have done this without your support and unconditional love. Thanks for always believing in me and for making my days better. Thanks for taking care of me and for being such an amazing husband and friend. I couldn't have asked for a better partner to go through this journey.

TABLE OF CONTENTS

LIST OF TABLES

LIST OF FIGURES

KEY TO ABBREVIATIONS

ABX: antibiotics

AGEs: advance glycation end products

ALP: alkaline phosphatase

ap2: adipocyte protein 2

APCs: antigen presenting cells

BMC: bone mineral content

BMD: bone mineral density

BMPs: bone morphogenic proteins

BV/TV: bone volume/total volume

BVF: bone volume fraction

CFU-M: macrophage colony-forming units

CM: conditioned media

CONV-R: conventional raised

CTLA-4: cytotoxic T-lymphocyte-associated antigen-4

FPPS: farnesyl pyrophosphate synthase

GALT: gut associated lymphoid tissue

GF: germ free

GFP: green fluorescent protein

GI: gastrointestinal epithelium

GIP: gastric inhibitory polypeptide/ glucose-dependent insulinotropic polypeptide

GLP-1, GLP-2: glucagon- like peptides-1 and 2

HSCs: hematopoietic stem cells

IBD: inflammatory bowel disease

IBS: irritable bowel syndrome

IECs: intestinal epithelial cells

IELs: intraepithelial lymphocyte

IFN-γ: interferon gamma

IGF1: insulin-like growth factor 1

IL-1: interleukin-1

IL-10: Interleukin-10

IL-17A: interleukin 17 A

IL-2: interleukin 2

IL-4: interleukin 4

IL-6: interleukin 6

IL-6sR: IL-6 soluble receptor

IOM: Institute of Medicine

iPTH: intermittent parathyroid hormone

KO: knockout

LA: *Lactobacillus acidophilus*

LGG: *Lactobacillus rhamnosus* GG

LR; *L. reuteri*: *Lactobacillus reuteri* 6475

Lrp5: low-density lipoprotein receptor 5

M-CSF: macrophage colony stimulating factor

MLN: mesenteric lymph node

MOI: multiplicity of infection

MSCs: mesenchymal stem cells

NOD: non-obese diabetic

NOD: nucleotide-binding oligomerization domain

OC: osteocalcin

OPG: osteoprotegerin

OSX: osterix

OTUs: operational taxonomic units

OVX: ovariectomized

PAMPs: pathogen-associated molecular pattern

PBS: phosphate-buffered saline

PPAR-γ: peroxisome proliferator-activated receptors

PRRs: pattern-recognition receptors

PTH: parathyroid hormone

PYY: Peptide YY

RA: rheumatoid arthritis

RANKL: receptor nuclear factor kappa beta ligand

RUNX2: runt-related transcription factor 2

SCFA: short chain fatty acids

SERMs: selective estrogen receptor modulators

SPF: specific pathogen-free

STZ: streptozotocin

T1D: Type 1 diabetes

T2D: Type 2 diabetes

Tb. N: trabecular number

Tb. Sp: trabecular spacing

Tb. Th: trabecular thickness

TGFβ: transforming growth factor beta

Th1: T helper 1

Th17: T helper 17

Th2: T helper 2

TJ: tight junction

TLR: toll-like receptor

TNF-α: tumor necrosis alpha

Tph1: tryptophan hydroxylase 1

TRAP5b: tartrate-resistant acid phosphatase 5b

Treg: T regulatory cells

WT: wild type

μCT: microcomputed tomography

Chapter 1. Introduction

1.1 The skeletal system

The human skeletal system is composed of a framework of bones, ligaments, tendons, and cartilage. The skeleton has a variety of functions: provides structural support for the body, allows for movement and locomotion of the body by providing support to the muscles, serves as a reservoir for minerals, protects vital internal organs, and maintains mineral homeostasis and hematopoiesis (Figure 1.1).

1.1.1 General structure of the bone

The adult human skeleton has a total of 206 bones, excluding the sesamoid bones. This system is divided into the axial skeleton which is composed of 80 bones and the appendicular skeleton which is made up of the remaining 126 bones. There are four general categories of bone: long, short, flat, and irregular bones. Long bones such as the femur and tibia are composed of a region above the growth plate called the epiphyses. The epiphyses are filled with spongy bone containing the red bone marrow. Below the epiphyses is the metaphysis region which is important for bone growth during childhood and contains the growth plate. The largest part of the long bone is the long, cylindrical middle known as the diaphysis. The diaphysis, also called the shaft, is primarily made up of dense, strong bone (cortical bone) and contains the medullary cavity. The medullary cavity is surrounded by two membranes: endosteum and periosteum. The endosteum is a thin connective tissue where bone growth, remodeling, and repairs occur. The outer layer, the periosteum is a dense fibrous membrane that contains blood vessels, nerves, and lymphatic vessels. While the diaphysis is mostly composed of cortical bone, the metaphysis and epiphysis are composed of a honeycomb-like network of spongy trabecular bone surrounded by a relatively thin shell of dense cortical bone. The trabecular bone is highly porous and highly metabolic active. The cortical bone is heavily calcified, is typically less metabolically active than the trabecular bone and

is crucial for providing structure and support (Figure 1.2). Around 20% of the human adult skeleton is made up of trabecular bone and 80% of cortical bone, however this number can change depending on the bone. Long bones have more cortical bone than trabecular whereas the vertebrae mostly contains trabecular bone.

Bone marrow, present inside the bone, is a semi-solid tissue and its primary function is to produce blood cells (hematopoiesis) and store fat. Bone marrow is characterized as red or yellow marrow, a characteristic that will depend on the prevalence of hematopoietic vs fat cells. At birth, the majority of the bone marrow is red marrow, however as we grow, the red marrow is replaced by yellow due to the accumulation of fat. There are two types of cells located in the bone marrow: hematopoietic (HSCs) and mesenchymal stem cells (MSCs). These stem cells can differentiate into several types of specialized cells. MSCs are multipotent stem cells that can differentiate into myocytes, adipocyte, chondrocyte, and osteoblasts. HSCs give rise to myeloid and lymphoid lineages. Myeloid cells differentiate into erythrocytes, monocytes, neutrophils, basophils, eosinophils and megakaryocytes. Lymphoid cells differentiate into T and B lymphocytes and natural killer cells. The cellular composition of the bone marrow is described in table 1.1.

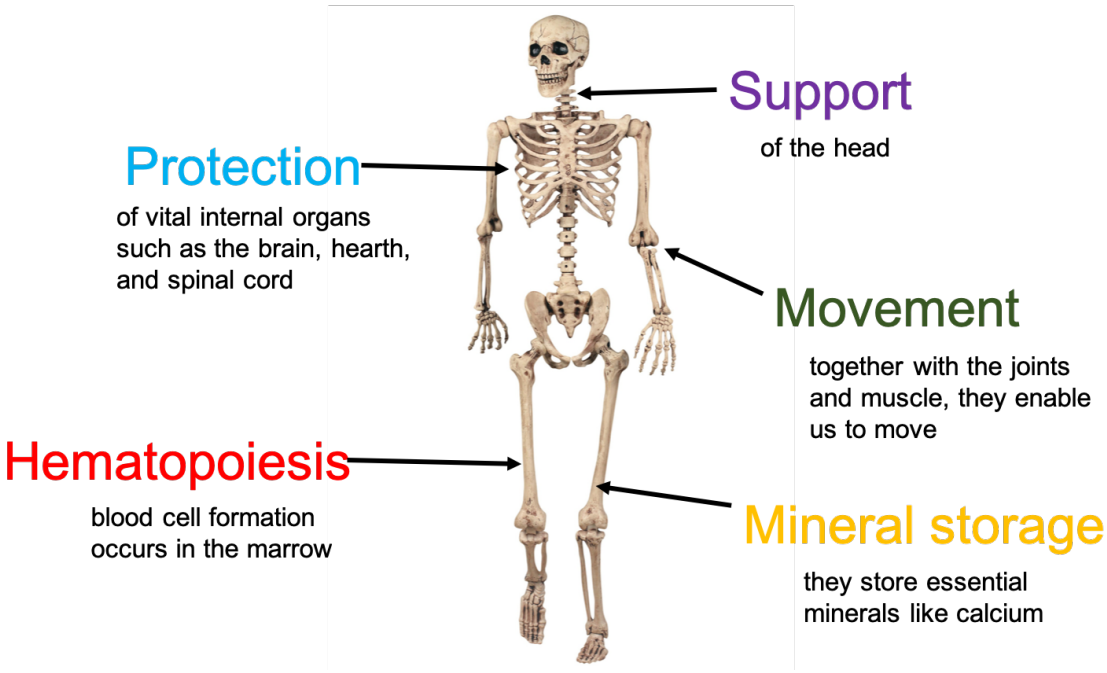

Figure 1.1. Functions of the bone.

The skeletal system is composed of bones and cartilage and performs critical functions: it provides structural support for the body, facilitates movement and locomotion by serving as a point of attachment to the muscles, serves as a reservoir for minerals such as a calcium and phosphorus, it protects vital internal organs by covering or surrounding them, and maintains mineral homeostasis and hematopoiesis.

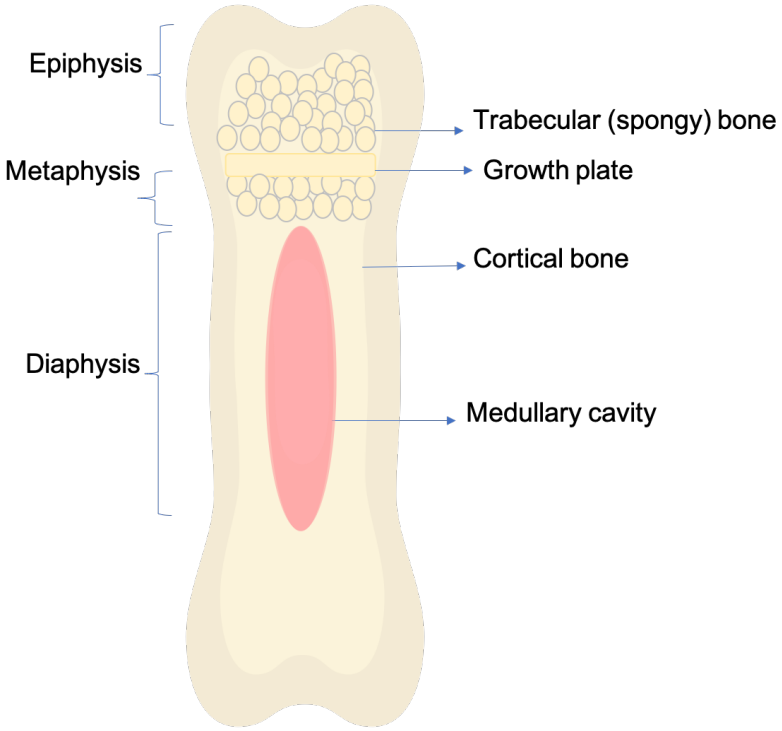

Figure 1.2. Bone anatomy.

The epiphysis is located at the end of the long bones and is composed of spongy trabecular bone covered by a thin layer of cortical bone. The metaphysis is located between the epiphysis and diaphysis and contains the growth plate. Like the epiphysis, the metaphysis is also composed of spongy trabecular bone. The diaphysis, which is surrounded by cortical bone, is the long cylindrical middle that contains the medullary cavity.

Immune cells			Percent
Lymphocytes			~8-20%
	T cells		~1-5%
		CD4 +	~1.5%
		CD8 +	~2-2.5%
		Treg	~0.5%
	B cells		~1%
CD11c+ dendritic cells			~1-2%
Plasma cells			~0.5%
Natural killer T cells			~0.4-4%
Mesenchymal stem cells			~0.01-0.1%
Myeloid- derived cells			~20-64%

Table 1.1. Cell population in the bone marrow.

The bone marrow is a primary lymphoid organ that generates lymphocytes from hematopoietic stem cells. Hematopoietic stem cells differentiate into myeloid and lymphoid cells. Myeloid-derived cells such as monocytes/macrophages and neutrophils constitute approximately 20 to 64% of the cells in the bone marrow. Lymphocytes represent about 8 to 20% of the cells. In terms of T cell population, $CD8^+$ T cells are most abundant than $CD4^+$ T cells. Only a small proportion of the cells in the bone marrow are mesenchymal stem cells (1).

1.1.2 Bone formation and development

Bone formation, also known as ossification, is the process by which new bones are produced. This process consists of both endochondral and intramembranous bone formation and it begins around the third month of fetal life in humans. During endochondral fetal development, bone develops by replacing hyaline cartilage with osteoblasts. This cartilage serves as a template that will be replaced by new bone. During intramembranous ossification, compact and spongy bone evolve directly from MSCs that differentiate into osteoblasts without using the cartilaginous matrix as intermediate. Intramembranous ossification is the process responsible for the development of flat bones of the cranial vault, some facial bones, and parts of the mandible and clavicle. While these two processes lead to the formation of bone, endochondral ossification takes much longer that intramembranous ossification.

Bone undergoes longitudinal and radial growth at the growth plate, a process similar to endochondral ossification. The process begins when chondrocytes at the epiphyseal plate (growth plate) start dividing, leading to the movement of cells toward the diaphysis. This process replaces cartilage with bone, resulting in a lengthening of the bone. Longitudinal and radial growth occurs during childhood and adolescence. However, in males, long bones stop growing around the age of 21 and in females at the age of 18. During this process, chondrocytes stop dividing and all of the cartilage undergoes mineralization and new bone is formed. Radial growth is the increase in bone diameter by the addition of bony tissue at the surface of bones. This process occurs by the deposition of new bone on the periosteal surface by the osteoblasts and equivalent resorption at the endosteal surface by osteoclasts. A balance in signaling between osteoclast and osteoblast allows the thickening of the bone.

1.1.3 Cellular components of bone

There are three major components of the bone: 1) the organic matrix which consists of 95% type 1 collagen and 5% proteoglycans and constitutes approximately 25% of the bone mass; 2) the inorganic matrix which makes up 70% of the bone and contains phosphate and calcium in the form of hydroxyapatite; and 3) the osteogenic cells which include osteoblasts, osteocytes, and osteoclasts.

1.1.3.1 Osteoblasts

Osteoblasts are the cells responsible for bone formation. Morphologically, osteoblasts are cuboidal cells located in the interface of newly synthesized bone. They differentiate from mesenchymal stem cells (MCSs). Commitment of MSCs to the osteoblast lineage is regulated by the transforming growth factor beta (TGF-β), bone morphogenetic proteins (BMPs), and the canonical Wnt catenin pathway. Osteoblast function is regulated at three main levels: lineage selection, maturation, and apoptosis. Lineage selection occurs in response to the expression of the transcription factor runt-related transcription factor 2 (RUNX2). Once RUNX2 is activated, pre-osteoblasts undergo differentiation into mature osteoblasts. Osteoblast differentiation is a 3-stage process characterized by the expression of several markers. In stage 1, the cells continue to proliferate, and they express fibronectin, collagen 1 and osteopontin. In stage 2, they start to differentiate into mature osteoblasts, and they express alkaline phosphatase (ALP). During the last stage, matrix mineralization occurs and osteocalcin is highly expressed (2) (Figure 1.3). Through the secretion of type I collagen and bone organic matrix proteins osteoblast regulate bone formation. At the end of bone formation, osteoblasts either undergo apoptosis or become embedded within the mineralized bone matrix where they become osteocytes.

1.1.3.2 Osteocytes

Osteocytes, known as the mechanosensory cells, are former osteoblasts that have been embedded into the bone matrix (Figure 1.3). They are the most abundant cell type in mature bone tissue, comprising more than 90% of cells within the bone matrix (3). Osteocytes communicate with each other via cytoplasmic extensions known as canaliculi and are connected via gap junctions. Their strategic location in the lacuna- canalicular network enables osteocytes to detect variations in mechanical signals (4), as well as levels of circulating factors such as ions and hormones. In response to these signals, osteocytes coordinate the function of osteoblasts and osteoclasts. Osteocytes can detect fatigue-induced microdamage and secrete factors such as osteoprotegerin (OPG), receptor activator of nuclear factor kappa-B ligand (RANKL), and sclerostin to induce replacement of damaged bone. Sclerostin is solely produced by osteocytes and antagonizes several members of the BMP family of proteins and prevents activation of Wnt signaling and therefore osteoblast differentiation.

1.1.3.3 Osteoclasts

Osteoclasts are multinucleated cells formed by the fusion of monocyte and macrophage precursors cells. Osteoclasts are derived from hematopoietic stem cells (HSCs). Differentiation of HSCs into osteoclasts is regulated by macrophage colony stimulating factor (M-CSF), RANKL, and the soluble RANKL receptor OPG, the last two being produced by osteoblasts. In the initial stages of differentiation, HSCs undergo differentiation into macrophage colony-forming units (CFU-M) in response to M-CSF signaling (Figure 1.3). CFU-M is the common precursor cells of macrophages and osteoclasts. Soluble or membrane-bound RANKL binds to its receptor RANK on the precursor cells which results in the transcription and activation of osteoclast genes (cathepsin K and tartrate-resistant acid phosphatase). The next step is the fusion of cells to form the multinucleated osteoclast. Osteoclast differentiation can be regulated by osteoblasts through

the secretion of OPG, which competes with RANK and prevents its interaction with the RANKL, thus inhibiting osteoclast differentiation. Conversely, osteoclasts can also modulate osteoblast differentiation through the secretion of coupling factors such as BMP-6 and Wnt10b. Together, osteoclast and osteoblast differentiation and function can be regulated by interconnected signals.

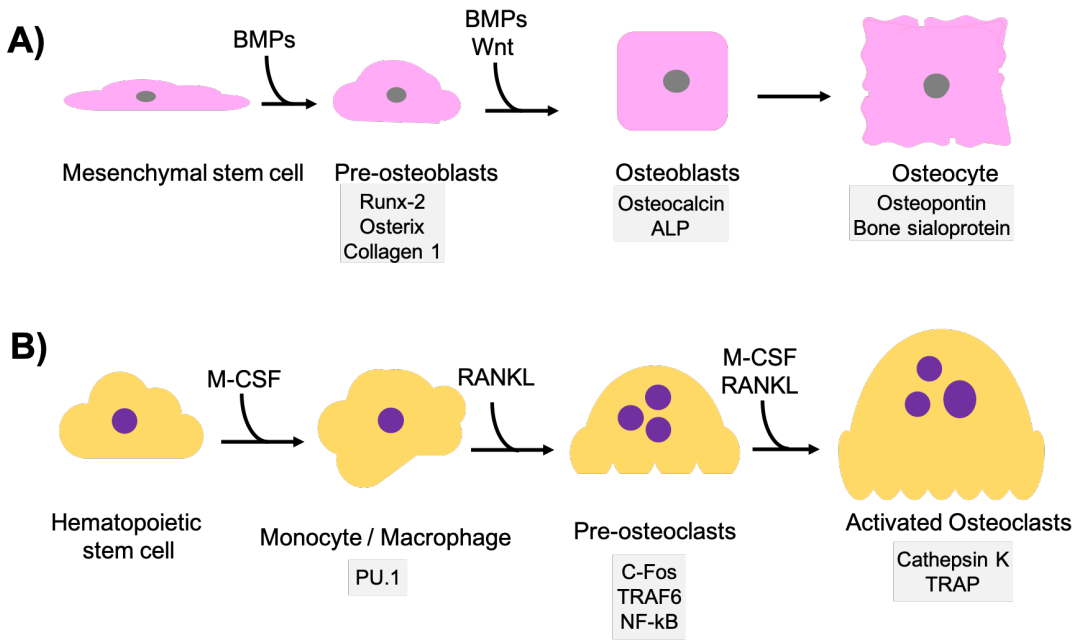

Figure 1.3. Osteoblast and osteoclast differentiation and markers.

(A) In response to BMPs, mesenchymal stem cells undergo differentiation into pre-osteoblast which express RUNX-2, osterix and collagen 1. In the next step, pre-osteoblasts differentiate into mature osteoblasts, a process in which Wnt/β-catenin signaling plays an essential role. At this point, mature osteoblasts will express osteocalcin and alkaline phosphatase (ALP). Osteoblasts become osteocytes when they are embedded within the bone.

(B) Osteoclasts differentiate from the hematopoietic stem cells. In response to M-CSF, hematopoietic stem cells undergo differentiation into macrophage colony-forming units (CFU-M), which are the common precursor cells of macrophages and osteoclasts. The differentiation step from CFU-M to multinucleated osteoclasts is characterized by cell–cell fusion, which is mainly induced by RANKL. In the activation (maturation) stage, osteoclasts acquire bone resorbing activity.

1.1.4 Bone modeling and remodeling

Bone undergoes both modeling and remodeling throughout life. Bone modeling is the process by which bones are shaped or reshaped in response to biomechanical forces. Bone modeling defines skeletal development and growth. This process is independent of the action of osteoblast and osteoclasts and is controlled by physical activity. One example of bone modeling can be seen in tennis players. In tennis players the arm that is used to play tennis has higher bone mass than the other one due to physical loading. Other factors such as hormones can also regulate bone modeling as in the case of the parathyroid hormone (PTH) and inhibition of sclerostin that can stimulate modeling-based bone formation (5). During bone modeling, bone formation and resorption are not tightly coupled. Bone modeling continues throughout life but is less frequent than bone remodeling in adults (6).

Bone is a highly dynamic organ that is continuously undergoing remodeling. Bone remodeling is the replacement of old bone tissue by new bone with the goals of maintaining bone strength, mineral homeostasis, and preventing accumulation of bone microdamage. This process begins before birth and continues throughout life. Approximately 5 to 10% of the existing bone in the adult human skeleton is replaced every year. This process is accomplished by the balance between the osteoblasts and osteoclasts and an imbalance in this communication can detrimentally affect bone health. Bone remodeling can be triggered by different signals such as changes in mechanical force, endocrine and paracrine signals, cytokines, and modulation of calcium levels (7,8). The basic multicellular units that constitute bone remodeling are the osteoblasts, which produce the new bone matrix; the osteoclasts, which are in charge of bone resorption; and the osteocytes, which are osteoblast derived cells that act as mechanosensors. A fourth type of cells that may be involved in this process are the bone lining cells, which are suggested to play a role in coupling bone formation to resorption, but their role is not completely understood (9) (Figure 1.4).

The bone remodeling cycle is composed of four sequential phases: activation, resorption, reversal, and bone formation. Activation begins by the recruitment, activation, migration, and proliferation of osteoclast precursor cells by the osteoblasts to the bone-resorbing compartments. Osteoblasts stimulate and recruit osteoclasts by the secretion of factors such as RANKL and M-CSF (10). Osteoblasts can also secrete OPG, which can stop osteoclast activation (11). The resorption phase begins when multinucleated preosteoclasts bind to the bone matrix via interactions with integrin receptors (12). After the osteoclasts attach to the bone matrix, they form unique membrane domains, including the sealing zone, ruffled border, and the functional secretory domain. These domains create an acidic environment, in which the osteoclast will release lysosomal enzymes to dissolve the bone matrix. Activated osteoclasts can secrete tartrate-resistant acid phosphatase 5b (TRAP5b) into the serum which is used as a quantification marker of whole-body bone resorption. Activated osteoclasts will also secrete cathepsin K, and matrix metalloproteases (13). Following resorption of the old or damaged bone, the process undergoes reversal. During the reversal phase, the osteoclasts recruit osteoblasts by releasing growth factors from the bone matrix, such as TGFβ, insulin-like growth factor (IGF), and BMPs to increase osteoblast number and activity (13). Bone formation is a two steps process: first, the osteoblast secretes unmineralized osteoid, which is then mineralized through the incorporation of hydroxyapatite; second, some osteoblasts will undergo apoptosis while others become embedded within the bone and differentiate into osteocytes (14). During this phase, the process of "coupling" bone resorption to bone formation also occurs to ensure that the volume of bone removed is replaced by new bone. Osteocytes play an important role in responding to mechanical stimuli and signaling to the other cells types to initiate the remodeling process (4).

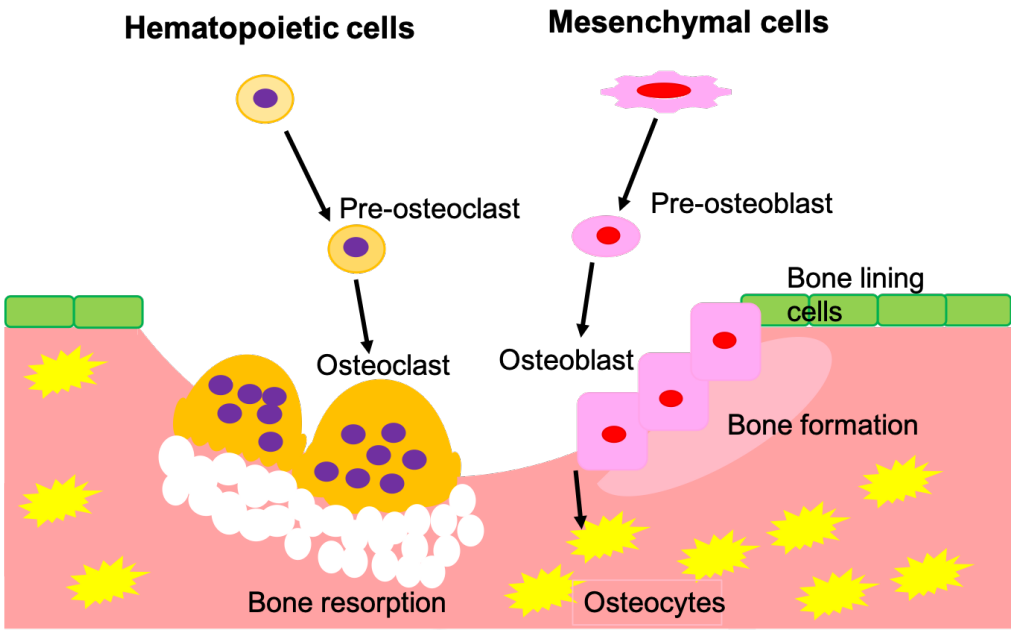

Figure 1.4. Bone remodeling.

Bone remodeling is a continuous process that maintains the integrity of the bone tissue. This process involves communication between the osteoblasts, osteoclasts, and osteocytes. During this process, old bone is removed by osteoclasts and replaced by osteoblasts, the bone forming cells. Osteoblasts will then undergo apoptosis, or they will become embedded within the bone and differentiate into osteocytes. Bone lining cells will help by coupling bone formation to bone resorption.

1.2. Bone pathophysiology

Disruption of the skeletal system can result in a variety of bone diseases and disorders. Some of these disorders are (15):

- Osteomalacia or soft bones: is a disease that affects adults and is defined as the inadequate mineralization of the bones due to the lack of vitamin D.
- Rickets: is the equivalent of osteomalacia in children and is characterized by deformation and widening bones.
- Paget's disease: is a chronic bone disorder in which the osteoclast become abnormally active. This results in an intense osteoblastic response that leads to irregular new bone formation. This disease causes the affected bones to become larger and misshapen.
- Rheumatoid arthritis: is a chronic autoimmune disease that leads to the destruction of bone architecture.
- Osteoarthritis: is the most common form of arthritis. This disease occurs when the cartilage between the joints break down.
- Osteoporosis: is characterized by low bone mineral density and is the most common type of bone disease. In this dissertation we will focus on this disease.

1.2.1 Osteoporosis: definition and classification

Osteoporosis is a condition that occurs when the bone deteriorates and becomes fragile due to a decrease in bone density. This decrease in bone density can be attributed to an imbalance in bone remodeling, with increased or decreased bone resorption and formation respectively. This imbalance in bone remodeling can lead to a decrease in bone mineral density (BMD), trabecular thickness, trabecular number, and an increase in trabecular space, resulting in fragile bone. Osteoporosis is primarily determined by measuring BMD and is diagnosed when the patient has a

T score of -2.5 or lower, meaning a BMD that is 2.5 standard deviations below the average population BMD. Clinically, osteoporosis can be classified in 4 subgroups based on the T score: 1) normal bone density: a T score of -1.0 or above. 2) osteopenia (low bone density): a T score between -1 to -2.5. 3) osteoporosis: a T score of -2.5 or lower. 4) severe osteoporosis: a T score lower than -2.5 with one or more fractures (16). Osteoporosis can also be categorized into primary and secondary osteoporosis. Primary or idiopathic osteoporosis, which is the most common form of osteoporosis, occurs as a consequence of the normal human aging process. In females it is accelerated due to menopause. On the other hand, secondary osteoporosis is caused by diseases or treatments that interfere with bone remodeling/formation. Some conditions and treatments that are known to lead to osteoporosis, regardless of age, include inflammatory bowel disease, glucocorticoid treatment, and type 1 diabetes (17–20).

1.2.2 Epidemiology of osteoporosis

Worldwide, osteoporosis is estimated to affect 200 million people (21). In the United States, osteoporosis affects >10 million people and accounts for more than 2 million fractures, with a total cost of $17 billion (22). By 2020, the prevalence of osteoporosis in the United States is expected to surpass 14 million people and by 2025 the annual cost associated with osteoporosis will increase by a 50% (22). Nonvertebral fractures represent 73% of total incident fractures and 94% of total costs. A around 30% of people with hip fractures die during the first year and 50% have permanent disability (22). Although osteoporosis is more common in women (50% of women over fifty can have a fracture due to osteoporosis), men can also be affected. Osteoporosis can affect 1 in 4 men over fifty. About 39% of bone fracture occurs in men between 50-64 years old. In addition, during the first year following a hip fracture the mortality rate for men is higher(36%) than for women (21%) (23).

1.2.3 Treatments for osteoporosis

While there has been a lot of progress in finding effective treatments against osteoporosis, the treatments that are currently available are not effective for everyone, they can be expensive and tend to have unwanted and detrimental side effects (24–26). Osteoporosis treatments can be divided into non-pharmacological and pharmacological treatments.

1.2.3.1 Non-pharmacological treatments

Non-pharmacological treatments include a diet high in calcium and vitamin D, lifestyle modifications such as decreasing alcohol and drug consumption as well as increasing physical activity, specifically weight bearing exercises. Dietary modification of calcium or calcium rich foods and vitamin D is essential to improve bone mass. The Institute of Medicine (IOM) suggests that men between the ages of 50 - 70 should consume 1,000 mg of calcium daily while women older than 50 and men older than 71 years old should consume around 1,200 mg of calcium daily (27). However, there are negative side effects associated with high intake of calcium supplements including a higher risk of developing kidney stones and myocardial infarction, particularly in women (28). Further studies however, are required to better understand the side effects of calcium supplements. In terms of vitamin D intake, the IOM recommends for men and women 51 to 70 years of age 600 international units (IU) per day and 800 IU per day for people over 70 years old (27).

1.2.3.2 Pharmacological treatments

Current pharmacological treatments for osteoporosis include antiresorptive drugs which are designed to prevent bone resorption and anabolic agents that increase bone formation. Antiresorptive drugs include bisphosphonates, calcitonin, and selective estrogen receptor modulators (SERMs) while anabolic agents consist of parathyroid hormone analogues (PTH). Bisphosphonates are commonly used as a first line treatment for osteoporosis. Bisphosphonates

are chemically stable inorganic pyrophosphate analogues with extremely high affinity for the mineral component of bone (29). Once embedded into bone mineral, actively resorbing osteoclasts take up bisphosphonates which in turn inhibits farnesyl pyrophosphate synthase (FPPS) (30,31). Inhibition of FPPS induces lipid modification within osteoclasts, ultimately leading to apoptosis (30). Therefore, bisphosphonates prevent bone resorption by inducing osteoclast apoptosis and reducing their recruitment and activity (32). Newer generation bisphosphonates have nitrogen side chains which allow them to adhere more tightly to the hydroxyapatite mineral than previous generations (29,33). Besides the beneficial effects of bisphosphonates, several studies have shown that long term use of bisphosphonates can increase the risk of osteonecrosis of the jaw (34). Calcitonin is a naturally produced hormone that inhibits osteoclast function (35). Calcitonin use is recommended for postmenopausal women who are at least five years beyond menopause and when other medicines are not suitable. Salmon calcitonin nasal spray was shown to decrease the risk of new vertebral fractures in postmenopausal women that already have osteoporosis (36). Despite these findings, calcitonin treatment does not appear to be as effective as bisphosphonates in preventing non-vertebral fractures and side effects including increase risk of cancer (37). SERMs such as raloxifene have tissue-specific effects and act either as an estrogen agonist in bone or as an estrogen antagonist in breast tissue. Raloxifene treatment may also increase the risk of venous thromboembolic disease and stroke (24). In addition, similar to calcitonin, raloxifene treatment does not prevent hip fractures (24,25). Teriparatide, a recombinant human PTH analogue, is the first anabolic agent approved for osteoporosis treatment. Subcutaneous, daily low doses of PTH promotes osteoblast differentiation and inhibits osteoblast and osteocyte apoptosis (38). However, the duration of teriparatide therapy is limited to two years due to the risk of development of osteosarcoma (26). Taken together, novel therapies against osteoporosis with limited side effects are necessary.

1.2.3.3 Emerging therapies for osteoporosis

Many studies are currently investigating new approaches for the treatment of osteoporosis. These pharmacological approaches include: 1) humanized monoclonal antibodies to inhibit sclerostin. Sclerostin is secreted by the osteocytes and prevents bone formation by inhibiting osteoblasts activity. Romosozumab, a humanized monoclonal antibody that inhibits sclerostin decreased the risk of new vertebral fractures and increased bone mineral density in postmenopausal women after 12 months of treatment. Romosozumab treatment has recently been approved by the Food and Drug Administration (39); 2) selective inhibitors of cathepsin K. Cathepsin K is a protease released by osteoclast to degrade bone matrix. Cathepsin K inhibitors can potentially prevent bone loss by preventing bone resorption. However, in 2016 Merck discontinued the development of the cathepsin K inhibitor Odanacatib due to an increased risk of stroke (40); 3) integrin antagonists can prevent bone resorption by preventing the attachment of osteoclast to the extracellular matrix and therefore bone resorption (41); and 4) stimulators of osteoprogenitor cells (42,43). Non-pharmacological approaches include: stem cell therapy and probiotics. Stem cells can promote bone formation through their differentiation into osteoblast cells. Intravenously injected mouse mesenchymal stem cells into ovariectomized mice restored bone volume and prevented bone loss (44), demonstrating a beneficial effect of this treatment in bone regulation. Recently, several studies have demonstrated a beneficial effect of probiotic consumption in preventing bone loss. Probiotic treatment against osteoporosis is a promising therapeutic target due to the lack of side effects. Probiotics beneficial effects on bone density are described in section 1.5.3.3.

1.2.4 Risk factors for osteoporosis

A number of factors have been linked to an increased risk of developing osteoporosis. Some of these factors can be controlled while most of them are uncontrollable. Controllable risk

factors associated with osteoporosis include: a sedentary lifestyle, excessive drug consumption, and a diet low in calcium and vitamin D. Eating disorders can also lead to bone loss mainly due to the poor consumption of calcium and vitamin D. A study in South Korean postmenopausal women found that postmenopausal women that consumed alcohol 4 times a week had lower bone mineral density than non-drinkers (45). Uncontrollable factors include gender, family history of osteoporosis, age, certain medications, and ethnicity. Females are at a higher risk of developing osteoporosis after menopause. Lighter and thinner bones are more prone to osteoporosis. The chance of losing bone density also increases with age, which may be due in part to complications from secondary diseases that can affect bones. Having other medicals conditions including inflammatory bowel disease and diabetes (see section 1.3) can also increase the risk for osteoporosis. Certain medications such as glucocorticoids can lead to bone loss and increase the risk of fracture. In summary, many factors can contribute to bone loss and osteoporosis.

1.3. Bone loss in diabetes mellitus

1.3.1 Types of diabetes mellitus

Diabetes mellitus is a chronic metabolic disease in which the body's ability to produce and respond to insulin is affected, resulting in increased blood glucose levels. There are two main types of diabetes: type 1 diabetes (T1D) and type 2 diabetes (T2D). T1D is an autoimmune disease in which the pancreatic beta cells produce little or no insulin, leading to impaired glucose uptake in tissues and therefore increase in blood glucose (46–48). T1D can be controlled by insulin delivery and regulation of blood glucose. T2D is the most common type of diabetes and mostly develops in adulthood (49). T2D is characterized by insulin resistance. Insulin signaling and glucose uptake are also impaired in insulin-dependent cells. Both types of diabetes can result in complications such as neuropathy, nephropathy, cardiomyopathy, and retinopathy. In addition to these common complications, diabetes mellitus can also lead to secondary osteoporosis.

1.3.2 Epidemiology of diabetes mellitus-induced bone loss

Studies in humans as well as in animals have shown that both types of diabetes can affect bone health however, the pathophysiology is different (50–54). T1D in animal models and humans is associated with bone loss. On the contrary, the effects of T2D on bone density are variable with some studies showing either no change, decreased or increased bone density (51,52,55). The discrepancy in these studies can be explained in part by the changes in bone load due to the increase in body weight seen in these patients (51,55). In addition, the increase in risk of fractures in people with T1D is higher when compared with T2D patients (56). T2D is associated with a 19% increase in risk fracture while T1D is associated with 30% (57,58). Women with T1D, between the ages 40-49 had an 82% increased risk in having a fracture than women without diabetes. Similarly, men with T1D (ages 60-69) had double the risk of fracture than men without diabetes (59). In terms of bone mineral density (BMD), T1D patients (both sexes) had lower BMD when compared to

controls (60). In a study in pre-pubertal children, (5.8 months after T1D diagnosis) BMD was found to be lower in the T1D kids when compared to controls (61). In summary, both T1D and T2D can affect the bone, however T1D is mostly associated with bone loss while T2D is not. Since T1D is clearly associated with bone loss, in this study we will focus on understanding T1D effects on bone density.

1.3.3 Mouse models of type 1 diabetes-induced bone loss

Several animal models have been used to better understand the effect of T1D on bone density. These models consist of both spontaneous and pharmacologically induced T1D (62). The $Ins2^{+/-Akita}$ and non-obese diabetic (NOD) mice develop T1D spontaneously. The $Ins2^{+/-Akita}$ mouse has a point mutation in the insulin 2 gene that leads to incorrect folding of the insulin protein producing toxicity in pancreatic ß cells and resulting in pancreatic ß cell apoptosis and hyperglycemia. The $Ins2^{+/-Akita}$ mice develop insulin dependent diabetes within 4-6 weeks of life (63). T1D susceptibility in the NOD mice is not entirely understood, however, it has been suggested that a polymorphism in the cytotoxic T-lymphocyte-associated antigen-4 (CTLA-4) can play a role in this process. CTLA-4 is a member of the immunoglobulin superfamily that contributes to the suppressor function of regulatory T cells (64). Polymorphism in CTLA-4 is associated with autoimmune diseases such as lupus, rheumatoid arthritis, multiple sclerosis and diabetes (65–67). The pathogenesis in the NOD mice is characterized by leukocytic infiltration of the pancreatic islets that leads to impaired insulin release and hyperglycemia. Since these are spontaneous models that do not consistently develop diabetes; which is the case for the NOD mice in which only 60% of male mice develop diabetes (62,68), pharmacological treatments are also used. The most common pharmacological drug used to induce T1D phenotype in animals is streptozotocin (STZ). STZ is a drug derived from *Streptomyces achromogenes* that leads to pancreatic β cell apoptosis, impaired insulin secretion and consequent hyperglycemia (62). STZ is

taken up by pancreatic B cells via glucose transporter 2 GLUT2 (62). Despite the difference in these animal models, our lab and others have shown bone loss in both the genetic and pharmacological models of T1D (20).

1.3.4 Mechanisms of type 1 diabetes induced-bone loss

There are several suggested mechanisms by which diabetes can affect bone health. Some of these mechanisms include the direct effect of hyperglycemia and insulin/ IGF-1 on osteoblasts, increase in bone marrow adiposity, and systemic and local (bone) increase in pro-inflammatory cytokines. Specifically, most of these mechanisms have been shown to regulate bone density by affecting osteoblasts. T1D animal models often present with a decrease in osteocalcin, osterix, RUNX2, osteoblast numbers, as well as bone formation (69–71). On the contrary, the effects of diabetes in bone resorption and in osteoclasts are variable. Several studies have shown no changes, increased or decreased levels of osteoclasts in T1D animal models (70,72,73). Clinical studies looking at osteoclast activity in the serum, by measuring c-terminal telopeptide of type 1 collagen (CTX), have shown no changes in diabetic patients (74–77), suggesting that in humans, osteoclasts are not the primary cells involved in diabetes-induced bone loss.

1.3.4.1 Hyperglycemia and bone loss

Different mechanisms have been suggested to be involved in hyperglycemia-induced bone loss. These mechanisms include alterations in mesenchymal stem cells (MSCs) lineage selection, prevention of osteoblast maturation, as well as increased osteoblast death. Despite the fact that diabetes is mostly associated with osteoblast effects, hyperglycemia can also affect osteoclasts. In addition, high glucose conditions can increase advance glycation end products (AGEs) and oxidative stress which indirectly affects bone cells.

1.3.4.1.1 Effects of hyperglycemia in mesenchymal stem cells lineage selection

Hyperglycemia can regulate bone density by promoting the differentiation of MSCs towards adipogenesis. MSCs can differentiate into osteoblasts and adipocytes, a process that is controlled by the canonical Wnt signaling (78). Activation of the Wnt signaling pathway induces MSCs differentiation towards osteoblasts while the peroxisome proliferator-activated receptors – γ (PPAR-γ) pathway promotes adipogenesis (79). *In vitro*, high glucose induces bone marrow MSCs differentiation towards adipocytes by suppressing the osteogenic transcription factors RUNX2 and osterix, and by increasing the levels of PPAR-γ (80,81). Among the Wnt ligands, Wnt10b is a major regulator of bone density and lineage selection. Wnt10b increases the expression of RUNX2 and osterix and promotes osteoblast differentiation (82). T1D mouse models present a decrease in Wnt10b expression and osteoblast number, together with an increase in adipocyte area and number (83). Indeed, Wnt10b transgenic mice are protected against T1D induced bone loss (83).

1.3.4.1.2 Effects of hyperglycemia on osteoblast maturation and death

High glucose levels can affect bone formation by preventing osteoblast maturation and inducing osteoblast death (84–86). T1D mouse models express low levels of osteocalcin, osterix, and RUNX2. Osteoblast numbers are also decreased in the bone of T1D mice (83,87). An increase in osteoblast TUNEL staining and pro-apoptotic factors in T1D mouse models has also been shown (19). *In vitro*, exposure of pre-osteoblast cell lines (i.e., MC3T3-E1 cells) to high glucose conditions (30 mM) decreased osteocalcin and alkaline phosphatase gene expression (85,88), inhibited osteoblast differentiation, and calcium deposition (89). Similarly, sustained exposure of human osteoblast-like cells (MG-63) to high glucose for 7 days inhibited cell proliferation in a concentration-dependent manner compared to cells cultured under normal glucose concentration (84). In addition, MC3T3-E1 cells cultured under conditions associated with T1D (high glucose

or pro-inflammatory cytokines such as TNFα) display reduced levels of RUNX2, osteocalcin, and Wnt10b (83,90). Together, these studies support the role of high glucose in affecting osteoblasts differentiation and bone formation in patients with T1D.

1.3.4.1.2 Effects of hyperglycemia on osteoclasts

Hyperglycemia can also affect osteoclasts by inhibiting their formation and function. *In vitro*, high levels of D(+)glucose inhibited osteoclast formation, ROS production (needed for bone resorption), caspase-3 activity (necessary for RANKL-induced differentiation), and migration of osteoclasts in response to RANKL (91). Monocytes isolated from the bone marrow of C57BL/6 mice treated with 33.6mmol/L glucose for four days had less osteoclast cells and expressed lower levels of RANK and cathepsin K when compared to normal glucose-treated isolated monocytes. This study demonstrates that osteoclastogenesis can be suppressed *in vitro* under hyperglycemic conditions (92). On the contrary, *in vivo*, high doses of STZ in female mice increased TRAP5b levels in the serum but had no effects on osteoclast numbers (87), suggesting that high glucose effects on osteoclasts are variable.

1.3.4.1.3 Role of AGEs and oxidative stress in hyperglycemia and bone

Other mechanisms by which hyperglycemia can affect bone density includes an increase in advance glycation end products (AGEs) and oxidative stress. During diabetes, there is an increase in AGE (93). AGEs can regulate both osteoblasts and osteoclasts by interacting with it is receptor (e.g., RAGE). This interaction can decrease osteoblast maturation, induce osteoblast apoptosis, and increase bone resorption by osteoclasts (94,95). An increase in oxidative stress by hyperglycemia can also inhibit osteoblast differentiation and promote osteoclastogenesis (96,97).

1.3.4.2 Role of hyperlipidemia in type 1 diabetes-induced bone loss

Insulin is a major regulator of lipoprotein lipase (LPL). LPL is an enzyme that breaks down triglycerides from the blood and transfers them to the tissue to either to be used for fuel or re-

assembled into triglycerides for storage. Insulin regulates LPL activity by increasing LPL gene transcription in adipocytes and by stimulating the levels of LPL mRNA through posttranscriptional and posttranslational mechanisms (98). In insulin deficient conditions, the activity of the lipoprotein lipases is decreased (99) which leads to an increase in serum lipids and hyperlipidemia. Hyperlipidemia has been associated with low bone mass. However, studies in humans are not consistent, mainly due to the sample size, gender, age and other diseases that can affect the outcome (100–102). An increase in serum lipids can promote mesenchymal stem cells to differentiate into adipocytes by activating PPARγ2 and thus could play a role in suppressing osteoblast activity. The effects of hyperlipidemia on bone density has also been shown in T1D conditions. One study done in T1D female patients found a significant correlation between increased serum lipid levels and decreased bone density (103). T1D mouse models have also shown an increase in bone marrow adipocyte number (69,83). However, inhibition of T1D-induced marrow adiposity in mice using a PPARγ antagonist did not prevent bone loss (103,104). In addition, vertebral bone loss is also seen in T1D conditions. However, T1D vertebral bone does not display increased adiposity like the marrow compartment of the femoral bone (105), suggesting that an increase in bone marrow adipogenesis is not the primary driver in T1D-induced bone loss.

1.3.4.3 Insulin and IGF-1 signaling in the regulation of bone density

IGF-1 and insulin can both regulate osteoblasts. Osteoblasts express insulin receptors (70) and insulin increases transcription factor RUNX2 and promotes osteoblast differentiation (106). IGF-1 binds to its receptor (IGF1R) and promotes osteoblast maturation, proliferation, and matrix generation (107). Indirectly, insulin regulates osteoblasts by controlling blood glucose (108). IGF-1have also been suggested to be involved in diabetes induced bone loss. Several studies have shown low serum IGF-1 levels in children and adolescents with T1D (109–111). In postmenopausal diabetic women, serum IGF-I levels were inversely associated with the number

of prevalent vertebral bone fractures (112). In addition, low levels of IGF-1 in T1D patients are linked to an increase in pro-inflammatory cytokines, which are known to negatively affect bone density (113).

1.3.4.4 Cytokine dysregulation in type 1 diabetes and bone loss

While many factors are associated with diabetes-induced bone loss, cytokines have also been demonstrated to be involved in this effect. During diabetes, there is a systemic increase in pro-inflammatory cytokines (114–118). Studies in both human and diabetic murine models have demonstrated an increase in pro-inflammatory cytokines and a decrease in anti-inflammatory cytokines during diabetes (73,114–116,119). Changes in cytokines levels are well known to affect the bone (see section 1.4), and several studies in human and animal models have shown an association between pro-inflammatory cytokines and bone loss (17,120–123). In addition, not only are pro-inflammatory cytokines elevated in the serum of diabetic mice, but they are also expressed at high levels in the bone, suggesting a link between pro-inflammatory cytokines and diabetes-induced bone loss.

1.3.4.4.1 Role of pro-inflammatory cytokines in T1D-induced bone loss

Several studies have tested the role of pro-inflammatory cytokines in diabetes-induced bone loss. One study looking at the effect of interferon gamma (IFN-γ) in T1D-induced bone loss demonstrated that absence of IFN-γ does not protect against bone loss, suggesting potential compensation by, or role for other cytokines in T1D effects on bone density (116). Tumor necrosis factor alpha (TNF-α) is well known to negatively affect osteoblasts and promote bone resorption (124,125). Since TNF-α levels are highly up-regulated in diabetes, many studies have assessed its role in diabetes-induced bone loss. An increase in TNF-α in T1D mice, induced by the bacterial antigen lipopolysaccharides (LPS), resulted in enhanced osteoclast differentiation and osteoclast bone resorption activity (126). During estrogen deficiency along with T1D, high levels of TNF-α

correlated with bone loss and osteoblast death in female mice (87). In addition, inhibition of TNF-α during T1D can prevent a decrease in callus bone formation induced by T1D (127). Furthermore, inhibition of TNFα decreased osteoclast numbers and increased periodontal bone formation and osteoblasts in diabetes-induced periodontal bone loss (128). Diabetes can also decrease mesenchymal stem cell proliferation and increase their apoptosis, an effect that can be prevented by the TNF-α inhibitor pegsunercept (127). These findings demonstrated that pro-inflammatory cytokines contribute to the loss of bone density seen in T1D patients.

1.3.4.4.2 Role of anti-inflammatory cytokines in T1D-induced bone loss

Diabetes is also characterized by a decrease in the anti-inflammatory cytokine interleukin 10 (IL-10). Circulating levels of interleukin 10 (IL-10) were markedly low prior to diabetes onset in the NOD mouse model (117). Similarly to NOD mice, diabetic patients exhibit significantly lower serum IL-10 levels compared to non-diabetic subjects (118). Interestingly, administration of IL-10 protected NOD mice from developing diabetes (129). Despite these findings, the role of IL-10 in diabetes-induced bone loss is poorly understood. In chapter two of this thesis, we demonstrate that during early stages of T1D IL-10 deficiency exacerbates femoral and cortical bone loss.

In summary, diabetes can lead to bone loss, osteoporosis, and increased risk fracture. Several mechanisms have been demonstrated to be involved in diabetes-induced bone loss. However, more research needs to be done to further understand these mechanisms. In chapter two we add to the current knowledge by demonstrating an important role for IL-10 in the early stages of T1D- induced bone loss.

1.4. Immune regulation of bone density

One of the main modulators of bone remodeling is the immune system. Conditions in which the immune system is dysregulated such as in colitis and rheumatoid arthritis bone health is profoundly affected (17,123,130). B and T lymphocytes are well known to regulate bone density by altering osteoblasts and osteoclasts through the secretion of several pro and anti-inflammatory cytokines or via direct cell to cell contact (131–133). Other components of the immune system such as neutrophils, macrophages and dendritic cells can also modulate bone health. Cytokines such as IL-10, IFN-γ, TNF-α, interleukin 17A (IL-17A), and IL-6 have all been demonstrated to affect the bone remodeling processes (134–139) (Figure 1.5). Since the effect that these cells and cytokines have in the bone are distinct, we will discuss their role on bone density regulation individually.

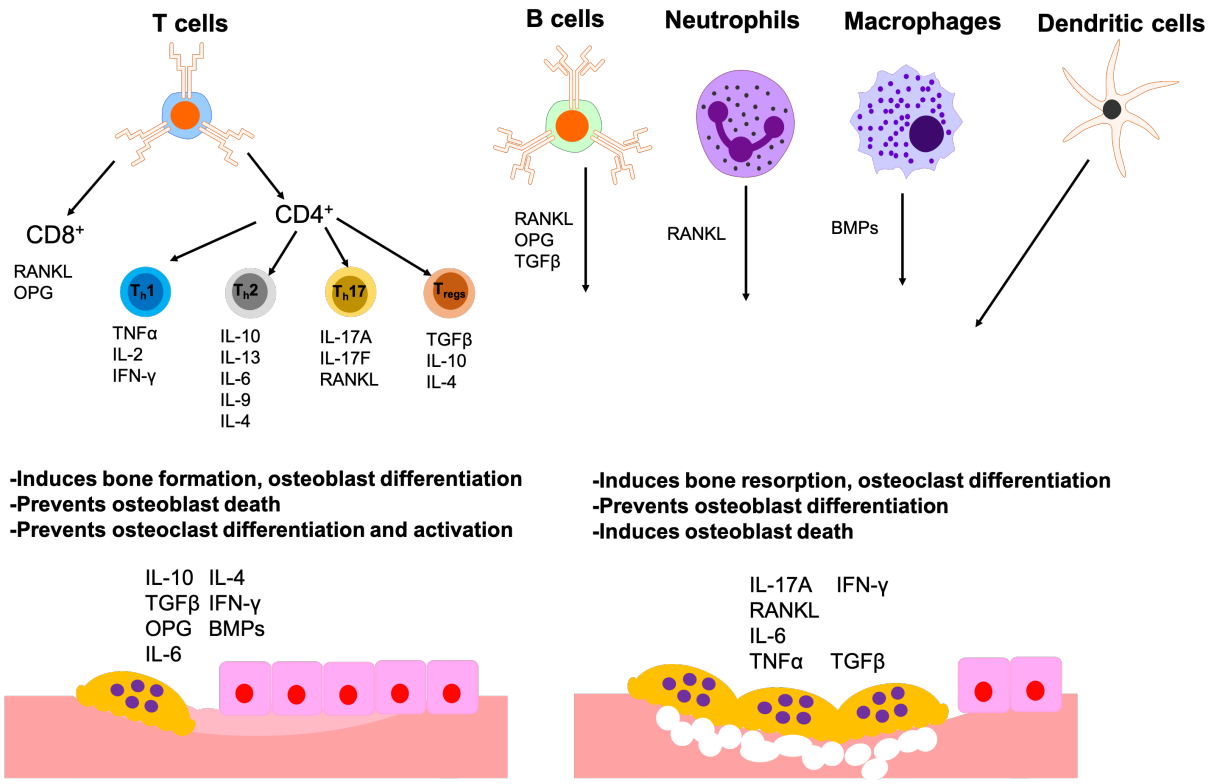

Figure 1.5. Modulation of bone remodeling by immune cells.

Some of the immune cells that regulate bone density include T and B lymphocytes, neutrophils, macrophages, and dendritic cells. Each one of these cells can modulate bone remodeling by directly interacting with bone cells or via the secretion of cytokines. Cytokines such as interleukin 10 (IL-10), interleukin 6 (IL-6), interleukin 17 (IL-17), and tumor necrosis alpha (TNF-α) are well known modulators of bone remodeling. Each one of these cells/cytokines regulate bone density by acting on the osteoblasts and promoting bone formation or by preventing bone resorption by the osteoclasts. Abbreviations: receptor activator of nuclear factor kappa-B ligand (RANKL), bone morphogenetic protein (BMP), osteoprotegerin (OPG), transforming growth factor beta (TGFβ), interferon gamma (IFN-γ).

1.4.1 Lymphocyte regulation of bone

Several studies have highlighted the role of T and B lymphocytes in the regulation of bone density. Interestingly, not only can these cells individually affect bone density, they can also interact with each other to regulate the bone response. For example, T and B cell interaction through the CD40L/CD40 receptors enhances the secretion of osteoprotegerin (OPG), an inhibitor of bone resorption, by B cells (132). Under basal conditions, CD40L, CD40, and B cell deficient mice present lower bone density (132,140). On the contrary, after activation, T and B cells can secrete pro-osteoclastogenic cytokines which can increase bone resorption and lead to bone loss.

1.4.1.1 T lymphocytes and bone regulation

T lymphocytes are major components of the adaptive immune system and are crucial for recognizing antigens to mediate an immune response. T cells can express either αβ or γδ T cell receptor subunits. Most T cells express the αβ subunits while only a small fraction express γδ subunits. These cells can be classified as CD4 and CD8 positive T cells based on the expression of the CD4 or CD8 glycoproteins on their surfaces. $CD4^+$ T cells can be further subdivided in T helper 1 (Th1), 2 (Th2), 17 (Th17), and T regulatory cells (Treg), all of which can produce different cytokines and can have a variety of effects on bone. Th1 cells are characterized by the secretion of TNF-α, IFNγ, and interleukin (IL)-2; Th2 cells can produce interleukins 4 (IL-4), 5 (IL-5), 6 (IL-6), 9 (IL-9), 10 (IL-10), and 13 (IL-13) (141,142); Th17 can secrete IL-17A, IL-17F, IL-21, and IL-22 (143); and Treg can produce IL-10 and TGFβ.

The role of T cells on bone density regulation has been tested in different mouse models. In 10 week old TCRβ deficient mice, a strain that is deficient in αβ T-cell receptor, total body bone mass density was reduced, but no changes were seen in the femoral bone, or osteoclasts and osteoblasts markers in the serum. Mechanical testing of the femoral bone did not show any significant differences (144). Similarly, in the nude mice, a strain that also lacks αβ T cells, no

changes in femoral trabecular bone volume or osteocalcin serum levels were noticed (144). In contrast, in a different study, 10 to 12 weeks old female nude and TCRα deficient mice presented lower bone mass density in the femur and tibia when compared to the wild type control, suggesting that T cells are required for the normal development of bone. However, one caveat of this last study is that the wild type and deficient mice were bought from different companies and were not littermates. Therefore littermates wild type controls from the same company are required to confirm these results (140). In a different study, 12-16 weeks old T-cell–deficient nude mice also presented decreased bone mass density due to a decrease in bone marrow osteoprotegerin production and increased bone resorption (132). The discrepancies in these results might be explained by the different ages of the mice used (10 vs 16 weeks). The role of T cells on bone density regulation in estrogen depleted conditions (OVX) has also been tested. TCRα deficient mice were not protected against OVX-induced bone loss, suggesting that bone loss in estrogen depleted condition is not mediated by T cells (140). Interestingly, T cell nude mice prevented the increase of total body and femoral bone density induced by intermittent parathyroid hormone (iPTH) treatment (144). Taken together, T cell regulation of bone density might be influenced by the age of the mice and the specific knockout model that was used.

1.4.1.1.1 CD 4^+ T cells

In healthy conditions, $CD4^+$ T cells do not seem to play a role in bone density regulation. Reduction of $CD4^+$ T cells in the class II MHC knockout mice does not show any bone phenotype. Trabecular femoral bone volume and serum osteocalcin levels in the class II MHC knockout mice are not different from wild type mice (144). However, $CD4^+$ T cells that were activated with *Actinobacillus actinomycetemcomitans* antigens promoted bone loss in periodontitis (145), demonstrating a different response between naïve vs activated $CD4^+$ T cells. Intermittent PTH treatment did not improve bone architecture in T cell deficient mice reconstituted with $CD4^+$ T

cells, suggesting that these cells are not regulated by iPTH treatment (144). *In vitro*, $CD4^+$ T cells can regulate osteoclast differentiation. Depletion of $CD4^+$ T cells (*in vivo*), significantly increased the number of osteoclasts formed (*in vitro*) after stimulation with 1,25-$(OH)_2D_3$ (146). Subsets of $CD4^+$ T cells (Th1, Th2, and Th17) can also regulate bone density through the secretion of cytokines such as TNF-α, IFNγ, and IL-10.

1.4.1.1.2 CD 8^+ T cells

In vitro, $CD8^+$ T cell prevents osteoclastogenesis. Co-culture of osteoclast precursors with activated $CD8^+$ T cells in the presence of macrophage colony-stimulating factor (M-CSF) and RANKL prevent osteoclast differentiation (147). Depletion of bone marrow $CD8^+$ T cells significantly increased the number of osteoclasts formed in bone marrow cell cultures stimulated with 1,25-$(OH)_2D_3$ for 7 days (146). $CD8^+$ T cells can also regulate osteoblasts via increasing Wnt signaling. Treatment of mice with intermittent PTH was found to increase the production of Wnt10b by bone marrow $CD8^+$T cells, which stimulates bone formation by activating Wnt signaling in osteoblasts (144). Indeed, Wnt signaling in pre-osteoblasts was diminished in T cell null mice and T cell null mice failed to increase total body and femoral bone density after intermittent PTH administration. However incorporation of $CD8^+$ T cells prevented this effect (144), suggesting that the beneficial effect of intermittent PTH treatment on osteoblasts is mediated by $CD8^+$ T cell stimulation of Wnt10b. In summary, $CD8^+$ T cells benefit the bone by inducing osteoblast differentiation and preventing osteoclastogenesis.

One subset of $CD8^+$ T cells are the $CD8^+$ Treg cells. These cells express CD25 and the transcription factor FoxP3 and similar to $CD8^+$ T cells, $Foxp3^+$ $CD8^+$ Treg can also suppress bone resorption induced by osteoclasts (148). In estrogen depleted conditions (OVX), $Foxp3^+$ $CD8^+$ Tregs transferred into two weeks post-OVX mice prevented bone resorption and limited bone loss (149).

1.4.1.1.3 T regulatory cells

T regulatory cells (Treg) play a crucial role in suppressing the immune response in various immune conditions. Treg cells form when naive $CD4^+$ cells are exposed to antigen in the presence of TGF-β. They express the transcription factor Foxp3, which is essential for Treg development. Treg can modulate the bone remodeling process, specifically osteoclast activity, via two mechanisms. First, Tregs inhibit osteoclast differentiation from peripheral blood mononuclear cells through the secretion of cytokines including TGFβ and IL-4 (150). Second, Treg regulates osteoclast differentiation via direct cell-to-cell contact through cytotoxic T-lymphocyte antigen 4 (CTLA-4). CTLA-4 is expressed on Treg and inhibits osteoclast formation. Co-culture of bone marrow derived monocyte cells with activated Tregs inhibited osteoclast formation and bone resorption, an effect that was prevented when cell-to-cell contact was inhibited (151), suggesting a direct role of CTLA-4 in Treg effect on monocytes. Indeed, treatment of osteoclast precursor cells with CTLA-4 suppresses osteoclast formation in a dose dependent manner (151). In a collagen-induced arthritis model, transfer of activated Treg reduced the differentiation of splenocytes into osteoclasts and increased the expression of IL-10, which can further prevent osteoclast differentiation (152). Bone marrow transferred from Foxp3-transgenic (Foxp3tg) mice fully protected wild type mice from local bone erosion in a model of TNF-mediated arthritis. The bone protective effect by Treg cells was associated with reduced osteoclast numbers and bone resorption (153). In conclusion, Treg can benefit the bone through the secretion of cytokines and via direct interaction with osteoclast precursor cells.

1.4.1.1.4 Gamma delta T cells

The vast majority of T cells express the αβ subunits and only 1-10% of the human peripheral circulating T cells are γδ T cells (154). γδ T cells are mostly present in the columnar epithelium of the crypts in the intestine (154). Despite the well-known role of these cells in the

immune response, their role in bone biology is not completely known and needs to be studied further. One study demonstrated that anti- CD3/CD28-stimulated γδ T cells can inhibit osteoclast differentiation and resorptive activity *in vitro* via decreasing IL-17 levels (155). This effect was further supported by another study that showed inhibition of osteoclastogenesis by activated γδ T cells but not freshly isolated γδ T cells. Indeed, freshly isolated γδ T cells enhanced osteoclast generation and function (156). Other studies have also shown activation of γδ T cells by several drugs used to regulate bone density such as bisphosphonates (157), but the role of γδ T cells on bone health during this drug treatment is not entirely understood.

1.4.1.2 B lymphocytes and bone regulation

B cells differentiate from lymphoid progenitors and together with T cells, play an important role in the adaptive immune response. Like T cells, B cells can also influence the bone through the production of factors that are important for bone maintenance such as osteoprotegerin (OPG) and receptor activator of nuclear factor kappa-B ligand (RANKL). OPG inhibits bone resorption via interacting with RANKL and preventing it from interacting with RANK in the osteoclasts. This interaction prevents osteoclast activation and differentiation. B cells have been demonstrated to be responsible for around 64% of total bone marrow OPG production, with 45% derived from mature B cells. B-cell knockout mice present a bone phenotype that is characterized by deficiency in bone marrow OPG production, stimulation of bone resorption via an increase in osteoclast activation, and lower total body bone mineral density (132).

B cells have also been reported to have the ability to enhance osteoclastogenesis via the production of RANKL. Resting B cells are not known to produce high amounts of RANKL. However, activation of B cells with either IL-2 or IFN-γ can produce RANKL and induce osteoclast differentiation *in vitro* (158,159). B cells can also inhibit osteoclast formation indirectly via the secretion of TGFβ, a factor that induces osteoclast apoptosis (160).

In addition to the homeostatic role of B cell in bone health, these cells have also been shown to be involved in the regulation of bone density in several disease models. For example, in two mouse models of rheumatoid arthritis (RA): collagen- induced arthritis and the TNF-transgenic mice, bone marrow B lymphocytes prevented bone formation by inhibiting osteoblast differentiation (133). In addition, B cells isolated from peripheral blood from RA patients inhibited human mesenchymal stem cell (hMSC) differentiation into osteoblasts. B cells significantly inhibited osteoblast differentiation by reducing expression of RUNX2, a key transcription factor associated with osteoblast differentiation (133). HIV infection is also associated with low bone mass. In the HIV transgenic rat model, upregulation of RANKL by B cells, together with a decrease in OPG, was associated with bone loss seen in the HIV group (161,162). In estrogen depleted conditions, B cell-specific RANKL deficient mice were partially protected against ovariectomy-induced trabecular bone loss (163). In addition, B cells isolated from the bone marrow of early postmenopausal women express high levels of RANKL (164), suggesting that high levels of RANKL expressed by B cells contribute to bone loss. Together, these results highlight the important role of B cells in the regulation of bone density in physiological and pathophysiological conditions.

1.4.2 Innate immune regulation of bone

Cells of the innate immune system (especially neutrophils, macrophages and dendritic cells) can also regulate bone density.

1.4.2.1 Neutrophils

Neutrophils are the most abundant type of granulocytes and they play an essential role in the immune system. They differentiate from stem cells in the bone marrow. The role of neutrophils in the regulation of bone density is not completely understood, however it has been suggested that they can act on both osteoclasts and osteoblasts. In patients with rheumatoid arthritis (165) and

after *ex vivo* LPS stimulation (166), neutrophils express high levels of RANKL. Expression of membrane bound RANKL in neutrophils suggests that these cells can regulate bone resorption through neutrophil-osteoclast interaction (166). Indeed, coculture of LPS-stimulated neutrophils with human monocyte-derived osteoclasts and Raw 264.7 cells stimulated osteoclast activity and bone resorption (166). On the contrary, supernatant from LPS stimulated neutrophils did not have an osteoclastogenic effect, demonstrating that neutrophils do not express soluble RANKL and its effects on osteoclasts is mediated through cell to cell contact (166). Neutrophils can also affect osteoblast function by changing their morphology and preventing their interaction with the bone matrix. The effect of neutrophils on osteoblast is also mediated through cell to cell contact and results in decreased bone formation and increased bone resorption (167).

1.4.2.2 Macrophages

Macrophages play a crucial role in bone density as they share the same precursor cells with osteoclasts and can also differentiate into osteoclasts (168). There are three known distinct macrophage populations in the bone and bone marrow: bone marrow macrophages (erythroid island macrophages and hematopoietic stem cell macrophages), osteoclasts, and osteal macrophages or osteomacs. Erythroid island macrophages and hematopoietic stem cell macrophages are important in erythroid maturation and they can influence the hematopoietic stem cell niches (169). Osteomacs are bone tissue specific macrophages that constitute about one sixth of the total cells within the osteal tissue (170). Osteomacs are distinguishable from osteoclasts by the expression of the murine macrophage marker F4/80 and the absence of TRAP, a marker of osteoclast (171). They can be near osteoblasts and can support osteoblast function. Indeed, depletion of osteomacs from calvarial cultures significantly decreased osteocalcin mRNA and osteoblast mineralization *in vitro* (171). In human bone marrow-derived mesenchymal stem cells (MSCs) osteomacs induced MSCs differentiation into osteoblasts (172). Depletion of

osteomacs/macrophages (either using the Mafia transgenic mouse model or clodronate liposome delivery) in the mouse tibial injury model resulted in suppression of new bone formation and demonstrated that osteomacs are required for deposition of collagen type 1 matrix and bone mineralization (173). Human and murine macrophages also produce bone morphogenetic proteins 2 and 6 (BMPs), which increased osteoblast differentiation. Treatment of macrophages with anti-BMP-2 prevented the pro-osteogenic effects (174). These data suggest that contrary to osteoclasts, macrophages and bone specific macrophages are beneficial to the bone. However, macrophages are known to be an important source of pro-inflammatory cytokines such as IL-1β, IL-6, and TNF-α, all of which can enhance osteoclast differentiation and activity and lead to bone loss. Despite these findings, the exact role of macrophages in osteoporosis is still not completely understood.

1.4.2.3 Dendritic cells

Under steady-state conditions, dendritic cells do not seem to play a role in bone remodeling (175). However, under conditions where high levels of pro-inflammatory cytokines are expressed, dendritic cells can indirectly regulate bone density by activating T cells or through the secretion of cytokines such as TNFα, TGFβ, and IL-10 (175). Both osteoclasts and dendritic cells are derived from monocyte/macrophage precursor cells and in the presence of MCSF and RANKL myeloid dendritic cells of human peripheral blood can transdifferentiate into functional osteoclasts (176). In a model of osteolysis, dendritic cells were recruited to the site of bone resorption and they express high levels of cathepsin K (marker of osteoclast and bone resorption) and enhanced bone resorption (177). In rheumatoid arthritis, dendritic cells can serve as osteoclast precursors and therefore contribute to bone loss (176). In general, these data suggest that under pro-inflammatory conditions dendritic cells regulate osteoclastogenesis and bone loss.

1.4.3 Regulation of bone remodeling by cytokines

Bone remodeling is also regulated by pro and anti-inflammatory cytokines. These cytokines interact with both osteoblasts and osteoclasts. Some of the cytokines that are known to regulate bone density are tumor necrosis factor alpha, interferon-γ, interleukin 10, interleukin 6, interleukin 4, interleukin 17A, and transforming growth factor beta.

1.4.3.1 Tumor necrosis alpha

Macrophages are the major producers of tumor necrosis alpha (TNFα), although TNFα can also be produced by activated lymphocytes, natural killer cells, neutrophils, astrocytes, and adipose tissue (178). TNFα is a major pro-inflammatory cytokine involved in the inflammatory response through the regulation of cell functions such as cell proliferation, survival, differentiation, and apoptosis (178). The effects of TNFα on bone density are well described. TNFα can act on both osteoclasts and osteoblasts. TNFα upregulates the expression of RANKL and MCSF and therefore increase osteoclast differentiation (134,135). High levels of TNFα during menopause have been associated with bone loss (87) and TNF-α knockout mice are protected against ovariectomized (OVX) induced bone loss (179). Accordingly, treatment with a TNF binding protein inhibitor prevents bone loss in OVX mice (180). Inhibition of TNFα also prevents periodontal bone loss induced by diabetes (128). *In vitro*, TNFα promotes osteoclast differentiation (134,181), prevents osteoblast differentiation (182,183), and increase osteoblast apoptosis (184). Conversely, low levels of TNFα can induce osteogenic differentiation from MSCs via upregulation of the transcription factors osterix and RUNX2 (185), which suggests that low levels of TNFα can be beneficial to the bone, however more studies are needed to understand this effect. In general, TNFα has detrimental effects on bone density by promoting and increasing osteoclast differentiation, and by preventing osteoblast differentiation and enhancing osteoblast death.

1.4.3.2 Interferon gamma

Interferon-γ (IFN-γ) is a pro-inflammatory cytokine that plays a crucial role in the innate and adaptive immune response. IFN-γ is produced predominantly by natural killer cells, natural killer T cells, and by Th1 $CD4^+$ T cells and CD8 cytotoxic T lymphocytes once antigen-specific immunity develops (186). Unlike TNF-α, the effect of IFN-γ on bone density is more variable. *In vitro*, IFN-γ inhibited osteoclastogenesis (136) and prevented the effects of 1,25-dihydroxyvitamin D3, PTH, and IL-1 on stimulation of osteoclast formation in human bone marrow cells (187). On the contrary, IFN-γ can stimulate osteoclast resorptive activity by enhancing RANKL and TNFα production by T cells (188). Indeed, treatment of T cell-deficient nude mice with recombinant IFNγ did not affect bone density however, reconstitution of T cells in these animals induced vertebral bone loss (188). In rats, intraperitoneal injections of IFN-γ induced osteopenia via decreasing bone formation rate (189). In humans with osteopetrosis (dense bones), administration of IFNγ three times a week for six months stimulated bone resorption and significantly decreased trabecular bone volume (190). These results demonstrate the complexity of IFNγ effects on bone density.

1.4.3.3 Interleukin 10

IL-10 is an anti-inflammatory cytokine that inhibits the activity of Th1 cells, natural killer cells, and macrophages, all of which enhance the inflammatory response and contribute to tissue damage. Many different cell types such as macrophages, dendritic cells and activated T and B cells can produce IL-10 (191). Besides its anti-inflammatory role, IL-10 can also regulate bone density. Studies in IL-10 deficient mice have demonstrated accelerated alveolar bone loss, decreased trabecular number, and cortical bone area when compared to wild type controls (137–139). IL-10 deficient mice also have lower expression of osteoblast and osteocyte markers in the periodontal tissue (138). *In vitro*, IL-10 prevents RAW264.7 cells and mouse bone marrow cells differentiation

into osteoclasts via suppressing c-Fos and c-Jun (192,193). IL-10 can also modulate osteoclast formation by increasing OPG and decreasing RANKL gene expression in dental follicle cells (194). Our studies also add to the current knowledge about IL-10 effects on bone density by demonstrating its role in type 1 diabetes and bone loss *in vitro* and *in vivo* (see chapter 2).

1.4.3.4 Interleukin 6

Interleukin 6 (IL-6) can be secreted by many cells including macrophages, T and B lymphocytes, monocytes, fibroblasts, endothelial cells, and mesangial cells (195). The role of IL-6 in bone remodeling is variable with studies showing stimulation of bone resorption, inhibition of osteoclast differentiation or no changes on bone density. This variability can be attributed to the differing effects that IL-6 has in different models. For example, under healthy conditions, IL-6 deficient mice show no bone phenotype when compared to control mice (179), however, overexpression of circulating IL-6 in growing prepubertal mice resulted in lower trabecular and cortical bone volume due to an increase in osteoclast activity and decrease in osteoblast numbers (196). In both the glucocorticoid and OVX - induced osteoporosis model, administration of IL-6 neutralizing antibody prevented bone loss (179,197,198). IL-6 and its soluble receptor (IL-6sR) can also indirectly control osteoblast proliferation and/or differentiation by stimulation of local factors such as IGF-1(199) and BMP-6 (200). Together with the osteogenic protein 1, IL-6 and IL-6sR enhanced alkaline phosphatase activity in primary culture of rat osteoblasts (200). In conclusion, IL-6 effects on bone density are variable and more studies are needed to completely understand it is role in different bone conditions.

1.4.3.5 Interleukin 4

Interleukin 4 (IL-4) is a cytokine produced by $CD4^+$ T cells, mast cells and basophils. IL-4 acts on a variety of cells including bone cells. *In vitro*, IL-4 inhibited bone marrow osteoclast precursor cell differentiation (201). In rheumatoid arthritis, IL-4 inhibited bone resorption by

inhibiting osteoclasts differentiation and activity (202). In contrast, overproduction of IL-4 in T cells in mice leads to trabecular and cortical bone loss (203). On the murine osteoblastic cell line MC3T3-E1, IL-4 together with IL-3 stimulated osteoblast proliferation but inhibited cell differentiation (204).

1.4.3.6 Interleukin 17A

TGFβ and IL-6 are responsible for the differentiation of T cells into Th17. Th17 are the primary producers of interleukin 17A (IL-17A), in addition, other cells such as $CD8^+$ T cells, natural killer, and γδ T cells can also secrete IL-17A (205). IL-17A has numerous immune regulatory properties such as stimulation of chemokines and matrix metalloproteinases release and activation of neutrophils. In addition to these functions, IL-17A can also regulate bone cells. *In vivo*, IL-17A deficient mice show no bone phenotype. Trabecular bone and serum osteoclast and osteoblast markers in the IL-17A deficient group were not different from the wild type mice. However, *in vitro* IL-17A can act on both osteoblasts and osteoclasts. In humans peripheral blood monocytes IL-17A enhanced osteoclast differentiation, activation, and bone resorption (206). In primary calvarial osteoblasts, IL-17A inhibited the expression of alkaline phosphatase, RUNX2, and osteocalcin (207), suggesting a negative role of IL-17A on bone formation. Indirectly, IL-17A regulates bone density by recruiting and activating immune cells that can enhance the secretion of cytokines such as TNFα and RANKL (208).

1.4.3.7 Transforming growth factor beta

TGFβ can be secreted by a variety of cells such as Treg, macrophages, and osteoblasts. TGFβ induces regulatory T cells, and in the presence of IL-6 promotes Th17 differentiation. In humans, three isoforms of TGF-β have been described, TGF-β1, TGF-β2 and TGF-β3. In the bone, TGFβ has been shown to regulate both osteoblasts and osteoclasts. In osteoclast precursor cells TGFβ can have both positive and negative effects on osteoclast differentiation. *In vitro*, TGFβ

induces osteoclast formation (209) and osteoclast apoptosis (210), suggesting that it acts via more than one mechanism. In cell culture of osteoblasts, TGFβ strongly decreases RANKL (209), suppresses osteoblast differentiation (211), prevents osteoblast apoptosis (212), and induces osteoblast proliferation (213). *In vivo*, the role of TGFβ on bone density seems to be positive. In the TGF-β1 knockout mice, alkaline phosphatase activity, collagen maturity, bone mineral content and bone mineral density decreased significantly when compared to the wild type (214,215). TGF-β2 knockout mice also present bone development abnormalities such as a decrease in bone size (216).

1.5 Gut and bone axis

This section is an edited version of the review article that was published in Understanding the Gut-Bone Signaling Axis; Chapter: Epithelial Barrier Function in Gut-Bone Signaling

Authors**: Naiomy Deliz Rios-Arce**, Fraser L. Collins, Jonathan D. Schepper, Michael D. Steury, Sandi Raehtz, Heather Mallin, Danny T. Schoenherr, Narayanan Parameswaran, and Laura R. McCabe

The gastrointestinal (GI) epithelium play an essential role in maintaining host health through its ability to digest and absorb nutrients. At the same time, it is essential for providing a selective barrier that prevents translocation of harmful substances as well as pathogens and their products from the external environment to the blood stream. The intestinal epithelium is composed of a continuous single layer of intestinal epithelial cells (IECs) that are sealed together by tight junction (TJ) proteins (Figure 1.6). This epithelial layer allows the movement of materials from the mucosal side of the epithelium to the serosal side via transcellular and paracellular pathways. A mucus layer, secreted by specialized epithelial cells (goblet cells), is located on the surface of the epithelium and is important for limiting the ability of gut bacteria and pathogens to access host cells. The lumen of the GI tract also harbors a variety of commensal microorganisms referred to as the gut microbiota which accounts for 90% of the cells in the human body, approximately 10^{14} bacteria total, in which the colon usually has the highest content with approximately 10^{11} CFU/ml (217). The intestine also secretes immunoglobulins, defensins, and other antimicrobial products that contribute to maintaining a healthy environment. Beneath the epithelial layer is the lamina propria which contains immune cells, fibroblasts and plasma cells.

Disruption of the epithelial barrier can 1) affect efficient nutrient absorption, 2) facilitate pathogen translocation into the bloodstream and cause systemic inflammation, and 3) alter gut microbiota composition (218). As a consequence, barrier disruption can trigger the development

of GI diseases such as IBD, celiac disease, and colon cancer (219–222). Other systemic and metabolic diseases such as type I diabetes can also be influenced by barrier changes (223,224). However, whether barrier dysfunction is causal or a consequence of these systemic and metabolic diseases is controversial. Recent studies from our lab and others demonstrate that GI barrier dysregulation can critically affect bone health (225,226). Indeed, in diseases characterized by a malfunction of the GI tract such as in IBD, bone health is significantly affected resulting in bone loss (17).

For many years, the interaction between the gut and the bone has been described. These interactions were mostly attributed to the role of the GI tract in the absorption of minerals such as calcium and phosphorous. However, the gut is also known to secrete endocrine factors that can signal to bone cells. In addition, the integrity of the gut epithelial layer, as well as it is immune response, can affect bone health. More recent studies from our lab and others have also shown a role of the gut microbiota in the regulation of bone density.

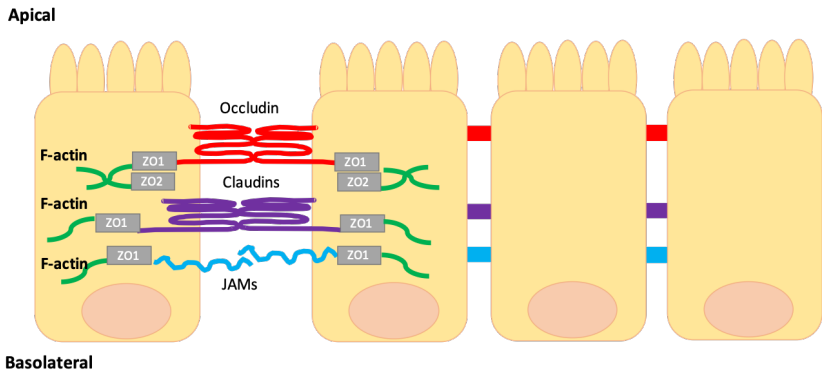

Figure 1.6. Schematic representation of the intestinal tight junction proteins and their location.

Tight junctions are protein complexes that span between epithelial cells to form a tight barrier. They are comprised of transmembrane proteins, such as occludin (red) and claudins (purple), and they are connected to the actin cytoskeleton via a zona occludens (ZO-1 and ZO-2 (gray)). The transmembrane receptor JAM (junctional adhesion molecule (blue)) is also found at tight junction complexes. Abbreviations: JAM junctional adhesion molecule, ZO zona occludens.

1.5.1 Mineral absorption in gut-bone signaling

One well-characterized function of the gut is the absorption of minerals such as calcium and phosphorus. These two minerals are found in the hydroxyapatite in the bones and play a crucial role in bone formation and maintenance. Calcium absorption occurs in the small intestine via two routes: active transport (transcellular) and passive diffusion (paracellular). Transcellular calcium absorption occurs predominantly in the duodenum and is regulated by calcitriol, the active form of vitamin D. The importance of vitamin D in calcium absorption and bone health is emphasized by the consequences of vitamin D deficiency on bone which includes rickets in children and osteomalacia in adults (227). In addition, when the vitamin D receptor is specifically deleted in the intestine, this results in lower intestinal calcium absorption, inhibition of bone mineralization, and an increase in bone fractures (228). Conversely, paracellular calcium absorption is independent of vitamin D and occurs throughout the length of the intestine. Paracellular calcium absorption is a concentration-dependent diffusional process that occurs through the tight junctions and structures within intercellular spaces (229).

1.5.1.1 Hormonal regulation of mineral absorption

There are three well known calcium regulating hormones; parathyroid hormone (PTH), calcitriol, and calcitonin. PTH maintains the levels of calcium in the blood by regulating bone resorption and bone formation. Calcitriol, the active form of vitamin D, increases the level of calcium in the blood by increasing uptake of calcium from the gut into the blood, enhancing reabsorption of calcium by the kidneys, and increasing the release of calcium from the bone. Calcitonin, on the other hand, is secreted when calcium serum levels are high and prevents bone resorption. Calcitonin is produced by the parafollicular cells of the thyroid gland and reduces blood calcium levels by two main mechanisms; 1) prevents the activity of osteoclasts by mediating the loss of the ruffled osteoclast border; and 2) prevents reabsorption of calcium by the kidneys, which

together decreases blood calcium levels. The interaction between these hormones determines calcium levels in the bone and serum. For example, during vitamin D deficiency, circulating PTH increases leading to an increase in the activity of 1α-hydroxylase in the kidney. 1α-hydroxylase then converts vitamin D into calcitriol which them stimulates calcium absorption through its interaction with the vitamin D receptor. Indirectly, PTH can also stimulate calcium release from the bone by acting on osteoblasts and stimulating the release of RANKL which will induce bone degradation via osteoclasts. An uncontrolled increase in RANKL secretion by PTH can lead to osteopenia and osteoporosis. A negative feedback loop then regulates the levels of PTH; when blood calcium levels increase, calcium-sensing receptor in the parathyroid gland slows PTH synthesis and release by inhibiting vesicle fusion and exocytosis. One human study has shown a negative correlation between serum PTH and bone mineral density (BMD) (230). In another study, patients with hyperparathyroidism have the lowest BMD values (231).

Interestingly, low doses of intermittent PTH (iPTH) treatment is associated with bone anabolic effects. iPTH treatment increases BMD and reduces the risk of fracture in post-menopausal women with osteoporosis (232). iPTH treatment increases bone density by promoting osteoblast differentiation. Daily PTH injections in mice with either normal bone mass or osteopenia increased bone formation by increasing the life-span of mature osteoblasts and preventing their apoptosis (233). iPTH can also induce Wnt10b production from bone marrow $CD8^+$ T cells that then activates canonical Wnt signaling in preosteoblasts, activation of the Wnt signaling promotes osteoblast differentiation (144). In T1D, iPTH treatment suppressed osteoblast apoptosis and reversed preexisting bone loss from diabetes (234). Currently, iPTH is the only bone anabolic treatment approved by the Food and Drug Administration to treat osteoporosis. However, the duration of this treatment (teriparatide) is limited to two years due to the development of osteosarcoma (26).

1.5.2 Gut-derived endocrine factors and their effects on bone density regulation

Another mechanism by which the gut regulates the bone is through the secretion of hormones such as serotonin, incretins, and peptide YY.

1.5.2.1 Serotonin as a regulator of bone density

Serotonin (5- hydroxytryptamine; 5-HT) is a neurotransmitter with a variety of physiological roles in the body including modulation of bone density. The vast majority of serotonin (around 95%) is secreted by the enterochromaffin cells in the GI tract and a small fraction is secreted in the brain (235,236). Serotonin can signal via as many as 15 different receptors. Osteoblasts express three serotonin receptors: Htr1b, Htr2a, and Htr2b (237). Interestingly, the effects of serotonin on bone modulation differ depending on whether it is secreted by the brain or by the GI tract (238).

When serotonin is produced in the brain, serotonin promotes bone formation and prevents bone resorption by acting on the Htr2c receptor in the ventromedial hypothalamic (VHM) neurons. This interaction inhibits the synthesis of epinephrine and decreases sympathetic tone. This decrease in sympathetic tone decreases beta 2 adrenergic receptor signaling in osteoblasts; beta 2 adrenergic receptors are known to decrease osteoblast proliferation, and to increase bone resorption. Therefore, inhibition of the sympathetic activity by brain-derived serotonin increases bone formation and decreases bone resorption (238).

When serotonin is produced peripherally, it inhibits bone formation by binding to the Htr1b receptor on the osteoblasts and decreases osteoblast proliferation. The role of gut-produced serotonin was first described in low-density lipoprotein receptor (Lrp5) family 5 knockout mice. Lrp5 inhibits the expression of tryptophan hydroxylase (Tph1), which is the rate limiting enzyme in the synthesis of serotonin, in the duodenum, in turn decreasing serotonin biosynthesis. In the absence of Lrp5, serotonin levels are high and there is a decrease in osteoblast differentiation and

bone density (237,239). In contrast, Tph1 deficient mice, which have decreased serotonin levels, have increased bone mineral density (240). In both the Lrp5-knockout and Tph1-knockout mice, changes in bone density are attributed to changes in osteoblast proliferation with no changes in osteoclasts. In addition, an association between the use of selective serotonin reuptake inhibitors (SSRIs), an increase in bone fracture, and a decrease in bone density in humans has been shown (241,242). One meta-analysis found that consumption of SSRIs increases the fracture risk by 70% (243). In another study, the risk of hip fracture was elevated in Australian people, over the age of 65, that were taking SSRIs (244). In older women, over the age of 65, the use of SSRIs was associated with a higher risk of any non-spine fracture (245). These studies demonstrate that elevated serotonin levels can lead to bone loss.

Another cell type that has recently been discovered to secrete serotonin is the osteoclast. One study found that in the presence of RANKL, osteoclast precursors can express Tph1 and synthesize serotonin. They also show a decrease in osteoclastogenesis in Tph1 knockout mice (246). However, the role of serotonin release from osteoclasts and its effects on bone density needs further study. Taken together, these studies suggest that secretion of serotonin from the gut or the brain can have different and opposite effects on the bone.

1.5.2.2 Incretins and bone

Incretins are a group of metabolic intestinal peptide hormones that are secreted in response to food ingestion. The most widely recognized incretins are gastric inhibitory polypeptide (also known as glucose-dependent insulinotropic polypeptide or GIP) and glucagon- like peptides-1 and 2 (GLP-1, GLP2). GIP is secreted by the “K-cells” from the mucosa of the small intestine (duodenum and jejunum), while GLP-1 and GLP-2 are secreted by the “L-cells” located in the distal jejunum, ileum, and colon (247,248). These incretins act on the pancreas to regulate blood glucose by modifying the release of insulin.

In addition to its role in the secretion of insulin, GIP can also stimulate glucagon release and it can prevent pancreatic beta cell apoptosis. GIP receptors (GIPR) are widely expressed throughout the intestine and many other organs, and therefore, GIP can have a variety of effects. In the bone, GIPR is expressed in both osteoblasts and osteoclasts (249). *In* vitro, treatment of osteoblasts with GIP results in elevated expression of collagen type I messenger RNA as well as an increase in alkaline phosphatase activity, suggesting an increase in osteoblast activity (249). *In vivo*, the role of GIP on bone density is controversial. In one study, GIPR-deficient mice were found to have a significant increase in trabecular bone mineral density (250), while in a similar study GIPR-deficient mice had lower cortical thickness and higher osteoclast number (251). On the contrary, overexpression of GIP in mice resulted in higher trabecular bone mass, serum osteocalcin, and increased bone formation (252). In euglycemic humans, GIP infusion (4 pmol/kg/min for 15 min, followed by 2 pmol/kg/min for 45 min) decreases c-terminal telopeptide of type I collagen, a marker of bone resorption, in the serum (253), suggesting that GIP can prevent bone resorption.

Similar to GIP, GLP-1 and GLP-2 are released in response to food intake and they regulate blood glucose by the stimulation of insulin release. Both types of GLP work through their receptors (GLP-1R and GLP-2R) which are also widely expressed in many organs, but unlike GIP, in the bone GLP-1R and GLP-2R are only expressed in immature osteoblasts (254). The role of GLP-1 in bone was first demonstrated in GLP-1 receptor knockout mice. In this model, absence of GLP-1R led to a decrease in cortical bone mineral density, and an increase in bone fragility, bone resorption, and osteoclast cell numbers (255,256). However, this effect was only seen in the cortical bone and not in the trabecular bone. In a different study, administration of GLP-1 for 3 consecutive days into STZ diabetic rats reversed hyperglycemia and up-regulated the expression of bone formation markers such as osteocalcin (257).

The role of GLP-2 on bone density has also been studied in postmenopausal women. A single dose of GLP2 in postmenopausal women significantly reduced markers of bone resorption in the serum, with a slightly increase in bone formation markers (258). Treatment with GLP-2 for four months in postmenopausal women resulted in a significant increase in total hip bone mineral density (259). Incretins can also indirectly regulate bone density by the regulation of insulin and insulin like growth factor (IGF-1) (Section 1.3.4.3). Together these studies demonstrate the role of incretins in the regulation of bone density.

1.5.2.3 Peptide YY effects on bone

Peptide YY (PYY), a gut-derived satiety peptide of the neuropeptide Y family, is secreted by the endocrine L cells from the ileum and colon in response to feeding (260). This peptide binds with high affinity to receptors of the Y-receptor family Y1, Y2 and Y5 (261). Whereas Y1 and Y5 receptors are shown to be involved in controlling feeding behavior (262), Y2 receptors have been shown to be involved in bone mineral density (BMD) regulation. Y2 receptor deficient mice present a two fold increase in trabecular bone volume, number, and thickness in response to an increase in osteoblast activity, bone mineralization, and formation (263). Both male and female PYY knockout mice present a significant increase in lumbar BMD, content, and femoral cancellous bone volume. Opposite results were seen in a different study in which PYY deficient mice presented a reduction in trabecular bone mass and bone strength (264). The discrepancy in results between these studies may be related to the different design of the targeting vector, variations in the genetic background, as well as the age at which the bone analysis was performed (6-9 months vs 3-4 months) (265). However, in women with anorexia nervosa, elevated levels of PYY were strongly associated with lower BMD in the spine (266). These results suggest that elevated levels of PYY can be detrimental to the bone, however more studies are required to further understand it is effects on bone density.

1.5.3 Regulation of bone density by gut microbiota

The human gastrointestinal (GI) tract harbors a complex and dynamic population of microorganisms which includes bacteria, fungi and viruses. The intestinal microbiota is acquired at birth and evolves from low complexity into a highly diverse population. Fungi are generally considered to be a relatively minor component of the gut microbiota, accounting for approximately 0.1% of the microbes, while bacteria account for 99% (267). The human intestinal microbiota comprises about 1200 bacterial species, in which the main phyla represented are Bacteroidetes, Firmicutes, Actinobacteria, Proteobacteria, and Verrucomicrobia (268). A number of factors can alter intestinal microbial composition. These include medications such as antibiotics, psychological and physical stress, radiation, altered peristalsis and dietary changes (269–273). This can lead to alterations in bacterial metabolism as well as overgrowth of potential pathogenic bacteria (274). Changes to the gut microbiota during dysbiosis have now been linked to a myriad of diseases such as IBD, irritable bowel syndrome (IBS), obesity and rheumatoid arthritis (275–278). Importantly, dysbiosis can also lead to disruption of epithelial barrier leading to unwanted consequences (279) (Figure 1.7).

Altered gut microbiota can signal through pattern recognition receptors on gut epithelial cells, activating the NF-κB pathway and leading to changes in gut homeostasis (280). Epithelial cell NF-κB activation increases pro-inflammatory cytokines such as TNFα, IL-1, and INFγ (281). An increase in gut INFγ and TNFα protein levels have been shown to increase intestinal permeability (282,283). This altered protein composition decreases barrier properties and leads to leaky gut properties. The exact mechanism behind these effects is not well characterized (20). Dysbiosis has also been linked to increase in IL-1β, which has also been shown to increase permeability by decreasing TJ protein occludin expression (284).

Additionally, dysbiosis of the gut microbiota also influences other adaptations such as mucin production which in turn influences gut barrier function. Intestinal mucins can inhibit bacterial adhesion to the intestinal epithelial cells, limiting immune responses and maintaining barrier function. The commensal microbiota has been shown to regulate production of intestinal mucins (285). The abundance of mucolytic bacterium, which has the ability to degrade mucins, has been shown to increase 100 fold during dysbiosis observed in IBD (286). In addition, under dysbiosis pathogens can secrete proteases that have been shown to cleave MUC2, the main mucin-component, thereby decreasing mucin levels (287). Decreases in the mucin layers have been shown to compromise the intestinal barrier function leading to increases in intestinal permeability and microbe penetration (288). All of the effects of dysbiosis on the gut barrier function can also lead to systemic changes in the body including bone loss (289–291).

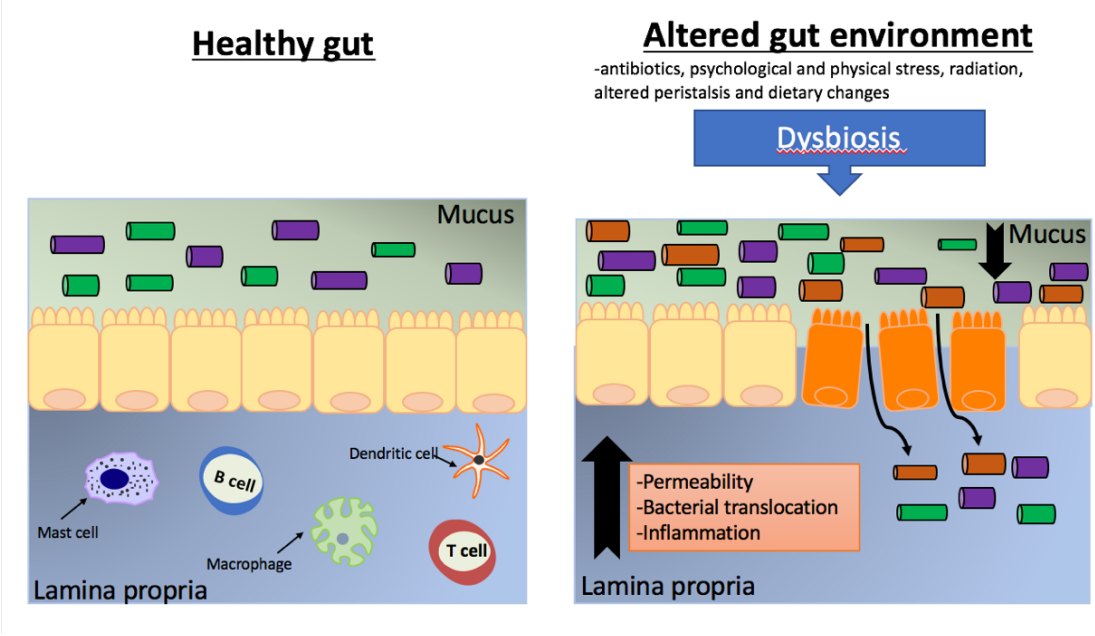

Figure 1.7. Schematic representation of the gut epithelial layer in healthy gut vs dysbiosis. In the normal state, the mucus layer prevents the interaction between the gut microbiota and the intestinal epithelial barrier. Underneath the epithelial layer is the lamina propria. The lamina propria is composed of connective tissue and cells of the innate and adaptive immune system: mast cells, macrophages, dendritic cells, and lymphocytes (T and B). The composition of the intestinal epithelial layer can be influenced by many factors including antibiotic treatment, psychological and physical stress, radiation, age, and diet. This can lead to alterations in bacterial metabolism as well as overgrowth of potential pathogenic bacteria (dysbiosis). This dysbiosis is associated with increased levels of permeability, bacterial translocation and inflammation.

1.5.3.1 Models to study the role of gut microbiota on bone density

Several approaches are used to study the role of gut microbiota on bone density. The most direct approach is germ-free (GF) mice which are devoid of microorganisms. Another approach involves the use of antibiotics to deplete the gut microbiota.

1.5.3.1.1 Gut microbiota effects on bone density in germ free mice

One of the first studies that demonstrates the role of the gut microbiota on bone density used GF mice. In this study, GF female mice had higher femoral trabecular and cortical bone when compared to conventional raised (CONV-R) mice (291). However, a later study found no changes in femoral trabecular bone volume between GF and CONV-R female mice (225). To further understand the role of gut microbiota on bone density, GF mice were colonized with conventional specific pathogen-free (SPF) gut microbiota. Colonization of GF mice with SPF for one month induced bone loss, while colonization for eight months increased bone density in female mice, but no changes were seen in male mice (289). In a different study, colonization of GF mice with SPF decreased bone mineral density, bone formation, and mineral apposition rate (292). Our lab has shown that reconstitution of the gut microbiota in GF mice with human microbiota samples from different donors does not alter bone density (293), demonstrating that the effects of gut microbiota on bone density in GF mice are variable. This variation in results can be attributed to the differences in gut microbiota samples used, age, sex, and strain of the mice. In addition, one downside of using GF mice is the developmental defects that they present. Since GF mice lack intestinal microbiota, they can't develop a normal immune system. Indeed, GF mice present extensive deficits in the development of the gut associated lymphoid tissue (GALT). GF mice have lower $CD4^+$ T cells in the lamina propria, smaller Peyer's patches and less germinal centres (294). In the bone, GF mice express lower levels of TNFα and RANKL (295). In summary, studies done in GF mice should be interpreted carefully due to the role that the immune system can play in the

bone. In Chapters 3 and 4 we demonstrate the importance of T and B lymphocytes in gut microbiota effects on bone density.

1.5.3.1.2 Depletion of the gut microbiota by antibiotic treatment and its effects on bone density.

Another approach to study the role of the gut microbiota on bone density is by using antibiotics. Antibiotics are antimicrobial agents that are used to kill bacteria. By using this technique, researchers study the role of gut bacteria in the host by 1) using broad-spectrum antibiotics to deplete the intestinal microbiota. 2) targeting specific bacteria population such as gram-positive or negative bacteria through the use of specific antibiotics. 3) induce gut microbiota dysbiosis. Interestingly, not only can antibiotics influence gut microbiota, but they can also influence bone homeostasis.

Several studies have shown the effect that chronic antibiotic use can have on the bone. For example, early life (at weaning) exposure to subtherapeutic antibiotic treatment (penicillin, vancomycin, penicillin plus vancomycin, chlortetracycline, or all together) for three weeks significantly increased bone mineral density in female C57BL/6J mice, an effect that did not persist after 7 weeks of treatment (296). However, low doses of penicillin at weaning for 20 weeks increased bone mineral density and bone mineral content in female mice (297). Treatment of 2-month old female BALB/c mice with a broad-spectrum antibiotic cocktail (ampicillin, vancomycin, metronidazole, and neomycin) or just vancomycin for one month increased bone mineral density with no changes in serum osteoclasts or osteoblasts markers (289). Female C57BL/6J mice that received three short courses of therapeutic-dose amoxicillin and tylosin, to mimic pediatric antibiotic use, presented larger bones than the control group one month after treatment. Increase in bone area and mineral content were most pronounced in the amoxicillin treated group than in the tylosin (298). These results suggest that early in life exposure to antibiotic

and chronic antibiotic treatment in female mice can modulate the bone. However, this effect does not always persist over time and it can depend on the type of antibiotics used and the duration of the treatment.

In male mice, chronic antibiotics also affect bone density but is also variable. Continuous low dose of penicillin from birth or weaning for 20 weeks decreased total body bone mineral content significantly when compared to non-treated mice (297). Chronic antibiotic treatment (ampicillin and neomycin) from weaning until 16 weeks of age, decreased femoral cortical area and thickness (299). Interestingly, all of these studies were focused on the effect that chronic antibiotic use can have on the bone. Conversely, our lab has shown the effect that 4-weeks post-antibiotic treatment have on the femoral and vertebral bones. In this study, twelve-week-old BALB/c male mice were treated with ampicillin and neomycin in the drinking water for two weeks. Depletion of the microbiota for two weeks did not affect femoral trabecular bone volume fraction. However, 4-weeks post-antibiotic induced gut microbiota dysbiosis and bone loss. Bone loss in the post-antibiotic group was associated with a significant decrease in femoral and vertebral trabecular thickness and an increase in trabecular spacing. In addition, osteoclast number, and serum levels of TRAP5b were increased in the post-antibiotic treated group, while serum osteocalcin, mineral apposition rate and bone formation rate were decreased. These data indicate that though microbiome depletion for 2 weeks does not affect bone volume, repopulation of the gut microbiota after antibiotic treatment can have detrimental effects on the bone (300). Together these studies demonstrate that antibiotics can be useful to study the contribution of the gut microbiota on bone density. However, one caveat of this approach is the effect that the antibiotics can directly have on the bone (301). Therefore, the use of antibiotics that are poorly absorbed in the gut should be considered.

1.5.3.2.1 Probiotic as a treatment to prevent bone loss

Probiotics are living microorganisms that when administered in adequate amounts confer a health benefit to the host (302). Probiotics effects in the host are strain specific. Therefore, strain identity is important to link a strain of bacteria to a specific health effect as well as to enable accurate epidemiological studies. Many genera of bacteria such as Bifidobacterium, Escherichia, Lactobacillus, Enterococcus and Bacillus have all been used as probiotics (303). Moreover, some yeast strains from the genus Saccharomyces are also commonly used in probiotic products. Probiotic products contain one or more selected microbial strains and are generally consumed as dietary supplements in the form of powder, capsules or tablets. They can also be in dairy products such as yogurt or as inoculants in milk-based foods. More recently, probiotic bacteria have also been added to unconventional products such as toothpaste, ice cream, and beer. Probiotic bacteria can also be found in the mucus membranes of our body. Probiotic consumption can bring numerous benefits to the host. They contribute to the host via improvement of intestinal health, restoration of the gut microbiota after antibiotic treatment, inhibition of pathogenic bacteria, modulation of the immune response, enhancement of vitamins and mineral absorption, and secretion of enzymes (304–306). Recently, probiotic strains have also been shown to be beneficial for bone health in both humans and animal models.

1.5.3.2.1 Probiotic effects on bone density in healthy conditions

The earliest studies demonstrating a beneficial effect of probiotic consumption in bone health came from the poultry industry. The use of probiotics in the poultry industry began when probiotics administration improved egg-shell quality and egg laying performance. Later studies found that treatment of broilers with the probiotics *Bacillus licheniformis* and *Bacillus subtilis* significantly increased tibial thickness (307). Since these findings, many researchers have looked at the role of several probiotic strains in bone health in different animal models as well as in

humans. Treatment with *Bifidobacterium longum* by daily gavage for 28 days in intact male Wistar rats increased femoral fracture strength and calcium content (308). In C57Bl/6 healthy male mice, treatment with the probiotic *Lactobacillus reuteri* 6475 (*L. reuteri*) for four weeks enhanced femoral trabecular bone volume fraction, bone mineral density, number, and thickness. An increase in serum osteocalcin and bone formation rate, with no changes in serum osteoclast markers, were seen in the *L. reuteri* treated group, suggesting that the beneficial effects of this probiotic on bone density are mediated by bone formation. Interestingly, intact C57Bl/6 female mice treated with *L. reuteri* had no changes in either femoral or vertebral trabecular bone density (309). However, in BALB/c female mice with a moderate inflammatory status, induced by dorsal surgical incision, treatment with *L. reuteri* for eight weeks significantly increased femoral trabecular bone volume fraction, numbers, and mineral apposition rate (310), suggesting that this probiotic requires an inflammatory setting to increase bone density. Conversely, treatment of female mice with *Lactobacillus rhamnosus* GG (LGG) twice a week for four weeks increased femoral trabecular bone volume fraction and serum osteocalcin levels (311). Together, these studies demonstrate the beneficial effect that probiotic consumption can have on the bone.

1.5.3.2.2 Probiotic effects on bone density in low estrogen conditions

Not only can probiotics improve bone health in healthy conditions, but they can also prevent bone loss in many conditions that are well known to induce bone loss such as low estrogen. The loss of estrogen due to menopause is the most important risk factor for osteoporosis in women. Therefore, many studies have look at the role of probiotics in preventing bone loss during ovariectomized (OVX) conditions in animals and menopause in women. Supplementation of conventional mice with *Lactobacillus rhamnosus* GG (LGG) or the probiotic supplement VSL#3 for four weeks protected mice against OVX-induced bone loss. Importantly, nonpathogenic bacteria such as Escherichia coli DH5alpha did not provide any protection from bone loss,

suggesting strain specificity. The beneficial effects of LGG and VSL#3 on the bone were accompanied by an increase in serum osteocalcin and a decrease in pro-inflammatory cytokines in the bone marrow (225). In the same OVX model, treatment with *L. reuteri* for four weeks also prevented bone loss, but no changes in osteocalcin levels were noticed. *L. reuteri* beneficial effects on the bone were associated with regulation of bone resorption. *L. reuteri* treated mice had lower serum osteoclast marker and bone marrow cell differentiation towards osteoclasts was decreased in this group (312). A mixture of three different strains of probiotics (*Lactobacillus paracasei* DSM13434, *Lactobacillus plantarum* DSM 15312 and DSM 15313) also protected mice from OVX-induced cortical bone loss and bone resorption (313). OVX- mice treated with this mixture of probiotics for 6 weeks had higher trabecular bone mineral density, trabecular thickness and cortical bone mineral content than the OVX-non-treated group. Serum osteocalcin levels were also higher in the OVX-probiotic treated group (313). In humans, administration of *L. reuteri* for 12 months, to women between the ages 75-80, prevented a decrease in bone mineral density (314). In postmenopausal women (mean age 65, range 50–78) milk fermented with *Lactobacillus helveticus* reduced serum parathyroid hormone and increased serum calcium compared to the control milk, however, no direct bone measurements were done in this study (315). Similarly, probiotic supplementation in osteopenic postmenopausal women with a multispecies probiotic supplement (7 different probiotic strain) decreased serum parathyroid hormone and cross-linked C-telopeptide (a marker of bone resorption) with no changes in bone density. The lack of changes in bone density in this study can be attributed to the short duration of the treatment (6 months) (316). Together these results demonstrate the beneficial effects of probiotics in preventing bone loss in low estrogen conditions.

1.5.3.2.3 Probiotic effects in type 1 diabetes and gut dysbiosis induced bone loss

The beneficial effects of probiotics in inhibiting bone loss is also shown in other animal models (317). In the STZ T1D-induced animal model *L. reuteri* supplementation for four weeks prevented bone loss by increasing mineral apposition rate, serum osteocalcin, osteoblast numbers, and Wnt10b gene expression. *L. reuteri* supplementation also significantly decreased adipocytes number in the bone marrow of T1D mice (83). Interestingly, *L. reuteri* also prevented bone loss induced by gut dysbiosis. This beneficial effect was mediated by an increase in bone mineral apposition rate, bone formation, serum osteocalcin, and a decrease in bone resorption markers in the serum (300). These results demonstrated that the probiotic *L. reuteri* can affect multiple mechanisms of bone remodeling under different pathophysiological conditions.

1. 5.3.3 Mechanisms of gut microbiota regulation of bone density

The mechanisms through which probiotics or modulation of the gut microbiota exert it is effects on bone density has not been fully elucidated and is likely to be a complex communication between the gut microbiota, immune system, gut epithelial barrier, and bone cells. In addition, different probiotic bacterial strains will probably act via distinct and/or overlapping mechanisms. Some of the suggested and better described mechanisms include (1) enhancement of barrier integrity and mineral absorption; (2) modulation of the host immune system; (3) and changes in gut bacteria composition.

1.5.3.3.1 Enhancement of barrier integrity and mineral absorption by gut microbiota and its effects on bone density

The integrity of the gut epithelial layer is crucial to maintain healthy bones. Several studies have shown that an increase in intestinal permeability, in diseases such as IBD, correlates with bone loss (226,318). Therefore, improvement of this barrier by probiotics has been suggested to be one of the mechanisms by which they benefit the bone. How an increase in intestinal

permeability can lead to bone loss? An increase in intestinal permeability will allow bacteria and their molecules to get in contact with the epithelial submucosa, which may initiate aberrant intestinal and systemic pro-inflammatory responses. This increase in pro-inflammatory cytokines can further lead to the secretion of osteoclastogenic cytokines, such as IL-17A and TNF-α that can promote bone resorption and therefore bone loss. Our lab has tested the direct role of intestinal barrier leak and bone loss by using the mucus supplement (MDY). MDY is a non-absorbed, non-metabolized high molecular weight polyethylene glycol that has been shown to benefit the intestinal barrier by increasing mucus production and preventing barrier leaks (unpublished data). We have found that treatment of male mice with MDY for four weeks prevented the post antibiotic-induced increase in intestinal permeability and bone loss, demonstrating the link between intestinal permeability and bone loss (300). Probiotics have also been shown to prevent an increase in intestinal permeability. Administration of the antibiotic ampicillin for 2 weeks in young male mice increased gut permeability and treatment with a probiotic cocktail of four Lactobacillus species (JUP-Y4) for four weeks prevented this effect. JUP-Y4 treatment reduced the levels of D-lactate and endotoxin (markers of intestinal permeability) in the serum and increased the expression of tight-junction proteins. JUP-Y4 treatment also reduced the expression of TNFα, IL-6, and IL-1β in the colon of antibiotic-treated group. Another study from our lab that demonstrates the link between gut permeability and bone loss used the probiotic *L. reuteri*. In this study, mature male mice were treated with an antibiotic mixture for two weeks followed by four weeks of no treatment (repopulation) or treatment with *L. reuteri*. Natural repopulation of the gut microbiota for four weeks increased intestinal permeability and decreased bone density, while treatment with *L. reuteri* completely prevented both effects (300). Treatment with LGG and the probiotic supplement VSL#3 for four weeks also decreased gut permeability and completely protected

against bone loss induced by estrogen depletion (225). Together, these studies demonstrate the link between probiotics regulation of intestinal permeability and bone loss.

Another way that probiotics effects on the intestinal barrier can regulate bone remodeling is via nutrient absorption. Probiotics can produce short-chain fatty acids. Short-chain fatty acids can reduce the intestinal tract pH, subsequently increasing the absorption of minerals. Probiotics such as *Bifidobacterium longum* and *Lactobacillus paracasei* increased calcium content in the bone (308) and prevented urine excretion of calcium induced by ovariectomizing (313). Postmenopausal women treated with *Lactobacillus helveticus* fermented milk had an increase in serum calcium at the same time that they present healthier bones (315). However, calcium changes by probiotic treatment are not always observed. For example, in ovariectomized (OVX) rat the probiotic *Bifidobacterium longum* increased bone mineral density but failed to enhance calcium absorption (308). These results suggest that while calcium plays a crucial role in the regulation of bone density, changes in bone density by probiotics are not always mediated by an increase in calcium absorption and that other mechanisms are involved.

1.5.3.3.2 Modulation of the host immune system by gut microbiota and its effects on bone density

As described in section 1.4, bone density is also regulated by the immune system. Probiotics are well known to regulate the immune system. Indeed, several studies have shown that the beneficial effect of probiotics on bone health is associated with changes in immune cell population and cytokine expression. Supplementation with the probiotic LGG or the probiotic supplement VSL#3 in OVX mice prevented bone loss and reduced the expression of the pro-osteoclastogenic cytokines TNFα, IL-17, and RANKL from the small intestine and bone marrow (225). Furthermore, another study using LGG demonstrated that its beneficial effect on bone density in female mice is mediated via an increase in Treg cells in the bone marrow. LGG treatment

stimulates the production of butyrate. Butyrate is a short chain fatty acid that increases Treg cells in the gut and also in the bone marrow. An increase in Treg cells upregulates the expression of Wnt10b in the bone marrow and promote osteoblast differentiation and bone formation. In the absence of Treg cells, LGG treatment had no effect on bone density (311), demonstrating the important role of these cells on bone density regulation by LGG. *Lactobacillus acidophilus* (LA) also benefits bone density via regulation of Treg-Th17 cell balance. LA inhibits osteoclastogenic Th17 cells and promotes anti-osteoclastogenic Treg cells in bone marrow of OVX mice. In the serum, LA treatment also suppresses the expression of pro-osteoclastogenic cytokines IL-17, TNF-α and RANKL and increases the expression of the anti-osteoclastogenic cytokine IL-10 (319). *L. reuteri* treatment in healthy male mice decreases TNFα levels in the small intestine at the same time that increases bone density (309). Correspondingly, in the absence of estrogen, *L. reuteri* suppressed $CD4^+$ T (which are associated with bone loss) in the bone marrow of OVX mice (312). Interestingly, in the absence of T and B lymphocytes, *L. reuteri* does not enhance bone density, demonstrating that T and B lymphocytes are required for *L. reuteri* beneficial effects on the bone (Chapter 3). In general, regulation of the immune system by different probiotics is one of the mechanisms by which they can benefit the bone.

1.5.3.3.3 Changes in gut microbiota composition and its effects on bone density

The direct contribution of gut microbiota composition on bone density is complicated and more studies are required to further understand this. A recent study demonstrated that LGG treatment benefits the bone via increasing the relative frequency of Clostridia in the gut of female mice. An increase in Clostridia leads to an increase in butyrate secretion and Treg cells in the intestine and in the bone marrow which enhances bone density through the secretion of Wnt10b (311). However, in the same study, the abundance of other bacteria also changed after probiotic treatment, suggesting that other bacteria can also contribute to this effect. A study from our group

shows that gut microbiota repopulation after antibiotic treatment can induce gut microbiota dysbiosis (as indicated by an increase in Firmicutes to Bacteroidetes ratio), enhance intestinal permeability, increase pro-inflammatory cytokines, and decrease bone density. Interestingly, treatment with *L. reuteri* prevented all of these effects and bone loss (300), demonstrating a role of *L. reuteri* in preventing gut microbiota disturbances and bone loss. However how modifications of different microbial communities contribute to regulation of bone density still unknown.

1.6. Summary

Bone remodeling is a highly regulated process and dysregulation of this process can result in low bone density and osteoporosis. Osteoporosis is characterized by an increase in bone fragility and fractures, therefore, proper function of the bone remodeling process is crucial for maintaining healthy bones. Numerous factors can regulate this process and one of these factors is the immune system. The immune system and its cytokines play a key role in the regulation of bone density under physiological and pathophysiological conditions such as in type 1 diabetes and gut microbiota dysbiosis. In addition, supplementation with probiotic bacteria exerts a beneficial effect on the bone, in part dependent on the immune system. However, more research is needed to understand the signaling pathways that link the gut microbiome, immune system and bone. Understanding the role of the immune system, its cytokines, and the gut microbiota in several osteoporotic conditions can lead to the development of new treatments against bone loss and osteoporosis.

1.7. Aims of the study

Based on the knowledge gaps in the literature and the rationale provided in the introduction, the overall aim of this study was to investigate and identify the role of the immune system and its cytokines in different models of bone loss. First, in the T1D mouse model we hypothesized that in the absence of IL-10 bone loss will be exacerbated in T1D conditions. Second, we hypothesized that lymphocytes are important in mediating the bone effects induced by *Lactobacillus reuteri* as well as during gut dysbiosis. These hypotheses were tested in the following aims:

Aim 1: Determine the role of IL-10 in T1D-induced bone loss. (Chapter 2)

As previously mentioned, T1D is well known to induce bone loss. This study was designed to understand the contribution of the cytokine IL-10 in T1D- induced bone loss. We first evaluated the role of IL-10 in T1D induced bone loss *in vivo* by using a mouse model that is deficient in IL-10 (IL-10 deficient mice). Then, we used an *in vitro* approach to explore the specific role and mechanisms of IL-10 regulation of osteoblast gene expression during high glucose conditions.

Aim 2: Identify the mechanism by which *L. reuteri* increases bone density in healthy male mice. (Chapter 3)

Our lab has shown the beneficial effect of the probiotic *L. reuteri* in enhancing bone density and preventing bone loss in several animal models. This study was designed to investigate the role of T and B lymphocytes in mediating the beneficial effect of *L. reuteri* in regulating bone density in healthy, mature male mice. We used the Rag-deficient mouse model (lack mature T and B cells) to test the hypothesis that T and B lymphocytes are important for *L. reuteri* effects on bone density.

Aim 3: Identify the mechanism by which gut dysbiosis induces bone loss in male mice. (Chapter 4)

This study aimed to investigate the role of lymphocytes in a mouse model of bone loss induced by gut microbiota dysbiosis. An antibiotic approach was used to induce gut microbiota dysbiosis and bone loss. Together with the Rag deficient mice we tested the hypothesis that absence of T and B lymphocytes prevents bone loss induced by gut dysbiosis.

REFERENCES

REFERENCES

1. Zhao E, Xu H, Wang L, Kryczek I, Wu K, Hu Y, et al. Bone marrow and the control of immunity. Cell Mol Immunol. 2012;9(1):11–9.

2. Rutkovskiy A, Stensløkken K-O, Vaage IJ. Osteoblast Differentiation at a Glance. Med Sci Monit Basic Res. 2016;22:95–106.

3. Bellido T, Plotkin LI, Bruzzaniti A. Bone Cells. In: Burr DB, Allen MR, editors. Basic and applied bone biology. Elsevier Inc.; 2014. p. 27–45.

4. Bonewald LF, Johnson ML. Osteocytes, mechanosensing and Wnt signaling. Bone. 2008;42(4):606–15.

5. Langdahl B, Ferrari S, Dempster DW. Bone modeling and remodeling: potential as therapeutic targets for the treatment of osteoporosis. Ther Adv Musculoskelet Dis. 2016;8(6):225–35.

6. Clarke B. Normal bone anatomy and physiology. Clin J Am Soc Nephrol. 2008;3 Suppl 3:131–9.

7. Jacobs CR, Temiyasathit S, Castillo AB. Osteocyte Mechanobiology and Pericellular Mechanics. Annu Rev Biomed Eng. 2010;12(1):369–400.

8. Sims N a, Gooi JH. Bone remodeling: Multiple cellular interactions required for coupling of bone formation and resorption. Vol. 19, Seminars in Cell and Developmental Biology. 2008. p. 444–51.

9. Wein MN. Bone Lining Cells: Normal Physiology and Role in Response to Anabolic Osteoporosis Treatments. Curr Mol Biol Reports. 2017;3(2):79–84.

10. Kearns AE, Khosla S, Kostenuik PJ. Receptor activator of nuclear factor κB ligand and osteoprotegerin regulation of bone remodeling in health and disease. Vol. 29, Endocrine Reviews. 2008. p. 155–92.

11. Blair HC, Larrouture QC, Li Y, Lin H, Beer-Stoltz D, Liu L, et al. Osteoblast Differentiation and Bone Matrix Formation *In Vivo* and *In Vitro*. Tissue Eng Part B Rev. 2017;23(3):268–80.

12. Helfrich MH, Nesbitt SA, Lakkakorpi PT, Barnes MJ, Bodary SC, Shankar G, et al. β1integrins and osteoclast function: Involvement in collagen recognition and bone resorption. Bone. 1996;19(4):317–28.

13. Teitelbaum SL. Osteoclasts: What do they do and how do they do it? Am J Pathol.

2007;170(2):427–35.

14. Florencio-silva R, Rodrigues G, Sasso-cerri E, Simões MJ, Cerri PS, Cells B. Biology of Bone Tissue : Structure , Function , and Factors That Influence Bone Cells. 2015;2015.

15. Rockville. Bone health and osteoporosis: a report of the Surgeon General. US Heal Hum Serv. 2004;437.

16. Sözen T, Özışık L, Başaran NÇ. An overview and management of osteoporosis. Eur J Rheumatol. 2017 Mar;4(1):46–56.

17. Irwin R, Lee T, Young VB, Parameswaran N, McCabe LR. Colitis-induced bone loss is gender dependent and associated with increased inflammation. Inflamm Bowel Dis. 2013;19(8):1586–97.

18. Kinlein SA, Shahanoor Z, Romeo RD, Karatsoreos IN. Chronic corticosterone treatment during adolescence has significant effects on metabolism and skeletal development in male C57BL6/N mice. Endocrinology. 2017;158(7):2239–54.

19. Coe LM, Irwin R, Lippner D, McCabe LR. The bone marrow microenvironment contributes to type I diabetes induced osteoblast death. J Cell Physiol. 2011;226(2):477–83.

20. Coe LM, Zhang J, McCabe LR. Both spontaneous Ins2+/- and streptozotocin-induced type I diabetes cause bone loss in young mice. J Cell Physiol. 2013 Apr;228(4):689–95.

21. Reginster JY, Burlet N. Osteoporosis: A still increasing prevalence. Bone. 2006;38(2 SUPPL. 1):1998–2003.

22. Burge R, Dawson-Hughes B, Solomon DH, Wong JB, King A, Tosteson A. Incidence and Economic Burden of Osteoporosis-Related Fractures in the United States, 2005-2025. J Bone Miner Res. 2006;22(3):465–75.

23. Epidemiology | International Osteoporosis Foundation.

24. Hadji P. The evolution of selective estrogen receptor modulators in osteoporosis therapy. Climacteric. 2012;15(6):513–23.

25. Siris ES, Harris ST, Eastell R, Zanchetta JR, Goemaere S, Diez-Perez A, et al. Skeletal effects of raloxifene after 8 years: Results from the Continuing Outcomes Relevant to Evista (CORE) study. J Bone Miner Res. 2005;20(9):1514–24.

26. Gallagher JC, Tella SH. Prevention and treatment of postmenopausal osteoporosis. J Steroid Biochem Mol Biol. 2013 Oct;1–16.

27. Ross AC, Taylor CL, Yaktine AL, Del Valle HB. Dietary reference intakes for calcium and vitamin D. A. Catharine Ross, Christine L. Taylor, Ann L. Yaktine and HBDV, editor. Vol. 32, Endocrinology and Metabolism Clinics of North America. 2011. 181-194 p.

28. Daly RM, Ebeling PR. Is excess calcium harmful to health? Nutrients. 2010;2(5):505–22.

29. Drake MT, Cremers SCLM. Bisphosphonate Therapeutics in Bone Disease: The Hard and Soft Data on Osteoclast Inhibition. Mol Interv. 2010 Jun;10(3):141–52.

30. Dunford JE, Thompson K, Coxon FP, Luckman SP, Hahn FM, Poulter CD, et al. Structure-activity relationships for inhibition of farnesyl diphosphate synthase in vitro and inhibition of bone resorption in vivo by nitrogen-containing bisphosphonates. J Pharmacol Exp Ther. 2001 Feb;296(2):235–42.

31. Kavanagh KL, Guo K, Dunford JE, Wu X, Knapp S, Ebetino FH, et al. The molecular mechanism of nitrogen-containing bisphosphonates as antiosteoporosis drugs. Proc Natl Acad Sci. 2006 May;103(20):7829–34.

32. Baron R, Ferrari S, Russell RGG. Denosumab and bisphosphonates: different mechanisms of action and effects. Bone. 2011 Apr;48(4):677–92.

33. Papapoulos SE. Bisphosphonates : how do they work ? Best Pract Res Clin Endocrinol Metab. 2008 Oct;22(5):831–47.

34. Khosla S, Burr D, Cauley J, Dempster DW, Ebeling PR, Felsenberg D, et al. Bisphosphonate-associated osteonecrosis of the jaw: Report of a Task Force of the American Society for Bone and Mineral Research. Vol. 22, Journal of Bone and Mineral Research. 2007. p. 1479–91.

35. Naot D, Cornish J. The role of peptides and receptors of the calcitonin family in the regulation of bone metabolism. Bone. 2008;43(5):813–8.

36. Chesnut CH, Silverman S, Andriano K, Genant H, Gimona A, Harris S, et al. A Randomized Trial ofNasal Spray Salmon Calcitonin in Postmenopausal Women with Established Osteoporosis: the Prevent Recurrence ofOsteoporotic Fractures Study. 9343(00):267–76.

37. Trovas GP, Lyritis GP, Galanos A, Raptou P, Constantelou E. A Randomized Trial of Nasal Spray Salmon Calcitonin in Men With Idiopathic Osteoporosis: Effects on Bone Mineral Density and Bone Markers. J Bone Miner Res. 2002;17(3):521–7.

38. Bellido T, Ali AA, Plotkin LI, Fu Q, Gubrij I, Roberson PK, et al. Proteasomal degradation of Runx2 shortens parathyroid hormone-induced anti-apoptotic signaling in osteoblasts. A putative explanation for why intermittent administration is needed for bone anabolism. J Biol Chem. 2003 Dec;278(50):50259–72.

39. Cosman F, Crittenden DB, Adachi JD, Binkley N, Czerwinski E, Ferrari S, et al. Romosozumab Treatment in Postmenopausal Women with Osteoporosis. N Engl J Med. 2016;375(16):1532–43.

40. Mullard A. Merck & Co. drops osteoporosis drug odanacatib. Nat Rev Drug Discov. 2016;15(10):669–669.

41. Yang R-S, Tu H-J, Lin Y-M, Chuang W-J, Liou H-C, Fu W-M, et al. Inhibition of osteoporosis by the αvβ3 integrin antagonist of rhodostomin variants. Eur J Pharmacol. 2017;804(March):94–101.

42. Tu KN, Lie JD, King C, Wan V, Candidate P, Cameron M, et al. Osteoporosis : A Review of Treatment Options. 2018;43(2):92–104.

43. J D, P D. Advances in Non-Pharmacological and Pharmacological Management of Osteoporosis. Gerontol Geriatr. 2016;2(4):1–6.

44. Lin S-P, Fang Y-T, Cheng EC-H, Jan M-L, Huang H-Y, Cheng C-C, et al. Isolation of therapeutically functional mouse bone marrow mesenchymal stem cells within 3 h by an effective single-step plastic-adherent method. Cell Prolif. 2010;43(3):235–48.

45. Jang H-D, Hong J-Y, Han K, Lee JC, Shin B-J, Choi S-W, et al. Relationship between bone mineral density and alcohol intake: A nationwide health survey analysis of postmenopausal women. PLoS One. 2017;12(6):e0180132.

46. Abel ED, Peroni O, Kim JK, Kim Y-B, Boss O, Hadro E, et al. Adipose-selective targeting of the GLUT4 gene impairs insulin action in muscle and liver. Nature. 2002;409(6821):729–33.

47. Zisman A, Peroni OD, Abel DE, Michael DM, Mauvais-Jarvis F, Lowell BB, et al. Targeted disruption of the glucose transporter 4 selectively in muscle caused insulin resistance and glucose intolerance. Nat Med. 2000;(6):924–8.

48. Shaw RJ, Lamia K a, Vasquez D, Koo S, Depinho R a, Montminy M, et al. The Kinase LKB1 Mediates Glucose Homeostasis in Liver and Therapeutic Effects on Metformin. Science (80-). 2005;310(5754):1642–6.

49. Xu G, Liu B, Sun Y, Du Y, Snetselaar LG, Hu FB, et al. Prevalence of diagnosed type 1 and type 2 diabetes among US adults in 2016 and 2017: Population based study. BMJ. 2018;362.

50. Burghardt AJ, Issever AS, Schwartz A V., Davis KA, Masharani U, Majumdar S, et al. High-resolution peripheral quantitative computed tomographic imaging of cortical and trabecular bone microarchitecture in patients with type 2 diabetes mellitus. J Clin Endocrinol Metab. 2010 Nov;95(11):5045–55.

51. Bonds DE, Larson JC, Schwartz A V., Strotmeyer ES, Robbins J, Rodriguez BL, et al. Risk of Fracture in Women with Type 2 Diabetes: the Women's Health Initiative Observational Study. J Clin Endocrinol Metab. 2006 Sep;91(9):3404–10.

52. Petit MA, Paudel ML, Taylor BC, Hughes JM, Strotmeyer ES, Schwartz A V, et al. Bone mass and strength in older men with type 2 diabetes: the Osteoporotic Fractures in Men Study. J Bone Miner Res. 2010 Feb;25(2):285–91.

53. Strotmeyer ES, Cauley JA, Schwartz A V, Nevitt MC, Resnick HE, Zmuda JM, et al. Diabetes is associated independently of body composition with BMD and bone volume in older white and black men and women: The Health, Aging, and Body Composition Study. J Bone Miner Res. 2004 Mar 15;19(7):1084–91.

54. Hanley D a, Brown JP, Tenenhouse A, Olszynski WP, Ioannidis G, Berger C, et al. Associations among disease conditions, bone mineral density, and prevalent vertebral deformities in men and women 50 years of age and older: cross-sectional results from the Canadian Multicentre Osteoporosis Study. J Bone Miner Res. 2003 Apr 1;18(4):784–90.

55. Chen HH, Horng MH, Yeh SY, Lin IC, Yeh CJ, Muo CH, et al. Glycemic control with thiazolidinedione is associated with fracture of T2DM patients. PLoS One. 2015;10(8).

56. Shah VN, Shah CS, Pharm M, Snell-bergeon JK. Type 1 Diabetes and Risk for Fracture: Meta-analysis and Review of the Literature. Diabet Med. 2016;32(9):1134–42.

57. Linares MI. Diabetes mellitus and bone health : epidemiology , etiology and implications for fracture risk stratification. 2018;1–8.

58. Vestergaard P, Rejnmark L, Mosekilde L. Relative fracture risk in patients with diabetes mellitus, and the impact of insulin and oral antidiabetic medication on relative fracture risk. Diabetologia. 2005;48(7):1292–9.

59. Weber DR, Haynes K, Leonard MB, Willi SM, Denburg MR. Type 1 diabetes is associated with an increased risk of fracture across the life span: a population-based cohort study using the health improvement network (THIN). Diabetes Care. 2015;38(10):1913–20.

60. Eller-Vainicher C, Zhukouskaya V V, Tolkachev Y V, Koritko SS, Cairoli E, Grossi E, et al. Low bone mineral density and its predictors in type 1 diabetic patients evaluated by the classic statistics and artificial neural network analysis. Diabetes Care. 2011 Oct;34(10):2186–91.

61. Gunczler P, Lanes R, Paoli M, Martinis R, Villaroel O, Weisinger JR. Decreased Bone Mineral Density and Bone Formation Markers Shortly After Diagnosis of Clinical Type 1 Diabetes Mellitus. J Pediatr Endocrinol Metab. 2001;115:525–8.

62. Szkudelski T. The mechanism of alloxan and streptozotocin action in B cells of the rat

pancreas. Vol. 50, Physiological Research. 2001. p. 537–46.

63. Yoshioka M, Kayo T, Ikeda T, Koizumi A. A novel locus, Mody4, distal to D7Mit189 on chromosome 7 determines early-onset NIDDM in nonobese C57BL/6 (Akita) mutant mice. Diabetes. 1997 May;46(5):887–94.

64. Tai X, Van Laethem F, Pobezinsky L, Guinter T, Sharrow SO, Adams A, et al. Basis of CTLA-4 function in regulatory and conventional CD4+ T cells. Blood. 2012;119(22):5155–63.

65. Liu J, Zhang H-X. CTLA-4 Polymorphisms and Systemic Lupus Erythematosus: A Comprehensive Meta-Analysis . Genet Test Mol Biomarkers. 2013;17(3):226–31.

66. Vaidya B, Pearce S. The emerging role of the CTLA-4 gene in autoimmune endocrinopathies. Eur J Endocrinol. 2004;150(5):619–26.

67. Qu HQ, Bradfield JP, Grant SFA, Hakonarson H, Polychronakos C. Remapping the type i diabetes association of the CTLA4 locus. Genes Immun. 2009;10(1):27–32.

68. Atkinson MA, Leiter EH. The NOD mouse model of type 1 diabetes: As good as it gets? Vol. 5, Nature Medicine. 1999. p. 601–4.

69. Botolin S, Faugere M-C, Malluche H, Orth M, Meyer R, McCabe LR. Increased bone adiposity and peroxisomal proliferator-activated receptor-gamma2 expression in type I diabetic mice. Endocrinology. 2005 Aug;146(8):3622–31.

70. McCabe L, Zhang J, Raehtz S. Understanding the skeletal pathology of type 1 and 2 diabetes mellitus. Crit Rev Eukaryot Gene Expr. 2011;21(2):187–206.

71. Manavalan JS, Cremers S, Dempster DW, Zhou H, Dworakowski E, Kode A, et al. Circulating osteogenic precursor cells in type 2 diabetes mellitus. J Clin Endocrinol Metab. 2012 Sep;97(9):3240–50.

72. Verhaeghe J, Thomsen JS, Van Bree R, Van Herck E, Bouillon R, Mosekilde L. Effects of exercise and disuse on bone remodeling, bone mass, and biomechanical competence in spontaneously diabetic female rats. Bone. 2000;27(2):249–56.

73. Motyl K, McCabe LR. Streptozotocin, type 1 diabetes severity and bone. Biol Proced Online. 2009 Mar 6;11(1):296–315.

74. Kemink SA, Hermus AR, Swinkels LM, Lutterman JA, Smals AG. Osteopenia in insulin-dependent diabetes mellitus; prevalence and aspects of pathophysiology. J Endocrinol Invest. 2000 May;23(5):295–303.

75. Cakatay U, Telci A, Kayali R, Akçay T, Sivas A, Aral F. Changes in bone turnover on deoxypyridinoline levels in diabetic patients. Diabetes Res Clin Pract. 1998

May;40(2):75–9.

76. Bjørgaas M, Haug E, Johnsen HJ. The urinary excretion of deoxypyridinium cross-links is higher in diabetic than in nondiabetic adolescents. Calcif Tissue Int. 1999 Aug;65(2):121–4.

77. Cloos C, Wahl P, Hasslacher C, Traber L, Kistner M, Jurkuhn K, et al. Urinary glycosylated, free and total pyridinoline and free and total deoxypyridinoline in diabetes mellitus. Clin Endocrinol (Oxf). 1998 Mar;48(3):317–23.

78. Rosen CJ, Ackert-Bicknell C, Rodriguez JP, Pino AM. Marrow fat and the bone microenvironment: developmental, functional, and pathological implications. Crit Rev Eukaryot Gene Expr. 2009 Jan;19(2):109–24.

79. Sadie-Van Gijsen H, Crowther NJ, Hough FS, Ferris WF. The interrelationship between bone and fat: from cellular see-saw to endocrine reciprocity. Cell Mol Life Sci. 2013 Jul;70(13):2331–49.

80. Kennell JA, MacDougald OA. Wnt signaling inhibits adipogenesis through beta-catenin-dependent and -independent mechanisms. J Biol Chem. 2005 Jun;280(25):24004–10.

81. Keats E, Khan ZA. Unique responses of stem cell-derived vascular endothelial and mesenchymal cells to high levels of glucose. PLoS One. 2012;7(6).

82. Bennett CN, Longo KA, Wright WS, Suva LJ, Lane TF, Hankenson KD, et al. Regulation of osteoblastogenesis and bone mass by Wnt10b. Proc Natl Acad Sci. 2005;102(9):3324–9.

83. Zhang J, Motyl KJ, Irwin R, MacDougald OA, Britton RA, McCabe LR. Loss of bone and Wnt10b expression in male type 1 diabetic mice is blocked by the probiotic Lactobacillus reuteri. Endocrinology. 2015;156(9):3169–82.

84. Terada M, Inaba M, Yano Y, Hasuma T, Nishizawa Y, Morii H, et al. Growth-inhibitory effect of a high glucose concentration on osteoblast-like cells. Bone. 1998;22(1):17–23.

85. Zayzafoon M, Stell C, Irwin R, McCabe LR. Extracellular glucose influences osteoblast differentiation and c-jun expression. J Cell Biochem. 2000 Aug 2;79(2):301–10.

86. Wang X, Feng Z, Li J, Chen L, Tang W. High glucose induces autophagy of MC3T3-E1 cells via ROS-AKT-mTOR axis. Mol Cell Endocrinol. 2016;429:62–72.

87. Raehtz S, Bierhalter H, Schoenherr D, Parameswaran N, McCabe LR. Estrogen Deficiency Exacerbates Type 1 Diabetes Induced Bone TNFα expression and Osteoporosis in Female Mice. Endocrinology. 2017 Apr 14;

88. Cunha JS, Ferreira VM, Maquigussa E, Naves MA, Boim MA. Effects of high glucose

and high insulin concentrations on osteoblast function in vitro. Cell Tissue Res. 2014;358(1):249–56.

89. Balint E, Szabo P, Marshall CF, Sprague SM. Glucose-induced inhibition of in vitro bone mineralization. Bone. 2001;28(1):21–8.

90. Gilbert L, He X, Farmer P, Rubin J, Drissi H, van Wijnen AJ, et al. Expression of the Osteoblast Differentiation Factor RUNX2 (Cbfa1/AML3/Pebp2αA) Is Inhibited by Tumor Necrosis Factor-α. J Biol Chem. 2002;277(4):2695–701.

91. Wittrant Y, Gorin Y, Woodruff K, Horn D, Abboud HE, Mohan S, et al. High d(+)glucose concentration inhibits RANKL-induced osteoclastogenesis. Bone. 2008;42(6):1122–30.

92. Xu F, Ye Y, Dong Y, Guo F, Chen A, Huang S. Inhibitory effects of high glucose/insulin environment on osteoclast formation and resorption in vitro. J Huazhong Univ Sci Technol - Med Sci. 2013;33(2):244–9.

93. Schwartz A V., Garnero P, Hillier TA, Sellmeyer DE, Strotmeyer ES, Feingold KR, et al. Pentosidine and increased fracture risk in older adults with type 2 diabetes. J Clin Endocrinol Metab. 2009;94(7):2380–6.

94. Alikhani M, Alikhani Z, Boyd C, MacLellan CM, Raptis M, Liu R, et al. Advanced glycation end products stimulate osteoblast apoptosis via the MAP kinase and cytosolic apoptotic pathways. Bone. 2007;40(2):345–53.

95. Miyata T, Notoya K, Yoshida K, Horie K, Maeda K, Kurokawa K, et al. Advanced glycation end products enhance osteoclast-induced bone resorption in cultured mouse unfractionated bone cells and in rats implanted subcutaneously with devitalized bone particles. J Am Soc Nephrol. 1996;8(2):260–70.

96. Bai XC, Lu D, Bai J, Zheng H, Ke ZY, Li XM, et al. Oxidative stress inhibits osteoblastic differentiation of bone cells by ERK and NF-κB. Biochem Biophys Res Commun. 2004;314(1):197–207.

97. Domazetovic V, Marcucci G, Lantomasi T, Brandi ML, Vincenzini MT. Oxidative stress in bone remodeling: role of antioxidants. Clin Cases Miner Bone Metab. 2017;14(2):209.

98. Goldberg IJ, Eckel RH, Abumrad NA. Regulation of fatty acid uptake into tissues: lipoprotein lipase- and CD36-mediated pathways. J Lipid Res. 2008;50(Supplement):S86–90.

99. Vergès B. Lipid disorders in type 1 diabetes. Diabetes Metab. 2009;35(5):353–60.

100. Yamaguchi T, Sugimoto T, Yano S, Yamauchi M, Sowa H, Chen Q, et al. Plasma Lipids and Osteoporosis in Postmenopausal Women. Endocr J. 2002;49(2):211–7.

101. Jiang J, Qiu P, Wang Y, Zhao C, Fan S, Lin X. Association between serum high-density lipoprotein cholesterol and bone health in the general population : a large and multicenter study. Arch Osteoporos. 2019;14(36):1–9.

102. Solomon DH, Avorn J, Canning CF, Wang PS. Lipid levels and bone mineral density. Am J Med. 2005;118(12):1414.e1-1414.e5.

103. Slade JM, Coe LM, Meyer RA, McCabe LR. Human bone marrow adiposity is linked with serum lipid levels not T1-diabetes. J Diabetes Complications. 2012;26(1):1–9.

104. Botolin S, McCabe LR. Inhibition of PPARγ prevents type I diabetic bone marrow adiposity but not bone loss. J Cell Physiol. 2006;209:967–76.

105. Martin LM, McCabe LR. Type I diabetic bone phenotype is location but not gender dependent. Histochem Cell Biol. 2007;128(2):125–33.

106. Eghbali-Fatourechi GZ, Lamsam J, Fraser D, Nagel D, Riggs BL, Khosla S. Circulating osteoblast-lineage cells in humans. N Engl J Med. 2005 May;352(19):1959–66.

107. Zhang M, Xuan S, Bouxsein ML, Von Stechow D, Akeno N, Faugere MC, et al. Osteoblast-specific knockout of the insulin-like growth factor (IGF) receptor gene reveals an essential role of IGF signaling in bone matrix mineralization. J Biol Chem. 2002;277(46):44005–12.

108. Ikeda K, Matsumoto T, Morita K, Yamato H, Hiroo T, Ezawa I, et al. The role of insulin in the stimulation of renal 1,25-dihydroxyvitamin D synthesis by parathyroid hormone in rats. 1987;121(5).

109. Bideci A, Çamurdan OM, Cinaz P, Dursun H, Demirel F. Serum zinc, insulin-like growth factor-I and insulin-like growth factor binding protein-3 levels in children with type 1 diabetes mellitus. J Pediatr Endocrinol Metab. 2005;18:1007–11.

110. Radetti G, Paganini C, Antoniazzi F, Pasquino B, Valentini R, Gentili L, et al. Growth Hormone-Binding Proteins, IGF-1 and IGF-Binding Proteins in Children and Adolescents with Type 1 Diabetes mellitus. Horm Res. 1997;47:110–5.

111. Jehle PM, Schulten K, Schulz W, Jehle DR, Stracke S, Manfras B, et al. Serum levels of insulin-like growth factor (IGF)-I and IGF binding protein (IGFBP)-1 to -6 and their relationship to bone metabolism in osteoporosis patients. Euro J Intern Med. 2003;14(1):32–8.

112. Kanazawa I, Yamaguchi T, Sugimoto T. Serum insulin-like growth factor-I is a marker for assessing the severity of vertebral fractures in postmenopausal women with type 2 diabetes mellitus. Osteoporos Int. 2011;22(4):1191–8.

113. Van Sickle BJ, Simmons J, Hall R, Raines M, Ness K, Spagnoli A. Increased circulating

IL-8 is associated with reduced IGF-1 and related to poor metabolic control in adolescents with type 1 diabetes mellitus. Cytokine. 2009;48(3):290–4.

114. Erbagci AB, Tarakcioglu M, Coskun Y, Sivasli E, Sibel Namiduru E. Mediators of inflammation in children with type I diabetes mellitus: cytokines in type I diabetic children. Clin Biochem. 2001;34(8):645–50.

115. Snell-Bergeon JK, West NA, Mayer-Davis EJ, Liese AD, Marcovina SM, D'Agostino RB, et al. Inflammatory markers are increased in youth with type 1 diabetes: The SEARCH case-control study. J Clin Endocrinol Metab. 2010 Jun;95(6):2868–76.

116. Motyl KJ, Botolin S, Irwin R, Appledorn DM, Kadakia T, Amalfitano A, et al. Bone inflammation and altered gene expression with type I diabetes early onset. J Cell Physiol. 2009 Mar;218(3):575–83.

117. Schloot NC, Hanifi-Moghaddam P, Goebel C, Shatavi S V, Flohe S, Kolb H, et al. Serum IFN-gamma and IL-10 levels are associated with disease progression in non-obese diabetic mice. Diabetes Metab Res Rev. 2002;18(1):64–70.

118. Van Exel E, Gussekloo J, De Craen AJM, Frölich M, Wiel AB Van Der, Westendorp RGJ. Low production capacity of interleukin-10 associates with the metabolic syndrome and type 2 diabetes: The Leiden 85-plus study. Diabetes. 2002;51(4):1088–92.

119. Lee J-H, Lee W, Kwon OH, Kim J-H, Kwon OW, Kim KH, et al. Cytokine profile of peripheral blood in type 2 diabetes mellitus patients with diabetic retinopathy. Ann Clin Lab Sci. 2008;38(4):361–7.

120. Compston JE, Judd D, Crawley EO, Evans WD, Evans C, Church HA, et al. Osteoporosis in patients with inflammatory bowel disease. Gut. 1987 Apr;28(4):410–5.

121. Harris L, Senagore P, Young VB, McCabe LR. Inflammatory bowel disease causes reversible suppression of osteoblast and chondrocyte function in mice. AJP Gastrointest Liver Physiol. 2009 May;296(5):G1020–9.

122. Irwin R, Raehtz S, Parameswaran N, McCabe LR. Intestinal inflammation without weight loss decreases bone density and growth. Am J Physiol - Regul Integr Comp Physiol. 2016;311(6):R1149–57.

123. Hardy R, Cooper MS. Bone loss in inflammatory disorders. J Endocrinol. 2009;201(3):309–20.

124. Qiao YC, Chen YL, Pan YH, Tian F, Xu Y, Zhang X, et al. The change of serum tumor necrosis factor alpha in patients with type 1 diabetes mellitus: A systematic review and meta-analysis. PLoS One. 2017;12(4):1–14.

125. Chen Y ling, Qiao Y chao, Xu Y, Ling W, Pan Y hong, Huang Y cheng, et al. Serum

TNF-α concentrations in type 2 diabetes mellitus patients and diabetic nephropathy patients: A systematic review and meta-analysis. Immunol Lett. 2017;186(March):52–8.

126. Catalfamo DL, Calderon NL, Harden SW, Sorenson HL, Neiva KG, Wallet SM. Augmented LPS responsiveness in type 1 diabetes-derived osteoclasts. J Cell Physiol. 2012;228(2):349–61.

127. Ko KI, Coimbra LS, Tian C, Alblowi J, Kayal RA, Einhorn T, et al. Diabetes reduces mesenchymal stem cells in fracture healing through a TNFα-mediated mechanism. Diabetologia. 2015;58(3):633–42.

128. Pacios S, Kang J, Galicia J, Gluck K, Patel H, Ovaydi-Mandel A, et al. Diabetes aggravates periodontitis by limiting repair through enhanced inflammation. FASEB J. 2012;26(4):1423–30.

129. Pennline K, Roque-Gaffney E, Monahan M. Recombinant human IL-10 prevents the onset of diabetes in the nonobese diabetic mouse. Clin Immunol Immunopathol. 1994;71(2):169–75.

130. Schett G. Rheumatoid arthritis: Inflammation and bone loss. Wiener Medizinische Wochenschrift. 2006;156(1–2):34–41.

131. Klausen B, Hougen HP, Fiehn N -E. Increased periodontal bone loss in temporarily B lymphocyte-deficient rats. J Periodontal Res. 1989;24(6):384–90.

132. Li Y, Toraldo G, Li A, Yang X, Zhang H, Qian WP, et al. B cells and T cells are critical for the preservation of bone homeostasis and attainment of peak bone mass in vivo. Blood. 2007;109(9):3839–48.

133. Sun W, Meednu N, Rosenberg A, Rangel-Moreno J, Wang V, Glanzman J, et al. B cells inhibit bone formation in rheumatoid arthritis by suppressing osteoblast differentiation. Nat Commun. 2018;9(1):5127.

134. Zhang YH, Heulsmann A, Tondravi MM, Mukherjee A, Abu-Amer Y. Tumor necrosis factor-α (TNF) stimulates RANKL-induced osteoclastogenesis via coupling of TNF type 1 receptor and RANK signaling pathways. J Biol Chem. 2001 Jan 5;276(1):563–8.

135. Wei S, Kitaura H, Zhou P, Ross PF, Teitelbaum SL. IL-1 mediates TNF-induced osteoclastogenesis. J Clin Invest. 2005;115(282–290).

136. Kim JW, Lee MS, Lee CH, Kim HY, Chae SU, Kwak HB, et al. Effect of interferon- γ on the fusion of mononuclear osteoclasts into bone-resorbing osteoclasts. BMB Rep. 2012;

137. Al-Rasheed A, Scheerens H, Srivastava AK, Rennick DM, Tatakis DN. Accelerated alveolar bone loss in mice lacking interleukin-10: Late onset. J Periodontal Res. 2004;39(3):194–8.

138. Claudino M, Garlet TP, Cardoso CRB, de Assis GF, Taga R, Cunha FQ, et al. Down-regulation of expression of osteoblast and osteocyte markers in periodontal tissues associated with the spontaneous alveolar bone loss of interleukin-10 knockout mice. Eur J Oral Sci. 2010;118(1):19–28.

139. Dresner-Pollak R, Gelb N, Rachmilewitz D, Karmeli F, Weinreb M. Interleukin 10-deficient mice develop osteopenia, decreased bone formation, and mechanical fragility of long bones. Gastroenterology. 2004;127(3):792–801.

140. Lee S-K, Kadono Y, Okada F, Jacquin C, Koczon-Jaremko B, Gronowicz G, et al. T Lymphocyte-Deficient Mice Lose Trabecular Bone Mass With Ovariectomy. J Bone Miner Res. 2006;21(11):1704–12.

141. Mosmann VR, Cherwinski H, Bond MW, Giedlin MA, Coffman RL. Two types of murine helper T cell clone. I. Definition according to profiles of lymphokine activities and secreted proteins. J Immunol. 1986;136(7):2348–57.

142. Romagnani S. T-cell subsets (Th1 versus Th2). Ann Allergy Asthma Immunol. 2000;85(1):9–19.

143. McGeachy MJ, Cua DJ. Th17 Cell Differentiation: The Long and Winding Road. Immunity. 2008;28(4):445–53.

144. Terauchi M, Li JY, Bedi B, Baek KH, Tawfeek H, Galley S, et al. T Lymphocytes Amplify the Anabolic Activity of Parathyroid Hormone through Wnt10b Signaling. Cell Metab. 2009;10(3):229–40.

145. Teng Y-TA, Nguyen H, Gao X, Kong Y-Y, Gorczynski RM, Singh B, et al. Functional human T-cell immunity and osteoprotegerin ligand control alveolar bone destruction in periodontal infection. J Clin Invest. 2011;106(6):R59–67.

146. Grcevic D, Lee S-K, Marusic A, Lorenzo JA. Depletion of CD4 and CD8 T Lymphocytes in Mice In Vivo Enhances 1,25-Dihydroxyvitamin D3-Stimulated Osteoclast-Like Cell Formation In Vitro by a Mechanism That Is Dependent on Prostaglandin Synthesis. J Immunol. 2000;165(8):4231–8.

147. Choi Y, Woo KM, Ko SH, Lee YJ, Park SJ, Kim HM, et al. Osteoclastogenesis is enhanced by activated B cells but suppressed by activated CD8+T cells. Eur J Immunol. 2001;31(7):2179–88.

148. Buchwald ZS, Kiesel JR, DiPaolo R, Pagadala MS, Aurora R. Osteoclast activated FoxP3+CD8+T-cells suppress bone resorption in vitro. PLoS One. 2012;7(6).

149. Buchwald ZS, Kiesel JR, Yang C, DiPaolo R, Novack D V, Aurora R. Osteoclast- induced FOXP3+ CD8 T-cells limit bone loss in mice. Bone. 2013;56(1):163–73.

150. Kim YG, Lee CK, Nah SS, Mun SH, Yoo B, Moon HB. Human CD4+CD25+ regulatory T cells inhibit the differentiation of osteoclasts from peripheral blood mononuclear cells. Biochem Biophys Res Commun. 2007;357(4):1046–52.

151. Zaiss MM, Axmann R, Zwerina J, Polzer K, Gückel E, Skapenko A, et al. Treg cells suppress osteoclast formation: A new link between the immune system and bone. Arthritis Rheum. 2007;56(12):4104–12.

152. Kelchtermans H, Geboes L, Mitera T, Huskens D, Leclercq G, Matthys P. Activated CD4+CD25+ regulatory T cells inhibit osteoclastogenesis and collagen-induced arthritis. Ann Rheum Dis. 2009;68(5):744–50.

153. Zaiss MM, Frey B, Hess A, Zwerina J, Luther J, Nimmerjahn F, et al. Regulatory T Cells Protect from Local and Systemic Bone Destruction in Arthritis. J Immunol. 2010;184(12):7238–46.

154. Vroom TM, Scholte G, Ossendorp F, Borst J. Tissue distribution of human γδ T cells: No evidence for general epithelial tropism. J Clin Pathol. 1991;44(12):1012–7.

155. Pappalardo A, Thompson K. Activated γδ T cells inhibit osteoclast differentiation and resorptive activity in vitro. Clin Exp Immunol. 2013;174(2):281–91.

156. Phalke SP, Chiplunkar S V. Activation status of γδ T cells dictates their effect on osteoclast generation and bone resorption. Bone Reports. 2015;3:95–103.

157. Thompson K, Roelofs AJ, Jauhiainen M, Mönkkönen H, Mönkkönen J, Rogers MJ. Activation of γδ T Cells by Bisphosphonates. In: Advances in Experimental Medicine and Biology. 2010. p. 11–20.

158. Manabe N, Kawaguchi H, Chikuda H, Miyaura C, Inada M, Nagai R, et al. Connection between B lymphocyte and osteoclast differentiation pathways. J Immunol. 2001;167(5):2625–31.

159. Kawai T, Matsuyama T, Hosokawa Y, Makihira S, Seki M, Karimbux NY, et al. B and T lymphocytes are the primary sources of RANKL in the bone resorptive lesion of periodontal disease. Am J Pathol. 2006;169(3):987–98.

160. Weitzmann MN, Cenci S, Haug J, Brown C, DiPersio J, Pacifici R. B lymphocytes inhibit human osteoclastogenesis by secretion of TGFβ. J Cell Biochem. 2000;78(2):318–24.

161. Titanji K, Vunnava A, Sheth AN, Delille C, Lennox JL, Sanford SE, et al. Dysregulated B Cell Expression of RANKL and OPG Correlates with Loss of Bone Mineral Density in HIV Infection. PLoS Pathog. 2014;10(11):1–14.

162. Titanji K. Beyond antibodies: B cells and the OPG/RANK-RANKL pathway in health, non-HIV disease and HIV-induced bone loss. Front Immunol. 2017;8(DEC):1–9.

163. Onal M, Xiong J, Chen X, Thostenson JD, Almeida M, Manolagas SC, et al. Receptor activator of nuclear factor κB ligand (RANKL) protein expression by B lymphocytes contributes to ovariectomy-induced bone loss. J Biol Chem. 2012;287(35):29851–60.

164. Eghbali-fatourechi G, Khosla S, Sanyal A, Boyle WJ, Lacey DL, Riggs BL. Role of RANK ligand in mediating increased bone resorption in early postmenopausal women. J Clin Invest. 2003;111(8):1221–30.

165. Poubelle PE, Chakravarti A, Fernandes MJ, Doiron K, Marceau A-A. Differential expression of RANK, RANK- L, and osteoprotegerin by synovial fluid neutrophils from patients with rheumatoid arthritis and by healthy human blood neutrophils. Arthritis Res Ther. 2007;9(2):1–12.

166. Chakravarti A, Raquil MA, Tessier P, Poubelle PE. Surface RANKL of Toll-like receptor 4-stimulated human neutrophils activates osteoclastic bone resorption. Blood. 2009;114(8):1633–44.

167. Allaeys I, Rusu D, Picard S, Pouliot M, Borgeat P, Poubelle PE. Osteoblast retraction induced by adherent neutrophils promotes osteoclast bone resorption: Implication for altered bone remodeling in chronic gout. Lab Investig. 2011;91(6):905–20.

168. Michalski MN, McCauley LK. Macrophages and Skeletal Health. Pharmacol Ther. 2017;1–30.

169. Manwani D, Bieke JJ. The Erythroblastic Island. Curr Top Dev Biol. 2008;82:23–53.

170. Pettit AR, Chang MK, Hume DA, Raggatt LJ. Osteal macrophages: A new twist on coupling during bone dynamics. Bone. 2008;43(6):976–82.

171. Chang MK, Raggatt L-J, Alexander KA, Kuliwaba JS, Fazzalari NL, Schroder K, et al. Osteal Tissue Macrophages Are Intercalated throughout Human and Mouse Bone Lining Tissues and Regulate Osteoblast Function In Vitro and In Vivo. J Immunol. 2008;181(2):1232–44.

172. Nicolaidou V, Wong MM, Redpath AN, Ersek A, Baban DF, Williams LM, et al. Monocytes induce STAT3 activation in human mesenchymal stem cells to promote osteoblast formation. PLoS One. 2012;7(7).

173. Alexander KA, Chang MK, Maylin ER, Kohler T, Müller R, Wu AC, et al. Osteal macrophages promote in vivo intramembranous bone healing in a mouse tibial injury model. J Bone Miner Res. 2011;26(7):1517–32.

174. Champagne CM, Takebe J, Offenbacher S, Cooper LF. Macrophage cell lines produce osteoinductive signals that include bone morphogenetic protein-2. Bone. 2002;30(1):26–31.

175. Plekhova NG, Lyapun IN, Gnedenkov S, Sinebryukhov S, Mashtalyar D. The Role of Dendritic Cells in Bone Loss and Repair. Dendritic Cells. 2018;(Dc).

176. Rivollier A, Tebib J, Piperno M, Aitsiselmi T, Rabourdin-combe C, Jurdic P, et al. Immature dendritic cell transdifferentiation into osteoclasts: a novel pathway sustained by the rheumatoid arthritis microenvironment. Blood. 2004;104(13):4029–37.

177. Maitra R, Follenzi A, Yaghoobian A, Montagna C, Merlin S, Cannizzo ES, et al. Dendritic Cell-Mediated In Vivo Bone Resorption. J Immunol. 2010;185(3):1485–91.

178. Parameswaran N, Patial S. Tumor Necrosis Factor-α Signaling in Macrophages Narayanan. Crit Rev Eukaryot Gene Expr. 2010;20(2):87–103.

179. Zhu S, He H, Gao C, Luo G, Xie Y, Wang H, et al. Ovariectomy-induced bone loss in TNFα and IL6 gene knockout mice is regulated by different mechanisms. J Mol Endocrinol. 2018;60(3):185–98.

180. Kimble RB, Bain S, Pacifici R. The functional block of TNF but not of IL-6 prevents bone loss in ovariectomized mice. J Bone Miner Res. 1997;12(6):935–41.

181. Kobayashi K, Takahashi N, Jimi E, Udagawa N, Takami M, Kotake S, et al. Tumor Necrosis Factor Stimulates Osteoclast Differentiation by a Mechanism Independent of the Odf/Rankl-Rank Interaction. J Exp Med. 2000 Jan;191(2):275–86.

182. Wang LM, Zhao N, Zhang J, Sun QF, Yang CZ, Yang PS. Tumor necrosis factor-alpha inhibits osteogenic differentiation of pre-osteoblasts by downregulation of EphB4 signaling via activated nuclear factor-kappaB signaling pathway. J Periodontal Res. 2018;53(1):66–72.

183. Zuo C, Zhao X, Shi Y, Wu W, Zhang N, Xu J, et al. TNF-alpha inhibits SATB2 expression and osteoblast differentiation through NF-kappaB and MAPK pathways. Oncotarget. 2018;9(4):4833–50.

184. Zheng L, Wang W, Ni J, Mao X, Song D, Liu T, et al. Role of autophagy in tumor necrosis factor-α-induced apoptosis of osteoblast cells. J Investig Med. 2017;65(6):1014–20.

185. Huang H, Zhao N, Xu X, Xu Y, Li S, Zhang J, et al. Dose-specific effects of tumor necrosis factor alpha on osteogenic differentiation of mesenchymal stem cells. Cell Prolif. 2011;44(5):420–7.

186. Schoenborn JR, Wilson CB. Regulation of Interferon-γ During Innate and Adaptive Immune Responses. Adv Immunol. 2007;96(07):41–101.

187. Takahashi N, Mundy GR, Roodman GD. Recombinant human interferon-gamma inhibits formation of human osteoclast-like cells. JImmunol. 1986;137(11):3544–9.

188. Gao Y, Grassi F, Ryan MR, Terauchi M, Page K, Yang X, et al. IFN-gamma stimulates osteoclast formation and bone loss in vivo via antigen-driven T cell activation. J Clin Invest. 2007;117(1):122–32.

189. Mann GN, Jacobs TW, Buchinsky FJ, Armstrong EC, Li M, Ke HZ, et al. Interferon-γ causes loss of bone volume in vivo and fails to ameliorate cyclosporin A-induced osteopenia. Endocrinology. 1994;135(3):1077–83.

190. L L, Ries WL, Rodriguiz M, Hatcher HC. Recombinant human interferon gamma therapy for osteopetrosis. Pediatr Pharmacol Ther. 1992;119–24.

191. Couper KN, Blount DG, Riley EM. IL-10: The Master Regulator of Immunity to Infection. J Immunol. 2014;180(9):5771–7.

192. Xu LX, Kukita T, Kukita A, Otsuka T, Niho Y, Iijima T. Interleukin-10 selectively inhibits osteoclastogenesis by inhibiting differentiation of osteoclast progenitors into preosteoclast-like cells in rat bone marrow culture system. J Cell Physiol. 1995;165(3):624–9.

193. Mohamed SGK, Sugiyama E, Shinoda K, Taki H, Hounoki H, Abdel-Aziz HO, et al. Interleukin-10 inhibits RANKL-mediated expression of NFATc1 in part via suppression of c-Fos and c-Jun in RAW264.7 cells and mouse bone marrow cells. Bone. 2007;41(4):592–602.

194. Liu D, Yao S, Wise GE. Effect of interleukin-10 on gene expression of osteoclastogenic regulatory molecules in the rat dental follicle. Eur J Oral Sci. 2006;114(18):42–9.

195. Keystone E, Omair MA. Interleukin-6 inhibition. In: Rheumatology. 2015. p. 485–91.

196. De Benedetti F, Rucci N, Del Fattore A, Peruzzi B, Paro R, Longo M, et al. Impaired skeletal development in interleukin-6-transgenic mice: A model for the impact of chronic inflammation on the growing skeletal system. Arthritis Rheum. 2006;54(11):3551–63.

197. Li X, Zhou ZY, Zhang YY, Yang HL. IL-6 contributes to the defective osteogenesis of bone marrow stromal cells from the vertebral body of the glucocorticoid-induced osteoporotic mouse. PLoS One. 2016;11(4):1–19.

198. Jilka RL, Hangoc G, Girasole G, Passeri G, Daniel C, Abrams JS, et al. Increased Osteoclast Development After Estrogen Loss : Mediation by Interleukin-6. Science (80-). 1992;257(5066):88–91.

199. Franchimont N, Gangji V, Durant D, Canalis E. Interleukin-6 with its soluble receptor enhances the expression of insulin-like growth factor-I in osteoblasts. Endocrinology. 1997;138(12):5248–55.

200. Yeh LCC, Zavala MC, Lee JC. Osteogenic Protein-1 and interleukin-6 with its soluble

receptor synergistically stimulate rat osteoblastic cell differentiation. J Cell Physiol. 2002;190(3):322–31.

201. Riancho JA, Zarrabeitia MT, Gonzalez-Macias J. Interleukin-4 modulates osteoclast differentiation and inhibits the formation of resorption pits in mouse osteoclast cultures. Biochem Biophys Res Commun. 1993;196(2):678–85.

202. Miossec P, Chomarat P, Dechanet J, Moreau J-F, Roux J-P, Delmas P, et al. Interleukin-4 inhibits bone resorption through an effect on osteoclasts and proinflammatory cytokines in an ex vivo model of bone resorption in rheumatoid arthritis. 1994;37(12):1715–22.

203. Lewis DB, Liggitt HD, Effmann EL, Motley ST, Teitelbaum SL, Jepsen KJ, et al. Osteoporosis induced in mice by overproduction of interleukin 4. Proc Natl Acad Sci U S A. 1993;90(24):11618–22.

204. Ura K, Watanabe K, Eto S, Yanagihara N. Interleukin (IL) -4 and IL-13 Inhibit the Differentiation of Murine Osteoblastic MC3T3-E1 Cells. Endocr J. 2000;47(3):293–302.

205. Pappu BP, Angkasekwinai P, Dong C. Regulatory mechanisms of helper T cell differentiation: New lessons learned from interleukin 17 family cytokines. Pharmacol Ther. 2008;117(3):374–84.

206. Adamopoulos IE, Chao C chi, Geissler R, Laface D, Blumenschein W, Iwakura Y, et al. Interleukin-17A upregulates receptor activator of NF-κB on osteoclast precursors. Arthritis Res Ther. 2010;12(1):1–11.

207. Zhang JR, Pang DD, Tong Q, Liu X, Su DF, Dai SM. Different Modulatory Effects of IL-17, IL-22, and IL-23 on Osteoblast Differentiation. Mediators Inflamm. 2017;2017.

208. Adamopoulos IE, Bowman EP. Immune regulation of bone loss by Th17 cells. Arthritis Res Ther. 2008;10(5):1–9.

209. Quinn JMW, Itoh K, Udagawa N, Häusler K, Yasuda H, Shima N, et al. Transforming growth factor β affects osteoclast differentiation via direct and indirect actions. J Bone Miner Res. 2001;16(10):1787–94.

210. Fuller K, Lean J, Bayley K, Wani M, Chambers T. A role for TGFβ1 in osteoclast differentiation and survival. J Cell Sci. 2000;113:2445–53.

211. Lian N, Lin T, Liu W, Wang W, Li N, Sun S, et al. Transforming growth factor β suppresses osteoblast differentiation via the vimentin activating transcription factor 4 (ATF4) axis. J Biol Chem. 2012;287(43):35975–84.

212. Karsdal MA, Larsen L, Engsig MT, Lou H, Ferreras M, Lochter A, et al. Matrix metalloproteinase-dependent activation of latent transforming growth factor-β controls the conversion of osteoblasts into osteocytes by blocking osteoblast apoptosis. J Biol Chem.

2002;277(46):44061–7.

213. Matsunobu T, Torigoe K, Ishikawa M, De Vega S, Kulkarni AB, Iwamoto Y, et al. Critical roles of the TGF-β type I receptor ALK5 in perichondrial formation and function, cartilage integrity, and osteoblast differentiation during growth plate development. Dev Biol. 2009;332(2):325–38.

214. Atti E, Gomez S, Wahl SM, Mendelsohn R, Paschalis E, Boskey AL. Effects of transforming growth factor-β deficiency on bone development: A Fourier Transform-Infrared imaging analysis. Bone. 2002;31(6):675–84.

215. Geiser AG, Zeng QQ, Sato M, Helvering LM, Hirano T, Turner CH. Decreased bone mass and bone elasticity in mice lacking the transforming growth factor-β1 gene. Bone. 1998;23(2):87–93.

216. Sanford LP, Ormsby I, Gittenberger-de Groot AC, Sariola H, Rick F, Boivin GP, et al. TGFβ2 knockout mice have multiple developmental defects that are non-overlapping with other TGFβ knockout phenotypes. Development. 1997;24(13):2659–70.

217. Loh G, Blaut M. Role of commensal gut bacteria in inflammatory bowel diseases. Gut Microbes. 2012;3(6):544–55.

218. Ma TY, Anderson JM, Turner JR. Tight Junctions and the Intestinal Barrier. Vol. 1, Physiology of the Gastrointestinal Tract. 2012. 1043-1088 p.

219. König J, Wells J, Cani PD, García-Ródenas CL, MacDonald T, Mercenier A, et al. Human Intestinal Barrier Function in Health and Disease. Clin Transl Gastroenterol. 2016;7(10):e196.

220. Nagao-Kitamoto H, Kitamoto S, Kuffa P, Kamada N. Pathogenic role of the gut microbiota in gastrointestinal diseases. Intest Res. 2016 Apr;14(2):127–38.

221. Lee SH. Intestinal Permeability Regulation by Tight Junction: Implication on Inflammatory Bowel Diseases. Intest Res. 2015;13(1):11–8.

222. Soler AP, Miller RD, Laughlin K V, Carp NZ, Klurfeld DM, Mullin JM. Increased tight junctional permeability is associated with the development of colon cancer. Carcinogenesis. 1999;20(8):1425–31.

223. Gong J, Hu M, Huang Z, Fang K, Wang D, Chen Q, et al. Berberine Attenuates Intestinal Mucosal Barrier Dysfunction in Type 2 Diabetic Rats. Front Pharmacol. 2017;8:42.

224. Cox AJ, Zhang P, Bowden DW, Devereaux B, Davoren PM, Cripps AW, et al. Increased intestinal permeability as a risk factor for type 2 diabetes. Diabetes Metab. 2016;43:2–5.

225. Li JY, Chassaing B, Tyagi AM, Vaccaro C, Luo T, Adams J, et al. Sex steroid deficiency-

associated bone loss is microbiota dependent and prevented by probiotics. J Clin Invest. 2016 Apr;126(6):2049–63.

226. Katz S, Weinerman S. Osteoporosis and gastrointestinal disease. Vol. 6, Gastroenterology and Hepatology. 2010. p. 506–17.

227. Holick MF. Resurrection of vitamin D deficiency and rickets. J Clin Invest. 2006;116(8):2062–72.

228. Lieben L, Masuyama R, Torrekens S, Looveren R Van, Schrooten J, Baatsen P, et al. Normocalcemia is maintained in mice under conditions of calcium malabsorption by vitamin D–induced inhibition of bone mineralization. J Clin Invest. 2012;122(5):1803–15.

229. Bronner F. Mechanisms of intestinal calcium absorption. In: Journal of Cellular Biochemistry. 2003. p. 387–93.

230. Kota S, Jammula S, Kota S, Meher L, Modi K. Correlation of vitamin D, bone mineral density and parathyroid hormone levels in adults with low bone density. Indian J Orthop. 2013;47(4):402.

231. Deplas A, Debiais F, Alcalay M, Bontoux D, Thomas P. Bone density, parathyroid hormone, calcium and vitamin D nutritional status of institutionalized elderly subjects. J Nutr Health Aging. 2004;8(5):400–4.

232. Neer RM, Arnaud CD, Zanchetta JR, Prince R, Gaich GA, Reginster J-Y, et al. Effect of Parathyroid Hormone (1-34) on Fractures and Bone Mineral Density in Postmenopausal Women with Osteoporosis. N Engl J Med. 2001;344(19):1434–41.

233. Jilka RL, Weinstein RS, Bellido T, Roberson P, Parfitt AM, Manolagas SC. Increased bone formation byprevention of osteoblast apoptosis with parathyroid hormone. J Clin Invest. 1999;104(4):439–46.

234. Motyl KJ, Mccabe LR. Amelioration of Type I Diabetes-induced Osteoporosis by Parathyroid Hormone is Associated with Improved Osteoblast Survival. J Cell Physilogy. 2014;227(4):1326–34.

235. de Vernejoul M-C, Collet C, Chabbi-Achengli Y. Serotonin: good or bad for bone. Bonekey Rep. 2012;1(May):1–6.

236. Gershon MD, Tack J. The Serotonin Signaling System: From Basic Understanding To Drug Development for Functional GI Disorders. Gastroenterology. 2007;132(1):397–414.

237. Yadav VK, Ryu JH, Suda N, Tanaka KF, Gingrich JA, Schütz G, et al. Lrp5 Controls Bone Formation by Inhibiting Serotonin Synthesis in the Duodenum. Cell. 2008;135(5):825–37.

238. Patricia D, Karsenty G. The two faces of serotonin in bone biology. J Cell Biol. 2010;191(1):7–13.

239. Yadav VK, Ducy P. Lrp5 and bone formation: A serotonin-dependent pathway. Ann N Y Acad Sci. 2010;1192:103–9.

240. Yadav VK, Oury F, Suda N, Liu ZW, Gao XB, Confavreux C, et al. A Serotonin-Dependent Mechanism Explains the Leptin Regulation of Bone Mass, Appetite, and Energy Expenditure. Cell. 2009;138(5):976–89.

241. Warden SJ, Fuchs RK. Do Selective Serotonin Reuptake Inhibitors (SSRIs) Cause Fractures? Curr Osteoporos Rep. 2016;14(5):211–8.

242. Wadhwa R, Kumar M, Talegaonkar S, Vohora D. Serotonin reuptake inhibitors and bone health: A review of clinical studies and plausible mechanisms. Osteoporos Sarcopenia. 2017;3(2):75–81.

243. Eom CS, Lee HK, Ye S, Park SM, Cho KH. Use of selective serotonin reuptake inhibitors and risk of fracture: A systematic review and meta-analysis. J Bone Miner Res. 2012;27(5):1186–95.

244. Leach MJ, Pratt NL, Roughead EE. Risk of Hip Fracture in Older People Using Selective Serotonin Reuptake Inhibitors and Other Psychoactive Medicines Concurrently: A Matched Case–Control Study in Australia. Drugs - Real World Outcomes. 2017;4(2):87–96.

245. Diem SJ, Blackwell TL, Stone KL, Cauley JA, Hillier TA, Haney EM, et al. Use of Antidepressant Medications and Risk of Fracture in Older Women. Calcif Tissue Int. 2011;88(6):474–84.

246. Chabbi-Achengli Y, Coudert AE, Callebert J, Geoffroy V, Cote F, Collet C, et al. Decreased osteoclastogenesis in serotonin-deficient mice. Proc Natl Acad Sci. 2012;109(7):2567–72.

247. Kieffer TJ, Habener JF. The glucagon-like peptides. Endocr Rev. 1999;20(6):876–913.

248. Drucker DJ. The biology of incretin hormones. Cell Metab. 2006;3(3):153–65.

249. Bollag RJ, Zhong Q, Phillips P, Min L, Zhong L, Cameron R, et al. Osteoblast-Derived Cells Express Functional Glucose- Dependent Insulinotropic Peptide Receptors. Endocr Rev. 2000;141(3):1228–35.

250. Gaudin-Audrain C, Irwin N, Mansur S, Flatt PR, Thorens B, Baslé M, et al. Glucose-dependent insulinotropic polypeptide receptor deficiency leads to modifications of trabecular bone volume and quality in mice. Bone. 2013;53(1):221–30.

251. Mieczkowska A, Irwin N, Flatt PR, Chappard D, Mabilleau G. Glucose-dependent insulinotropic polypeptide (GIP) receptor deletion leads to reduced bone strength and quality. Bone. 2013;56(2):337–42.

252. Xie D, Zhong Q, Ding KH, Cheng H, Williams S, Correa D, et al. Glucose-dependent insulinotropic peptide-overexpressing transgenic mice have increased bone mass. Bone. 2007;40(5):1352–60.

253. Nissen A, Christensen M, Knop FK, Vilsbøll T, Holst JJ, Hartmann B. Glucose-dependent insulinotropic polypeptide inhibits bone resorption in humans. J Clin Endocrinol Metab. 2014;99(11):E2325–9.

254. Pacheco-Pantoja EL, Ranganath LR, Gallagher JA, Wilson PJ, Fraser WD. Receptors and effects of gut hormones in three osteoblastic cell lines. BMC Physiol. 2011;11:1–14.

255. Yamada C, Yamada Y, Tsukiyama K, Yamada K, Udagawa N, Takahashi N, et al. The murine glucagon-like peptide-1 receptor is essential for control of bone resorption. Endocrinology. 2008;149(2):574–9.

256. Mabilleau G, Mieczkowska A, Irwin N, Flatt PR, Chappard D. Optimal bone mechanical and material properties require a functional glucagon-like peptide-1 receptor. J Endocrinol. 2013;219(1):59–68.

257. Nuche-Berenguer B, Moreno P, Esbrit P, Dapía S, Caeiro JR, Cancelas J, et al. Effect of GLP-1 treatment on bone turnover in normal, type 2 diabetic, and insulin-resistant states. Calcif Tissue Int. 2009;84(6):453–61.

258. Henriksen DB, Alexandersen P, Byrjalsen I, Hartmann B, Bone HG, Christiansen C, et al. Reduction of nocturnal rise in bone resorption by subcutaneous GLP-2. Bone. 2004;34(1):140–7.

259. Henriksen DB, Alexandersen P, Hartmann B, Adrian CL, Byrjalsen I, Bone HG, et al. Four-month treatment with GLP-2 significantly increases hip BMD. A randomized, placebo-controlled, dose-ranging study in postmenopausal women with low BMD. Bone. 2009;45(5):833–42.

260. Adrian TE, Ferri G-L, Bacarese-Hamilton AJ, Fuessl HS, Polak JM, Bloom SR. Human distribution and release of a putative new gut hormone, peptide YY. Gastroenterology. 1985;89(11):1070–7.

261. Dumont Y, Fournier A, ST-Pierre S, Quirion R. Characterization of neuropeptide Y binding sites in rat brain membrane preparations using [125I][Leu31,Pro34]peptide YY and [125I]peptide YY3-36 as selective Y1 and Y2 radioligands. J Pharmacol Exp Ther. 1994;272(2):673–80.

262. Marsh DJ, Hollopeter G, Kafer KE, Palmiter RD. Role of the Y5 neuropeptide Y receptor

in feeding and obesity. Nat Med. 1998;4:31–6.

263. Baldock PA, Sainsbury A, Couzens M, Enriquez RF, Thomas GP, Gardiner EM, et al. Hypothalamic Y2 receptors regulate bone formation. J Clin Invest. 2002;109(7):915–21.

264. Wortley KE, Garcia K, Okamoto H, Thabet K, Anderson KD, Shen V, et al. Peptide YY Regulates Bone Turnover in Rodents. Gastroenterology. 2007;133(5):1534–43.

265. Wong IPL, Driessler F, Khor EC, Shi YC, Hörmer B, Nguyen AD, et al. Peptide YY regulates bone remodeling in mice: A link between gut and skeletal biology. PLoS One. 2012;7(7).

266. Utz AL, Lawson EA, Misra M, Mickley D, Gleysteen S, Herzog DB, et al. Peptide YY (PYY) Levels and Bone Mineral Density (BMD) in Women with Anorexia Nervosa. Bone. 2008;43(1):135–9.

267. Qin J, Li R, Raes J, Arumugam M, Burgdorf S, Manichanh C, et al. A human gut microbial gene catalogue established by metagenomic sequencing. Nature. 2010;464(7285):59–65.

268. Huttenhower C, Gevers D, Knight R, Abubucker S, Badger JH, Chinwalla AT, et al. Structure, function and diversity of the healthy human microbiome. Nature. 2012 Jun 13;486(7402):207–14.

269. Jakobsson HE, Jernberg C, Andersson AAF, Sjölund-Karlsson M, Jansson JJK, Engstrand L, et al. Short-Term Antibiotic Treatment Has Differing Long-Term Impacts on the Human Throat and Gut Microbiome. Ratner AJ, editor. PLoS One. 2010 Mar;5(3):e9836.

270. Dethlefsen L, Relman DA. Incomplete recovery and individualized responses of the human distal gut microbiota to repeated antibiotic perturbation. Proc Natl Acad Sci. 2011 Mar;108(Supplement_1):4554–61.

271. Cryan JF, Dinan TG. Mind-altering microorganisms: the impact of the gut microbiota on brain and behaviour. Nat Rev Neurosci. 2012 Sep;13(10):701–12.

272. Kang SS, Jeraldo PR, Kurti A, Miller ME, Cook MD, Whitlock K, et al. Diet and exercise orthogonally alter the gut microbiome and reveal independent associations with anxiety and cognition. Mol Neurodegener. 2014 Sep;9(1):36.

273. Touchefeu Y, Montassier E, Nieman K, Gastinne T, Potel G, Bruley des Varannes S, et al. Systematic review: the role of the gut microbiota in chemotherapy- or radiation-induced gastrointestinal mucositis - current evidence and potential clinical applications. Aliment Pharmacol Ther. 2014 Jul;40(5):n/a-n/a.

274. Myers SP. The Causes of Intestinal Dysbiosis. Altern Med Rev xAltern Med Rev. 2004;99(22):180–97.

275. Takaishi H, Matsuki T, Nakazawa A, Takada T, Kado S, Asahara T, et al. Imbalance in intestinal microflora constitution could be involved in the pathogenesis of inflammatory bowel disease. Int J Med Microbiol. 2008 Jul;298(5–6):463–72.

276. Spiller RC. Role of infection in irritable bowel syndrome. J Gastroenterol. 2007 Jan;42 Suppl 1:41–7.

277. Evans CC, LePard KJ, Kwak JW, Stancukas MC, Laskowski S, Dougherty J, et al. Exercise Prevents Weight Gain and Alters the Gut Microbiota in a Mouse Model of High Fat Diet-Induced Obesity. Federici M, editor. PLoS One. 2014 Mar;9(3):e92193.

278. Scher JU, Abramson SB. The microbiome and rheumatoid arthritis. Nat Rev Rheumatol. 2011 Aug;7(10):569.

279. Arrieta MC, Bistritz L, Meddings JB. Alterations in intestinal permeability. Gut. 2006;55(10):1512–20.

280. Nenci A, Becker C, Wullaert A, Gareus R, van Loo G, Danese S, et al. Epithelial NEMO links innate immunity to chronic intestinal inflammation. Nature. 2007 Mar;446(7135):557–61.

281. Capaldo CT, Nusrat A. Cytokine regulation of tight junctions. Biochim Biophys Acta. 2009 Apr;1788(4):864–71.

282. Ozaki H, Ishii K, Horiuchi H, Arai H, Kawamoto T, Okawa K, et al. Cutting edge: combined treatment of TNF-alpha and IFN-gamma causes redistribution of junctional adhesion molecule in human endothelial cells. J Immunol. 1999 Jul;163(2):553–7.

283. Youakim A, Ahdieh M. Interferon-gamma decreases barrier function in T84 cells by reducing ZO-1 levels and disrupting apical actin. Am J Physiol. 1999 May;276(5 Pt 1):G1279-88.

284. Al-Sadi RM, Ma TY. IL-1beta causes an increase in intestinal epithelial tight junction permeability. J Immunol. 2007 Apr 1;178(7):4641–9.

285. Wrzosek L, Miquel S, Noordine M-L, Bouet S, Chevalier-Curt M, Robert V, et al. Bacteroides thetaiotaomicron and Faecalibacterium prausnitzii influence the production of mucus glycans and the development of goblet cells in the colonic epithelium of a gnotobiotic model rodent. BMC Biol. 2013 May;11(1):61.

286. Png CW, Lindén SK, Gilshenan KS, Zoetendal EG, McSweeney CS, Sly LI, et al. Mucolytic Bacteria With Increased Prevalence in IBD Mucosa Augment In Vitro Utilization of Mucin by Other Bacteria. Am J Gastroenterol. 2010 Nov;105(11):2420–8.

287. van der Post S, Subramani DB, Backstrom M, Johansson ME V., Vester-Christensen MB, Mandel U, et al. Site-specific O-Glycosylation on the MUC2 Mucin Protein Inhibits

Cleavage by the Porphyromonas gingivalis Secreted Cysteine Protease (RgpB). J Biol Chem. 2013 May;288(20):14636–46.

288. Sun J, Shen X, Li Y, Guo Z, Zhu W, Zuo L, et al. Therapeutic Potential to Modify the Mucus Barrier in Inflammatory Bowel Disease. Nutrients. 2016 Jan;8(1).

289. Yan J, Herzog JW, Tsang K, Brennan CA, Bower MA, Garrett WS, et al. Gut microbiota induce IGF-1 and promote bone formation and growth. Proc Natl Acad Sci. 2016 Nov 22;E(47):E7554–63.

290. Villa CR, Ward WE, Comelli EM. Gut Microbiota-bone Axis. Crit Rev Food Sci Nutr. 2015;

291. Sjögren K, Engdahl C, Henning P, Lerner UH, Tremaroli V, Lagerquist MK, et al. The gut microbiota regulates bone mass in mice. J Bone Miner Res. 2012 Jun;27(6):1357–67.

292. Novince CM, Whittow CR, Aartun JD, Hathaway JD, Poulides N, Chavez MB, et al. Commensal Gut Microbiota Immunomodulatory Actions in Bone Marrow and Liver have Catabolic Effects on Skeletal Homeostasis in Health. Sci Rep. 2017;7(1):5747.

293. Quach D, Collins F, Parameswaran N, McCabe L, Britton RA, Bidwell J, et al. Microbiota Reconstitution Does Not Cause Bone Loss in Germ-Free Mice. mSphere. 2018;3(1):e00545-17.

294. Macpherson AJ, Hunziker L, McCoy K, Lamarre A. IgA responses in the intestinal mucosa against pathogenic and non-pathogenic microorganisms. Microbes Infect. 2001;3(12):1021–35.

295. Ohlsson C, Nigro G, Boneca IG, Bäckhed F, Sansonetti P, Sjögren K. Regulation of bone mass by the gut microbiota is dependent on NOD1 and NOD2 signaling. Cell Immunol. 2017;317:55–8.

296. Cho I, Yamanishi S, Cox L, Methé BA, Zavadil J, Li K, et al. Antibiotics in early life alter the murine colonic microbiome and adiposity. Nature. 2012 Aug;488(7413):621–6.

297. Cox LM, Yamanishi S, Sohn J, Alekseyenko A V, Leung JM, Cho I, et al. Altering the intestinal microbiota during a critical developmental window has lasting metabolic consequences. Cell. 2014;158(4):705–21.

298. Nobel YR, Cox LM, Kirigin FF, Bokulich NA, Yamanishi S, Teitler I, et al. Metabolic and metagenomic outcomes from early-life pulsed antibiotic treatment. Nat Commun. 2015;6.

299. Guss JD, Horsfield MW, Fontenele FF, Sandoval TN, Luna M, Apoorva F, et al. Alterations to the Gut Microbiome Impair Bone Strength and Tissue Material Properties. J Bone Miner Res. 2017;32(6):1343–53.

300. Schepper JD, Collins FL, Rios-Arce ND, Raehtz S, Schaefer L, Gardinier JD, et al. Probiotic Lactobacillus reuteri Prevents Postantibiotic Bone Loss by Reducing Intestinal Dysbiosis and Preventing Barrier Disruption. J Bone Miner Res. 2019;1–18.

301. Rathbone CR, Cross JD, Brown K V., Murray CK, Wenke JC. Effect of various concentrations of antibiotics on osteogenic cell viability and activity. J Orthop Res. 2011;29(7):1070–4.

302. Hill C, Guarner F, Reid G, Gibson GR, Merenstein DJ, Pot B, et al. Expert consensus document: the International Scientific Association for Probiotics and Prebiotics consensus statement on the scope and appropriate use of the term probiotic. Nat Rev Gastroenterol Hepatol. 2014;11(2):506–14.

303. Schepper JD, Irwin R, Kang J, Dagenais K, Lemon T, Shinouskis A, et al. Probiotics in Gut-Bone Signaling. Adv Exp Med Biol. 2017;225–47.

304. Macfarlane S, Macfarlane GT, Cummings JH. Review article: prebiotics in the gastrointestinal tract. Aliment Pharmacol Ther. 2006 Sep;24(5):701–14.

305. Kechagia M, Basoulis D, Konstantopoulou S, Dimitriadi D, Gyftopoulou K, Skarmoutsou N, et al. Health Benefits of Probiotics: A Review. ISRN Nutr. 2012;2013:11–7.

306. Markowiak P, Ślizewska K. Effects of probiotics, prebiotics, and synbiotics on human health. Nutrients. 2017;9(9).

307. Mutus R, Kocabagli N, Alp M, Acar N, Eren M, Gezen SS. The effect of dietary probiotic supplementation on tibial bone characteristics and strength in broilers. Poult Sci. 2006;85(9):1621–5.

308. Rodrigues FC, Castro ASB, Rodrigues VC, Fernandes SA, Fontes EAF, de Oliveira TT, et al. Yacon Flour and *Bifidobacterium longum* Modulate Bone Health in Rats. J Med Food. 2012;15(7):664–70.

309. McCabe LR, Irwin R, Schaefer L, Britton RA. Probiotic use decreases intestinal inflammation and increases bone density in healthy male but not female mice. J Cell Physiol. 2013 Aug;228(8):1793–8.

310. Collins FL, Irwin R, Bierhalter H, Schepper J, Britton RA, Parameswaran N, et al. Lactobacillus reuteri 6475 increases bone density in intact females only under an inflammatory setting. PLoS One. 2016;11(4).

311. Tyagi AM, Yu M, Darby TM, Vaccaro C, Li J-Y, Owens JA, et al. The Microbial Metabolite Butyrate Stimulates Bone Formation via T Regulatory Cell-Mediated Regulation of WNT10B Expression. Immunity. 2018;1–16.

312. Britton RA, Irwin R, Quach D, Schaefer L, Zhang J, Lee T, et al. Probiotic L. reuteri

Treatment Prevents Bone Loss in a Menopausal Ovariectomized Mouse Model. J Cell Physiol. 2014 Nov;229(11):1822–30.

313. Ohlsson C, Engdahl C, Fak F, Andersson A, Windahl SH, Farman HH, et al. Probiotics protect mice from ovariectomy-induced cortical bone loss. PLoS One. 2014 Jan;9(3):e92368.

314. Nilsson AG, Sundh D, Bäckhed F, Lorentzon M. *Lactobacillus reuteri* reduces bone loss in older women with low bone mineral density - a randomized, placebo-controlled, double-blind, clinical trial. J Intern Med. 2018;0–3.

315. Narva M, Nevala R, Poussa T, Korpela R. The effect of Lactobacillus helveticus fermented milk on acute changes in calcium metabolism in postmenopausal women. Eur J Nutr. 2004;43(2):61–8.

316. Jafarnejad S, Djafarian K, Fazeli MR, Yekaninejad MS, Rostamian A, Keshavarz SA. Effects of a Multispecies Probiotic Supplement on Bone Health in Osteopenic Postmenopausal Women: A Randomized, Double-blind, Controlled Trial. J Am Coll Nutr. 2017;36(7):497–506.

317. Parvaneh K, Ebrahimi M, Sabran MR, Karimi G, Hwei ANM, Abdul-Majeed S, et al. Probiotics (*Bifidobacterium longum*) Increase Bone Mass Density and Upregulate *Sparc* and *Bmp-2* Genes in Rats with Bone Loss Resulting from Ovariectomy. Biomed Res Int. 2015;2015:1–10.

318. Bianchi ML. Inflammatory bowel diseases, celiac disease, and bone. Vol. 503, Archives of Biochemistry and Biophysics. Elsevier Inc.; 2010. p. 54–65.

319. Dar HY, Shukla P, Mishra PK, Anupam R, Mondal RK, Tomar GB, et al. Lactobacillus acidophilus inhibits bone loss and increases bone heterogeneity in osteoporotic mice via modulating Treg-Th17 cell balance. Bone Reports. 2018;8(July 2017):46–56.

Chapter 2. Loss of interleukin 10 exacerbates early type 1 diabetes-induced bone loss.

This chapter has been submitted for publication in the *Journal of* Cellular Physiology.

Authors: **Naiomy Deliz Rios-Arce**, Andrew Dagenais, Derrick Feenstra, Brandon Coughlin, Susanne Mohr, Laura R. McCabe, Narayanan Parameswaran.

2.1 Abstract

Type-1 diabetes (T1D) increases systemic inflammation, bone loss, and risk for bone fractures. Levels of the anti-inflammatory cytokine IL-10 are decreased in T1D, however their role in T1D-induced osteoporosis is unknown. To address this, diabetes was induced in male IL-10 knockout (KO) and wild-type (WT) mice. Analyses of femur and vertebral trabecular bone volume fraction (BVF) identified bone loss in T1D-WT mice at 4- and 12-weeks which in T1D-IL-10-KO mice was further reduced at 4 but not 12 weeks. IL-10 deficiency also increased the negative effects of T1D on cortical bone. Osteoblast marker, osterix was decreased while osteoclast markers were unchanged, suggesting that IL-10 promotes anabolic processes. MC3T3-E1 osteoblasts cultured under high glucose conditions displayed a decrease in osterix which was prevented by addition of IL-10. Together, our results suggest that IL-10 is important for promoting osteoblast maturation and reducing bone loss during early stages of T1D.

2.2 Introduction

Diabetes mellitus is a chronic metabolic disease that occurs when the pancreatic β-cells do not produce sufficient insulin or when the body is unable to utilize the insulin. It affects millions of people in the US and worldwide and its prevalence is increasing at an alarming rate (1). While type 1 diabetes (T1D) is characterized by destruction of pancreatic β-cells by autoreactive T-cells, type 2 diabetes (T2D) is characterized by insulin resistance (2,3). The systemic hyperglycemia, metabolic derrangements and inflammation that occur in diabetes lead to a number of complications including nephropathy, cardiomyopathy, neuropathy, retinopathy and osteoporosis. Bone loss is an increasing concern for diabetic patients, especially T1D, which has been reported to increase the risk of hip fracture by 2-8 fold (4–7). T1D animal models also display reduced bone formation and bone loss similar to humans (8–14). T1D-induced bone loss can be exacerbated by factors such as estrogen deficiency (15), drug therapies (16,17) and inflammation (18).

Bone remodeling is a highly-regulated process that requires precise balance between osteoblasts (bone forming cells) and osteoclasts (bone resorbing cells). Imbalance in this process can lead to bone loss. We and others have shown that T1D bone loss is associated with an anabolic defect characterized by decreased osteoblast lineage selection and differentiation as well as increased osteoblast death (9,18,19). Both T1D patients and mouse models exhibit decreased levels of serum osteocalcin (osteoblast marker). In addition, as a result of altered lineage selection and lower Wnt10B signaling, T1D mice display increased bone marrow adiposity (19–23). T1D effect on osteoclast activity however, is less clear and dependent on the specific animal model used and disease severity (19,24,25). Bone remodeling is also modulated by many factors including cytokines (15,18,26–28). A role for inflammatory cytokines in T1D bone pathology has been suggested by systemic and local increases in cytokines during the pathogenesis of T1D (18,29–31). Circulating interferon gamma (IFN-γ) has been shown to be increased with age in the non-

obese diabetic (NOD) animal model (31). However, IFN-γ deficient mice are not protected from T1D induced bone loss, suggesting potential compensation by, or role for other cytokines in T1D effects on bone density (18). Several studies including ours have shown that levels of tumor necrosis factor alpha (TNF-α) are increased and play an important role in diabetes induced bone loss (15,18,32,33). Furthermore, we have also demonstrated an increase in expression of IFN-γ, interleukin-1 (IL-1) and interleukin-6 (IL-6) in the bone of T1D male mice (18). Also, during estrogen deficiency along with T1D, high levels of TNF-α correlated with bone loss and osteoblast death (15). Studies have also shown that inhibition of TNF-α during diabetes can prevent a decrease in callus bone formation induced by T1D (33). In contrast to increases in pro-inflammatory cytokines, the anti-inflammatory cytokine IL-10 has been shown to be markedly decreased prior to diabetic onset in the NOD mice (31). Interestingly, administration of IL-10 protected NOD mice from developing diabetes (34). Similar to NOD mice, diabetic patients exhibit significantly low serum IL-10 compared to non-diabetic subjects (35). In spite of these studies on IL-10 levels in diabetes, role of IL-10 in the bone during diabetes is not known.

Previous studies have demonstrated an important role for IL-10 in bone homeostasis (36–40). Studies have found that IL-10 KO mice, in addition to showing features of colitis, also demonstrate systemic skeletal disease with reduced bone mass, decreased bone formation and increased mechanical fragility (36–40). Bone loss in IL-10 KO mice was more severe in mice with colitis compared to mice without colitis (40). Similarly, 9-months old IL-10 KO mice have accelerated alveolar bone loss compared to age matched WT controls (36). While the mechanisms by which IL-10 regulates bone health is not completely understood, IL-10 has been shown to have direct effects on both osteoblasts (increase in osteoblast differentiation) and osteoclasts (inhibit osteoclast differentiation) (40–43). Even though past studies have shown that IL-10 levels are decreased during T1D and that IL-10 has direct effects on osteoblasts and osteoclasts, the role of

IL-10 in T1D-mediated bone pathology is not known. We demonstrate here that IL-10 regulation of osteoblasts plays an important role in T1D-induced bone loss during early but not later stages of disease.

2.3 Materials and Methods

2.3.1 Animals and experimental design

B6.129P2-*Il10*^{tm1Cgn}/J mutant mice (IL-10$^{-/-}$) and C57BL/6J male mice (6-7 weeks old) were purchased from Jackson Laboratories (Bar Harbor, Maine). Mice were allowed to acclimate to animal facility for 1-week prior to start of the experiment. After this period mice were randomly divided into four groups (8-10 per group): wild-type control, wild-type type 1 diabetes, IL-10$^{-/-}$ control and IL-10$^{-/-}$ type 1 diabetes. To induce diabetes, mice were injected (intraperitoneally) with 65 mg/kg body weight streptozotocin (STZ) for 5 consecutive days. Control mice received 0.1 M sodium citrate buffer (vehicle) for the same time period. Insulin injections (0.1 unit) were given to mice that lost 15% of their body weight. Blood glucose was measured four weeks after the first injection with an AccuChek compact glucometer (Roche), by collecting a drop of blood from the pedal dorsal vein. Mice with a blood glucose of >250 mg/dL were considered diabetic. Mice (4 - 5 per cage) were maintained on a 12-hour light/dark cycle at 23^{o}C and provided food and water ad libitum. Tissues were collected at 1- and 3-months after the first injection. All animal procedures were approved by the Michigan State University Institutional Animal Care and Use Committee and conformed to NIH guidelines.

2.3.2 µCT bone imaging

At harvest, femur and vertebrate bones were fixed in 10% formalin for 24 hours. After 24 hours, bones were transferred to 70% ethanol and scanned using a GE Explore Locus microcomputed tomography (µCT) system at a voxel resolution of 20 µm obtained from 720 views. The beam angle of increment was 0.5, and beam strength was set at 80 peak kV and 450 µA. Each run included bones from WT, KO (control and T1D groups), as well as a calibration phantom to standardize gray scale values and maintain consistency. Bone measurements were performed blind. On the basis of auto-threshold and isosurface analyses of multiple bone samples, a fixed

threshold (799) was used to separate bone from bone marrow. Femur trabecular bone analyses were performed from ~ 1% of the total length proximal to the growth plate, extending 10% of bone length toward the diaphysis and excluding the cortical bone. Trabecular bone mineral content (BMC), bone mineral density (BMD), percent bone volume fraction (% BVF), trabecular thickness (Tb. Th), spacing (Tb. Sp), and number (Tb. N) were computed using GE Healthcare MicroView software. Femoral trabecular isosurface images were taken from a region in the femur where analyses were performed measuring 1.0 mm in length and 1.0 mm in diameter. For vertebral analysis, the third lumbar vertebrae were used. Cortical measurements were performed in a 2x2x2 mm cube centered midway down the length of the bone.

2.3.3 Bone and colon RNA analysis

Immediately after euthanasia, bone samples were cleaned of all muscle and connective tissue, snap frozen in liquid nitrogen and stored at −80°C until RNA extraction (15). Colon samples were flushed of their contents with 1X PBS and frozen in liquid nitrogen and stored at -80 C until further processing (44). Frozen tissues were crushed under liquid nitrogen conditions using the Bessman Tissue Pulverizer (Spectrum Laboratories, Rancho Dominguez, CA). TriReagent (Molecular Research Center, Cincinnati, OH) was used to isolate RNA and RNA integrity was verified by agarose-gel electrophoresis. cDNA was synthesized by reverse transcription using Superscript II Reverse Transcriptase Kit and oligo dT primers (Invitrogen, Carlsbad, CA). Complementary DNA was amplified by PCR using iQ SYBR Green supermix (Bio-Rad Laboratories, Hercules, CA). Real time PCR was carried out for 40 cycles (95^{o} C for 15 seconds, 60^{o} C for 30 seconds, and 72^{o} C for 30 seconds) using an iCycler thermal cycler and data evaluated using the iCycler software. Negative controls included primers without cDNA. RNA levels of the housekeeping gene hypoxanthine guanine phosphoribosyl transferase (HPRT) did not fluctuate with treatment and were used as an internal control. Primers used for real-time polymerase chain

reaction are listed in Table 2.1.

2.3.4 *In vitro* cell culture system

Preosteoblast MC3T3-E1 cells (CRL-2593; ATCC, Manassas, VA) (passages between 18 to 24) were plated at a density of 3.9 x 10^3 cm^2 with α–minimal essential media (α-MEM) containing 10% fetal bovine serum (FBS) (Invitrogen and Atlanta Biologicals, Atlanta, GA) and 1% Penicillin-Streptomycin (Life Technologies). Cell media was changed every other day. After confluency, cells were treated with α-MEM with low (5 mM) and high (30mM) glucose for 3 days. Cells were then treated with 50 ng/ml recombinant murine IL-10 (Peprotech) for 24 hours. Cells were harvested with TriReagent (Molecular Research Center Inc.) and RNA extracted and analyzed as previously described.

2.3.5 *In vitro* cell protein extraction and Western blotting

Preosteoblast MC3T3-E1 cells (CRL-2593; ATCC, Manassas, VA) (passages between 18 to 24) were treated with low (5 mM) and high (30 mM) glucose for 3 days. Cells were then stimulated with 50 ng/ml recombinant murine IL-10 (Peprotech) for the indicated time points. Cells were lysed with lysis buffer containing 1% Triton X-100, protease and phosphatase inhibitors. Protein concentrations were determined using Bradford and equivalent protein (50 µg) was loaded into the wells of SDS-PAGE gels for western blot analysis. Blots were probed with antibodies diluted in LiCor blocking buffer (LiCor) or 5% BSA. Primary antibodies were against pERK1/2, p-JNK1/2, JNK1/2, and p-P38 (Cell Signaling Technology Inc. (Danvers, MA)), ERK-2 and tubulin (Santa Cruz). For immunoblotting, the secondary antibodies were IR-dye or HRP conjugated and analyzed by Licor's Odyssey or chemiluminescence respectively. The bands were quantified using Licor's Odyssey program (for IR dye) or densitometry (Image J for chemiluminescence).

2.3.6 Statistical Analysis

Data are presented as mean ± standard error or as box-plots (5-95 percentile) as indicated. Statistical analysis was performed using Student's t-test (two group comparisons) or ANOVA (more than 2 groups) with GraphPad Prism software version 7 (GraphPad, San Diego, CA, USA). Significant outliers (if present and indicated in figure legend) were removed using the ROUT test for outliers. A p-value < 0.05 was considered statistically significant.

Gene	Forward (5'-3')	Reverse (5'-3')
HPRT	AAGCCTAAGATGAGCGCAAG	TTACTAGGCAGATGGCCACA
TNFa	AGGCTGCCCCGACTACGT	GACTTTCTCCTGGTATGAGATAGCAA
Osteocalcin	AAGCAGGAGGGCAATAAGGT	TAGGCGGTCTTCAAGCCAT
Osterix	CTGCGGAAAGGAGGCACA AAGAAG	GGGTTAAGGGGAGCAAAGTCAGAT
TRAP	AATGCCTCGACCTGGGA	CGTAGTCCTCCTTGGCTGCT
Wnt10b	AATGCGGATCCACAACAACA	TTCCATGGCATTTGCACTTC
aP2	GCGTGGAATTCGATGAAATCA	CCCGCCATCTAGGGTTATGA
RUNX2	GACAGAAGCTTGATGACTCTAAACC	TCTGTAATCTGACTCTGTCCTTGTG
IL-6	ATCCAGTTGCCTTCTTGGGACTGA	TAAGCCTCCGACTTGTGAAGTGGT
IFNg	GGCTGTCCCTGAAAGAAAGC	GAGCGAGTTATTTGTCATTCGG

Table 2.1. List of genes measured and primer sequence for RT-PCR

2. 4 Results

2.4.1 Wild type and IL-10 knockout mice exhibit similar blood glucose levels

To induce T1D hyperglycemic conditions in mice, we used streptozotocin (STZ) a pharmacological compound (derived from *Streptomyces achromogenes)* that causes pancreatic β cell destruction and consequent marked hypoinsulinemia and hyperglycemia (45). Male mice, 7 to 8-week-old wild type (WT) and IL-10 knockout (KO) (both in C57BL/6J background), were injected with 65 mg of STZ per kilogram body weight for 5 consecutives days. Control mice received equal volume of vehicle (sodium citrate buffer). To confirm diabetes, blood glucose was measured 1 month after the first STZ injection. Blood glucose was significantly increased in both WT and KO groups ($p<0.0001$), whereas WT and KO control mice maintained normal blood glucose levels <200 mg/dL. No differences in blood glucose levels were observed between T1D WT and KO groups (Figure 2.1 A). As expected, T1D WT mice had decreased body weight compared to corresponding control mice ($p< 0.0001$) (19). Although control WT and KO groups did not differ in body weight, T1D KO mice lost significantly more weight compared to T1D WT mice at this time point ($p< 0.05$) (Figure 2.1 B).

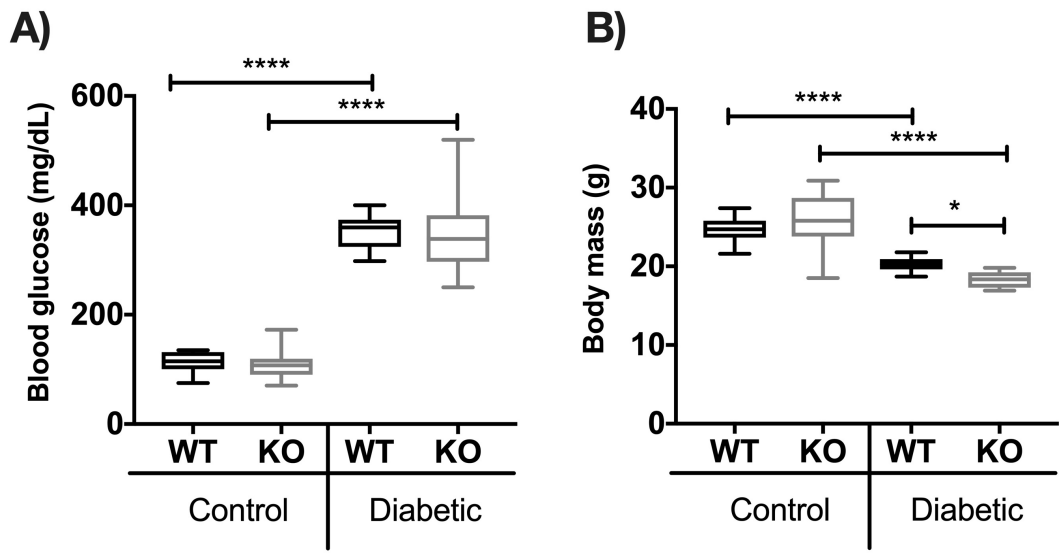

Figure 2.1. Induction of Type 1 diabetes with streptozotocin (STZ) in WT and IL-10 knockout mice.

C57BL/6 (WT) and IL-10 knockout (KO) mice were treated with citrate buffer (vehicle control) or STZ (diabetic) for 5 consecutives days. (A) Blood glucose levels (mg/dL) and (B) body weight in grams (g) were measured 4 weeks after the first STZ injection**.** Whiskers in the box plot represent 5-95 percentile values; n= 9-10 per group. *$p<0.05$, ****$p<0.0001$. Statistical analysis performed by One-way ANOVA followed by Fisher's LSD post-test. WT=wild type, KO= IL-10 knockout mice.

2.4.2 IL-10 deficiency enhances T1D-induced trabecular and cortical bone loss.

Bone density and structural parameters at the 1 month time point were assessed using microcomputed tomography (μCT). Distal femoral trabecular bone (Figure 2.2) and diaphyseal cortical bone (Figure 2.3) showed no significant differences between control WT and KO groups, suggesting that IL-10 is not essential for normal bone homeostasis in this age group. However, femur trabecular bone volume fraction (BVF corrected to body weight) was significantly decrease in T1D WT mice compared to control WT mice ($p<0.01$). Similarly, the KO diabetic group also displayed significant trabecular bone loss compared to KO control mice ($p<0.01$). When analyzed against the respective WT cohorts, trabecular bone loss in the T1D KO mice was significantly greater compared to the T1D WT mice ($p<0.05$; Figure 2.2 C). These results suggest that IL-10 plays an important role in preventing femur trabecular bone loss during diabetes and that loss of IL-10 exacerbates T1D bone loss. Further analyses of bone trabecular micro-architecture indicated a decrease in bone mineral density, trabecular thickness, number and an increase in trabecular spacing in the WT diabetic group compared to WT control mice. These parameters were exacerbated in the KO diabetic compared to WT diabetic mice. (Figure 2.2 D-H, table 2.2). Deficiency of IL-10 also increased the negative effects of T1D on cortical bone. Specifically, KO mice displayed less cortical area ($p<0.05$; Figure 2.3 C), bone mineral content ($p<0.001$), density ($p<0.001$), and thickness ($p<0.05$) when compared to the T1D WT group (Figure 2.3 A-I, table 2.2). To assess if these effects are bone site-specific we examined trabecular bone of the 3rd lumbar vertebrae using μCT analysis. Vertebrae from T1D WT mice showed a modest decrease in BVF compared to the WT controls (Figure 2.4 A-B). Importantly, the KO diabetic group exhibited a significant decrease in vertebral BVF compared to control KO mice vertebrae (Figure 2.4 A-B, table 2.2). When analyzed relative to the respective WT mouse groups, vertebral trabecular bone loss was significantly greater in the KO diabetic mice (Figure 2.4 C). Together, these data

demonstrate that lack of IL-10 can exacerbate T1D bone loss in femur and vertebrae.

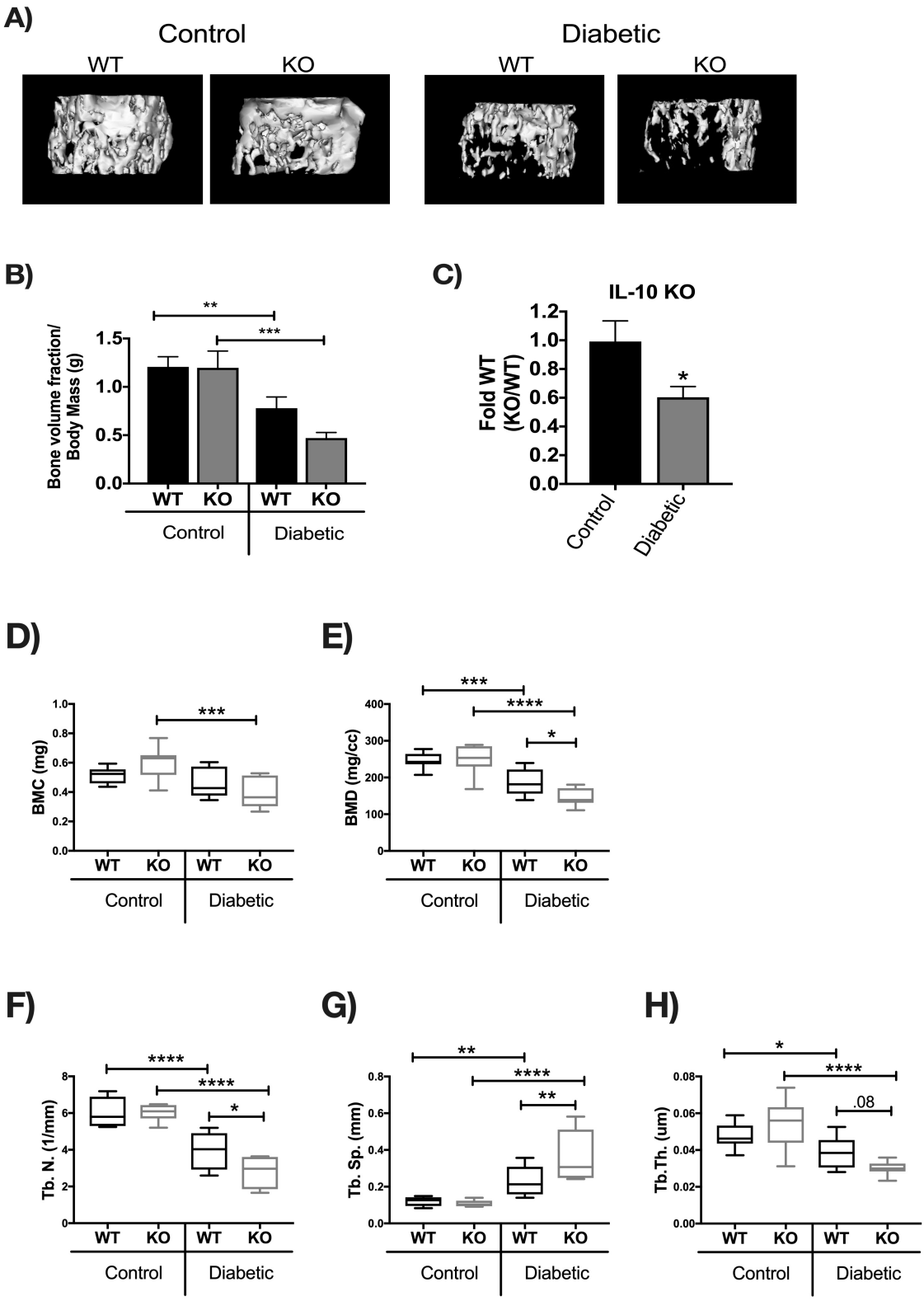

Figure 2.2. IL-10 knockout exacerbates trabecular bone loss 1 month after diabetes induction.

Figure 2.2. (cont'd)

Control and STZ treated WT and IL-10 knockout mice were euthanized 4 weeks after the first STZ injection. Femoral bones were collected and trabecular bone analyzed by uCT. (A) Representative micro-computed tomography isosurface images. (B) Bone volume fraction (corrected for weight loss). (C) Bone volume fraction (corrected for weight loss) from the KO group normalized to respective WT groups. * represent $p<0.05$ by T-test against WT diabetic group. (D) Bone mineral content (mg). (E) Bone mineral density (mg/cc). (F) Trabecular number (Tb. N, 1/mm). (G) Trabecular space (Tb. Sp, mm). (H) Trabecular thickness (Tb. Th, um). Bar graphs values are averages ± standard error; Whiskers in box plots represent 5-95 percentile values; n= 7-9 per group. *$p<0.05$, **$p<0.01$, ***$p<0.001$, ****$p<0.0001$. Statistical analysis performed by One-way ANOVA followed by Fisher's LSD post-test. WT=wild type, KO= IL-10 knockout mice.

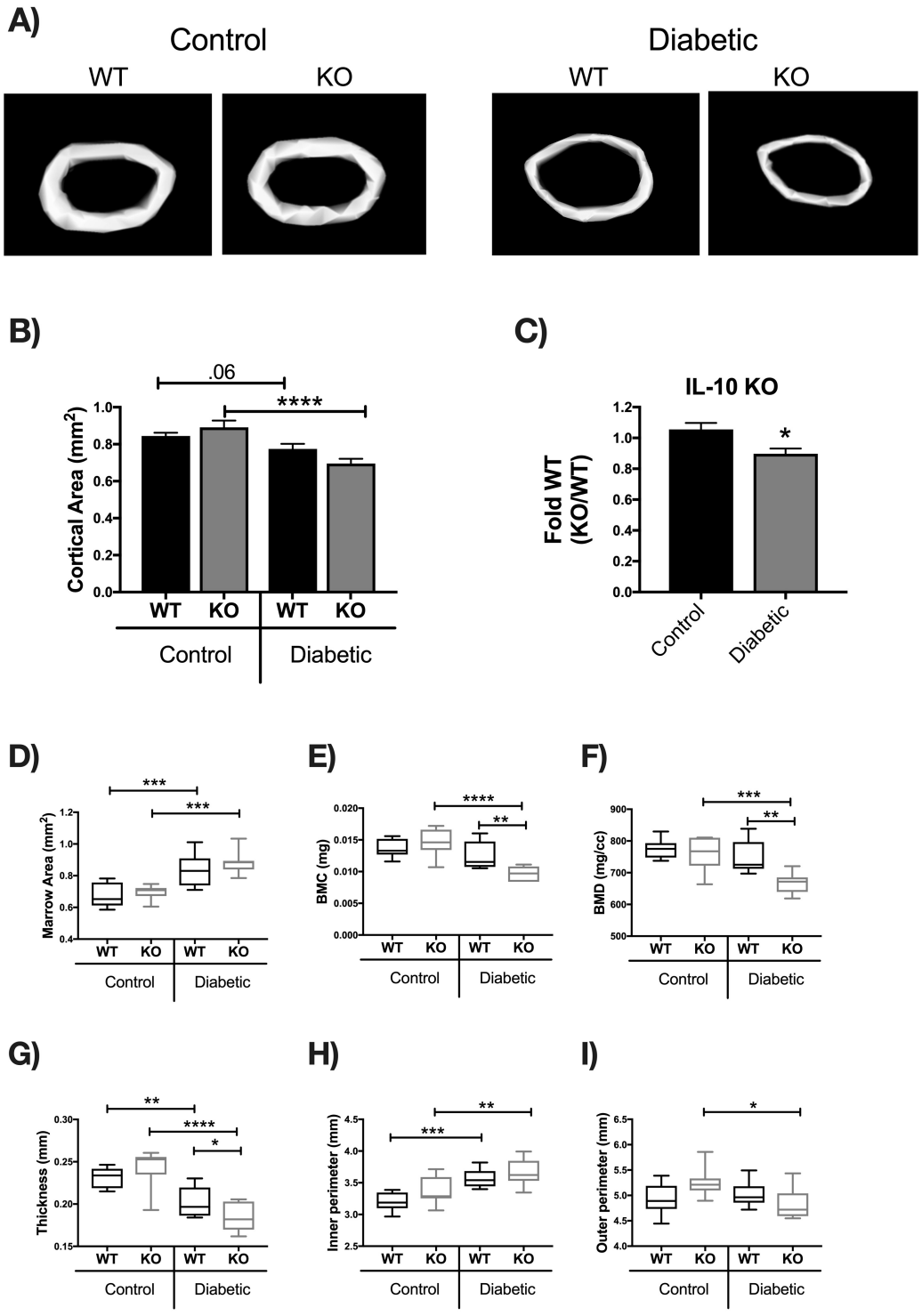

Figure 2.3. IL-10 deficiency exacerbates T1D-induced cortical bone loss 1 month after diabetes induction.

Figure 2.3. (cont'd)

Cortical bone analysis were performed using μCT, on femoral bones described in Figure 2. (A) Representative micro-computed tomography isosurface images. (B) Cortical area (mm^2). (C) Cortical area from the KO groups normalized to respective WT groups. * represent $p<0.05$ by T-test against WT diabetic group. (D) Marrow area (mm^2). (E) Bone mineral content (mg). (F) Bone mineral density (mg/cc). (G) Cortical thickness (mm). (H) Inner perimeter (mm). (I) Outer perimeter. Bar graphs values are averages ± standard error; Whiskers in box plots represent 5-95 percentile values; n= 7-9 per group. *$p<0.05$, **$p<0.01$, ***$p<0.001$, ****$p<0.0001$. Statistical analysis performed by One-way ANOVA followed by Fisher's LSD post-test. WT=wild type, KO= IL-10 knockout mice.

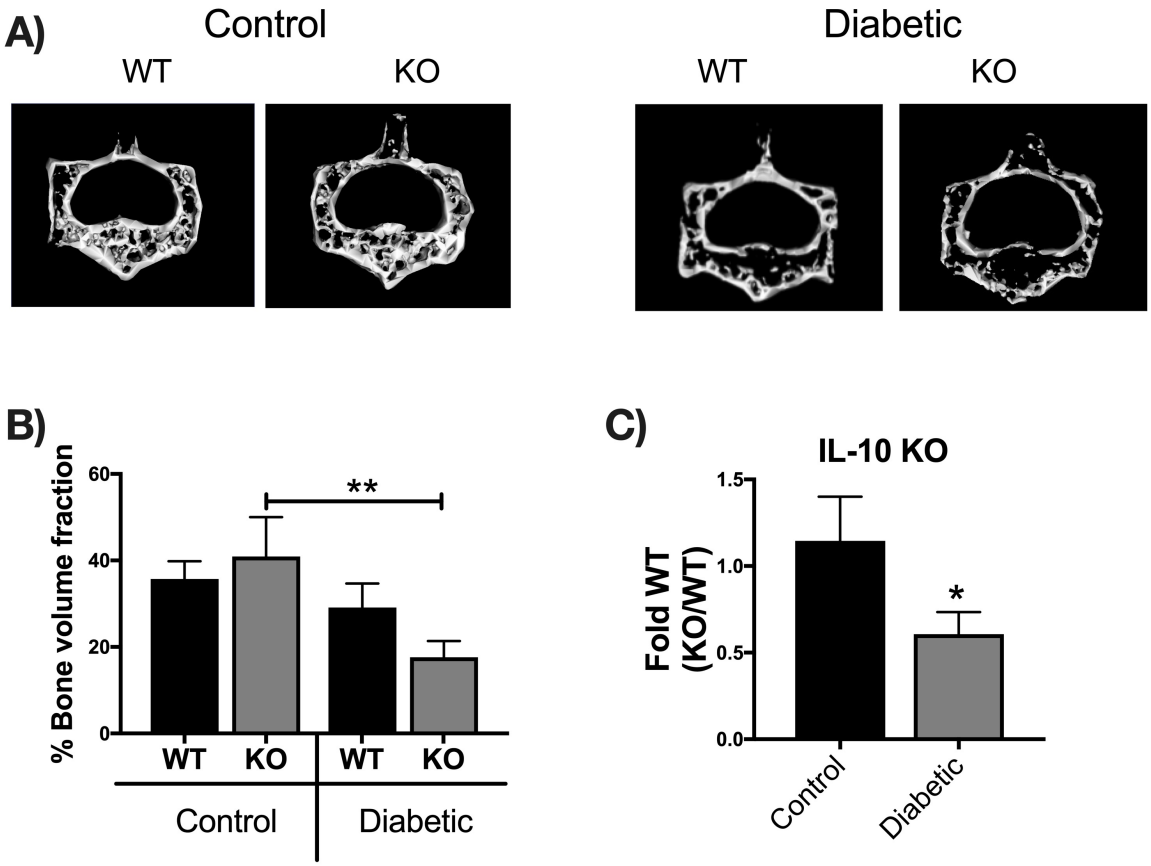

Figure 2.4. IL-10 knockout exacerbates vertebral trabecular bone loss 1 month after diabetes induction.

Vertebral bones were collected from mice groups described in Fig 2.2 and μCT analysis performed from the third lumbar vertebral body to assess trabecular bone. (A) Representative micro-computed tomography isosurface images. (B) Percent bone volume fraction and (C) bone volume fraction from the KO groups normalized to respective WT groups. * represent $p<0.05$ by T-test against WT diabetic group. Bar graphs values are averages ± standard error; n= 5-7 per group. *$p<0.05$, **$p<0.01$. Statistical analysis performed by One-way ANOVA followed by Fisher's LSD post-test. WT=wild type, KO=IL-10 knockout mice.

	Control		Diabetes	
Parameter: 1 month	WT	KO	WT	KO
Femur trabecular	**n=9**	**n=7**	**n=8**	**n=7**
BV/TV	29.11 ± 2.28	31.75 ± 4.36	15.86 ± 2.49#	8.70 ± 1.1 #*^
Tb. N. (1/mm)	6.066 ± 0.2745	6.030 ± 0.1902	3.947 ± 0.3575 #	2.808 ± 0.3024#*^
Tb. Th. (µm)	0.04768 ± 0.002295	0.05465 ± 0.005257	0.03862 ± 0.002988#	0.03031 ± 0.001496#*^
Tb. Sp. (mm)	0.1198 ± 0.008494	0.1328 ± 0.02549	0.2311 ± 0.02850#	0.3575 ± 0.05107#*^
BMD (mg/cc)	245.5 ± 7.267	249.7 ± 15.85	186.9 ± 12.70#	147.6 ± 9.583#*^
BMC (mg)	0.5135 ± 0.01820	0.5916 ± 0.04344	0.4575 ± 0.03558	0.3932 ± 0.03741#
Femur cortical				
Ct.Ar (mm^2)	0.8449 ± 0.01722	0.8915 ± 0.03604	0.7745 ± 0.02785	0.6953 ± 0.02603*^
Ma.Ar (mm^2)	0.6765 ± 0.02444	0.6950 ± 0.01762	0.8346 ± 0.03555#	0.8827 ± 0.02897*
Ct.Th (mm)	0.2311 ± 0.003951	0.2411 ± 0.008911	0.2021 ± 0.006329#	0.1827 ± 0.006381*^
Inner Perimeter (mm)	3.205 ± 0.04674	3.358 ± 0.08314	3.573 ± 0.05019#	3.653 ± 0.07993*
Outer Perimeter (mm)	4.923 ± 0.1009	5.258 ± 0.1129	5.015 ± 0.08671	4.844 ± 0.1203*
BMD (mg/cc)	772.8 ± 10.22	757.1 ± 19.55	745.9 ± 18.33	667.1 ± 12.55*^
BMC (mg)	0.01376 ± 0.000461	0.01459 ± 0.0008116	0.01236 ± 0.0007725	0.0096 ± 0.0004192*^
Vertebrate trabecular	**n=5**	**n=6**	**n=5**	**n=7**
BV/TV	35.08 ± 4.111	40.47 ± 9.086	28.48 ± 5.503	17.13 ± 3.652*
Tb. N.(1/mm)	8.665 ± 0.4628	7.336 ± 0.7394	7.57 ± 0.6047	5.855 ± 0.881
Tb. Th. (µm)	0.03995 ± 0.003171	0.05176 ± 0.009047	0.03635 ± 0.004281	0.02757 ± 0.001999*
Tb. Sp. (mm)	0.07689 ± 0.00951	0.09295 ± 0.02455	0.0994 ± 0.01545	0.1674 ± 0.02966*^
BMD (mg/cc)	267.2 ± 13.98	279.3 ± 30.85	242.8 ± 18.38	201.6 ± 15.63*
BMC (mg)	0.3898 ± 0.02712	0.4857 ± 0.07324	0.3613 ± 0.03889	0.2873 ±0.02571*

Table 2.2. Bone parameters after 1 month.

Values represent mean ± standard error

Abbreviations: BV/TV, bone volume/total volume; BMD, bone mineral density; BMC, bone mineral content, Tb.Th., trabecular thickness; Tb. N., trabecular number; Tb.Sp., trabecular space. Ct.Ar., cortical area; Ct.Th., cortical thickness; Ma.Ar., marrow area; Tt.Ar., total area.

# $p < 0.05$ with respect to WT-C

* $p < 0.05$ with respect to KO-C

^ $p < 0.05$ with respect to WT-Diabetic

2.4.3 Long term T1D effects on bone density are not affected by IL-10 deficiency

To determine if IL-10 KO diabetic mice continue to have excessive bone loss over-time (compared to WT diabetic mice), we examined mice 3 months after the first STZ injection. As seen in the 1 month experiments, blood glucose was similarly elevated in both T1D WT and KO mice ($p<0.0001$) (Figure 2.5 A). Compared to genotype controls, body weight was decreased in both WT and KO T1D mice ($p<0.0001$); however, unlike the 1 month time point, body weights were similar between the two genotypes (Figure 2.5 B). MicroCT analysis revealed that femur trabecular BVF was significantly decreased in the WT diabetic ($p<0.0001$) compared to WT control mice (Figure 2.5 C-D). Consistent with this, trabecular thickness ($p<0.0001$) and number ($p<0.0001$) were decreased and trabecular space ($p<0.0001$) increased markedly in the WT diabetic compared to WT control mice (Figure 2.5 D-J, table 2.3). Unlike the 1 month time point, when analyzed against the WT cohorts, KO diabetic showed similar trabecular bone loss compared to WT mice at the 3 months time point (Figure 2.5 E). In the cortical bone, T1D significantly decreased cortical area, bone mineral density and content, thickness and outer perimeter measures in both WT and KO diabetic mice compared to the respective control groups (Figure 2.6 A-I). When analyzed against the WT cohorts, IL-10 deficiency did not exacerbate T1D effects on cortical thickness (Figure 2.6 A-C, table 2.3). Measurment of vertebral trabecular BVF demonstrated no significant difference between any of the groups at this time point (Figure 2.7, table 2.3). Our results suggest that IL-10 plays an important role in inhibiting trabecular and cortical bone loss only during early diabetic time point but not at the later time point.

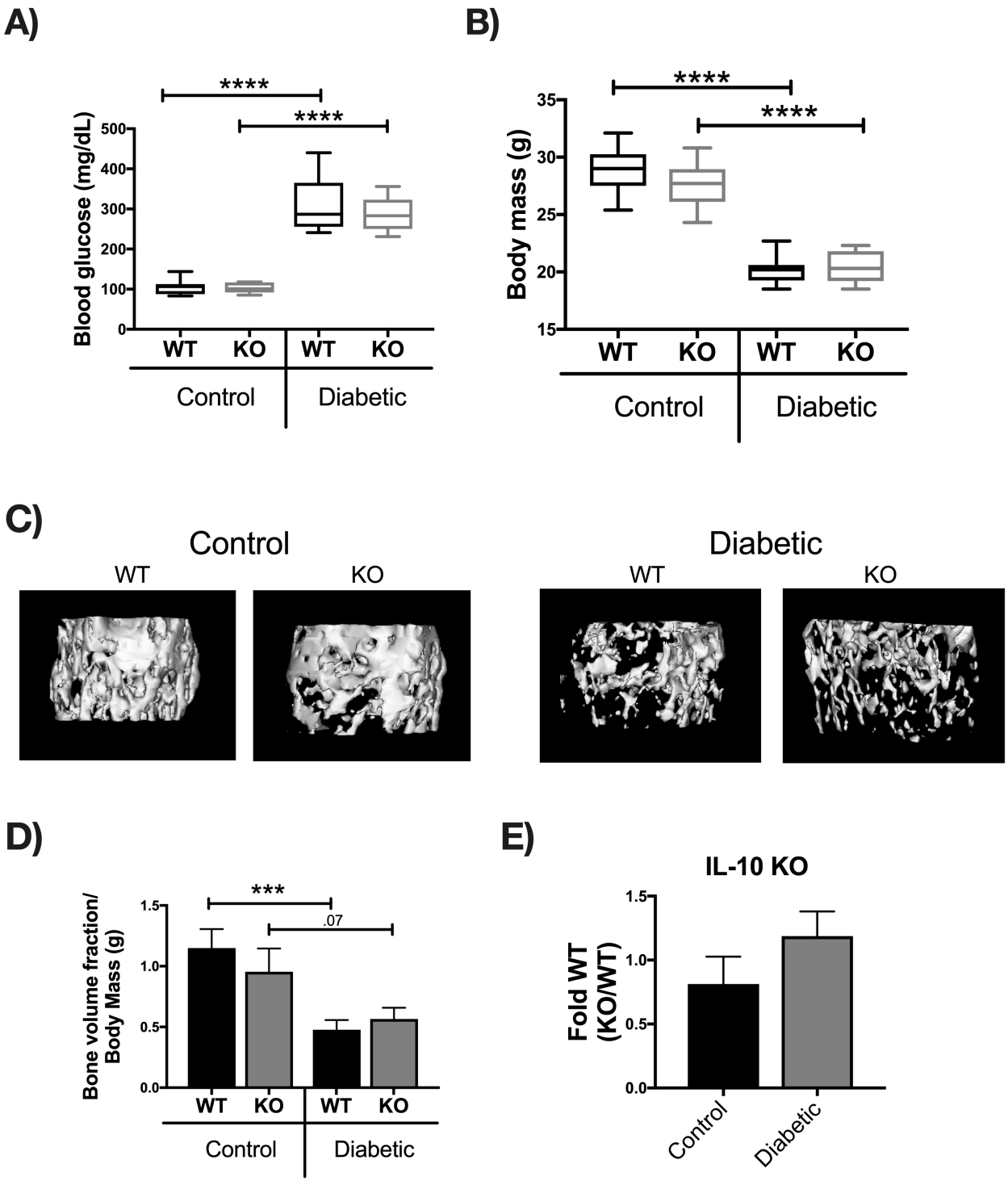

Figure 2.5. IL-10 knockout does not affect trabecular bone loss 3 months after diabetes induction. Control and STZ treated WT and IL-10 knockout mice were euthanized 12 weeks after the first STZ injection.

Figure 2.5. (cont'd)

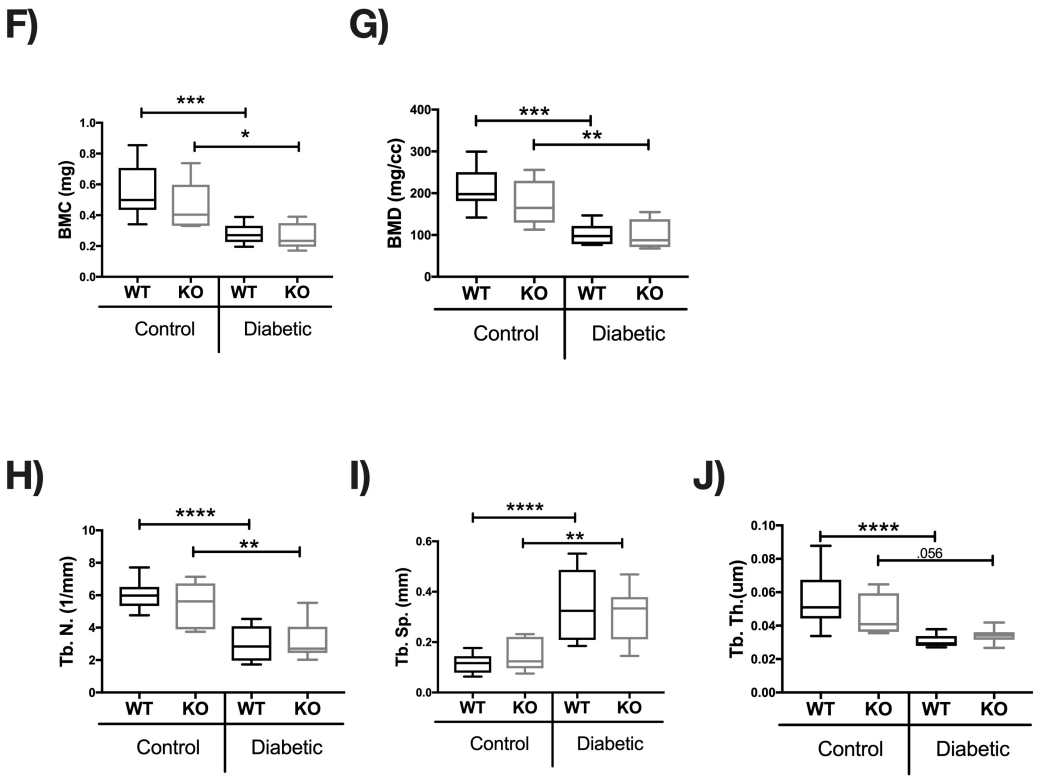

Femoral bones were collected and trabecular bone analyzed by uCT. (A) Blood glucose levels (mg/dL) and (B) body weight in grams (g); n=9-10. (C) Representative micro-computed tomography isosurface images. (D) Bone volume fraction (corrected for weight loss). (E) Bone volume fraction (corrected for weight loss) from the KO group normalized to respective WT groups. (F) Bone mineral content (mg). (G) Bone mineral density (mg/cc). (H) Trabecular number (Tb.N, 1/mm). (I) Trabecular space (Tb.Sp, mm). (J) Trabecular thickness (Tb.Th, um). Bar graphs values are averages ± standard error; Whiskers in box plots represent 5-95 percentile values; n= 5-9 per group. **p<0.01, ****p<0.0001. Statistical analysis performed by One-way ANOVA followed by Fisher's LSD post-test. WT=wild type, KO=IL-10 knockout mice.

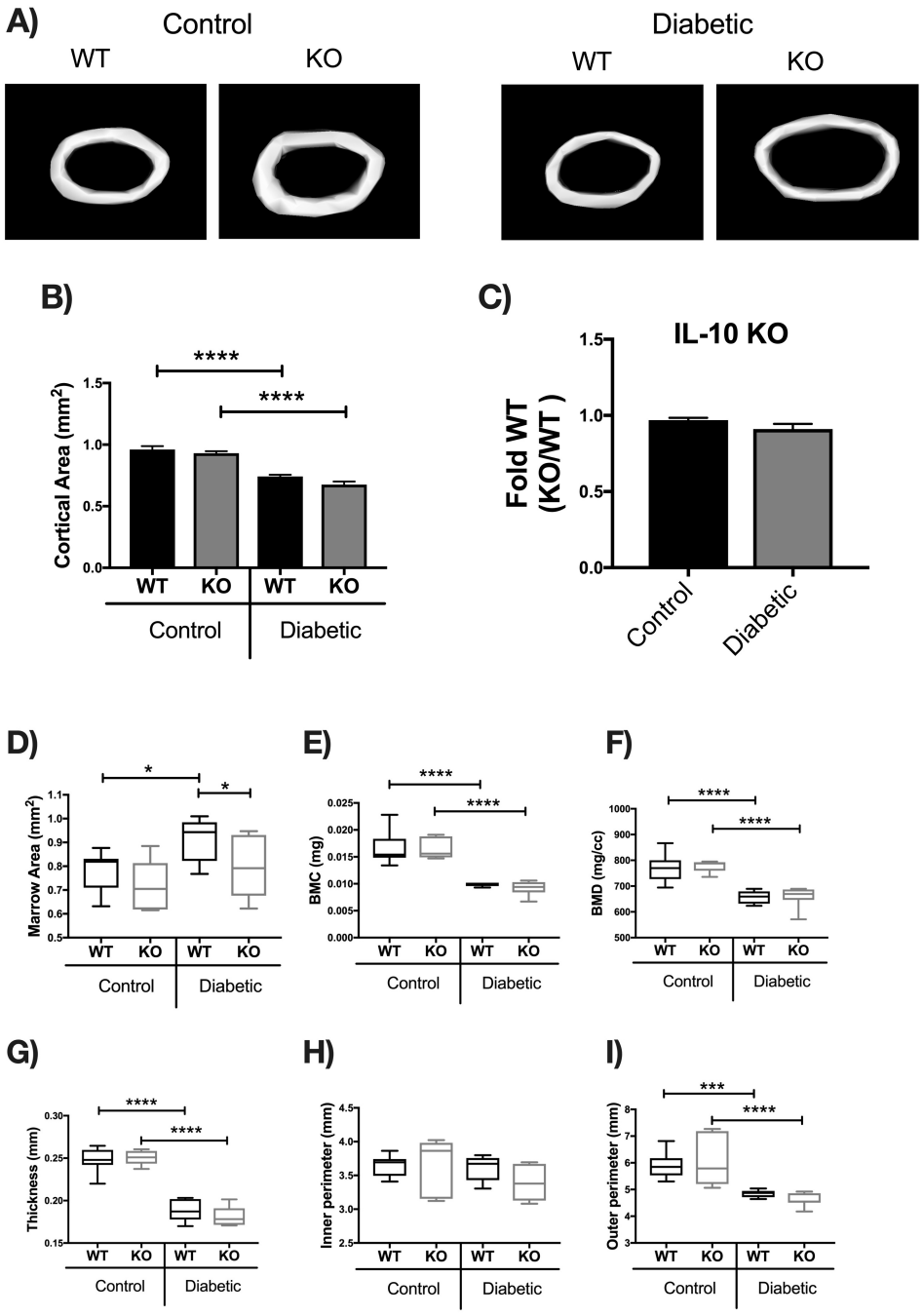

Figure 2.6. IL-10 knockout does not exacerbate T1D-induced cortical bone loss 3 months after diabetes induction.

Control and STZ treated WT and IL-10 knockout mice were euthanized 12 weeks after the first STZ injection. Femoral cortical bone analysis were performed using μCT. (A) Representative micro-computed tomography isosurface images. (B) Cortical area (mm^2).

Figure 2.6. (cont'd)

(C) Cortical area from the KO groups normalized to respective WT groups. (D) Marrow area (mm^2). (E) Bone mineral content (mg). (F) Bone mineral density (mg/cc). (G) Cortical thickness (mm). (H) Inner perimeter (mm). (I) Outer perimeter. Bar graphs values are averages ± standard error; Whiskers in box plots represent 5-95 percentile values; n= 5-9 per group. *p<0.05, **p<0.01, ***p<0.001, ****p<0.0001. Statistical analysis performed by One-way ANOVA followed by Fisher's LSD post-test. WT=wild type, KO= IL-10 knockout mice.

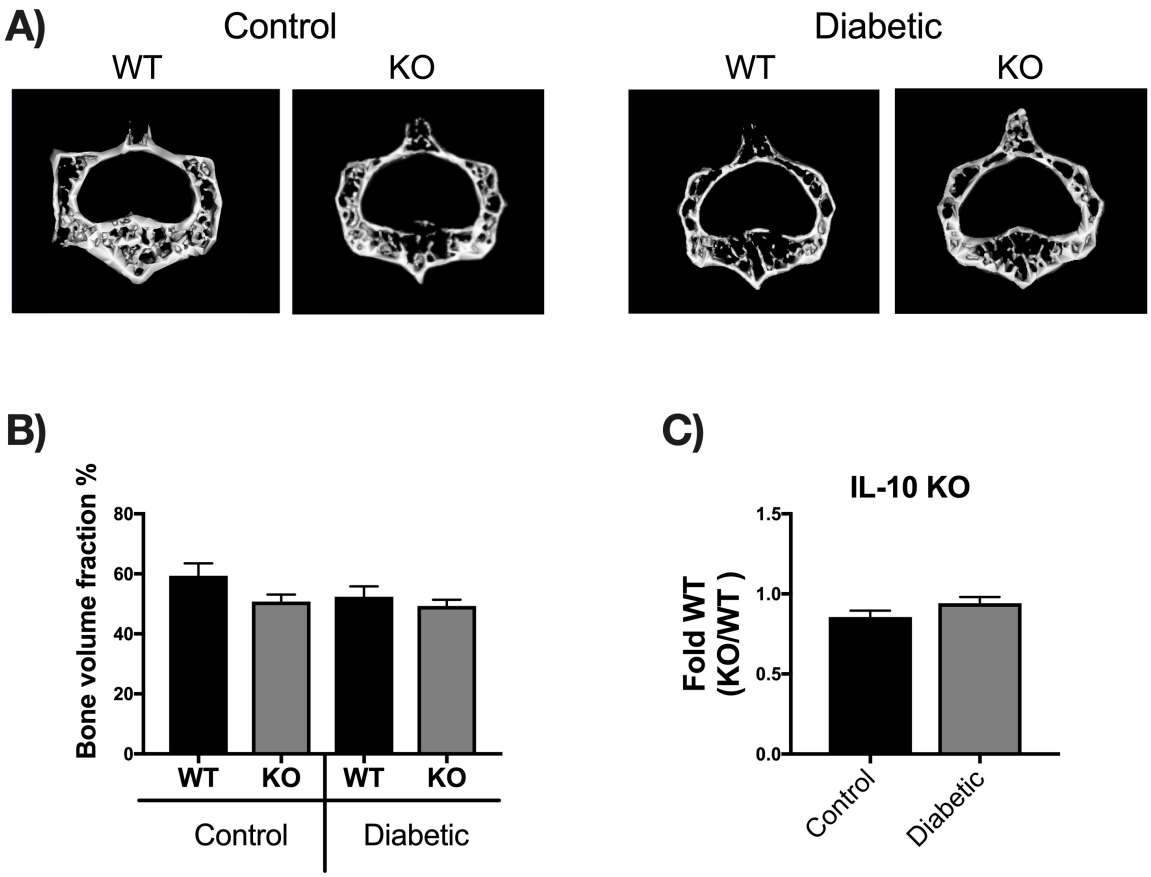

Figure 2.7. IL-10 knockout does not exacerbate vertebral trabecular bone loss 3 months after diabetes induction.

After 12 weeks of treatment vertebral bone was collected and the third lumbar vertebrae was analyzed via uCT. (A) Representative micro-computed tomography isosurface images. (B) Percentage bone volume fraction and (C) bone volume fraction from the KO groups normalized to respective WT groups. Bar graphs values are averages ± standard error; n= 5-7 per group. *$p<0.05$, **$p<0.01$. Statistical analysis performed by One-way ANOVA followed by Fisher's LSD post-test. WT=wild type, KO=IL-10 knockout mice.

	Control		Diabetes	
Parameter: 3 months	WT	KO	WT	KO
Femur trabecular	**n=10**	**n=5**	**n=8**	**n=8**
BV/TV	34.58 ± 4.20	26.13 ± 5.953	9.55 ± 1.55#	11.21 ± 1.69*
Tb. N. (1/mm)	5.839 ± 0.2134	5.138 ± 0.7827	3.037 ± 0.3828#	3.289 ± 0.4729
Tb. Th. (µm)	0.05480 ± 0.005527	0.04782 ± 0.007020	0.03060 ± 0.001359#	0.03375 ± 0.001749*
Tb. Sp. (mm)	0.1184 ± 0.01127	0.1602 ± 0.03659	0.3401 ± 0.04946#	0.3055 ± 0.04359*
BMD (mg/cc)	208.9 ± 15.77	179.6 ± 31.60	101.7 ± 8.954#	105.5 ± 13.05*
BMC (mg)	0.5393 ± 0.05679	0.4511 ± 0.09719	0.2787 ± 0.02268#	0.2735 ± 0.03087*
Femur cortical				
Ct.Ar (mm^2)	0.9608 ± 0.02682	0.9312 ± 0.01508	0.742 ± 0.01412#	0.6758 ± 0.02446*^
Ma.Ar (mm^2)	0.7831 ± 0.02668	0.7134 ± 0.0492	0.916 ± 0.03183#	0.8019 ± 0.04688^
Ct.Th (mm)	0.2489 ± 0.004543	0.251 ± 0.003923	0.1883 ± 0.004456#	0.1824 ± 0.004279*
Inner Perimeter (mm)	3.647 ± 0.05005	3.627 ± 0.1951	3.621 ± 0.06581	3.408 ± 0.09235
Outer Perimeter (mm)	5.888 ± 0.1607	6.114 ± 0.4526	4.853 ± 0.04784#	4.599 ± 0.09475*
BMD (mg/cc)	768.4 ± 17.5	778.6 ± 10.86	656.9 ± 8.463#	657 ± 15.56*
BMC (mg)	0.01653 ± 0.0009532	0.0166 ± 0.0009143	0.009888 ± 0.0001231#	0.009057 ± 0.0005009*
Vertebrate trabecular	**n=9**	**n=8**	**n=9**	**n=9**
BV/TV	58.98 ± 4.14	50.29 ± 2.39	52.00 ± 3.45	48.91 ± 2.01
Tb. N.(1/mm)	9.156 ± 0.1793	9.489 ± 0.2780	9.378 ± 0.2075	9.547 ± 0.2319
Tb. Th. (µm)	0.06497 ± 0.005353	0.05304 ± 0.002185#	0.05544 ± 0.003339	0.05119 ± 0.001501
Tb. Sp. (mm)	0.04458 ± 0.004274	0.05294 ± 0.003464	0.05163 ± 0.004185	0.05403 ± 0.003014
BMD (mg/cc)	233.4 ± 15.40	203.8 ± 8.199	203.1 ± 8.423#	189.4 ± 6.631
BMC (mg)	0.5265 ± 0.03183	0.4436 ± 0.02337#	0.4462 ± 0.02096#	0.3882 ± 0.01788

Table 2.3. Bone parameters after 3 months

Values represent mean ± standard error

Abbreviations: BV/TV, bone volume/total volume; BMD, bone mineral density; BMC, bone mineral content, Tb.Th., trabecular thickness; Tb. N., trabecular number; Tb.Sp., trabecular space.

Ct.Ar.,cortical area; Ct.Th., cortical thickness; Ma.Ar., marrow area; Tt.Ar., total area

# $p < 0.05$ with respect to WT-C

* $p < 0.05$ with respect to KO-C

^ $p < 0.05$ with respect to WT-Diabetic

2.4.4 T1D effects on osteoblast gene expression are exacerbated in IL-10 knockout mice

To understand the mechanisms by which IL-10 regulates T1D bone loss, especially during early stages of T1D (4 weeks), we examined mRNA markers of bone formation (osteoblasts) and bone resorption (osteoclasts). For this, we extracted RNA from tibia of the two genotypes under control and diabetic conditions and then examined the expression of bone formation markers (osteocalcin and osterix) and bone resorption markers (tartrate-resistant acid phosphatase, TRAP). As shown in Figure 2.8 A, expression of both osteocalcin (osteoblast differentiation marker) and osterix (osteoblast transcription factor) were significantly decreased in WT T1D mice ($p < 0.05$). Importantly, the KO diabetic mice displayed a significantly greater decrease in osterix than WT diabetic mice (Figure 2.8 A, $p<0.05$). KO diabetic mice also had lower osteocalcin levels compared to WT diabetic mice, however the difference did not reach statistical significance. Together, these results suggest that the presence of IL-10 reduces the negative effects of T1D on anabolic bone responses. In contrast, expression of TRAP was variable and did not significantly differ between the various groups suggesting that IL-10 likely does not regulate bone resorption in T1D mice (Figure 2.8 A).

Previous studies have shown that T1D can affect osteoblast lineage selection (9,20). Therefore, we examined the expression of Wnt10b, a major enhancer of osteoblast differentiation (46). In addition, we assessed expression of aP2, a fatty acid adipocyte protein whose expression in bone is indicative of increase in marrow adiposity (47). In previous studies we identified that bone Wnt10b is decreased while aP2 is increased in T1D mice (15,21). Similarly, in the current study, we found Wnt10b expression was significantly decreased in the WT diabetic ($p<0.05$) compared to WT control mice. In contrast to the WT, there was no significant difference between the KO control and KO diabetic mice. Note however, that Wnt10b expression was already significantly decreased in the KO control compared to the WT control bones (Figure 8A).

Expression of aP2, on the other hand, was significantly enhanced in both T1D WT and KO mice compared to their respective control genotype mice (Figure 2.8 A, $p<0.05$). These data suggest that under T1D conditions IL-10 effects on bone density are likely independent of Wnt10b and adipocyte lineage selection.

Since IL-10 is an important anti-inflammatory cytokine we next investigated the expression patterns of cytokines previously associated with T1D bone loss such as IFN-γ, TNF-α, and IL-6. Interestingly, our results showed no significant differences in expression of inflammatory cytokines in the bone between any of the groups (Figure 2.8 A). Unlike the bone, intestinal expression of TNFα was significantly enhanced in the KO group ($p<0.01$) (as expected (48)), suggesting an enhanced pro-inflammatory environment in the gut but likely not the bone.

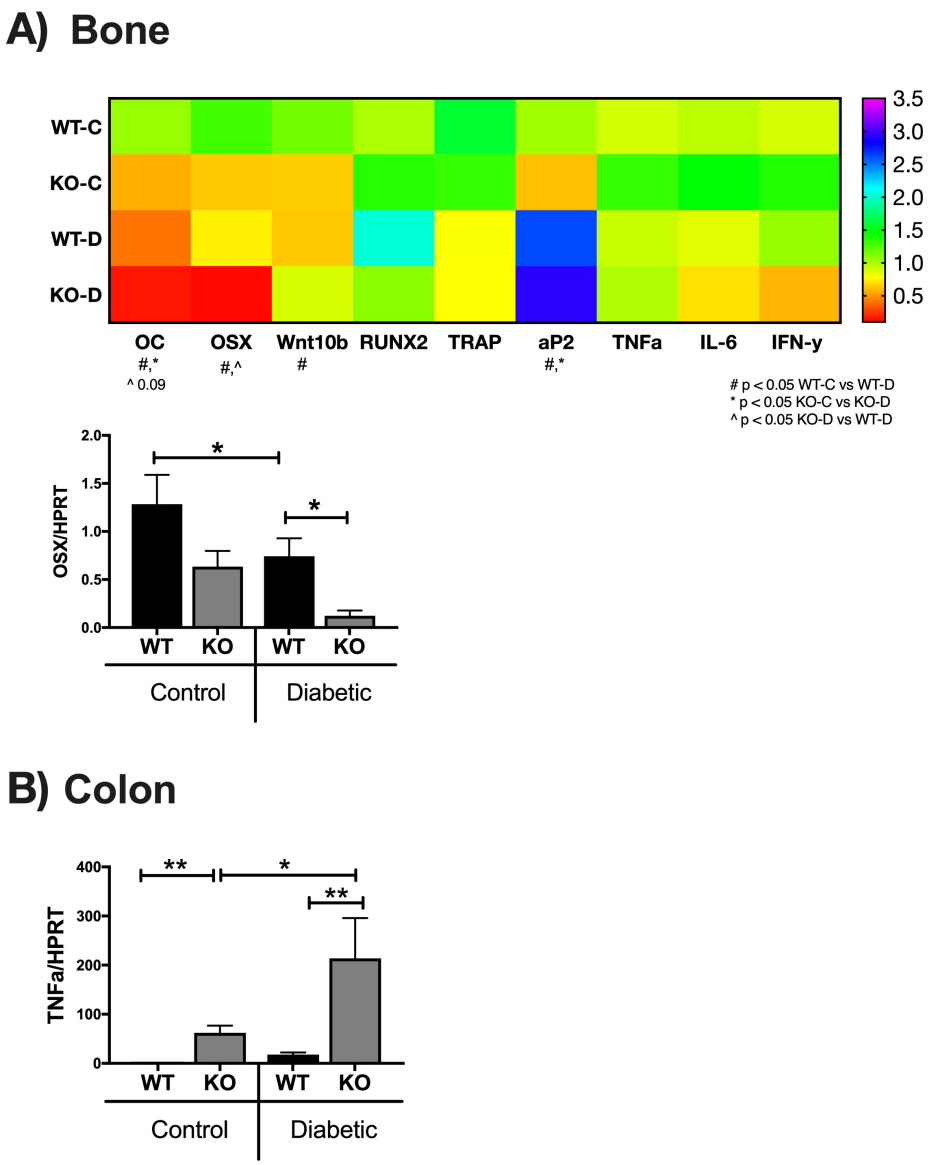

Figure 2.8. Gene expression of osteoblast, osteoclast, adipocyte and inflammatory markers in the tibia from WT and IL-10 knockout mice.

Control and STZ treated WT and IL-10 knockout mice were euthanized 4 weeks after the first STZ injection. Tibia and colon were collected, RNA extracted and mRNA analysis of indicated genes assessed by Q-RT-PCR. Genes were normalized to HPRT. (A) Bone data shown as heat map and osterix gene expression as a bar graphs. (B) Colon gene expression as bar graphs.

Figure 2.8. (cont'd)

Values are averages ± standard error; n= 8-10 per group. *p<0.05, **p<0.01, ****p<0.0001. Statistical analysis performed by One-way ANOVA followed by Fisher's LSD post-test. Outliers removed: OSX (1 outlier in the KO-C and WT-D),Wnt10b (1 outlier in the WT-D), RUNX2 (1 outlier in the WT-C and KO-D), TRAP (1 outlier in the WT-D), TNFA(1 outlier in the WT-C and WT-D), IL-6 (1 outlier in all of the groups), IFNY (1 outlier in the WT-C, WT-D, and KO-D), TNFA colon (2 outliers in the WT-control, 1 outlier in the KO-control).

2.4.5 IL-10 regulates osterix gene expression in osteoblasts via MAPK pathway

To further understand the mechanisms by which IL-10 regulates osteoblast markers under diabetic conditions, we used MC3T3-E1 osteoblasts treated with or without IL-10, under normal and high glucose conditions. Previous studies have shown *in vitro* that high glucose treatment of osteoblasts inhibits expression of anabolic genes (49–52). Since our *in vivo* studies suggest a role for IL-10 in osterix gene expression in the tibia, we focused on regulation of expression of osterix *in vitro*. MC3T3-E1 cells were treated with normal (5 mM) or high glucose (30 mM) for 72 hours followed by stimulation without or with IL-10 for 24 hours. As expected, osterix gene expression was significantly reduced under high glucose in the absence of IL-10 ($p<0.05$). However, in the presence of IL-10 under high glucose conditions, osterix expression reversed to control levels. Interestingly, IL-10 did not significantly affect osterix expression in cells grown under normal glucose conditions (Figure 2.9 A).

To understand the signaling mechanisms by which IL-10 regulates osterix gene expression, we focused on the MAPK pathways (JNK, p38 and ERK). Previous studies have shown that osterix expression is regulated by JNK, p38 or ERK depending on the stimulus (53,54). To understand the relationship between high glucose conditions and osterix in the context of these MAPK pathways, we first tested the effect of high glucose on the phosphorylation status of these three kinases. High glucose enhanced phosphorylation of JNK and p38 (as we have shown before (49)). Interestingly, high glucose decreased ERK phosphorylation (Figure 2.9 B, $p<0.05$). The ERK pathway is known to be a key stimulator of osteoblast differentiation. Consequently, we examined if IL-10 treatment prevents the high glucose suppression of ERK signaling. As expected, treatment with IL-10 prevented high glucose suppression of ERK phosphorylation (Figure 2.9.B). These results indicate that IL-10 likely sustains osteoblast ERK signaling and osterix expression under T1D conditions.

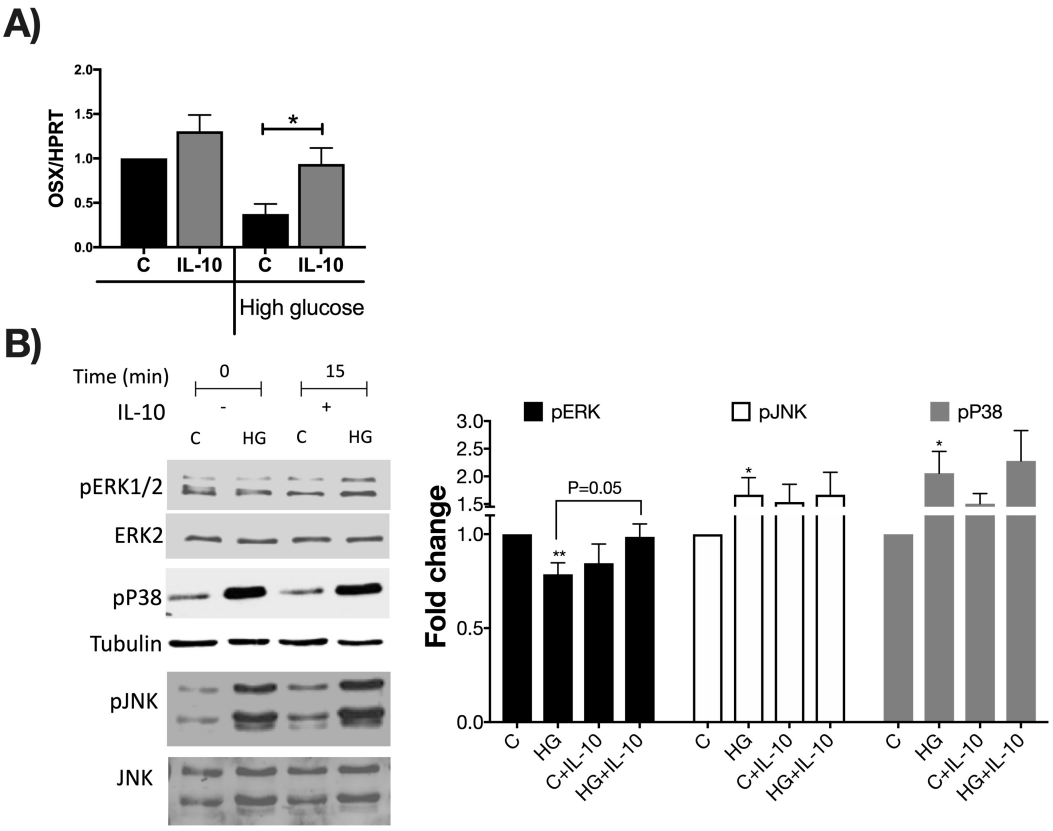

Figure 2.9 IL-10 prevents high glucose-mediated suppression of osterix expression via the ERK pathway.

(A) MC3T3-E1 cells were treated with high glucose (72 hours) +/- IL-10 for 24 hours. RNA extracted and mRNA analysis of osterix (OSX) gene assessed by Q-RT-PCR and normalized to HPRT. (B) MC3T3-E1 cells were treated with high glucose (72 hours) +/- IL-10 for 15 minutes. Representative blots show protein levels analyzed by Western Blot as well as loading controls (ERK and Tubulin). Quantification of western blots for p-ERK/ERK, p-p38, and p-JNK. Values are averages ± standard error; n= 4-5 per group, *$p<0.05$, **$p<0.01$. Statistical analysis performed by One-way ANOVA followed by Fisher's LSD post-test.

2.5 Discussion

Studies in human and diabetic murine models have demonstrated changes in the levels of pro and anti-inflammatory cytokines with unmanaged diabetes (18,19,29,30,55). Several proinflammatory cytokines have been reported to be elevated in T1D patients and animal models. For example, serum IFN-y is increased with age in the non-obese diabetic mice (NOD) and it reaches the highest levels at the onset of diabetes (31). T1D patients also present with elevated TNF-α serum levels (32). Other cytokines such as IL-6 and interleukin 1 beta (IL-1β) are also elevated under diabetic conditions (56). Interestingly, not only are these cytokines increased in the serum of diabetic mice, they are also expressed at high levels in the bone (e.g. IFN-y and TNF-α (18,19)), providing a link between inflammatory cytokines and T1D-induced bone loss. Furthermore, proinflammatory cytokines such as TNFα, IL-1β and prostaglandin E2 have been shown to play an important role in diabetes-induced periodontal bone loss (57–59). Inhibition of cytokine activity/levels, especially TNFα, has been shown to decrease osteoclast numbers and increase osteoblast and periodontal bone formation in a diabetes-induced periodontal bone loss model (60).

Compared to pro-inflammatory cytokines, levels of the anti-inflammatory cytokine IL-10 has been shown to be decreased in the serum and pancreas during diabetes progression in NOD mice (31). Remarkably, administration of recombinant IL-10 via daily subcutaneous injections or non-viral gene delivery protects NOD mice against the development of insulinitis and diabetes (34,61). Similar to NOD mice, diabetic patients also exhibit lower IL-10 serum levels compared to non-diabetic subjects (35). Given that other studies have shown a beneficial effect of IL-10 on bone mass (39,62) and that IL-10 levels are decreased during T1D (31,35), in the current report we investigated the importance of IL-10 in T1D-induced bone loss. Our results clearly demonstrate that during early stages of T1D-induced bone loss, IL-10 deficiency exacerbates bone loss in mice.

Thus reduced IL-10 levels during T1D in human patients may contribute to bone loss early on. However, our data also suggest that over time, IL-10 levels are not crucial to regulate bone density since by 6 months of age, diabetic IL-10 KO and WT mice exhibit similar levels of bone loss. These differences in time point response can be attributed to the rapid decline in bone density (60% decrease) in the absence of IL-10 at 1 month post-diabetes induction, while the wild type diabetic group only lost 39% bone volume. However, after 3 months of diabetes the decrease in bone density between the WT and IL-10 KO diabetic mice was similar, suggesting that bone loss in the IL-10 KO diabetic group is much faster and drastic but reaches a set point that is achieved by T1D WT mice at a later timepoint. Consistent with this, a progressive decline, over a 12-week period, in trabecular bone density, has been shown in T1D WT rats (63). Together, our results suggest that early decline in IL-10 during diabetes can be detrimental to the bone.

Consistent with our findings that IL-10 can play a role in bone density, many studies have demonstrated the importance of IL-10 in regulating bone health in non-diabetic models. IL-10 has been shown to regulate alveolar bone loss in aged mice (~9 month) compared to younger mice (3 months old) (36,38). In these studies, changes in bone density in the aged IL-10 KO mice were associated with down-regulation of osteoblast and osteocyte markers in the periodontal tissue (39). Another study looking at bone metabolism in IL-10 KO mice in the context of colitis development demonstrated a decrease in cancellous bone mass of the tibia as well as the trabecular bone surface and number, in the IL-10 KO mice compared to the WT group. Interestingly, these changes were most striking in IL-10 KO animals that showed colitis (40). Although these authors demonstrated this phenotype in 8 to 12 week old mice, in our studies we did not observe any signs of colitis in IL-10 KO mice (as demonstrated by equivalent body weight in control WT and KO mice at both time points tested). In addition, IL-10 KO mice in our facility did not display any overt clinical signs of colitis (such as diarrhea, bleeding etc). Because IL-10 KO mice in our study did not display

overt colitis, it is not surprising that non-diabetic IL-10 KO mice did not exhibit any bone pathology. It is important to note that a trend towards a lower femoral trabecular bone density in the IL-10 KO group was noted at the later time point (12 week treatment time @ which they are 6 months old). Even though we did not observe any clinical signs of colitis, colons from the IL-10 KO mice (non-diabetic and diabetic) showed markedly higher TNFα gene expression suggesting that the intestinal environment of these mice are skewed towards a pro-inflammatory state. This however, did not likely influence bone inflammatory environment since expression of inflammatory genes in the bone were similar between groups. These results suggest that the bone phenotype in the IL-10 KO diabetic group in this study is independent of changes in bone inflammation. Similar to our results, an increase in alveolar bone loss in IL-10 deficient mice was shown to be independent of changes in the inflammatory cytokines TNFα, IL1β, IL-6 and transforming growth factor beta (TGFβ) (39).

We and others have shown that T1D-induced bone loss is associated with suppression of osteoblast and an increase in adipogenesis (20,21). Similarly, we show here that T1D decreased markers of osteoblast maturation and increased markers of adipogenesis in the WT mice. In the IL-10 KO diabetic mice, although osteoblast markers were suppressed even further compared to the WT diabetic mice, expression of adipogenic markers were similar to that of the WT mice. A previous study using an *in vitro* model has shown that IL-10 can suppress lipid accumulation and adipogenesis in 3T3-L1 fibroblasts (64). However, in our *in vivo* T1D model, it appears that IL-10 deficiency does not significantly influence T1D-induced adipogenesis markers. Thus, our results suggest that the effect of diabetes on bone density in the absence of IL-10 is likely independent of changes in adipocytes.

IL-10 can also negatively influence osteoclastogenesis (39,42,43,62,65). Specifically, IL-10 prevents the differentiation of osteoclast progenitors to preosteoclasts (41,43). In a co-culture

system of mouse bone marrow cells and primary osteoblastic cells, IL-10 treatment for 7 days prevented osteoclast differentiation (42). In contrast, in IL-10 deficient mice (8 and 12 weeks old) osteoclast cell number were not affected (40). Our results on TRAP (a marker of osteoclast) gene expression, suggests that neither T1D nor IL-10 significantly influence osteoclastogenesis. Although previous studies have demonstrated that proinflammatory cytokines can promote and enhance osteoclastogenesis (66–69), deficiency of IL-10 did not upregulate pro-inflammatory cytokines in the bone. Consistent with that IL-10 KO did not affect TRAP gene expression in the control or diabetic mice. Together, these results are consistent with our previous studies showing that T1D does not influence osteoclast markers and further adds that IL-10 is not an important regulator of osteoclastogenesis in T1D model (20,21).

To understand the direct mechanisms by which IL-10 regulates osteoblasts, we examined the effects of IL-10 in osteoblasts cultured under normal and high glucose conditions. While studies looking at the role of IL-10 on osteoblast cells is limited, our results demonstrate a direct role for IL-10 in regulating osterix gene expression in osteoblasts especially under high glucose conditions. Previous studies have shown that high glucose can negatively influence osteoblast differentiation (70) and can decrease osteocalcin and osteoprotegerin gene expression is differentiated osteoblasts (50,71). Consistent with that, we found that high glucose exposure of pre-osteoblasts markedly decreases osterix gene expression. Osterix is an osteoblast-specific transcriptor factor that is required to induce preosteoblasts differentiation into mature osteoblasts (72). In addition, osterix null mice lack bone formation and have no trabeculae (73). Consistent with our findings, gene expression analysis of human osteoblastic cells, isolated from diabetic patients with osteoporotic fractures express significantly low levels of osterix (74). Our studies further demonstrate that IL-10 can directly reverse high glucose-mediated suppression of osterix expression. In an effort to identify signaling mechanisms, our studies further show that IL-10

increases in osterix expression via regulation of the ERK pathway. Regulation of ERK pathway by IL-10 have been shown in different models (75,76). In addition, previous studies using parathyroid hormone (PTH) and TNF-α have shown regulation of osterix gene expression via regulation of MAPK pathway (53,54). Thus, our results are consistent with these studies showing that ERK pathway is an important regulator of osterix under high glucose conditions in the presence of IL-10.

In summary, the present study demonstrates that IL-10 knockout mice are more susceptible to T1D bone loss, especially during the early disease process and therefore, decreases in IL-10 observed in animal models and human patients with T1D may have a detrimental role to bone health. We identified that IL-10 is able to regulate osterix gene expression and influence bone effects during T1D primarily through the regulation of osteoblasts. Together, our studies suggest that IL-10 and its signaling pathways are potential therapeutic targets for T1D bone loss.

REFERENCES

REFERENCES

1. Centers for Disease Control and Prevention. National Diabetes Statistics Report: Estimates of Diabetes and Its Burden in the United States, 2014. Atlanta, GA US Dep Heal Hum Serv. 2014;1–20.

2. Atkinson MA, Maclaren NK. The pathogenesis of insulin-dependent diabetes mellitus. N Engl J Med. 1994 Nov 24;331(21):1428–36.

3. Lebovitz HE. Type 2 Diabetes: An Overview. Clin Chem. 1999;45(8).

4. Hofbauer LC, Brueck CC, Singh SK, Dobnig H. Osteoporosis in patients with diabetes mellitus. J Bone Miner Res. 2007;22(9):1317–28.

5. Shah VN, Shah CS, Pharm M, Snell-bergeon JK. Type 1 Diabetes and Risk for Fracture: Meta-analysis and Review of the Literature. Diabet Med. 2016;32(9):1134–42.

6. Weber DR, Schwartz G. Epidemiology of Skeletal Health in Type 1 Diabetes. Curr Osteoporos Rep. 2016;14(6):327–36.

7. Miao J, Brismar K, Nyrén O, Ugarph-Morawski A, Ye W. Elevated Hip Fracture Risk in Type 1 Diabetic Patients. Diabetes Care. 2005;28(12):2850–5.

8. Eller-Vainicher C, Zhukouskaya V V, Tolkachev Y V, Koritko SS, Cairoli E, Grossi E, et al. Low bone mineral density and its predictors in type 1 diabetic patients evaluated by the classic statistics and artificial neural network analysis. Diabetes Care. 2011 Oct;34(10):2186–91.

9. Coe LM, Zhang J, McCabe LR. Both spontaneous Ins2+/- and streptozotocin-induced type I diabetes cause bone loss in young mice. J Cell Physiol. 2013 Apr;228(4):689–95.

10. Burghardt AJ, Issever AS, Schwartz A V., Davis KA, Masharani U, Majumdar S, et al. High-resolution peripheral quantitative computed tomographic imaging of cortical and trabecular bone microarchitecture in patients with type 2 diabetes mellitus. J Clin Endocrinol Metab. 2010 Nov;95(11):5045–55.

11. Bonds DE, Larson JC, Schwartz A V., Strotmeyer ES, Robbins J, Rodriguez BL, et al. Risk of Fracture in Women with Type 2 Diabetes: the Women's Health Initiative Observational Study. J Clin Endocrinol Metab. 2006 Sep;91(9):3404–10.

12. Petit MA, Paudel ML, Taylor BC, Hughes JM, Strotmeyer ES, Schwartz A V, et al. Bone mass and strength in older men with type 2 diabetes: the Osteoporotic Fractures in Men Study. J Bone Miner Res. 2010 Feb;25(2):285–91.

13. Strotmeyer ES, Cauley JA, Schwartz A V, Nevitt MC, Resnick HE, Zmuda JM, et al. Diabetes is associated independently of body composition with BMD and bone volume in older white and black men and women: The Health, Aging, and Body Composition Study. J Bone Miner Res. 2004 Mar 15;19(7):1084–91.

14. Hanley D a, Brown JP, Tenenhouse A, Olszynski WP, Ioannidis G, Berger C, et al. Associations among disease conditions, bone mineral density, and prevalent vertebral deformities in men and women 50 years of age and older: cross-sectional results from the Canadian Multicentre Osteoporosis Study. J Bone Miner Res. 2003 Apr 1;18(4):784–90.

15. Raehtz S, Bierhalter H, Schoenherr D, Parameswaran N, McCabe LR. Estrogen Deficiency Exacerbates Type 1 Diabetes Induced Bone TNFα expression and Osteoporosis in Female Mice. Endocrinology. 2017 Apr 14;

16. Chen HH, Horng MH, Yeh SY, Lin IC, Yeh CJ, Muo CH, et al. Glycemic control with thiazolidinedione is associated with fracture of T2DM patients. PLoS One. 2015;10(8).

17. Coe LM, Tekalur SA, Shu Y, Baumann MJ, Mccabe LR. Bisphosphonate treatment of type I diabetic mice prevents early bone loss but accentuates suppression of bone formation. J Cell Physiol. 2015;230(8):1944–53.

18. Motyl KJ, Botolin S, Irwin R, Appledorn DM, Kadakia T, Amalfitano A, et al. Bone inflammation and altered gene expression with type I diabetes early onset. J Cell Physiol. 2009 Mar;218(3):575–83.

19. Motyl K, McCabe LR. Streptozotocin, type 1 diabetes severity and bone. Biol Proced Online. 2009 Mar 6;11(1):296–315.

20. Botolin S, McCabe LR. Bone loss and increased bone adiposity in spontaneous and pharmacologically induced diabetic mice. Endocrinology. 2007 Jan;148(1):198–205.

21. Zhang J, Motyl KJ, Irwin R, MacDougald OA, Britton RA, McCabe LR. Loss of bone and Wnt10b expression in male type 1 diabetic mice is blocked by the probiotic Lactobacillus reuteri. Endocrinology. 2015;156(9):3169–82.

22. Pietschmann P, Schernthaner G, Woloszczuk W. Serum osteocalcin levels in diabetes mellitus: analysis of the type of diabetes and microvascular complications. Diabetologia. 1988 Dec;31(12):892–5.

23. McCabe LR. Understanding the pathology and mechanisms of type I diabetic bone loss. Vol. 102, Journal of Cellular Biochemistry. 2007. p. 1343–57.

24. McCabe L, Zhang J, Raehtz S. Understanding the skeletal pathology of type 1 and 2 diabetes mellitus. Crit Rev Eukaryot Gene Expr. 2011;21(2):187–206.

25. Verhaeghe J, Thomsen JS, Van Bree R, Van Herck E, Bouillon R, Mosekilde L. Effects of

exercise and disuse on bone remodeling, bone mass, and biomechanical competence in spontaneously diabetic female rats. Bone. 2000;27(2):249–56.

26. Irwin R, Lee T, Young VB, Parameswaran N, McCabe LR. Colitis-induced bone loss is gender dependent and associated with increased inflammation. Inflamm Bowel Dis. 2013;19(8):1586–97.

27. Chiang C, Kyritsis G, Graves DT, Amar S. Interleukin-1 and Tumor Necrosis Factor Activities Partially Account for Calvarial Bone Resorption Induced by Local Injection of Lipopolysaccharide. 1999;

28. Zhang YH, Heulsmann A, Tondravi MM, Mukherjee A, Abu-Amer Y. Tumor necrosis factor-α (TNF) stimulates RANKL-induced osteoclastogenesis via coupling of TNF type 1 receptor and RANK signaling pathways. J Biol Chem. 2001 Jan 5;276(1):563–8.

29. Erbagci AB, Tarakcioglu M, Coskun Y, Sivasli E, Sibel Namiduru E. Mediators of inflammation in children with type I diabetes mellitus: cytokines in type I diabetic children. Clin Biochem. 2001;34(8):645–50.

30. Snell-Bergeon JK, West NA, Mayer-Davis EJ, Liese AD, Marcovina SM, D'Agostino RB, et al. Inflammatory markers are increased in youth with type 1 diabetes: The SEARCH case-control study. J Clin Endocrinol Metab. 2010 Jun;95(6):2868–76.

31. Schloot NC, Hanifi-Moghaddam P, Goebel C, Shatavi S V, Flohe S, Kolb H, et al. Serum IFN-gamma and IL-10 levels are associated with disease progression in non-obese diabetic mice. Diabetes Metab Res Rev. 2002;18(1):64–70.

32. Qiao YC, Chen YL, Pan YH, Tian F, Xu Y, Zhang X, et al. The change of serum tumor necrosis factor alpha in patients with type 1 diabetes mellitus: A systematic review and meta-analysis. PLoS One. 2017;12(4):1–14.

33. Ko KI, Coimbra LS, Tian C, Alblowi J, Kayal RA, Einhorn T, et al. Diabetes reduces mesenchymal stem cells in fracture healing through a TNFα-mediated mechanism. Diabetologia. 2015;58(3):633–42.

34. Pennline K, Roque-Gaffney E, Monahan M. Recombinant human IL-10 prevents the onset of diabetes in the nonobese diabetic mouse. Clin Immunol Immunopathol. 1994;71(2):169–75.

35. Van Exel E, Gussekloo J, De Craen AJM, Frölich M, Wiel AB Van Der, Westendorp RGJ. Low production capacity of interleukin-10 associates with the metabolic syndrome and type 2 diabetes: The Leiden 85-plus study. Diabetes. 2002;51(4):1088–92.

36. Al-Rasheed A, Scheerens H, Srivastava AK, Rennick DM, Tatakis DN. Accelerated alveolar bone loss in mice lacking interleukin-10: Late onset. J Periodontal Res. 2004;39(3):194–8.

37. Alayan J, Ivanovski S, Farah CS. Alveolar bone loss in T helper 1/T helper 2 cytokine-deficient mice. J Periodontal Res. 2007;42(2):97–103.

38. Al-Rasheed A, Scheerens H, Rennick DM, Fletcher HM TD. Accelerated alveolar bone loss in mice lacking interleukin-10. J Dent Res. 2003;82(8):632–5.

39. Claudino M, Garlet TP, Cardoso CRB, de Assis GF, Taga R, Cunha FQ, et al. Down-regulation of expression of osteoblast and osteocyte markers in periodontal tissues associated with the spontaneous alveolar bone loss of interleukin-10 knockout mice. Eur J Oral Sci. 2010;118(1):19–28.

40. Dresner-Pollak R, Gelb N, Rachmilewitz D, Karmeli F, Weinreb M. Interleukin 10-deficient mice develop osteopenia, decreased bone formation, and mechanical fragility of long bones. Gastroenterology. 2004;127(3):792–801.

41. Evans KE, Fox SW. Interleukin-10 inhibits osteoclastogenesis by reducing NFATc1 expression and preventing its translocation to the nucleus. BMC Cell Biol. 2007;8:4.

42. Hong MH, Williams H, Jin CH, Pike JW. The Inhibitory Effect of Interleukin-10 on Mouse Osteoclast Formation Involves Novel Tyrosine-Phosphorylated Proteins. J Bone Miner Res. 2000 Feb 18;15(5):911–8.

43. Xu LX, Kukita T, Kukita A, Otsuka T, Niho Y, Iijima T. Interleukin-10 selectively inhibits osteoclastogenesis by inhibiting differentiation of osteoclast progenitors into preosteoclast-like cells in rat bone marrow culture system. J Cell Physiol. 1995;165(3):624–9.

44. Lee T, Lee E, Irwin R, Lucas PC, Mccabe LR, Parameswaran N. b -Arrestin-1 Deficiency Protects Mice from Experimental Colitis. 2013;182(4).

45. Szkudelski T. The mechanism of alloxan and streptozotocin action in B cells of the rat pancreas. Vol. 50, Physiological Research. 2001. p. 537–46.

46. Bennett CN, Ouyang H, Ma YL, Zeng Q, Gerin I, Sousa KM, et al. Wnt10b increases postnatal bone formation by enhancing osteoblast differentiation. J Bone Miner Res. 2007;22(12):1924–32.

47. Shan T, Liu W, Kuang S. Fatty acid binding protein 4 expression marks a population of adipocyte progenitors in white and brown adipose tissues. 2013;27:277–87.

48. Rennick DM, Fort MM. Lessons from genetically engineered animal models. XII. IL-10-deficient (IL-10(-/-) mice and intestinal inflammation. Am J Physiol Gastrointest Liver Physiol. 2000;(278):829–33.

49. Zayzafoon M, Botolin S, McCabe LR. p38 and activating transcription factor-2 involvement in osteoblast osmotic response to elevated extracellular glucose. J Biol

Chem. 2002;277(40):37212–8.

50. Zayzafoon M, Stell C, Irwin R, McCabe LR. Extracellular glucose influences osteoblast differentiation and c-jun expression. J Cell Biochem. 2000 Aug 2;79(2):301–10.

51. Balint E, Szabo P, Marshall CF, Sprague SM. Glucose-induced inhibition of in vitro bone mineralization. Bone. 2001;28(1):21–8.

52. Terada M, Inaba M, Yano Y, Hasuma T, Nishizawa Y, Morii H, et al. Growth-inhibitory effect of a high glucose concentration on osteoblast-like cells. Bone. 1998;22(1):17–23.

53. Lu X, Gilbert L, He X, Rubin J, Nanes MS. Transcriptional regulation of the osterix (Osx, Sp7) promoter by tumor necrosis factor identifies disparate effects of mitogen-activated protein kinase and NFKB pathways. J Biol Chem. 2006;281(10):6297–306.

54. Barbuto R, Mitchell J. Regulation of the osterix (Osx, Sp7) promoter by osterix and its inhibition by parathyroid hormone. J Mol Endocrinol. 2013;51(1):99–108.

55. Lee J-H, Lee W, Kwon OH, Kim J-H, Kwon OW, Kim KH, et al. Cytokine profile of peripheral blood in type 2 diabetes mellitus patients with diabetic retinopathy. Ann Clin Lab Sci. 2008;38(4):361–7.

56. Senn JJ, Klover PJ, Nowak IA, Mooney RA. Interleukin-6 induces cellular insulin resistance in hepatocytes. Diabetes. 2002;51(12):3391–9.

57. Liu R, Bal HS, Desta T, Krothapalli N, Alyasii M, Luan Q, et al. Diabetes Enhances Periodontal Bone Loss through Enhanced Resorption and Diminished Bone Formation. J Dent Res. 2006;85(6):510–4.

58. Salvi GE, Collins JG, Yalda B, Arnold RR, Lang NP, Offenbacher S. Monocytic TNFa secretion patterns in IDDM patients with periodontal diseases. J Clin Periodontol. 1997;4:8–16.

59. Salvi GE, Yalda B, Collins JG, Jones BH, Smith FW, Arnold RR, et al. Inflammatory Mediator Response as a Potential Risk Marker for Periodontal Diseases in Insulin-Dependent Diabetes Mellitus Patients. J Periodontol. 1997;68(2):127–35.

60. Pacios S, Kang J, Galicia J, Gluck K, Patel H, Ovaydi-Mandel A, et al. Diabetes aggravates periodontitis by limiting repair through enhanced inflammation. FASEB J. 2012;26(4):1423–30.

61. Lee M, Park H, Youn J, Eun TO, Ko K, Kim S, et al. Interleukin-10 plasmid construction and delivery for the prevention of type 1 diabetes. Ann N Y Acad Sci. 2006;1079:313–9.

62. Zhang Q, Chen B, Yan F, Guo J, Zhu X, Ma S, et al. Interleukin-10 inhibits bone resorption: A potential therapeutic strategy in periodontitis and other bone loss diseases.

Biomed Res Int. 2014;2014.

63. Silva MJ, Brodt MD, Lynch MA, McKenzie JA, Tanouye KM, Nyman JS, et al. Type 1 diabetes in young rats leads to progressive trabecular bone loss, cessation of cortical bone growth, and diminished whole bone strength and fatigue life. J bone Miner Res . 2009;24(9):1618–27.

64. Kim YH, Pyo S. Interleukin-10 suppresses adipogenesis via Wnt5a signaling pathway in 3T3-L1 preadipocytes. Biochem Biophys Res Commun. 2019;509(4):877–85.

65. Zhang L, Ding Y, Rao GZ, Miao D. Effects of IL-10 and glucose on expression of OPG and RANKL in human periodontal ligament fibroblasts. Brazilian J Med Biol Res. 2016;49(4).

66. Kobayashi K, Takahashi N, Jimi E, Udagawa N, Takami M, Kotake S, et al. Tumor Necrosis Factor Stimulates Osteoclast Differentiation by a Mechanism Independent of the Odf/Rankl-Rank Interaction. J Exp Med. 2000 Jan;191(2):275–86.

67. Ries WL, Seeds MC, Key L. Interleukin-2 stimulates osteoclastic activity : Increased acid production and radioactive calcium release. J Periodont Res. 989;24:242–6.

68. Azuma Y, Kaji K, Katogi R, Takeshita S, Kudo A. Tumor necrosis factor-alpha induces differentiation of and bone resorption by osteoclasts. J Biol Chem. 2000;275(7):4858–64.

69. Gao Y, Grassi F, Ryan MR, Terauchi M, Page K, Yang X, et al. IFN-gamma stimulates osteoclast formation and bone loss in vivo via antigen-driven T cell activation. J Clin Invest. 2007;117(1):122–32.

70. García-Hernández A, Arzate H, Gil-Chavarría I, Rojo R, Moreno-Fierros L. High glucose concentrations alter the biomineralization process in human osteoblastic cells. Bone. 2012;50(1):276–88.

71. Shao X, Cao X, Song G, Zhao Y, Shi B. Metformin rescues the MG63 osteoblasts against the effect of high glucose on proliferation. J Diabetes Res. 2014;2014.

72. Sinha KM, Zhou X. Genetic and molecular control of osterix in skeletal formation. J Cell Biochem. 2013;114(5):975–84.

73. Nakashima K, Zhou X, Kunkel G, Zhang Z, Deng JM, Behringer RR, et al. The Novel Zinc Finger-Containing Transcription Factor Osterix Is Required for Osteoblast Differentiation and Bone Formation. Cell. 2002;108(1):17–29.

74. Miranda C, Giner M, José Montoya M, Vázquez MA, Miranda MJ, Pérez-Cano R. Influence of high glucose and advanced glycation end-products (ages) levels in human osteoblast-like cells gene expression. BMC Musculoskelet Disord. 2016;17(1):1–9.

75. Hovsepian E, Penas F, Siffo S, Mirkin GA, Goren NB. IL-10 Inhibits the NF-κB and ERK/MAPK-Mediated Production of Pro-Inflammatory Mediators by Up-Regulation of SOCS-3 in Trypanosoma cruzi-Infected Cardiomyocytes. PLoS One. 2013;8(11):e79445.

76. Pereira L, Font-Nieves M, Van den Haute C, Baekelandt V, Planas AM, Pozas E. IL-10 regulates adult neurogenesis by modulating ERK and STAT3 activity. Front Cell Neurosci. 2015;9(February):1–9.

Chapter 3. Beneficial effects of *Lactobacillus reuteri* 6475 on bone density in male mice are dependent on lymphocytes.

This chapter is an edited version of the article that is being submitted for publication.

Authors: **Naiomy Deliz Rios-Arce**[*], Fraser L Collins[*], Jonathan Schepper, Daniel A. Jones, Laura Schaeffer, Robert A. Britton, Laura R McCabe, Narayanan Parameswaran.

[*]These authors contributed equally to this work

3.1 Abstract

Probiotic bacteria have been shown to prevent bone loss in several mouse osteoporosis models. In previous studies we demonstrated that oral administration of *Lactobacillus reuteri* ATCC 6475 increased bone density in healthy male mice. The objective of this study was to understand the role of the immune system, especially the lymphocytes, in mediating the beneficial effects of *L. reuteri* on the male mouse skeleton. We administered *L. reuteri* in drinking water for 4 weeks to wild type or Rag knockout (C57BL/6) male mice, which lack mature T and B lymphocytes. While *L. reuteri* treatment increased bone density in wild type mice, no significant increases were seen in Rag knockout mice, suggesting that lymphocytes are critical for mediating the beneficial effects of *L. reuteri* on bone density. Further analyses, revealed that orally administered *L. reuteri* translocated from the intestinal lumen to the mesenteric lymph nodes, where it can directly interact with immune cells. In *ex vivo* studies using whole mesenteric lymph node (MLN) as well as $CD3^+$ T-cells, we established that live *L. reuteri* and its secreted factors have concentration-dependent effects on the expression of cytokines, including anti-inflammatory cytokine IL-10. Fractionation studies identified that the active component of *L. reuteri* is highly water soluble and small in size (<3kDa) and is negatively regulated by a RIP2 inhibitor, suggesting a role for NOD signaling. Finally, we show that T-cells from MLNs treated with *L. reuteri* supernatants, secrete factors that enhance osterix (transcription factor involved in osteoblast differentiation) *in vitro*. Together, these data suggest that *L. reuteri* secreted factors regulate T-lymphocytes which play an important role in mediating the beneficial effects of *L. reuteri* on bone density.

3.2 Introduction

Osteoporosis is a growing medical and socioeconomic issue that is characterized by systemic low bone mineral density, deteriorated bone microarchitecture and an increased risk of fracture (1,2). One in two women and one in four men over the age of 50 will experience an osteoporotic fracture in their lifetime; costing over $25 billion annually in the United States alone by 2025 (3). While numerous therapies are available for reducing bone loss, they are associated with side-effects or high costs (4,5). Therefore, some patients choose to either not start the course of treatment or do not see it through to conclusion, increasing their risk of having an osteoporotic fracture and further complications (6). For these reasons novel osteoporosis therapeutics that are low-cost and that have fewer side-effects are desired.

In recent years the gut-bone axis has gained significant attention. Dysbiosis of the intestinal microbiota has been shown to be associated with pathogenesis of diseases including inflammatory bowel disease (IBD), diabetes, obesity and rheumatoid arthritis all of which are associated with bone loss and the development of osteoporosis (7–10). In contrast, supplementation with probiotic bacteria has been demonstrated to have beneficial effects on bone health. Our lab has previously shown that administration of *Lactobacillus reuteri* (*L. reuteri*) 6475 to male mice for 4 weeks increased femoral trabecular bone density (11). Interestingly, the beneficial bone effect of *L. reuteri* was observed in female mice only under a mild inflammatory state or if they were ovariectomized, suggesting a role for inflammation and/or sex hormones in modulating probiotic activity (12,13). Probiotic bacteria have also been tested for their potential therapeutic effects in a number of diseases associated with adverse bone loss (14,15). Our lab has demonstrated that *L. reuteri* 6475 prevents bone loss associated with type 1 diabetes, low estrogen, as well as dysbiosis-induced bone loss in mice (13,16–19). Still, the exact mechanism by which *L. reuteri* 6475 in the intestinal tract exerts a systemic effect to promote bone health remains to be fully elucidated.

The current paradigm for interaction between bacteria and the immune system in the intestine involves the uptake of bacteria by microfold cells (M cells) in the follicle-associated epithelium of Peyer's patches, transfer of bacteria via channels in goblet cells, or paracellular or transcytotic transport across the epithelium (20). These bacteria are then taken up by antigen presenting cells (APCs) in the Peyer's patches, lamina propria or mesenteric lymph nodes (MLNs) which then activate T-cells (20). Given that *L. reuteri* is administered orally, we wanted to examine whether the immune system, specifically the lymphocytes are involved in the beneficial effects of this probiotic bacteria on bone health. Using Rag knockout mice, deficient in mature T- and B-lymphocytes, we demonstrate that the benefits of *L. reuteri* on bone health require lymphocytes. We further show that *L. reuteri* translocates to the MLNs and interacts with cells in MLNs. In *ex vivo* studies, we demonstrate that live *L. reuteri* and its secreted components stimulate T-lymphocytes to secrete factors that can benefit osteoblasts. Together, our studies provide potential host as well as bacterial mechanisms by which *L. reuteri* enhances bone density in male mice.

3.3 Materials and Methods

3.3.1 Ethical approval

All animal procedures were approved by the Michigan State University Institutional Animal Care and Use Committee and conformed to NIH guidelines.

3.3.2 Animals and experimental design

For all experiments, mice were purchased from Jackson Laboratories (Bar Harbor, ME) and housed in a specific pathogen free facility at Michigan State University. All mice were maintained on a 12:12-h light-dark cycle at 23°C in groups of up to 5 animals per cage for the duration of the studies. Mice shipped from Jackson laboratories were allowed to acclimate to the animal facilities for at least one week prior to the start of experimentation.

For *in vivo* experiments, male mice at 12 weeks of age wild-type (C57BL/6) and Rag knockout ($Rag1^{tm1Mom}$, C57BL/6 background) were randomly divided into four cohorts: WT (+/- LR) and KO (+/- LR). Both strains of mice were housed in the same room and on the same rack to ensure adaptation to identical housing environment and to prevent cage effect. *L. reuteri* treated mice received $3.3x10^8$ cfu/ml of *L. reuteri* in drinking water for four weeks. Water bottles were changed every other day, and fresh *L. reuteri* added. Control mice received just water. Mice were given Teklad 7914 chow (Madison, WI) and water *ad libitum*. At the end of the experiment mice were sacrificed by overdose of anaesthesia (isoflurane) followed by cervical dislocation.

3.3.3 Bacterial culture conditions

L. reuteri ATCC PTA 6475 was initially cultured on deMan, Rogosa, Sharpe media (MRS, Difco) - agar plates and kept under anaerobic conditions at 37°C for a maximum of 1 week. For live bacteria, multiple colonies were picked and anaerobically cultured in 10 ml of MRS broth for 16-18 h at 37°C. Bacteria were washed by centrifugation at 4000 RCF for 10 minutes and re-suspended in 10 ml sterile PBS, twice, to remove all traces of MRS broth. Following the final

wash, bacteria were re-suspended in 10 ml RPMI (no serum or antibiotics). Bacterial concentration was calculated using the OD_{600} value. For heat killed bacteria, 1 ml of bacterial suspension was heated to 70°C for 50 minutes. Bacteria viability was confirmed by plating on MRS plates and culturing anaerobically overnight at 37°C.

For *in vivo* experiments *L. reuteri* was cultured as above with a few modifications to produce a higher concentration of bacteria. After sub-culturing into 10ml of fresh MRS broth for 16-18 hours the overnight culture was then sub-cultured anaerobically at 37°C in 800 ml fresh MRS broth and grown until log phase (OD_{600}=0.4). *L. reuteri* was then pelleted by centrifugation at 4000 RCF for 10 minutes and washed 3 times with PBS. The final pellet was re-suspended in 60 ml sterile PBS and one milliliter (ml) aliquots were made and stored at -80°C until use. Colony-forming units per milliliter (cfu/ml) were calculated the day before treatment by plating 10 µl of the aliquots onto MRS agar plates overnight at 37°C. Mice were treated with $3.3x10^8$ cfu/ml of *L. reuteri* in the drinking water. Drinking water was refilled with fresh water and/or probiotic 3X/week.

3.3.4 Generation of bacterial conditioned media

For generation of conditioned media (CM) live bacteria were cultured as above. Following re-suspension in RPMI, bacteria were incubated anaerobically on a rocker for 3 hours at 37°C. Bacteria was pelleted by centrifugation at 4000 RCF for 10 minutes and conditioned RPMI media collected, pH determined and sterile filtered (0.22µm). Control media was generated by adjusting the pH of RPMI media to that of the bacteria CM using lactic acid (Sigma, St Louis, MO, USA). Control media and CM were aliquoted and stored at -80°C for use in further experiments.

3.3.5 Generation of <3kDa fraction of *L. reuteri* conditioned media

L. reuteri conditioned media or RPMI control media was added to an Amicon Ultra-15 3K centrifugal filter unit (EMD Millipore, Billerica, MA, USA) and centrifuged at 4000 RCF for 30-

60 minutes. Flow through containing the <3kDa fraction was collected, sterile filtered (0.22µm), aliquoted and stored at -80°C for use in further experiments.

3.3.6 Solid-Phase extraction (SPE) fractionation of conditioned media

Fractionation of *L. reuteri* conditioned media or RPMI control media based on solubility was performed using Oasis PRiME HLB extraction columns (Waters, Milford, MA, USA). Briefly, CM or RPMI was added to the column and flow through collected (load). Components retained in the column were collected by washing with dH_20 (wash) followed by 90% acetonitrile / 10% dH_20 (elute). Solvents were removed from the fractions by evaporation via speed-vac until dryness. Samples were re-suspended in a comparable volume of RPMI, aliquoted and stored at -80°C until further use.

3.3.7 Carboxyfluorescein Succinimidyl Ester (CFSE) staining of bacteria and analysis of translocation to the mesenteric lymph nodes

Live *L. reuteri*, generated as described, was stained with CellTrace CFSE cell proliferation kit according to manufacturer's instructions (ThermoFisher Scientific, USA). Male C57BL/6 mice, 14 weeks of age, were gavaged with 300 µl (approx. $1x10^9$ cfu/ml) CFSE stained *L. reuteri*. Mice were sacrificed at 0 (n=2), 6 (n=2) and 24 (n=1) hours post gavage and the mesenteric lymph nodes isolated (21), homogenized and presence of $CFSE^+$ bacteria analyzed by flow cytometry.

3.3.8 Mesenteric lymph node stimulation

MLNs were isolated from adult male mice (12 – 18 weeks) and homogenized in RPMI media. Whole MLN cultures were plated in a 96 well U-bottom plate at $1x10^5$ cells per well. For $CD3^+$ MLN cultures, $CD3^+$ cells were isolated by magnetic cell sorting according to manufacturer's instructions (Miltenyi Biotec, San Diego, CA, USA) and plated at $1x10^5$ cells per well. Cells were cultured in the presence of live or heat killed (HK) *L. reuteri* 6475, at a multiplicity

of infection (MOI) of 1, 10 and 100, or conditioned media (+10% FBS) for 4 days at 37°C 5% CO_2 followed by flow cytometric analysis for the respective cytokines.

3.3.9 Isolation and treatment of naïve $CD4^+$ T cells

Spleens were isolated from male C57BL/6 mice (12 – 18 weeks), homogenized and re-suspended in RPMI media. Naïve $CD4^+$ T cells were isolated using a magnetic Naïve $CD4^+$ T Cell Isolation Kit according to manufacturer's instructions (Miltenyi Biotec). Isolated $CD4^+$ T cells ($1x10^5$) were then cultured under non-polarising conditions in the presence of conditioned media (whole or fractionated) or live or heat killed (HK) *L. reuteri* 6475 at a multiplicity of infection (MOI) of 1, 10 and 100, for 4 days at 37°C 5% CO_2 followed by flow cytometric analysis.

3.3.10 Flow cytometry analysis

For analysis, cells were pelleted and supernatant removed. Cells were incubated with Fc block (BD Pharmingen, CA, USA) for 15 min. Cells were stained with anti-mouse CD3-APC AlexaFluor 780 (500A2, eBioscience) and anti-mouse CD4-eF450 (RM 4–5, eBioscience) for 30 minutes at 4°C. Cells were then washed three times in assay buffer (PBS, 0.5% bovine serum albumin (BSA), 5mM EDTA) followed by permeabilization in cytofix / cytoperm per manufacturer's instructions (BD Pharmingen). Intracellular staining was performed with anti-mouse IL-10 FITC (JES5-16E3, eBioscience), anti-mouse IL-17A PE (TC11-18H10, BD Bioscience), anti-mouse IFNγ APC (XMG1.2, eBioscience) and anti-mouse LAP (TGFβ) PerCP-eF710 (TW7-16B4, eBioscience). Data were acquired on a BD LSRII (Becton Dickinson, Franklin Lakes, NJ) and analyzed with FlowJo (Version 10; FlowJo, LLC, Ashland OR).

3.3.11 *In vitro* cell culture system

Preosteoblast MC3T3-E1 cells (CRL-2593; ATCC, Manassas, VA) (passages between 18 to 24) were kept incomplete α–minimal essential media (α-MEM) containing 10% fetal bovine serum (FBS) (Invitrogen and Atlanta Biologicals, Atlanta, GA) and 1% Penicillin-Streptomycin

(Life Technologies). For gene expression analysis, cells were plated at a density of 20,000 cells/well in 96-well plates (Corning Incorporated, Corning NY) for 24 hours in complete α-MEM. Cells were treated as indicated for 6 hours. RNA extraction was completed as describe below.

For cell viability assay, MC3T3-E1 cells were plated at a density of 10,000 cells/well in white walled 96-well plates (Corning Incorporated, Corning NY) for 24 hours in complete α-MEM. Cells were treated as indicated for 6 hours. Cell viability (by assessing intracellular ATP levels) was measured by ApoSensor Cell Viability Assay kit (BioVision, San Francisco, CA) according to the manufacturer's instructions. Luminescence was measured by Synergy/neo2 multi-mode plate reader and calculated with Gen5 software (Bio-Tek). Duplicates wells were used for each condition and repeated at least three times.

3.3.12 RNA extraction

TriReagent (Molecular Research Center, Cincinnati, OH) was used to isolate RNA and RNA integrity was verified by agarose-gel electrophoresis. cDNA was synthesized by reverse transcription using Superscript II Reverse Transcriptase Kit and oligo dT primers (Invitrogen, Carlsbad, CA). Complementary DNA was amplified by PCR using iQ SYBR Green supermix (Bio-Rad Laboratories, Hercules, CA). Real time PCR was carried out for 40 cycles (95^{o} C for 15 seconds, 60^{o} C for 30 seconds, and 72^{o} C for 30 seconds) using an iCycler thermal cycler and data evaluated using the iCycler software. Negative controls included primers without cDNA. RNA levels of the housekeeping gene hypoxanthine guanine phosphoribosyl transferase (HPRT) did not fluctuate with treatment and were used as an internal control. Primers used for real-time polymerase chain were as follows: *HPRT* (Forward, **5**'- AAGCCTAAGATGAGCGCAAG- **3**', Reverse, **5**'- TTACTAGGCAGATGGCCACA), *Osterix* (Forward **5**'- CTGCGGAAAGGAGGCACAAAGAAG- **3**', Reverse, **5**'- GGGTTAAGGGGAGCAAAGTCAGAT-3'), *Bax* (Forward **5**' GACAGGGGGCTTTTTGCTA

3', Reverse, **5**'- TGTCCACGTCAGCAATCATC- **3**'), *Bcl-2* (Forward **5**'-GACAGAAGATCATGCCGTCC- **3**', Reverse, **5**'- GGTACCAATGGCACTTCAAG- **3**').

3.3.13 Microcomputed tomography (μCT) bone imaging

Femoral bones were collected at the day of harvest and fixed in 10% formalin for 24 hours. Bones were transferred to 70% ethanol and scanned using a GE Explore Locus microcomputed tomography (μCT) system at a voxel resolution of 20 μm obtained from 720 views. Each run included bones from all groups, as well as a calibration phantom to standardize gray scale values and maintain consistency. A fixed threshold (841) was used to separate bone from the bone marrow. Femur trabecular bone analyses were performed from 1% of the total length proximal to the growth plate, extending 2 mm toward the diaphysis, and excluding the outer cortical bone. Trabecular bone volume fraction (BVF), bone mineral content (BMC), bone mineral density (BMD), thickness (Tb. Th), spacing (Tb. Sp), and number (Tb. N) were computed using GE Healthcare MicroView software. Femoral trabecular isosurface images were taken from a region in the femur where analyses were performed measuring 1.0 mm in length and 1.0 mm in diameter. Cortical measurements were performed in a 2x2x2 mm cube centered midway down the length of the bone.

3.3.14 DNA extraction from colonic and fecal samples, 16S rRNA gene amplification, and sequencing

DNA was extracted from colonic and fecal samples as previously described (19). Briefly, fecal samples were transferred to Mo Bio Ultra Clean Fecal DNA bead Tubes (MoBio) containing 360 μl of buffer ATL (Qiagen) and homogenized for one minute in a BioSpec Mini-Beadbeater. Forty μL Proteinase K (Qiagen) was added and samples were incubated for 30 minutes at 55°C, then homogenized again for one minute and incubated at 55°C for additional 30 minutes. DNA was extracted modified extraction with Qiagen DNeasy Blood and Tissue kits as described

previously (13,22). Bacterial 16S sequences spanning variable region V4 were amplified by PCR with primers F515/R806 with a dual indexing approach and sequenced by Illumina MiSeq described previously (23). Twenty µl PCR reactions were prepared in duplicate and contained 40 ng DNA template, 1X Phusion High-Fidelity Buffer (New England Biolabs), 200 µM dNTPs (Promega or Invitrogen), 10 nM primers, 0.2 units of Phusion DNA Polymerase (New England Biolabs), and PCR grade water. Reactions were performed in an Eppendorf Prothermal cycler with an initial denaturation at 98 °C for 30 s, followed by 30 cycles of 10 s at 98 °C, 20 s at 51 °C, and 1 min at 72 °C. Replicates were pooled and purified with Agencourt AMPure XP magnetic beads (Beckman Coulter). DNA samples were quantified using the QuantIt High Sensitivity DNA assay kit (Invitrogen) and pooled at equilmolar ratios. The quality of the pooled sample was evaluated with the Bioanalyzer High Sensitivity DNA Kit (Agilent).

3.3.15 Microbial community analysis

Sequence data was processed using the MiSeq pipeline for mothur using software version 1.38.1 (24) as described previously (22). In brief, forward and reverse reads were aligned, sequences were quality trimmed and aligned to the Silva 16S rRNA gene reference database formatted for mother, and chimeric sequences were identified and removed using the mothur implementation of UCHIME. Sequences were classified according to the mothur-formatted Ribosomal Database Project (version 16, February 2016) using the Bayesian classifier in mothur, and those sequences classified as Eukarya, Archaea, chloroplast, mitochondria, or unknown were removed. The sequence data were then filtered to remove any sequences present only once in the data set. After building a distance matrix from the remaining sequences with the default parameters in mothur, sequences were clustered into operational taxonomic units (OTUs) with 97% similarity using the average-neighbor algorithm in mothur. 871 OTUs were identified across all samples with an average rarefaction depth of 54,791 reads per sample. Alpha and beta diversity analyses and

visualization of microbiome communities were performed with R, utilizing the phyloseq package (25,26). The Bray-Curtis dissimilarity matrix was used to describe differences in microbial community structure. Analysis of similarity (ANOSIM) was performed in mothur.

3.3.16 Statistical Analysis

All measurements are presented as the mean ± SEM or as box plots (whiskers indicate minimum to maximum values). Significance was tested using either Student's t test (2 groups) or ANOVA (more than 2 groups) with the indicated post-hoc test. Statistical analysis was performed using GraphPad Prism software version 7 (GraphPad, San Diego, CA, USA). Significant outliers (if present and indicated in figure legend) were removed using the ROUT test for outliers. A p-value of <0.05 was considered significant.

3.4 Results

3.4.1 *L. reuteri* requires lymphocytes to exert beneficial effects on bone

Previous studies have revealed that supplementation with the probiotic *L. reuteri* ATCC 6475 can have a beneficial effect on bone health (11–13,16,19) though the exact mechanisms are currently unknown. We and others have shown that *L. reuteri* has immuno-regulatory properties *in vitro* and *in vivo*, suggesting a role for the immune system in modulating the effects of *L. reuteri* on bone density (11,13,27). Although previous studies have shown that *L. reuteri* can modulate the immune system, the specific role of different immune cells in mediating effects on bone are not well known. To address this, we utilized male mice that are deficient in mature T and B lymphocytes (Rag1 knockout) and wild type (WT) controls. WT and KO mice were administered *L. reuteri* in their drinking water for 4 weeks. Control mice received water without the probiotic. After 4 weeks, *L. reuteri* administration had no significant effect on body weight or weights of organs including liver, muscle (tibialis), kidney, thymus and spleen (Figure 3.1). As expected, a significant decrease in thymus and spleen weights was observed in the KO group compared to the WT mice (Fig 1E and F). As we reported earlier (11), oral *L. reuteri* treatment significantly increased trabecular femoral bone density by 37% in the WT mice (Figure 3.2, $p<0.05$). In contrast, *L. reuteri* treatment did not enhance trabecular femoral bone density in the KO mice (Figure 3.2), suggesting that *L. reuteri* requires lymphocytes to increase trabecular bone density. Consistent with our findings, bone mineral density (BMD, $p<0.05$) and trabecular thickness increased (Tb. Th, $p<0.05$), while trabecular spacing decreased (Tb. Sp, $p<0.05$) in the *L. reuteri* treated WT mice (Table 3.1). Analysis of the cortical regions of the femur (diaphyseal region) showed that marrow area was decreased and outer perimeter increased by *L. reuteri* in the WT mice but not in the KO. Other parameters did not demonstrate any significant differences between the groups (Table 3.1).

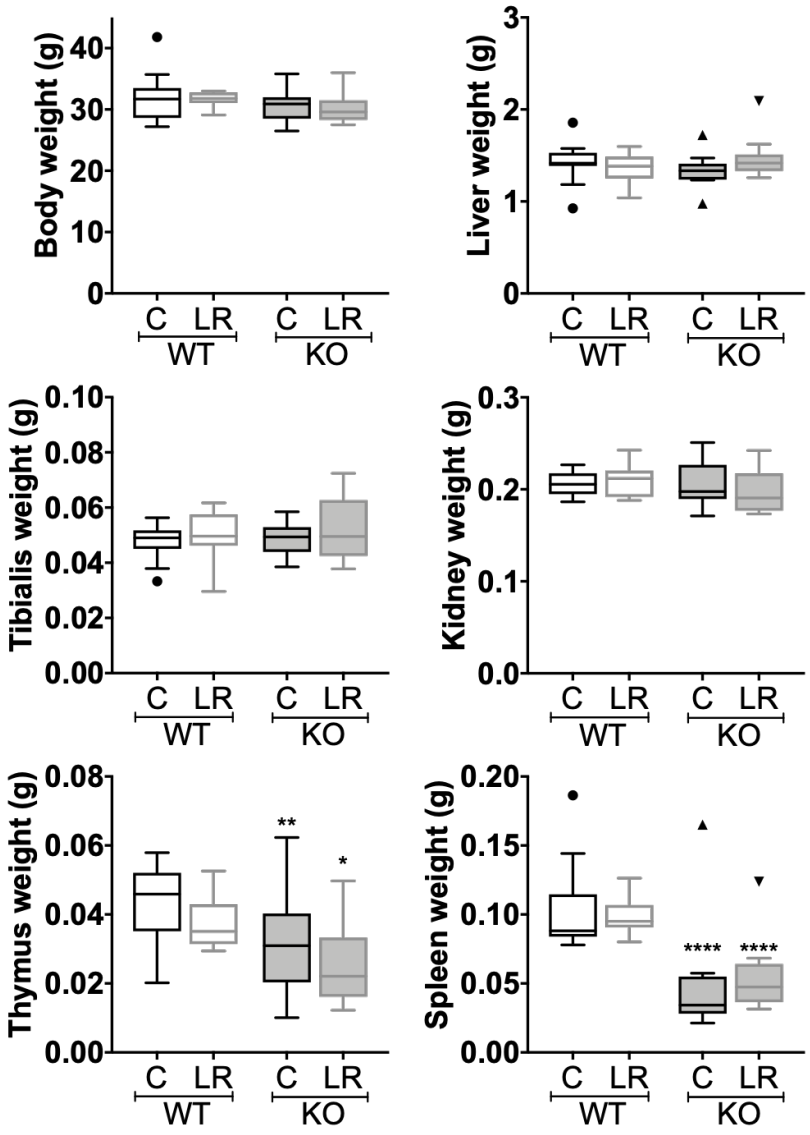

Figure 3.1. General body parameters.

12 weeks old C57BL/6 and Rag KO male mice were supplemented with water (n=11) or *L. reuteri* (n=10) for 4 weeks. General body parameters were measured the day of harvest. Body, liver, tibialis, kidney, thymus, and spleen weight in grams (g). *L. reuteri* treatment had no effect on general body parameters. Data presented as box plots with Whiskers using Tukey method. Statistical analysis performed by One-way ANOVA with Holm-Šídák correction for multiple comparisons. *=p<0.05, **=p<0.01

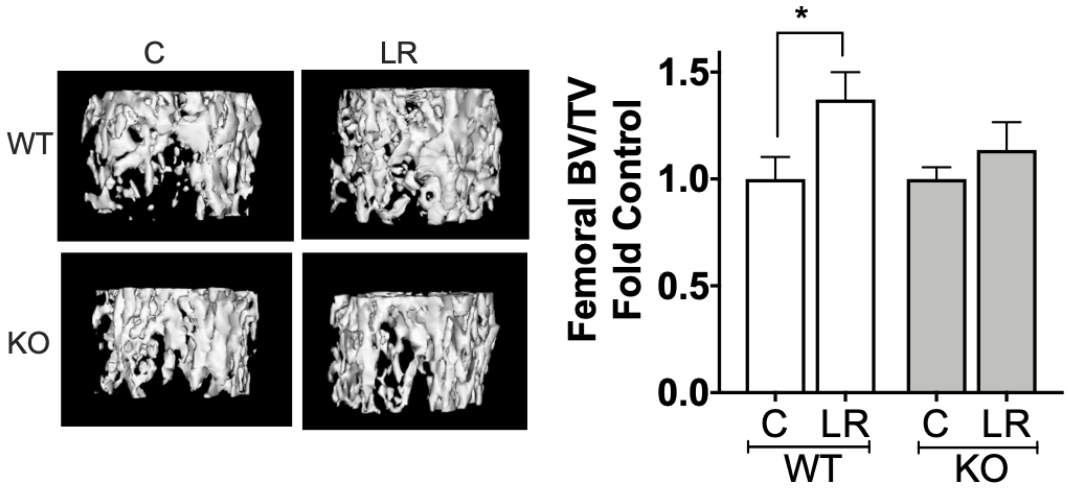

Figure 3.2. *L. reuteri* requires lymphocytes to exert beneficial effect on bone.

Twelve week old C57BL/6 and Rag KO male mice were supplemented with water (n=11) or *L. reuteri* (n=10) for 4 weeks. Femoral bone was collected, and trabecular and cortical bone analyzed by μCT. Representative micro-computed tomography isosurface images by uCT. Bone volume fraction (BV/TV) quantitative data obtained from the distal femur trabecular bone of control and *L. reuteri* treated mice. Statistical analysis performed one-way ANOVA with Dunnett's post-test. *=$p<0.05$

	Femoral Bone Parameters			
	WT		KO	
Parameter:	C (n=11)	LR (n=10)	C (n=11)	LR (n=10)
Femur trabecular				
BV/TV	32.28 ± 3.33	44.45 ± 4.16 #	40.53 ± 2.23	46.05 ± 5.25
BMD (mg/mL)	243.5 ± 8.13	282.5 ± 12.41 #	265.2 ± 6.27	290.3 ± 18.44
BMC (mg)	0.46 ±0 .02	0.52 ± 0.01	0.51 ±0 .01	0.52 ±0 .02
Tb. Th. (mm)	0.04 ±0 .002	0.06 ±0 .004 #	0.05 ± 0.002	0.07 ±0.006 *
Tb. N.(1/mm)	6.94 ±0 .46	7.24 ± 0.24	7.23 ±0.23	6.47 ± 0.35
Tb. Sp. (mm)	0.10 ± 0.01	0.08 ± 0.008	0.08 ± 0.006	0.07 ± 0.007
Femur Cortical				
Cortical area (mm^2)	0.96 ± 0.05	0.93 ± 0.04	0.94 ± 0.04	0.93 ± 0.04
Marrow area (mm^2)	0.81 ± 0.04	0.68 ± 0.03 #	0.67 ± 0.02	0.66 ± 0.04
Mean thickness (mm)	0.24 ± 0.008	0.25 ± 0.006	0.25 ± 0.007	0.25 ± 0.008
Inner perimeter (mm)	3.76 ± 0.07	3.73 ± 0.04	3.62 ± 0.09	3.77 ± 0.13
Outer perimeter (mm)	6.77 ± 0.43	7.96 ± 0.26 #	7.24 ± 0.42	8.08 ± 0.44
BMD (mg/mL)	784.3 ± 13.43	779.7 ± 7.17	784.1 ± 7.14	800 ± 11.65
BMC (mg)	0.01 ± 0.001	0.02 ± 0.00	0.01 ± 0.00	0.02 ± 0.00

Table 3.1 General mouse bone parameters.

Values represent mean ± standard error

Abbreviations: BV/TV, bone volume/total volume; BMD, bone mineral density; BMC, bone mineral content, Tb.Th., trabecular thickness; Tb. N., trabecular number; Tb.Sp., trabecular space $^{\#}$ $p < 0.05$ with respect to WT-C * $p < 0.05$ with respect to KO-C

3.4.2 Effect of *L. reuteri* on α and β diversity in gut microbiota in male mice

To assess if probiotic administration significantly modulated intestinal microbiota diversity in male mice and whether a difference in microbiota diversity could account for the lack of effect of *L. reuteri* in the Rag KO mice, we extracted DNA from colonic microbiota and performed 16S rRNA sequencing. Diversity metrics that utilize species richness and evenness (Bray-Curtis) showed no significant separation between the groups (WT±LR and KO±LR) (Figure 3.3B). Also, no significant differences were found in α diversity both in terms of OTUs and Shannon index (Figure 3.3A). These data suggest that *L. reuteri* treatment in either WT or Rag KO mice does not cause broad changes in bacterial communities in male mice. This result does not rule out changes in microbiota function or changes in specific bacterial species that may be impacted by *L. reuteri* supplementation. Given the absence of mature lymphocytes in Rag KO mice, we reasoned that the lymphocytes likely play an important and direct role in *L. reuteri* effects on bone.

3.4.3 *L. reuteri* translocates to mesenteric lymph node (MLN)

Because our *in vivo* studies were performed with *L. reuteri* administered orally, we reasoned that lymphocytes in MLNs would be one of the sites of *L. reuteri* interaction with lymphocytes. Therefore we examined if *L. reuteri* could be detected in MLNs in *L. reuteri* treated mice. C57BL/6 mice were gavaged with *L. reuteri* labelled with fluorescent CFSE (5(6)-Carboxyfluorescein N-hydroxysuccinimidyl ester). Mice were euthanized, and MLNs harvested at various time points (0, 6 and 24 hours). Isolated MLNs were then processed and analyzed by flow cytometry for CFSE labelled *L. reuteri*. The CFSE positive bacterial counts in the MLN increased ~32 fold at the 6 hour time point but returned to control levels by 24 hours after gavage. These results suggest that *L. reuteri* is able to translocate from the intestinal lumen to the MLNs early after oral administration and therefore could interact with cells in the lymph node (Figure 3.4).

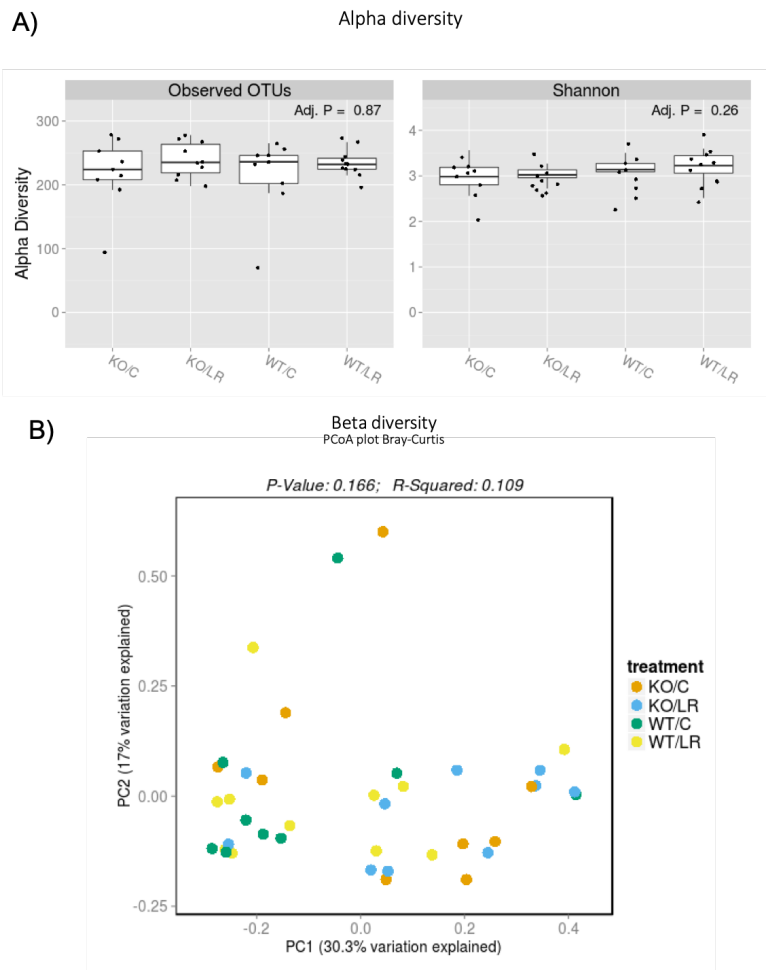

Figure 3.3. *L. reuteri* effects on gut microbiota.

Twelve week old C57BL/6 and Rag KO male mice were supplemented with water or *L. reuteri* for 4 weeks as indicated in Figure 3.2. Fecal samples were collected at the day of harvest and analyzed by 16S rRNA sequencing as described in the methods. A) Plots of alpha-diversity metrics of observed operational taxonomic units (OTUs) (richness) and Shannon diversity (richness and eveness) of the different treatment groups. B) Principle coordinate analysis of beta-diversity based on Bray-Curtis (richness and eveness) of the different treatment groups. WT/C = wild-type control, WT/LR = wild-type *L. reuteri* treated, KO/C = Rag1 KO control, KO/LR = Rag1 KO *L. reuteri* treated. n = 9-10/group.

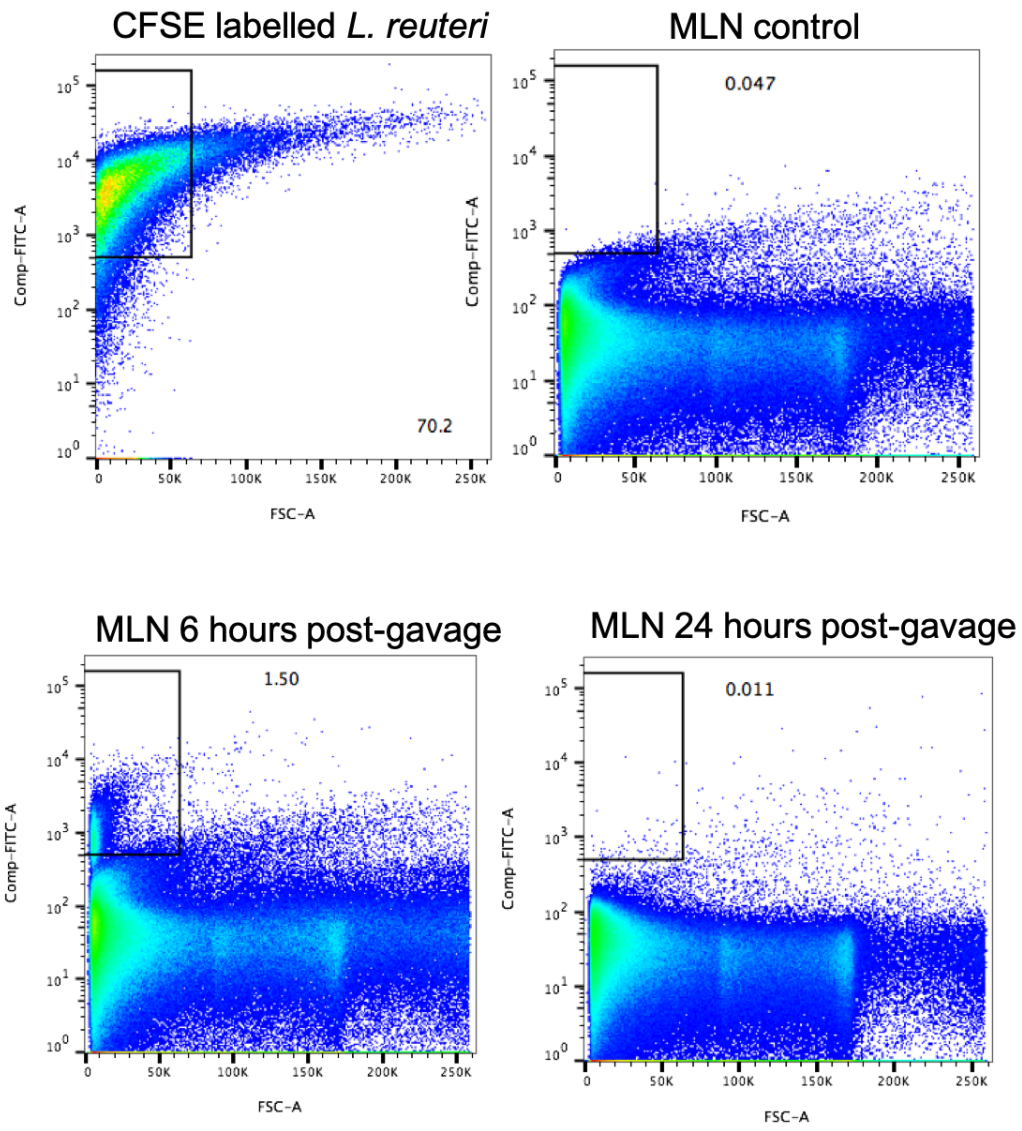

Figure 3.4. Translocation of CFSE-labeled *L. reuteri* from the intestinal lumen to the MLN. Male C57BL/6 mice (14 weeks) were gavaged with CFSE-labeled *L. reuteri*. After 0, 6 and 24 hours mice were sacrificed and MLNs collected and analyzed by flow cytometry. Representative scatter plots of CFSE-labeled with *L. reuteri* isolated from MLNs at 0, 6 and 24 hours, CFSE-labeled bacteria are present in the top-left quadrant.

3.4.4 Effect of live *L. reuteri* on cytokine expression in whole MLN *ex vivo* cultures

Our data thus far suggests that the bone effects of *L. reuteri* requires lymphocytes and that *L. reuteri* is able to translocate to MLNs upon oral administration. To examine the effect of *L. reuteri* on expression of cytokines in MLNs, we treated MLNs *ex vivo* with *L. reuteri* for 4 days and assessed expression of cytokines that have been shown to regulate bone health. We focused on IL-10 and TGFβ (can enhance bone health)(28–32) as well as IFNγ (negatively influences bone health) and IL-17A (has both negative and positive effects on bone) (33–35). These cytokines were assessed using flow cytometry. Treatment of MLN cultures with live *L. reuteri* significantly increased expression (as indicated by median fluorescent intensity; MFI) of IL-10 and IFNγ in a concentration-dependent manner ($p<0.01$). In addition, the number of IL-10+ and IFNγ+ cells also increased significantly ($p<0.01$). In contrast, TGFβ expression showed minimal change with live *L. reuteri*. However, TGFβ+ cell numbers were differentially modulated at different MOI, with an MOI of 1 causing an increase ($p<0.05$), and higher MOIs showing no difference. While expression of IL-17A increased only at the highest MOI, IL-17A$^+$ cell numbers were not affected by live *L. reuteri* (Figure 3.5A). Gating within the CD4$^+$ T cell population also revealed similar expression and +cell profiles, except for TGFβ which showed a biphasic response with both MFI for TGFβ as well as TGFβ+ cell numbers (Figure 3.5B). Compared to live *L. reuteri*, effect of heat killed *L. reuteri* was not consistent and in some cases showed a modest response only at high concentrations ($p<0.05$) (Figure 3.5B). Together, these results demonstrate that live but not heat killed *L. reuteri* can significantly induce concentration-dependent effects on the MLN immune cell cytokine profiles and the majority of these effects are similar between the whole MLN and the MLN CD4$^+$ T cell population.

Mesenteric lymph nodes contains a multitude of different cells types including antigen presenting cells (APCs). To identify whether the effects of *L. reuteri* on the CD4$^+$ T cells was

indirect via APCs or direct on the T cells, $CD3^+$ cells were isolated from whole MLNs and cultured with either live or heat killed *L. reuteri*. As with the whole MLN cultures, addition of live *L. reuteri* to $CD3^+$ MLN cells had a profound effect on cytokine expression (Figure 3.6A). Live *L. reuteri* significantly increased expression of IL-10, IL-17A, TGFβ and IFNγ in a concentration-dependent manner as determined by flow cytometry. Similarly, number of $CD3^+$ cells expressing these respective cytokines was also significantly increased by live *L. reuteri* treatment. Compared to this, heat killed *L. reuteri* had no significant effect on expression of any of the cytokines examined. When gated within the CD4+ T-cells, the results were similar to that of CD3+ T cells (Figure 3.6B).

Having revealed that *L. reuteri* directly modulates MLN $CD4^+$ T cell cytokine expression, we next sought to determine the effects of live *L. reuteri* on naïve $CD4^+$ T cells. $CD4^+$ T cells were isolated from spleens by magnetic isolation and treated with either live or heat killed *L. reuteri* under non-polarising culture conditions. Comparable to the responses of isolated $CD3^+$ MLN cultures, $CD4^+$ splenic T cells exhibited a concentration-dependent response to live *L. reuteri* for both IL-10 and IL-17A expression ($p<0.01$) (Figure 3.7). IFNγ expression increased significantly only at an MOI of 100 ($p<0.01$) while no effect was observed for TGFβ. Heat killed *L. reuteri* increased IL-10 ($p<0.05$) and IL-17A ($p<0.01$) expression modestly, only at an MOI of 100 (Figure 3.7). Together, these data suggest that live *L. reuteri* is able to stimulate T-cells directly and can modulate cytokine expression in cells that have potential modulatory effects on bone health.

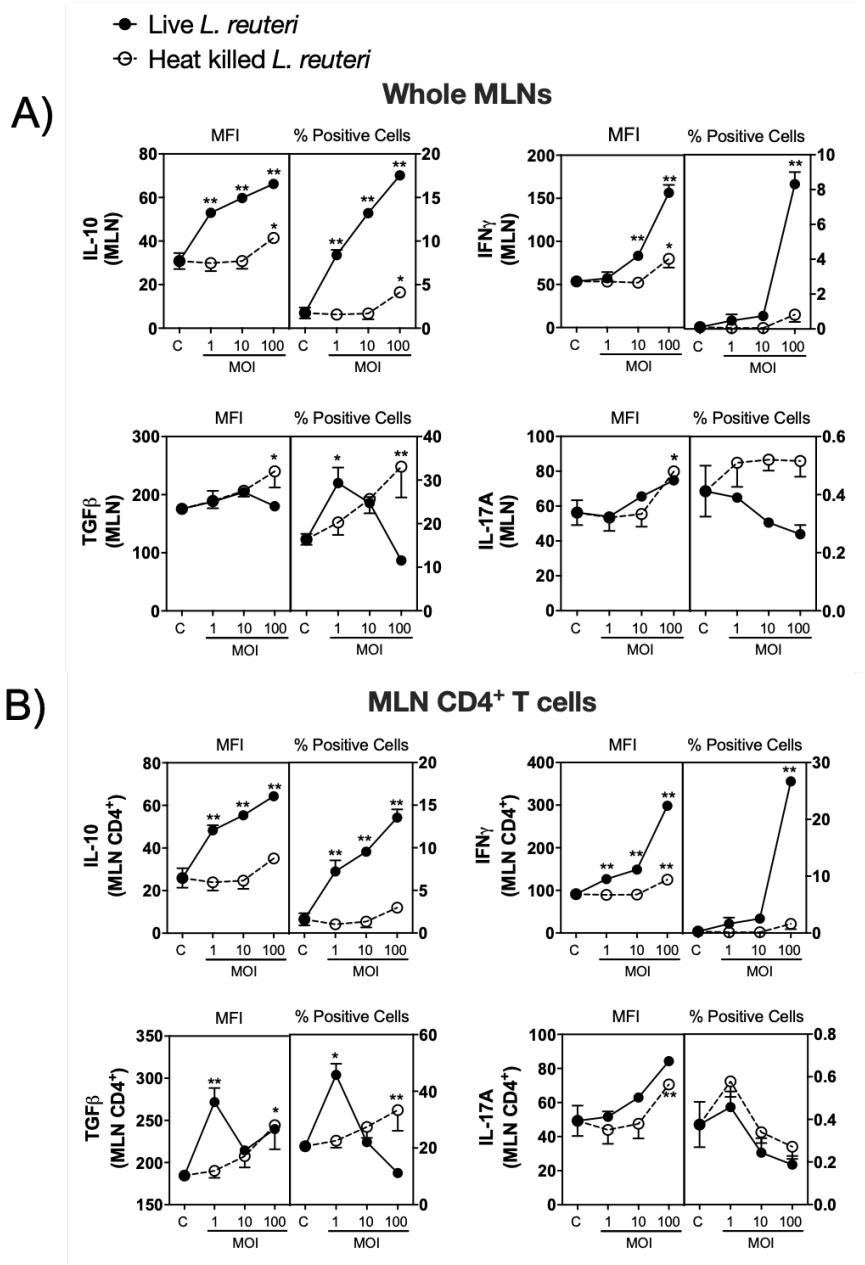

Figure 3.5. Effect of live and heat Killed *L. reuteri* 6475 on cytokine expression in whole MLN cultures.

Mesenteric lymph nodes were isolated from male C57BL/6 mice (12-18 weeks), homogenized and cultured with live or heat killed *L. reuteri* 6475 at an MOI of 1, 10 or 100 for 4 days. Cells were analyzed using flow cytometry for expression of IL-10, INFγ, IL-17 A and TGFβ.

Figure 3.5 (cont'd)

Results for MFI and % positive cells were analyzed as (A) the whole MLN or (B) gated on the MLN $CD4^+$ T cells. Statistical analysis performed by 2-way ANOVA with Dunnett's post-test and multiple t-tests corrected for multiple comparisons with Holm-Šídák method. *=$p<0.05$, **=$p<0.01$ compared to control. n=5

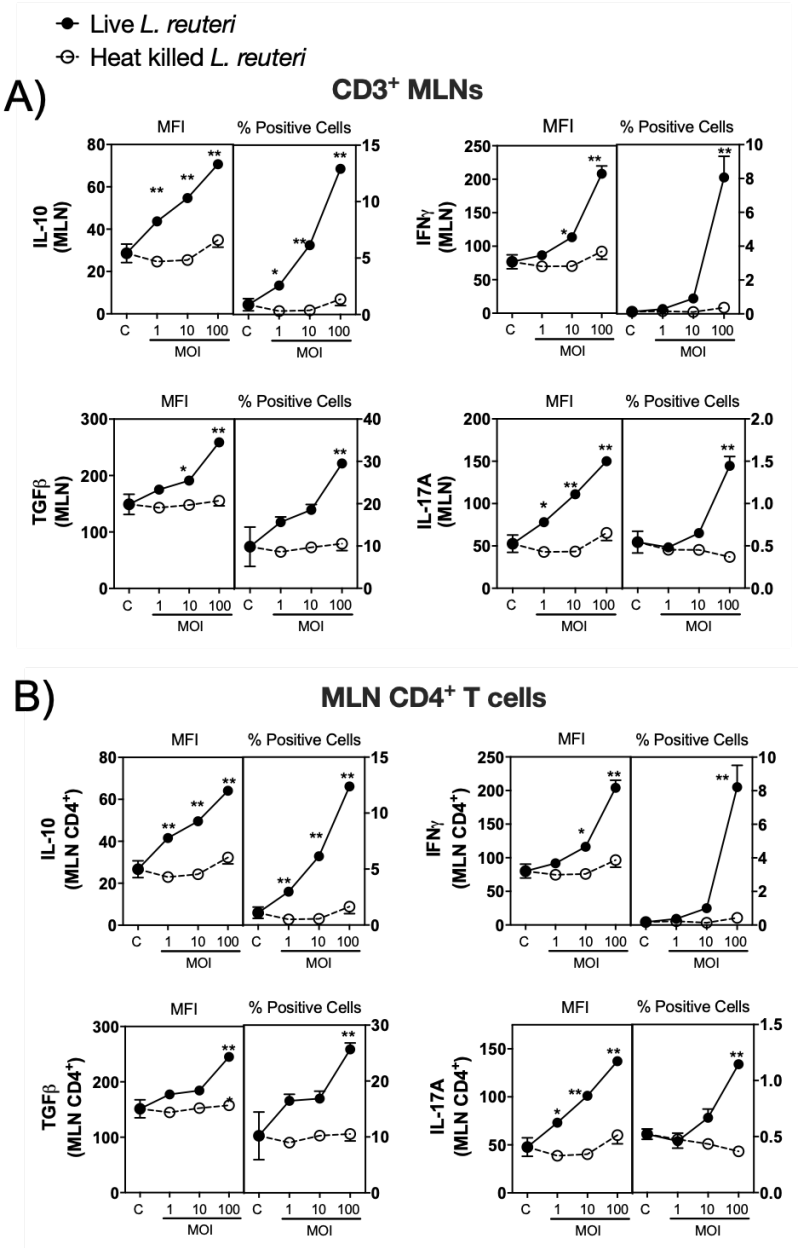

Figure 3.6. Effect of *L. reuteri* 6475 on cytokine expression in CD3$^+$ lymphocytes isolated from MLNs.

Mesenteric lymph nodes were isolated from male C57BL/6 mice (12-18 weeks), homogenized and CD3$^+$ cells obtained by magnetic separation. CD3$^+$ cells were cultured with live or heat killed *L. reuteri* 6475 at an MOI of 1, 10 or 100 for 4 days. Cells were analyzed using flow cytometry for

Figure 3.6 (cont'd)

expression of IL-10, INFγ, IL-17 A and TGFβ. Results for MFI and % positive cells were analyzed as (A) CD3+ cells or (B) gated on the MLN $CD4^+$ T cells. Statistical analysis performed by 2-way ANOVA with Dunnett's post-test and multiple t-tests corrected for multiple comparisons with Holm-Šídák method or by unpaired t-test. *=$p<0.05$, **=$p<0.01$ compared to relevant control. n=5.

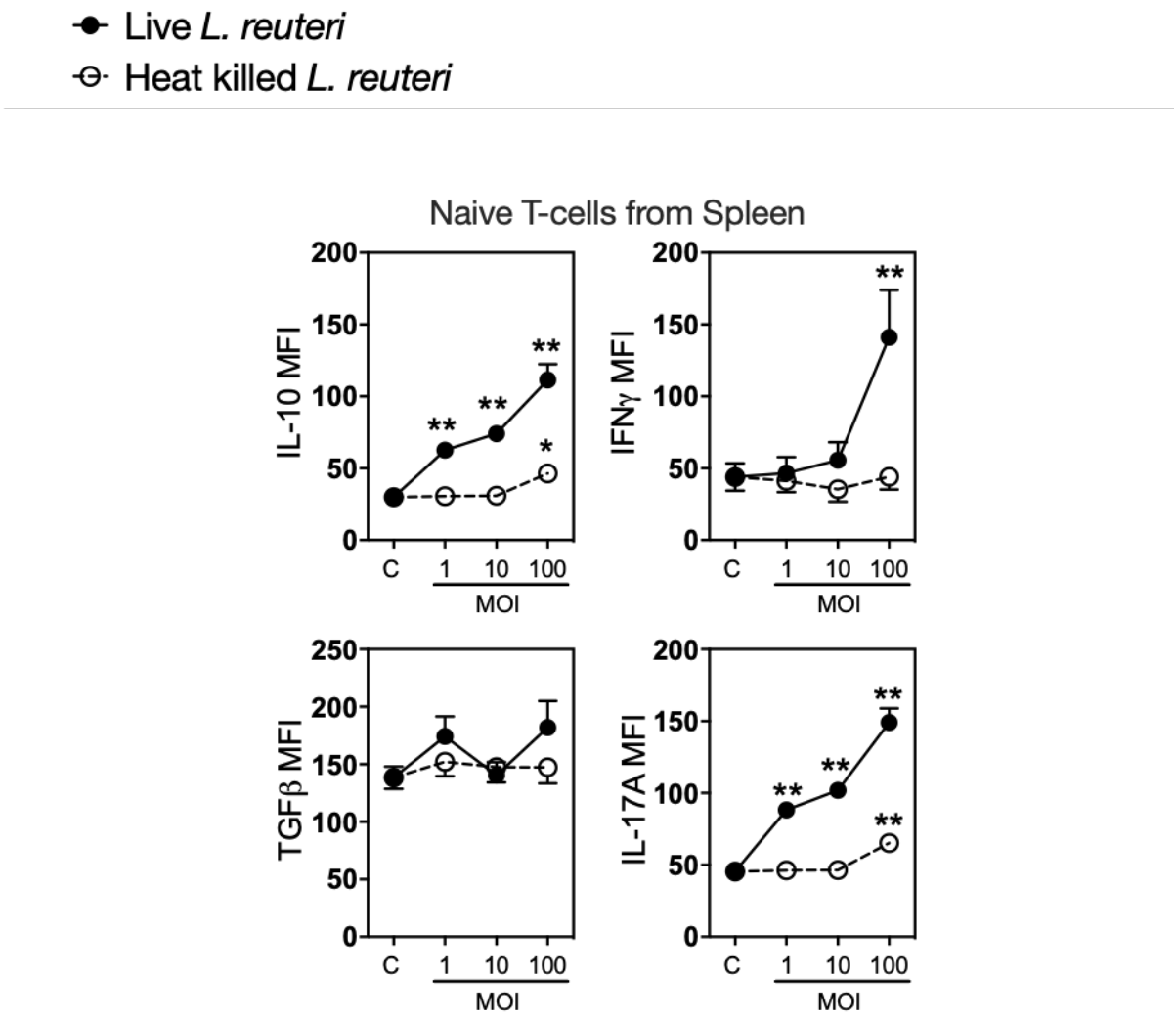

Figure 3.7. Effect of *L. reuteri* on naïve splenic CD4$^+$ T cells cytokine expression.

Spleens were isolated from male C57BL/6 mice (12-18 weeks) and naïve CD4$^+$ T cells obtained by magnetic separation. Cells were cultured under non-polarising conditions with live or heat killed *L. reuteri* 6475 at an MOI of 1, 10 or 100 for 4 days and cytokine expression (IL-10, INFγ, IL17A and TGFβ) analyzed by flow cytometry. Statistical analysis performed by 2-way ANOVA with Dunnett's post-test and multiple t-tests corrected for multiple comparisons with Holm-Šídák method or by unpaired t-test. *=p<0.05, **=p<0.01 compared to control. n=10.

3.4.5 Effect of *L. reuteri* secreted factors on T-lymphocyte cytokine expression

To identify whether the effects of live *L. reuteri* required direct cell-cell contact or whether the effects are induced by secreted factor(s), whole MLN cultures were treated *ex vivo* with *L. reuteri* conditioned media (CM). *L. reuteri* CM significantly elevated expression of all the cytokines assessed (IL-10, IFNγ, TGFβ and IL-17A) (Figure 3.8A). When gated within the CD4+ T-cells, expression of cytokines showed similar pattern (Figure 3.8A). Percentage of cytokine positive cells mostly followed a similar pattern to that of the MFI (data not shown). To determine whether *L. reuteri* secreted factor(s) were responsible for the observed direct effect of *L. reuteri* on T-lymphocytes, we further treated isolated $CD3^+$ T-cells from MLNs with *L. reuteri* CM. Similar to the effects on whole MLN cultures, *L. reuteri* CM treatment of isolated T-cells significantly increased $CD4^+$ T cell expression of all four cytokines (Figure 3.8B) as well as increased numbers of $CD4^+$ cytokine+ cells (data not shown). Similar to MLN cultures, treatment of CD4+ T cells (spleen) with *L. reuteri* CM also significantly increased the expression of all cytokines assessed (Figure 3.8C). Together, these results suggest that secreted component(s) of *L. reuteri* are able to directly stimulate T-cells and significantly modulate expression of cytokines.

3.4.6 RIP2 negatively regulates expression of IL-10 and IL-17A in lymphocytes

Probiotic bacteria and *Lactobacillus* bacteria in particular have previously been shown to induce their beneficial effects through toll-like receptor (TLR) signaling, specifically TLR2 (36,37). Furthermore, bacteria are able to induce a signaling cascade through activation of the Nucleotide-binding Oligomerization Domain (NOD) pathway (38). To determine whether *L. reuteri* secreted factors induce their modulatory effects through TLR or NOD signaling we inhibited MyD88 or RIP2 tyrosine kinase in splenic $CD4^+$ T cells prior to *L. reuteri* stimulation. To determine if *L. reuteri* was acting through a TLR in a MyD88-dependent manner, we used a MyD88 peptide inhibitor (Figure 3.9A). MyD88 inhibitor failed to block the effects of *L. reuteri*

on IL-10 and IL-17A. To further investigate whether *L. reuteri* signaled via the NOD pathway we utilized Gefitinib, a RIP2 tyrosine kinase inhibitor which inhibits RIP2 tyrosine phosphorylation and NOD2-induced NF-κB activation and cytokine release (39). *L. reuteri* CM significantly increased expression of IL-10, and IL-17A as expected; however, pretreatment of the cells with Gefitinib significantly augmented the expression of IL-10 ($p<0.01$), and IL-17A ($p<0.01$) suggesting that RIP2 negatively regulates expression of these cytokines in T-cells induced by *L. reuteri* CM (Figure 3.9B).

3.4.7 Fractionation of *L. reuteri* conditioned media

To identify the active components secreted by *L. reuteri* that influences T-cell cytokine expression, the conditioned media was subjected to a series of fractionations based on size and water solubility. Fractionation based on size revealed that the component in question is less than 3kD in size (Figure 3.10A). Treatment of splenic $CD4^+$ T cells with the <3kD fraction of *L. reuteri* CM significantly increased expression of IL-10 ($p<0.01$) and IL-17A ($p<0.01$) compared to control. To further define the active component in the *L. reuteri* CM, whole supernatants were fractionated based on water solubility using a solid-phase extraction (SPE) column and the resulting fractions (load, wash and elute) tested (Figure 3.10B). Normal RPMI media and *L. reuteri* CM were processed through the speed-vac (SV) to control for any effects the evaporation process. Analysis of cytokine expression in $CD4^+$ T cells revealed significantly increased expression of IL-10 ($p<0.05$) with the *L. reuteri* CM load sample over the control load sample. A modest increase in IL-17A was also observed. The wash and elute fractions of the *L. reuteri* CM failed to induce any cytokine response over the control suggesting that the active molecule in *L. reuteri* CM is highly water soluble.

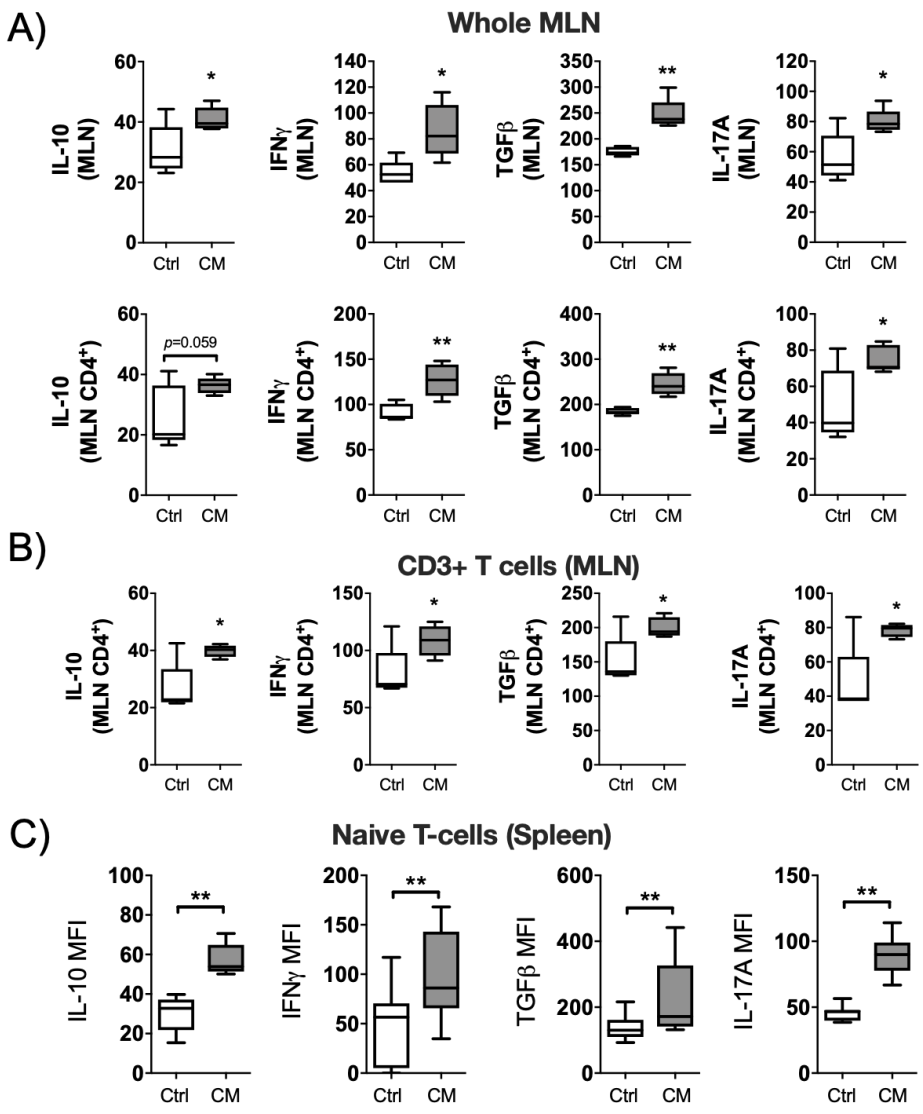

Figure 3.8. Effect of *L. reuteri* conditioned media on cytokine expression in T-cells.

Mesenteric lymph nodes and spleens were isolated from male C57BL/6 mice (12-18 weeks), homogenized and cultured with *L. reuteri* 6475 CM or control media for 4 days. Expression of cytokines (IL-10, IFNγ, TGFβ and IL-17A) was assessed using Flow cytometry. A) whole MLN cultures, B) $CD3^+$ T cells, and C) naïve $CD4^+$ T cells. Statistical analysis performed by unpaired t-test. *=p<0.05, **=p<0.01 compared to control. Whiskers in the box plots represent minimum to maximum values. n=5.

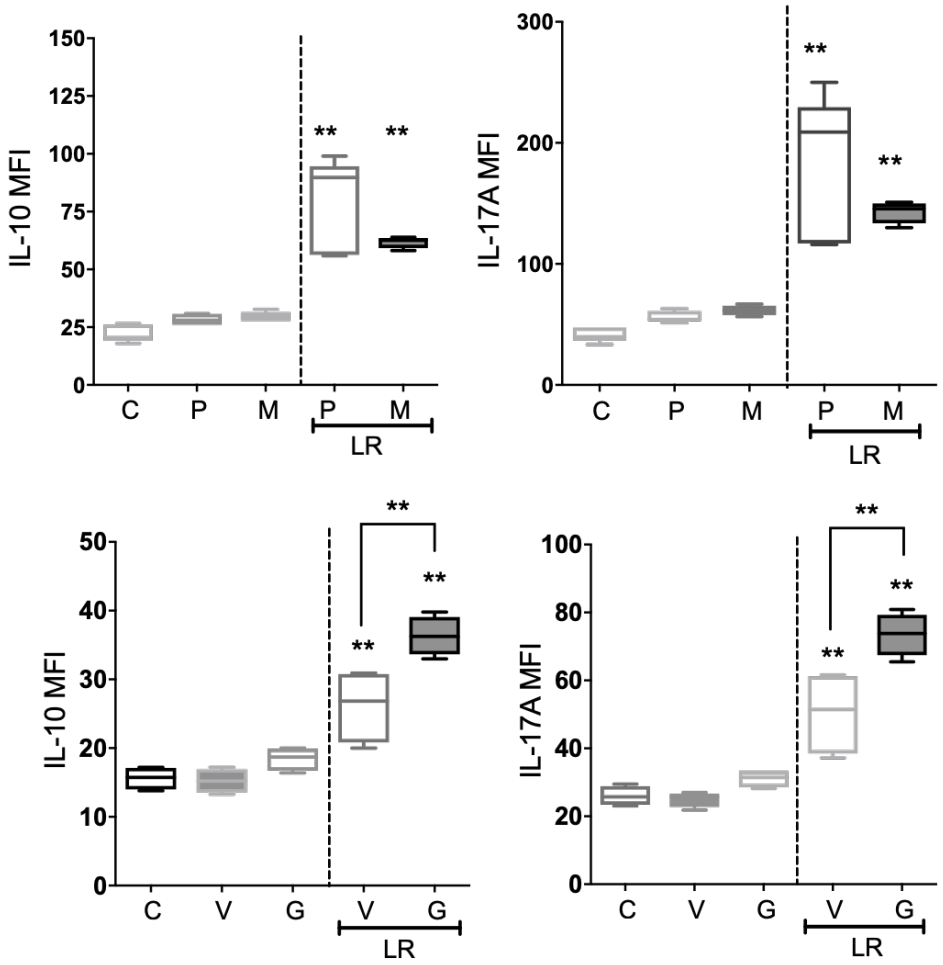

Figure 3.9. Effect of *L. reuteri* on CD4$^+$ T cells is negatively regulated by NOD pathway.

Spleens were isolated from male C57BL/6 mice (12-18 weeks) and naïve CD4$^+$ T cells obtained by magnetic separation. CD4$^+$ T cells were pre-treated with either A) MyD88 inhibitor (100 μM) or B) gefitinib (20 μM) for 24 hours before culture with *L. reuteri* CM for 4 days and cytokine expression (IL-10 and IL-17A) analyzed by flow cytometry. M = MyD88 inhibitor; P = control peptide; V = DMSO vehicle control; G = Gefitinib; LR = *L. reuteri* conditioned media. Statistical analysis performed by One-way ANOVA with Dunnett's multiple comparison post-test. *=p<0.05, **=p<0.01 compared to control; ^=p<0.05 compared to LR treated P. n=5.

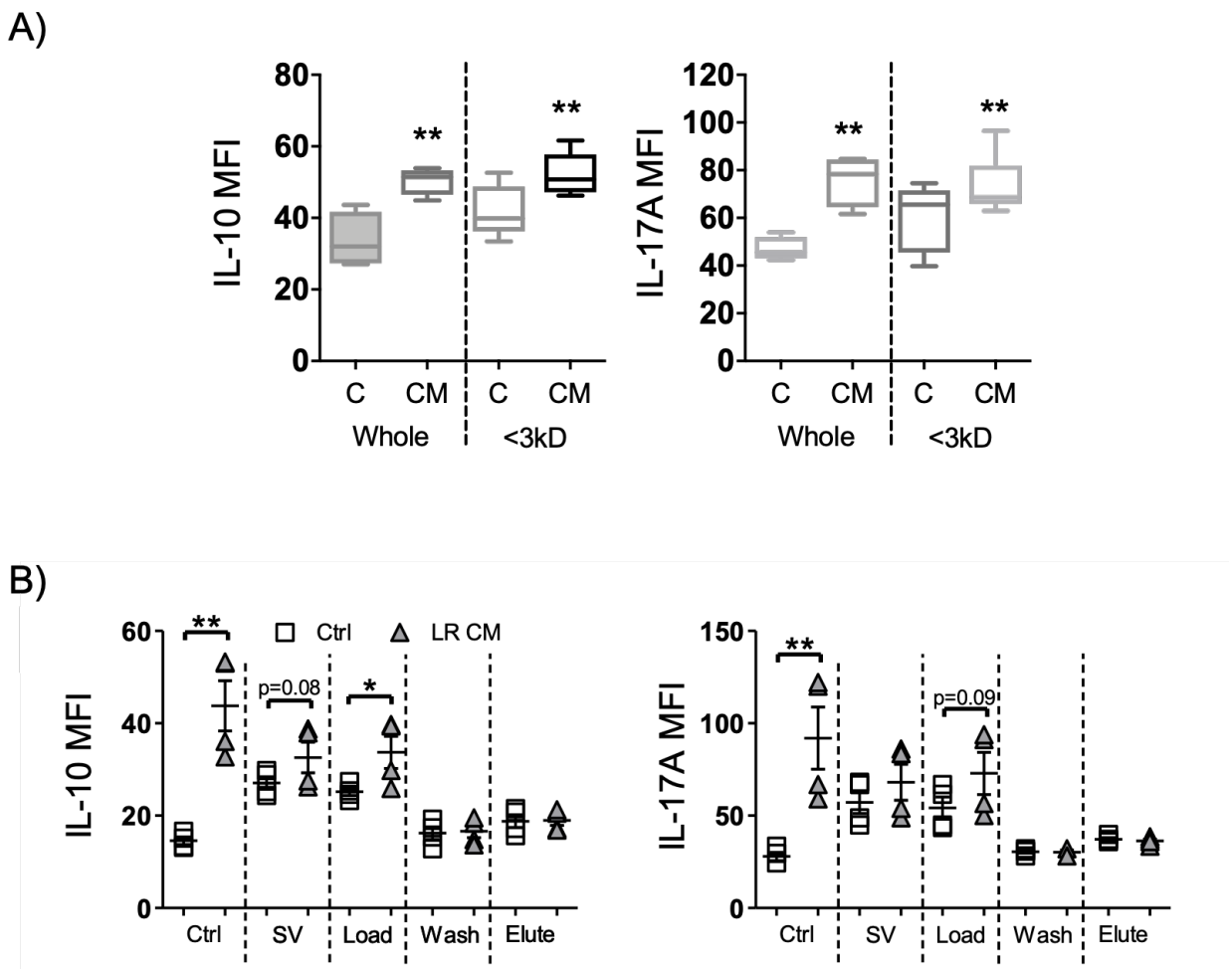

Figure 3.10. Effect of *L. reuteri* conditioned media fractions on naïve CD4$^+$ T cell cytokine expression.

Spleens were isolated from male C57BL/6 mice (12-18 weeks) and naïve CD4$^+$ T cells obtained by magnetic separation. CD4$^+$ T cells were cultured with either A) whole or <3kD CM or B) SPE fractionated CM and expression of cytokines analyzed by flow cytometry. SV=Speed-vac. Statistical analysis performed by unpaired t-test. *=p<0.05, **=p<0.01 compared to comparable control. n=4-5.

3.4.8 MLN and bone link

Data thus far suggest that oral *L. reuteri* administration likely interacts with MLNs and stimulates expression of multiple cytokines that have either osteoblastogenic or anti-osteoblastogenic activities. To determine the net effect of *L. reuteri* stimulation of T-cells on osteoblasts, we treated MC3T3-E1 pre-osteoblasts with T-cell supernatants (treated with or without *L. reuteri* stimulation). CD4+ T cells were isolated from MLNs and treated with *L. reuteri* CM or vehicle for 4 days. The supernatants from the T-cell cultures were then collected and added to osteoblast cultures for 6 hours. To rule out any residual activity of *L. reuteri* in the T-cell supernatant, the control *L. reuteri* CM was left in the incubator for 4 days (without any T-cells) similar to the T-cell treatment. Only the supernatants from T-cells treated with *L. reuteri* stimulated osteoblast ATP levels (Figure 3.11A). Importantly, *L. reuteri* CM, incubated without any cells for 4 days did not have any activity, suggesting that the ATP inducing effect of T-cell supernatants (treated) is due to secreted factors from T-cells. Consistent with this, Bcl2/Bax ratio was also significantly enhanced by *L. reuteri* treated T-cell supernatant ($p<0.05$), suggesting that T-cell secretory factor (stimulated by *L. reuteri*) is likely able to enhance the survival of osteoblasts (Figure 3.11A). Similarly, osterix expression (transcription factor important for osteoblast differentiation) was also induced by the *L. reuteri* treated T-cell supernatant ($p<0.05$) (Figure 3.11B). Together these data suggest that *L. reuteri* is able to stimulate T-cells in MLNs that can indeed beneficially affect osteoblasts.

Taken together, these results suggest that *L. reuteri*-induced bone responses are dependent on lymphocytes and that *L. reuteri* is able to stimulate T-lymphocytes to increase expression of cytokines and other factors that have potentially osteoblastogenic activity. In addition, our studies reveal that the active fraction that elicits these effects is in the <3KD fraction in the *L. reuteri* secreted component.

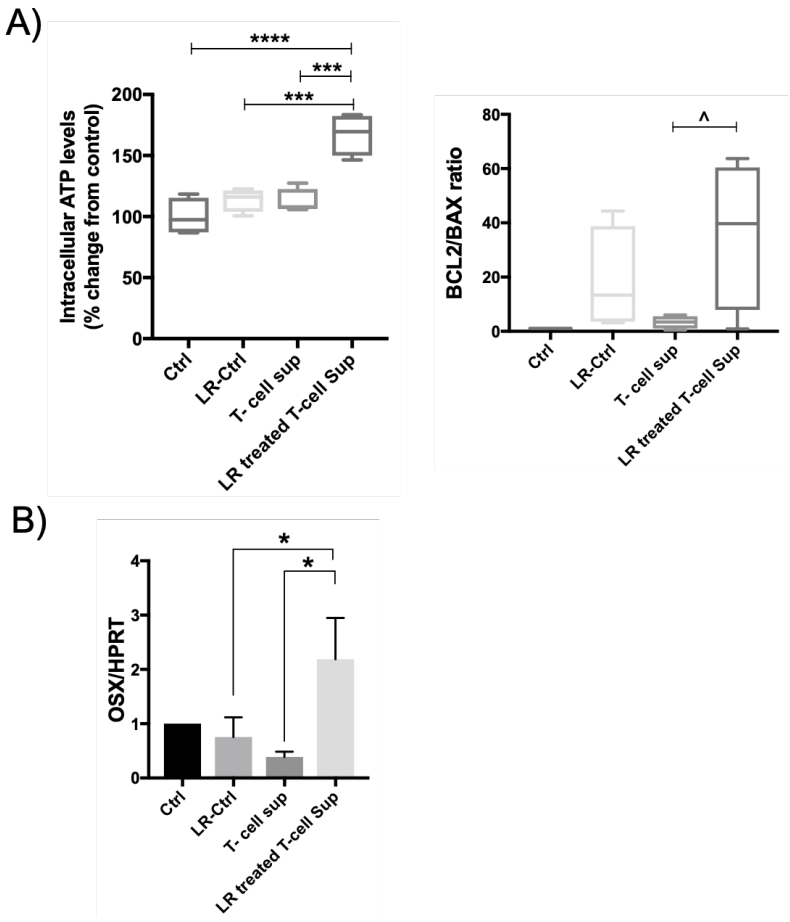

Figure 3.11. Secretory factors from *L. reuteri* CM treated T cells enhances osteoblast osterix gene expression.

Mesenteric lymph nodes were isolated from male C57BL/6 mice (12-18 weeks), homogenized and $CD4^+$ cells obtained by magnetic separation. $CD4^+$ T-cells were cultured with *L. reuteri* CM for 4 days. Supernatants from these cultures (secreted factors) were collected after 4 days and used to treat osteoblast cells for 6 hours. A) cell viability was measured by intracellular ATP levels and BCL2/BAX gene expression ratio. B) osterix gene expression. Ctrl= control, LR-Ctrl= *L. reuteri* CM with no cells, T-cell sup= T cells with no treatment. Statistical analysis performed one-way ANOVA with Tukey's post-test. *=p<0.05, ****=p<0.0001, ^ =p <0.05 by T test. n=5-6

3.5 Discussion

In recent years growing evidence from murine models has highlighted the benefit of probiotic bacteria in treating adverse bone pathology associated with numerous conditions, including estrogen-deficiency and type 1 diabetes (13–18). Furthermore, results from a recent randomized, double-blind placebo-controlled clinical trial have demonstrated that *L. reuteri* 6475 is able to reduce bone loss in older women (40), further demonstrating its potential as a novel therapeutic. Although different probiotic bacteria have been shown to have beneficial effects on bone health, the host and bacterial mechanisms that mediate these effects are not well understood. Our lab has shown that treatment with the probiotic *L. reuteri* ATCC 6475 can enhance femoral trabecular bone volume fraction, bone mineral density and bone mineral content in intact healthy male mice (11). Building upon these previous findings, in this study we have elucidated host as well as the bacterial mechanisms that enhance bone density in healthy male mice.

The intestine is residence to a significant population of immune cells that are in constant interaction with the intestinal microbiota. Immune cells present within the gut-associated lymphoid tissue (GALT), especially the mesenteric lymph nodes, play a critical role in inducing and maintaining tolerance to food proteins and commensal bacteria (41); these immune cells can then re-enter the blood stream and circulate throughout the body (42). Of the immune cells, T-lymphocytes are key players in maintaining the balance of bone remodeling and can exert an effect on both the bone forming osteoblasts and the bone resorbing osteoclasts. T cell-derived cytokines such as IL-10 and IL-17A have been demonstrated to inhibit / stimulate osteoclast differentiation as well as enhance mesenchymal stem cell proliferation and osteoblast differentiation (33–35,43). These data suggest that intestinal probiotics could exert systemic bone effects through the modulation of T cell cytokine expression. In this context, we have identified that the presence of lymphocytes is crucial for the beneficial effect of *L. reuteri* on bone health. Consistent with our

studies demonstrating that Rag KO mice do not respond to *L. reuteri* treatment, Dar et al suggested that the effect of *L. acidophilus* in preventing OVX-induced bone loss is dependent on T-reg-Th17 balance (44). Similarly, other probiotics such as LGG and the VSL#3 can decrease intestinal and bone marrow inflammation (18) that could potentially benefit bone.

Even though our recent studies suggest that *L. reuteri* is able to alter the microbial communities in a model of ABX-induced dysbiosis (19), our results here suggest that under healthy conditions, *L. reuteri* does not modify broad bacterial communities. These results prompted us to examine direct effects of *L. reuteri* on the host (versus indirect effects via microbiota modifications). Interestingly, we find that orally administered *L. reuteri* is able to translocate from the intestinal lumen to the mesenteric lymph nodes. Although this may only explain part of the mechanism by which lymphocytes are involved in *L. reuteri* effects on bone, we show that the bacteria, and its conditioned media and fractions thereof, affect MLN cytokine profile by increasing IL-10 expression and numbers of IL-10^+ cells as well as other cytokines including TGFβ, IFNγ and IL-17A. Intriguingly we also find that both *L. reuteri* and its secreted components have an immunomodulatory effect on $CD4^+$ T cell cytokine profile and that these actions of *L. reuteri* on $CD4^+$ T cells is negatively regulated by NOD signaling.

The most widely acknowledged paradigm of bacteria-immune cell interaction in the intestine involves the sampling of bacteria by dendritic cells and the presentation of these antigens to and subsequent programming of T cells (20). Recent studies however, have suggested that bacteria can cross the intestinal barrier independent of APCs. In cirrhotic patients with ascites, increased bacterial DNA has been detected in the serum (45) while in a murine model of social stress, DNA from commensal *Lactobacilli* have been detected in the spleen (46). In addition to these disease models of bacterial translocation, a study by Schultz et al (21) demonstrated that a green fluorescent protein (GFP) probiotic E. coli strain Nissle 1917 was able to translocate from

the intestinal lumen to the Peyer's patches and MLNs in a time-dependent manner, with peak levels detected 6 hours post-gavage. These data support the results from the current study where we find that orally gavaged *L. reuteri* is able to translocate to the MLNs, in a time-dependent manner, where it can potentially exert its immunomodulatory effect through direct contact with immune cells.

Based on the observations of translocation, we examined the direct effect of *L. reuteri* on cells in the MLNs and find that several cytokines including IL-10 and IL-17 are significantly modulated by probiotic bacteria and its secreted products. This observed immunomodulatory effect of *L. reuteri* is comparable to that reported with other species of lactobacilli; *L. rhamnosus* Lcr35 (47), *L. casei*, *L. fermentum* Lb20, *L. plantarum* (Lb1 and 299v), *L. johnsonii* La1 (48) and *L. gasseri* SBT2055 (49), have all been demonstrated to have concentration-dependent effects on dendritic cells. While the results from the whole MLN cultures suggested that the *L. reuteri* effects could be driven by APCs, the results from the $CD3^+$ MLN cultures raised the possibility that these probiotic bacteria could act directly on the T cells. This direct action of *L. reuteri* on T cells was further confirmed in the $CD4^+$ T cells where, as with the MLN cultures, *L. reuteri* had a concentration-dependent effect on cytokine expression. Perhaps the most interesting finding in this study however, is the discovery that soluble factors released by *L. reuteri* are able to modulate MLN and naïve $CD4^+$ T cell cytokine profile at levels comparable to that observed in the whole live bacteria cultures. The identity of these molecules is currently under active investigation. This finding provides a potential mechanism by which oral administration of *L. reuteri* could have systemic effects and modulate T cells, which is critical for the beneficial bone effects as demonstrated in the Rag knockout mice.

Dendritic cells, as well as other immune cells, recognize components of bacteria known as pathogen-associated molecular pattern (PAMPs), using specific pattern-recognition receptors

(PRRs) which are present on the host cell surface and in the cytosolic compartment (38,50). Of the extracellular PRRs, the family of toll-like receptors (TLRs) have been demonstrated to respond to a large variety of PAMPs and activate the innate immune system. Of the cytosolic PRRs, the nucleotide binding and oligomerization domain (NOD)-like receptor family members NOD1 and NOD2 are the most well understood (51). Studies have suggested that *Lactobacillus* species potentially interacts with the immune system and induces a response through TLR-2 (36,49,52), TLR-4 and DC-specific intracellular adhesion molecule 3-grabbing nonintegrin (DC-SIGN) (53). Furthermore, studies utilizing NOD1 and NOD2 knockout mice have identified that these receptors play a key role in the regulation of bone mass by the intestinal microbiota (54). Interestingly, TLR and NOD2 expression has been reported in T cells, suggesting that *L. reuteri* or its components could potentially act directly on the T cells, independent of APCs (55–57). Our results however, suggest that NOD signaling negatively affects *L. reuteri*-induced cytokine expression. Further studies however are needed to delineate *L. reuteri*-stimulated signaling pathways in lymphocytes.

Probiotic bacteria, including lactobacilli, are known to secrete many factors that can potentially modulate the immune system including extracellular proteins (58), short chain fatty acids (SCFA) (59) and soluble peptides (60). To try and identify the active molecules produced by *L. reuteri,* we fractionated the conditioned media. The active molecule was observed to be highly water soluble and within the <3kD fraction, suggesting either a non-protein molecule or a very small extracellular bacterial peptide. The characteristics of the *L. reuteri* active component in the present study had similar hallmarks to the active molecule(s) produced by the lactic acid bacteria *Bifidobacterium breve* and *Streptococcus thermophiles* (61); a non-protein molecule <3kD in size. Interestingly however, the authors suggest that the effects observed by *B. breve* and *S. thermophiles* may not be caused by the same active metabolite as some discordance was observed between experiments. Furthermore, the authors ruled out the SCFA butyrate and lactic acid as the

metabolites responsible; as concentrations were too low and no inhibitory effect of LPS-induced TNFα secretion was observed at the levels present, respectively (61). Butyrate is not a major component of lactobacilli fermentation; with different species and strains producing either very low levels or none at all (62–64). In contrast, acetate is produced at much higher concentrations (63). This could be of potential importance in suggesting a possible mechanism by which *L. reuteri* modulates T cell cytokine profile; treatment of $CD4^+$ T cells upon initiation of differentiation with acetate has been demonstrated to promote IL-10 expression in all T cell polarized conditions (T helper (Th)17 and Th1) and non-polarized T cells, without affecting expression of Foxp3 (65).

In summary we have identified that the beneficial effects of the probiotic bacteria *L. reuteri* 6475 on bone are dependent on mature lymphocytes and that it is able to directly stimulate T-cells in the mesenteric lymph nodes and spleen. We also demonstrate that *L. reuteri* secretes active metabolites that are able to directly modulate $CD4^+$ T cell cytokine profile and that this mechanism is negatively regulated by NOD signaling pathway. Furthermore, we have demonstrated that secreted factors from *L. reuteri* treated T cells can be beneficial to osteoblasts providing a link between the effect of bacteria on lymphocytes and its beneficial bone effects. These findings highlight the potential mechanism by which *L. reuteri* is able to exert its beneficial systemic bone effect and highlight potential targets for future therapeutic research.

REFERENCES

REFERENCES

1. Harvey N, Dennison E, Cooper C. Osteoporosis: impact on health and economics. Nat Rev Rheumatol. 2010;6(2):99–105.

2. Rachner TD, Khosla S, Hofbauer LC. Osteoporosis: now and the future. Lancet. 2011 Apr 9;377(9773):1276–87.

3. Foundation IO. International Osteoporosis Foundation - Facts and Statistics [Internet]. International Osteoporosis Foundation. Available from: https://www.iofbonehealth.org/facts-statistics

4. Ing-Lorenzini K, Desmeules J, Plachta O, Suva D, Dayer P, Peter R. Low-energy femoral fractures associated with the long-term use of bisphosphonates: a case series from a Swiss university hospital. Drug Saf. 2009;32(9):775–85.

5. Shannon J, Shannon J, Modelevsky S, Grippo A a. Bisphosphonates and osteonecrosis of the jaw. J Am Geriatr Soc. 2011;59:2350–5.

6. Khosla S, Shane E. A Crisis in the Treatment of Osteoporosis. J Bone Miner Res. 2016 Aug;31(8):1485–7.

7. Kostic AD, Xavier RJ, Gevers D. The microbiome in inflammatory bowel disease: Current status and the future ahead. Gastroenterology. 2014;146(6):1489–99.

8. Dunne JL, Triplett EW, Gevers D, Xavier R, Insel R, Danska J, et al. The intestinal microbiome in type 1 diabetes. Clin Exp Immunol. 2014;177(1):30–7.

9. Verdam FJ, Fuentes S, De Jonge C, Zoetendal EG, Erbil R, Greve JW, et al. Human intestinal microbiota composition is associated with local and systemic inflammation in obesity. Obesity. 2013;21(12):607–15.

10. Scher JU, Abramson SB. The microbiome and rheumatoid arthritis. Nat Rev Rheumatol. 2011;7(10):569–78.

11. McCabe LR, Irwin R, Schaefer L, Britton R a. Probiotic use decreases intestinal inflammation and increases bone density in healthy male but not female mice. J Cell Physiol. 2013 Aug;228(8):1793–8.

12. Collins FL, Irwin R, Bierhalter H, Schepper J, Britton RA, Parameswaran N, et al. Lactobacillus reuteri 6475 Increases Bone Density in Intact Females Only under an Inflammatory Setting. PLoS One. 2016;11(4):e0153180.

13. Britton R a, Irwin R, Quach D, Schaefer L, Zhang J, Lee T, et al. Probiotic L. reuteri treatment prevents bone loss in a menopausal ovariectomized mouse model. J Cell Physiol. 2014 Nov;229(11):1822–30.

14. Collins FL, Rios-Arce ND, Schepper JD, Parameswaran N, McCabe LR. The Potential of Probiotics as a Therapy for Osteoporosis. Microbiol Spectr. 2017 Aug;5(4):103–15.

15. Collins FL, Kim SM, McCabe LR, Weaver CM. Intestinal Microbiota and Bone Health: The Role of Prebiotics, Probiotics, and Diet. In: Smith SY, Varela A, Samadfam R, editors. Bone Toxicology. 1st ed. Cham: Springer International Publishing; 2017. p. 417–43.

16. Zhang J, Motyl KJ, Irwin R, MacDougald O a., Britton R a., McCabe LR. Loss of bone and Wnt10b expression in male type 1 diabetic mice is blocked by the probiotic L. reuteri. Endocrinology. 2015;(July):EN20151308.

17. Ohlsson C, Engdahl C, Fåk F, Andersson A, Windahl SH, Farman HH, et al. Probiotics protect mice from ovariectomy-induced cortical bone loss. PLoS One. 2014 Jan;9(3):e92368.

18. Li J-Y, Chassaing B, Tyagi AM, Vaccaro C, Luo T, Adams J, et al. Sex steroid deficiency-associated bone loss is microbiota dependent and prevented by probiotics. J Clin Invest. 2016 Jun 1;126(6):2049–63.

19. Schepper JD, Collins FL, Rios-Arce ND, Raehtz S, Schaefer L, Gardinier JD, et al. Probiotic Lactobacillus reuteri Prevents Postantibiotic Bone Loss by Reducing Intestinal Dysbiosis and Preventing Barrier Disruption. J Bone Miner Res. 2019 Jan 28;

20. Mowat AM, Agace WW. Regional specialization within the intestinal immune system. Nat Rev Immunol. 2014 Oct;14(10):667–85.

21. Schultz M, Watzl S, Oelschlaeger TA, Rath HC, Göttl C, Lehn N, et al. Green fluorescent protein for detection of the probiotic microorganism Escherichia coli strain Nissle 1917 (EcN) in vivo. J Microbiol Methods. 2005;61(3):389–98.

22. Quach D, Collins F, Parameswaran N, McCabe L, Britton RA. Microbiota Reconstitution Does Not Cause Bone Loss in Germ-Free Mice. mSphere. 2018;3(1):1–14.

23. Collins J, Auchtung JM, Schaefer L, Eaton KA, Britton RA. Humanized microbiota mice as a model of recurrent Clostridium difficile disease. Microbiome. 2015 Aug;3:35.

24. Kozich JJ, Westcott SL, Baxter NT, Highlander SK, Schloss PD. Development of a dual-index sequencing strategy and curation pipeline for analyzing amplicon sequence data on the MiSeq Illumina sequencing platform. Appl Environ Microbiol. 2013 Sep;79(17):5112–20.

25. Team RC. R: a language and environment for statistical computing. R Froundation for Statistical Computing, Vienna, Austria. 2017.

26. McMurdie PJ, Holmes S. phyloseq: An R Package for Reproducible Interactive Analysis and Graphics of Microbiome Census Data. Watson M, editor. PLoS One. 2013 Apr;8(4):e61217.

27. Thomas CM, Hong T, van Pijkeren JP, Hemarajata P, Trinh D V, Hu W, et al. Histamine derived from probiotic Lactobacillus reuteri suppresses TNF via modulation of PKA and ERK signaling. PLoS One. 2012 Jan;7(2):e31951.

28. Wu M, Chen G, Li YP. TGF-β and BMP signaling in osteoblast, skeletal development, and bone formation, homeostasis and disease. Bone Res. 2016;4(December 2015).

29. Mori G, D'Amelio P, Faccio R, Brunetti G. The Interplay between the bone and the immune system. Clin Dev Immunol. 2013;2013:720504.

30. Xu LX, Kukita T, Kukita A, Otsuka T, Niho Y, Iijima T. Interleukin-10 selectively inhibits osteoclastogenesis by inhibiting differentiation of osteoclast progenitors into preosteoclast-like cells in rat bone marrow culture system. J Cell Physiol. 1995 Dec;165(3):624–9.

31. Al-Rasheed A, Scheerens H, Srivastava AK, Rennick DM, Tatakis DN. Accelerated alveolar bone loss in mice lacking interleukin-10: Late onset. J Periodontal Res. 2004;39(3):194–8.

32. Hong MH, Williams H, Jin CH, Pike JW. The Inhibitory Effect of Interleukin-10 on Mouse Osteoclast Formation Involves Novel Tyrosine-Phosphorylated Proteins. J Bone Miner Res. 2010 Feb;15(5):911–8.

33. Sato K, Suematsu A, Okamoto K, Yamaguchi A, Morishita Y, Kadono Y, et al. Th17 functions as an osteoclastogenic helper T cell subset that links T cell activation and bone destruction. J Exp Med. 2006;203(12):2673–82.

34. Huang H, Kim HJ, Chang E-J, Lee ZH, Hwang SJ, Kim H-M, et al. IL-17 stimulates the proliferation and differentiation of human mesenchymal stem cells: implications for bone remodeling. Cell Death Differ. 2009;16(10):1332–43.

35. Croes M, Öner FC, van Neerven D, Sabir E, Kruyt MC, Blokhuis TJ, et al. Proinflammatory T cells and IL-17 stimulate osteoblast differentiation. Bone. 2016;84:262–70.

36. Ryu SH, Park JH, Choi SY, Jeon HY, Park J Il, Kim JY, et al. The probiotic Lactobacillus prevents citrobacter rodentium-induced murine colitis in a TLR2-dependent manner. J Microbiol Biotechnol. 2016;26(7):1333–40.

37. Moratalla A, Gómez-Hurtado I, Moya-Pérez Á, Zapater P, Peiró G, González-Navajas JM, et al. Bifidobacterium pseudocatenulatum CECT7765 promotes a TLR2-dependent anti-inflammatory response in intestinal lymphocytes from mice with cirrhosis. Eur J Nutr. 2016;55(1):197–206.

38. Moreira LO, Zamboni DS. NOD1 and NOD2 signaling in infection and inflammation. Front Immunol. 2012;3(NOV).

39. Tigno-Aranjuez JT, Asara JM, Abbott DW. Inhibition of RIP2's tyrosine kinase activity limits NOD2-driven cytokine responses. Genes Dev. 2010 Dec 1;24(23):2666–77.

40. Nilsson AG, Sundh D, Bäckhed F, Lorentzon M. *Lactobacillus reuteri* reduces bone loss in older women with low bone mineral density: a randomized, placebo-controlled, double-blind, clinical trial. J Intern Med. 2018;307–17.

41. Macpherson AJ, Smith K. Mesenteric lymph nodes at the center of immune anatomy. J Exp Med. 2006 Mar 20;203(3):497–500.

42. Hunter MC, Teijeira A, Halin C. T cell trafficking through lymphatic vessels. Front Immunol. 2016;7(DEC).

43. Zaiss MM, Axmann R, Zwerina J, Polzer K, Gückel E, Skapenko A, et al. Treg cells suppress osteoclast formation: A new link between the immune system and bone. Arthritis Rheum. 2007;56(12):4104–12.

44. Dar HY, Shukla P, Mishra PK, Anupam R, Mondal RK, Tomar GB, et al. Lactobacillus acidophilus inhibits bone loss and increases bone heterogeneity in osteoporotic mice via modulating Treg-Th17 cell balance. Bone Reports. 2018;8(July 2017):46–56.

45. Santiago A, Pozuelo M, Poca M, Gely C, Nieto JC, Torras X, et al. Alteration of the serum microbiome composition in cirrhotic patients with ascites. Sci Rep. 2016;6:25001.

46. Lafuse WP, Gearinger R, Fisher S, Nealer C, Mackos AR, Bailey MT. Exposure to a Social Stressor Induces Translocation of Commensal Lactobacilli to the Spleen and Priming of the Innate Immune System. J Immunol. 2017;1601269.

47. Evrard B, Coudeyras S, Dosgilbert A, Charbonnel N, Alamé J, Tridon A, et al. Dose-dependent immunomodulation of human dendritic cells by the probiotic lactobacillus rhamnosus lcr35. PLoS One. 2011;6(4):1–12.

48. Christensen HR, Frøkiaer H, Pestka JJ. Lactobacilli differentially modulate expression of cytokines and maturation surface markers in murine dendritic cells. J Immunol. 2002 Jan 1;168(1):171–8.

49. Sakai F, Hosoya T, Ono-Ohmachi A, Ukibe K, Ogawa A, Moriya T, et al. Lactobacillus gasseri SBT2055 Induces TGF-β Expression in Dendritic Cells and Activates TLR2

Signal to Produce IgA in the Small Intestine. PLoS One. 2014 Jan;9(8):e105370.

50. Janeway CA, Medzhitov R. Innate immune recognition. Annu Rev Immunol. 2002;20(1):197–216.

51. Fukata M, Vamadevan AS, Abreu MT. Toll-like receptors (TLRs) and Nod-like receptors (NLRs) in inflammatory disorders. Semin Immunol. 2009;21(4):242–53.

52. Mohamadzadeh M, Olson S, Kalina W V, Ruthel G, Demmin GL, Warfield KL, et al. Lactobacilli activate human dendritic cells that skew T cells toward T helper 1 polarization. Proc Natl Acad Sci U S A. 2005;102(8):2880–5.

53. Smits HH, Engering A, Van Der Kleij D, De Jong EC, Schipper K, Van Capel TMM, et al. Selective probiotic bacteria induce IL-10-producing regulatory T cells in vitro by modulating dendritic cell function through dendritic cell-specific intercellular adhesion molecule 3-grabbing nonintegrin. J Allergy Clin Immunol. 2005;115(6):1260–7.

54. Ohlsson C, Nigro G, Boneca IG, Bäckhed F, Sansonetti P, Sjögren K. Regulation of bone mass by the gut microbiota is dependent on NOD1 and NOD2 signaling. Cell Immunol. 2017;(March):0–1.

55. Komai-Koma M, Jones L, Ogg GS, Xu D, Liew FY. TLR2 is expressed on activated T cells as a costimulatory receptor. Proc Natl Acad Sci. 2004;101(9):3029–34.

56. Gelman AE, Zhang J, Choi Y, Turka LA. Toll-like receptor ligands directly promote activated CD4+ T cell survival. J Immunol. 2004;172(10):6065–73.

57. Zanello G, Goethel A, Forster K, Geddes K, Philpott DJ, Croitoru K. Nod2 activates NF-kB in CD4+ T cells but its expression is dispensable for T cell-induced colitis. PLoS One. 2013;8(12):1–10.

58. Sánchez B, Urdaci MC, Margolles A. Extracellular proteins secreted by probiotic bacteria as mediators of effects that promote mucosa-bacteria interactions. Microbiology. 2010;156(11):3232–42.

59. Kim CH, Park J, Kim M. Gut microbiota-derived short-chain Fatty acids, T cells, and inflammation. Immune Netw. 2014;14(6):277–88.

60. Lebeer S, Vanderleyden J, De Keersmaecker SCJ. Genes and Molecules of Lactobacilli Supporting Probiotic Action. Microbiol Mol Biol Rev. 2008;72(4):728–64.

61. Menard S. Lactic acid bacteria secrete metabolites retaining anti-inflammatory properties after intestinal transport. Gut. 2004;53(6):821–8.

62. Cummings JH, Macfarlane GT. The control and consequences of bacterial fermentation in the human colon. J Appl Bacteriol. 1991 Jun;70(6):443–59.

63. Kahouli I, Malhotra M, Saha S, Marinescu D, Ls R, Ma A, et al. Screening and In-Vitro Analysis of Lactobacillus reuteri Strains for Short Chain Fatty Acids Production , Stability and Therapeutic Potentials in Colorectal Cancer. Bioequivalence Bioavailab. 2015;7(1):39–50.

64. LeBlanc JG, Chain F, Martín R, Bermúdez-Humarán LG, Courau S, Langella P. Beneficial effects on host energy metabolism of short-chain fatty acids and vitamins produced by commensal and probiotic bacteria. Microb Cell Fact. 2017;16(1):79.

65. Park J, Kim M, Kang SG, Jannasch AH, Cooper B, Patterson J, et al. Short-chain fatty acids induce both effector and regulatory T cells by suppression of histone deacetylases and regulation of the mTOR-S6K pathway. Mucosal Immunol. 2015 Jan;8(1):80–93.

Chapter 4. Post-antibiotic gut dysbiosis-induced trabecular bone loss is dependent on lymphocytes

This chapter is an edited version of the article that is being submitted for publication.

Authors: **Naiomy Deliz Rios-Arce**, Jonathan D. Schepper, Andrew Dageanis, Laura Schaefer, Joseph D. Gardinier, Robert Britton, Laura R. McCabe, and Narayanan Parameswaran.

4.1 Abstract

Recent studies in mouse models have shown that gut microbiota significantly influences bone health. Our lab recently demonstrated that 2-week oral treatment with broad spectrum antibiotic followed by 4 weeks of natural repopulation of gut microbiota results in dysbiosis (microbiota imbalance)-induced bone loss in mice. Because gut microbiota is critical for the development of the immune system and since both microbiota and the immune system can regulate bone health, in this study, we tested the role of the immune system in mediating post-antibiotic dysbiosis-induced bone loss. For this, we treated wild-type (WT) and lymphocyte deficient (Rag-KO) mice with ampicillin/neomycin (ABX) cocktail in water for 2 weeks followed by 4 weeks of water without antibiotics to allow for natural repopulation. This led to a significant bone loss (31% decrease from control) in WT mice. Interestingly, no bone loss was observed in the Rag-KO mice suggesting that the lymphocytes are required for dysbiosis-induced bone loss. Bray-Curtis diversity metrics showed similar microbiota changes in both the WT and Rag-KO post-antibiotic treated groups. However, several operational taxonomic units (OTUs) classified as Lactobacillales were significantly higher in the repopulated Rag-KO when compared to the WT mice, suggesting that these bacteria might play a protective role in preventing bone loss in the Rag-KO mice after antibiotic treatment. To test this, we induced dysbiosis in WT mice in the presence or absence of oral *Lactobacillus reuteri* treatment for 4 weeks (post-ABX treatment). While the vehicle treated group exhibited significant bone loss, *L. reuteri* treated group did not demonstrate any bone loss, suggesting a bone protective role for this group of bacteria. Taken together, our studies elucidate an important role for lymphocytes in regulating post-antibiotic dysbiosis-induced bone loss.

4.2 Introduction

Osteoporosis is characterized by low bone mass and altered bone architecture (1). Worldwide, this disease is estimated to affect more than 200 million people (2). In the US, osteoporosis accounts for over 2 million bone fractures with an estimated $17 billion treatment cost (3). By 2025, the annual costs associated with osteoporosis are estimated to increase by ~50% (4). Osteoporosis enhances the risk for bone fractures that can lead to morbidity, mortality, loss of independence and decreased quality of life. Around 30% of people with hip fractures die during the first year and 50% have permanent disability (4). Many factors such as diet, age, sex, and certain medications can affect bone remodeling and lead to osteoporosis (5–9). Despite the development of new treatments against osteoporosis, patients are still concerned about drug effectiveness and unwanted side effects.

During the last decade the gut microbiota has emerged as an important regulator of host physiology including bone health. The intestinal microbiota comprises of ~1000 bacterial species of which the main phyla represented are Bacteroidetes, Firmicutes, Actinobacteria, Proteobacteria, and Verrucomicrobia (10). The intestinal microbiota is composed of both beneficial and harmful bacteria and thus, gut bacteria can be beneficial to the host as well as contribute to disease. For example, beneficial bacteria such as probiotics can increase bone density in multiple animal models (11–18) while pathogenic bacteria induce bone loss in male mice (19). Recent clinical studies further highlight the beneficial skeletal effects of ingesting probiotic bacteria (20–22). Studies have also shown that imbalance in gut microbiota (dysbiosis) is involved in the pathogenesis of several diseases including diabetes, and obesity (23,24).

Direct effects of the gut microbiota in regulating bone density was tested by Sjogren K et. al., who found higher femoral trabecular and cortical bone in germ free female mice compared to conventionally raised mice, suggesting a negative effect of the gut microbiota on bone density

(25). More recent studies in different animal models (age, sex, strain) have shown opposite effects or no changes in gut microbiota effects on bone density (14,26–28), demonstrating the complexity of this communication. This variation in results can be attributed to the duration of treatment, age (young vs mature), sex, and the different strains of mice used in the studies. In addition, studies in germ free mice are complicated due to the undeveloped immune system present in this model (25,29). Another important contributor, that can explain the discrepancies in results between gut microbiota and its effects on bone, is the source and composition of the gut microbiota used to conventionalize the germ-free mice. The composition of the mouse gut microbiota can be different between facilities, age, and mouse strain and thus can affect host functions differentially.

To better understand the role of the gut microbiota on bone density, our lab and others have used antibiotics to deplete commensal microbiota. Our lab recently demonstrated that administration of the broad spectrum antibiotics (ampicillin and neomycin) followed by natural gut microbiota repopulation for four weeks leads to dysbiosis and reduced trabecular femoral bone density (30). This experimental approach is especially useful to understand gut dysbiosis effects on bone density and is different from other studies that have used germ-free mice or have focused on chronic antibiotic treatment and its effects on skeletal health (26,31–33). The gut-bone signaling mechanisms that account for microbiota regulation of bone density are not fully understood but are thought to involve: improvement of intestinal barrier function (30), alteration of metabolic hormone levels (26), changes in nutrient absorption (34), regulation of the immune system (15,17,35,36), and microbial byproduct regulation of host cell functions (37). Our lab and others have shown that oral treatment with probiotics can influence the immune system as well as increase bone density in several different mouse models (14,15,17,36,38). In fact, recent studies have shown that microbiota metabolites can enhance bone health via regulation of T-regulatory

lymphocytes (36). These data suggest a critical role for the immune system in gut microbiota regulation of bone density.

In this study, we aimed to identify the requirement of T and B lymphocytes in dysbiosis-induced bone loss in the antibiotic-induced dysbiosis model in mice. Using mice deficient in mature T and B lymphocytes (Rag-KO), we demonstrate an important link between the gut microbiota and the lymphocytes in the modulation of bone density following antibiotic-induced dysbiosis.

4.3 Materials and Methods

4.3.1 Animals and experimental design

Wild-type (C57BL/6) and Rag knockout ($Rag2^{tm1Mom}$, C57BL/6 background) male mice were originally purchased from The Jackson Laboratory (Bar Harbour, Maine) and bred in-house. Both strains of mice were housed in the same room and on the same rack to ensure adaptation to identical housing environment and to prevent cage effect. At 12 weeks of age male mice were randomly divided into 4 experimental groups: 1) WT and 2) KO control groups that received water and 3) WT and 4) KO antibiotic groups that received antibiotics in water. The antibiotics ampicillin 1.0 g/L (Sigma, St. Louis, MO) and neomycin 0.5 g/L (Sigma, St. Louis, MO) were used to deplete the gut microbiota (30,39,40) and were given in the drinking water for 2-weeks. The drinking water, with or without antibiotics, was renewed every week. Antibiotic depletion of the gut microbiota was confirmed by the lack of fecal bacterial growth on agar plates as explained below. After 2-weeks, the antibiotic treatment ceased, and mice were treated for 4-weeks with water alone (WT and KO groups) or containing 3.3 x 10^8 cfu/ml of *Lactobacillus reuteri* 6475 (LR) (WT group). Mice were euthanized 4-weeks after cessation of antibiotic treatment (at age 18 weeks). During the study mice, were given Teklad 7914 chow (Madison, WI) and water ad libitum. Mice were housed in a 12:12-h light-dark cycle at 23°C in groups of up to 4 animals per cage. All animal procedures were approved by the Michigan State University Institutional Animal Care and Use Committee (IACUC) and conformed to NIH guidelines.

4.3.2 Bacterial culture

Lactobacillus reuteri ATCC PTA 6475 was cultured in deMan, Rogosa, Sharpe media (MRS, Difco) agar plates and kept under anaerobic conditions overnight at 37°C. The next day, 1 µl full loop of bacteria were sub-cultured into 10 ml of fresh MRS broth for 16-18 hours anaerobically at 37°C. The overnight culture was then sub-cultured anaerobically at 37°C in fresh

MRS broth and grown until log phase (OD600 =0.4). *L. reuteri* 6475 was then pelleted by centrifugation at 4000 RCF for 10 minutes and washed 3 times with 1 X sterile phosphate-buffered saline (PBS). The final pellet was re-suspended in 60 ml sterile PBS and one milliliter (ml) aliquots were made and stored at -80°C until use. Colony-forming units per milliliter (cfu/ml) were calculated the day before treatment by plating 10 µl of the aliquots into MRS agar plates overnight at 37°C. Mice were treated with $3.3x10^8$ cfu/ml of *L. reuteri* 6475 in the drinking water. Three times per week the drinking water was refilled with fresh water and/or probiotic.

4.3.3 Bacterial cultivation of feces

After two weeks of antibiotic treatment, fresh fecal samples were collected, weighed and then resuspended in 1 ml sterile PBS. Several dilutions were performed and 10 µl of the fecal suspension was plated-on Luria broth base agar plates (LB, Invitrogen). Plates were then incubated aerobically and anaerobically at 37° C for 24 hours. At the end of the incubation period, the number of colonies on the plates were counted, and the number of bacteria per gram of feces was calculated.

4.3.4 Microcomputed tomography (µCT) bone imaging

Femoral bone was collected at the day of harvest and fixed in 10% formalin for 24 hours. Bones were transferred to 70% ethanol and scanned using a GE Explore Locus microcomputed tomography (µCT) system at a voxel resolution of 20 µm obtained from 720 views. Each run included bones from mice of each experimental condition, as well as a calibration phantom to standardize gray scale values and maintain consistency across analyses. A fixed threshold (841) was used to separate bone from the bone marrow. Femur trabecular bone analyses were performed from 1% of the total length proximal to the growth plate, extending 10% of bone length toward the diaphysis, and excluding the outer cortical bone. Trabecular bone volume fraction (BVF), bone mineral content (BMC), bone mineral density (BMD), thickness (Tb. Th), spacing (Tb. Sp), and

number (Tb. N) were computed using GE Healthcare MicroView software. Femoral trabecular isosurface images were taken from a region in the femur where analyses were performed measuring 1.0 mm in length and 1.0 mm in diameter. Cortical measurements were performed in a 2- x 2- x 2 mm cube region of interest centered midway down the length of the bone. All bone analyses were done blinded to the experimental conditions.

4.3.5 Serum measurements

Sterile blood was collected at the end of the study and was allowed to clot at room temperature for 5 minutes and then centrifuged at 5000g for 10 minutes. Serum was removed and 30 µl were aliquoted and snap frozen in liquid nitrogen and stored at -80°C. Serum samples did not go through more than 1 freeze/thaw cycle. Serum osteocalcin (OC) and tartrate-resistant acid phosphatase (TRAP5b) were measured using a mouse OC and TRAP5b assay kits (BT – 470, Biomedical Technologies Inc., Stoughton, MA, and SB-TR103; Immunodiagnostic Systems Inc., Fountain Hills, AZ) respectively by the manufacturer's protocol.

4.3.6 DNA preparation of fecal samples

As previously described (30) fecal samples were transferred to Mo Bio Ultra Clean Fecal DNA bead Tubes (MoBio) containing 360µl of buffer ATL (Qiagen) and homogenized for one minute in a BioSpec Mini-Beadbeater. 40µL proteinase K (Qiagen) was added and samples were incubated for 30 minutes at 55°C, then homogenized again for one minute and incubated at 55°C for additional 30 minutes. DNA was extracted with Qiagen DNeasy Blood and Tissue kit.

4.3.7 DNA extraction from mouse fecal samples, 16S rRNA gene amplification, and sequencing

DNA for microbial sequence analysis was extracted from mouse fecal samples by bead-beating and modified extraction with Qiagen DNeasy Blood and Tissue kits as described previously (17,28). Bacterial 16S sequences spanning variable region V4 were amplified by PCR

with primers F515/R806 with a dual indexing approach and sequenced by Illumina MiSeq described previously (41). PCR reactions (20 µl) were prepared in duplicate and contained 40ng DNA template, 1X phu-sion high-fidelity buffer (New England Biolabs), 200 µMdNTPs (Promega or Invitrogen), 10 nM primers, 0.2 units of Phu- sion DNA Polymerase (New England Biolabs), and PCR grade. Reactions were performed in an Eppendorf Pro thermal cycler with an initial denaturation at 98 °C for 30 s, followed by 30 cycles of 10 s at 98 °C, 20 s at 51 °C, and 1 min at 72 °C. Replicates were pooled and purified with Agencourt AMPure XP magnetic beads (Beckman Coulter). DNA samples were quantified using the QuantIt High Sensitivity DNA assay kit (Invitrogen) and pooled at equilmolar ratios. The quality of the pooled sample was evaluated with the Bioanalyzer High Sensitivity DNA Kit (Agilent).

4.3.8 Microbial community analysis

Sequence data was processed using the MiSeq pipeline for mothur using software version 1.38.1 (42) as described previously (28). In brief, forward and reverse reads were aligned, sequences were quality trimmed and aligned to the Silva 16S rRNA gene reference database formatted for mother, and chimeric sequences were identified and removed using the mothur implementation of UCHIME. Sequences were classified according to the mothur-formatted Ribosomal Database Project (version 16, February 2016) using the Bayesian classifier in mothur, and those sequences classified as Eukarya, Archaea, chloroplast, mitochondria, or unknown were removed. The sequence data were then filtered to remove any sequences present only once in the data set. After building a distance matrix from the remaining sequences with the default parameters in mothur, sequences were clustered into operational taxonomic units (OTUs) with 97% similarity using the average-neighbor algorithm in mothur. 871 OTUs were identified across all samples with an average rarefaction depth of 54,791 reads per sample. Alpha and beta diversity analyses and visualization of microbiome communities were performed with R, utilizing the phyloseq package

(43,44). The Bray-Curtis dissimilarity matrix was used to describe differences in microbial community structure. Analysis of similarity (ANOSIM) was performed in mothur.

4.3.9 Mechanical Testing

Via microCT imaging the $I_{A/P}$ and c were determined at the site of fracturing as described above. Mechanical properties of the mouse tibias were determined under four-point bending using an EnduraTech ELF 3200 Series (Bose®, MA) (45). The base support span was 9mm with a load span of 3mm. The tibia was positioned in the loading device so the medial surface was in tension by placing the most distal portion of the tibia and fibula junction directly over the left-most support. Each tibia was loaded at 0.01 mm/s until failure, while the load and displacement were recorded. The force-deflection curve then used to calculate the structural-level properties, while tissue-level properties were estimated using the following beam-bending equations: Stress = $\sigma = f \cdot a \cdot c / 2 \cdot I_{A/P}$; Strain = $\varepsilon = 6 \cdot c \cdot d / a (3 \cdot L - 4 \cdot a)$. In each equation, f is the applied force, d is the resulting displacement, a is the distance between the inner spans (3mm), L is the distance of the outer spans (9mm), $I_{A/P}$ is the moment of inertia about the anterior/posterior axis, and c is the distance from the neutral axis to the medial surface under tension. The yield point was determined from the stress-strain relationship using a 20% offset method (46). Analyses were done blind to the experimental condition of the sample.

4.3.10 Statistical analysis

All measurements are presented as the mean ± standard error. To determine statistical significance between the groups One-way ANOVA followed by Tukey post hoc test (more than 2 groups) and T-test (for two groups) was performed using GraphPad Prism software version 7 (GraphPad, San Diego, CA, USA). Significant outliers (if present and indicated in figure legend) were removed using the ROUT test (Q=0.1%) for outliers. A p-value ≤ 0.05 was considered significant and <0.01 highly significant.

4.4 Results

4.4.1 Two week-broad spectrum antibiotic treatment depletes fecal microbiota in mice

Our lab and others have shown that treatment with the broad-spectrum antibiotics (ABX) ampicillin and neomycin can deplete the gut microbiota (30,39,40,47–49). We have chosen these two specific antibiotics because of their poor bioavailability in mice, thereby limiting extra-intestinal effects (50–52). Twelve-week-old WT and KO male mice were treated for two weeks with ABX (ampicillin: 144 mg /kg/day and neomycin: 72.46 mg/kg/day) in the drinking water. Microbiota depletion in the ABX groups was confirmed by plating fecal samples on Luria broth agar plates and incubating for 24 hours under aerobic and anaerobic conditions. Our results demonstrated no colony formation in any of the ABX treated groups (Figure 4.1B). ABX treated mice were allowed to repopulate for 4 weeks, following the 2-week ABX treatment (Figure 4.1A). General body parameters were assessed at this 4-week post-ABX time point when mice were euthanized and various organs harvested. Cecum weights in both WT and KO groups were increased in the post-ABX groups compared to the control groups (Table 4.1). As expected, a significant decrease in spleen weight was observed in the KO group compared to the WT mice. Other parameters such as body weight, liver, and kidney weights did not statistically differ between the various groups (Table 4.1).

4.4.2 Post-ABX dysbiosis-induced bone loss is abrogated in Rag KO mice

We recently demonstrated that natural gut microbiota repopulation for four weeks after broad spectrum ABX treatment causes dysbiosis and decreases bone density in BALB/c male mice (30). To examine if these effects are mouse strain specific as well as to determine the role of lymphocytes in post-ABX dysbiosis-induced bone loss we used Rag knockout (deficient in T and B lymphocyte) and their corresponding wild type mice, both in C57BL/6 background. We first determined the microbiota composition following repopulation to confirm dysbiosis in post-ABX

groups of both genotypes. Microbiota composition in colonic fecal samples was examined by 16S rRNA bacterial analysis. Similar to our previous study, antibiotic treatment increased gut microbiota dysbiosis (as described by increased Firmicutes to Bacteroidetes ratio) in both WT and KO groups (Figure 4.2A, $p<0.05$). Femoral bone showed a significant decrease (31%) in trabecular bone density in WT-ABX mice compared to non-ABX group (Figure 4.2B, $p<0.05$). Compared to the WT mice, gut microbiota repopulation did not affect trabecular femoral bone density in the KO-ABX group, suggesting that lymphocytes are important in microbiota-induced bone loss (Figure 4.2B). Consistent with these findings, trabecular thickness decreased (Tb. Th, $p<0.05$), while trabecular space increased (Tb. Sp, $p<0.05$) in the WT-ABX treated group compared to the WT untreated mice (Figure 4.2C, Table 4.2). No significant changes in these parameters were observed in the Rag KO groups. We also analyzed the diaphyseal region of the femur and did not find any significant differences between the groups (Table 4.2) indicating that post-ABX microbiota repopulation does not affect cortical bone at this timepoint in either of the genotypes.

To determine whether the post-ABX microbiota affects catabolic or anabolic bone parameters we measured serum markers of bone remodeling. Levels of tartrate-resistant acid phosphatase (TRAP5b), a marker of bone resorption, were not different between the groups (Figure 4.2D). However, osteocalcin (OC) levels, a marker of osteoblast activity/bone formation, were significantly lower in the WT-ABX treated group (Figure 4.2D, $p<0.05$). No changes in the KO-ABX group were noticed. Taken together, our results suggest that gut microbiota repopulation following ABX treatment regulates bone density by affecting bone anabolic processes in C57Bl/6 mouse strain and this effect requires the presence of T and B lymphocytes.

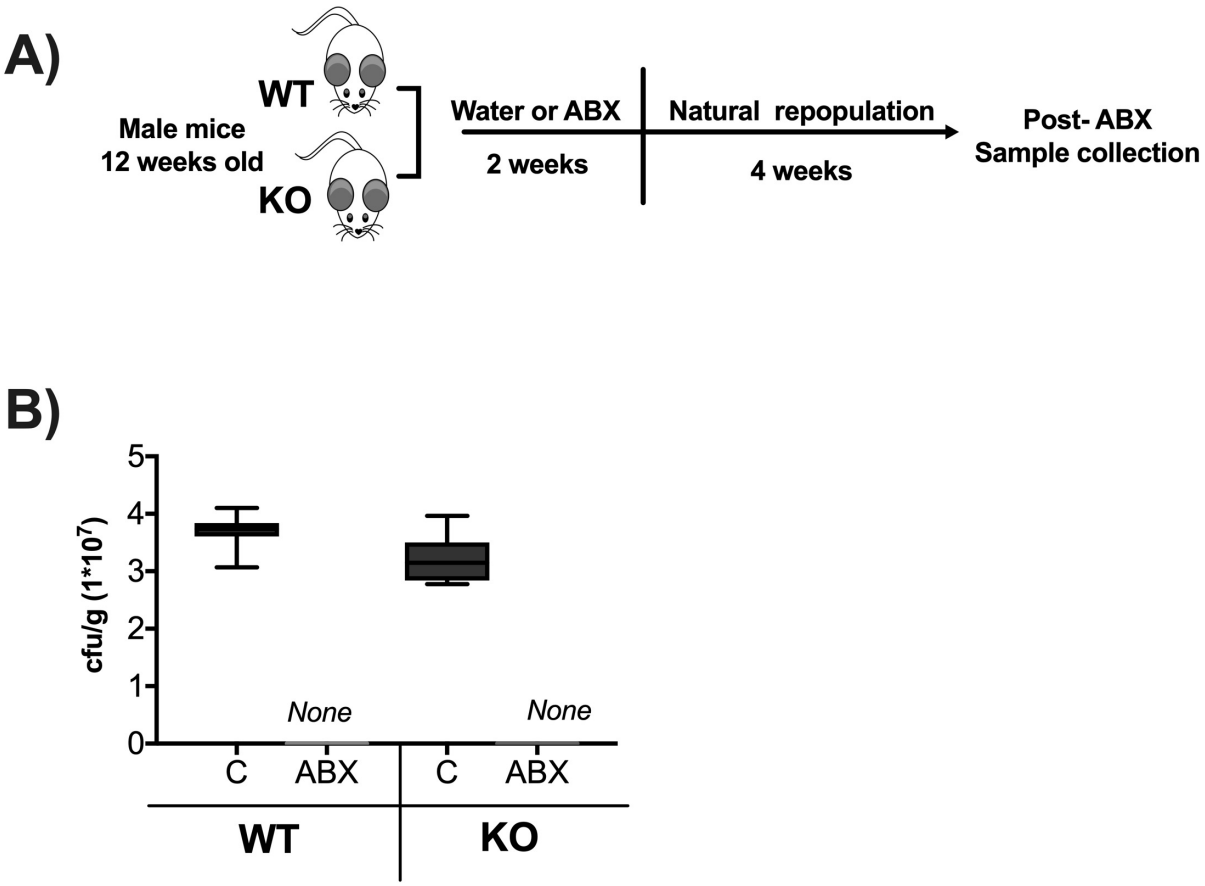

Figure 4.1. Two weeks antibiotic treatment decreases fecal microbiota composition.

12-week-old C57BL/6 and Rag-KO male mice were treated with water or the antibiotics (ABX) ampicillin and neomycin in the drinking water for 2-weeks followed by 4 weeks of no treatment (repopulation). A) Experimental design. B) Fecal samples were plated in agar dishes for 24 hours under anaerobic conditions to determine number of colony forming units per gram of feces (cfu/g) after 2-weeks ABX treatment. Control samples were diluted 1:7 while ABX were undiluted. Whiskers in the box plot represent 5-95 percentile. n=9-14 per group. Statistical analysis performed by 1-way ANOVA with Tukey post-test. C: control, ABX: antibiotic treated for 2 weeks. WT: wild type, KO: Rag-KO.

	General mouse parameters			
	WT		KO	
Parameters	C	Post-ABX	C	Post-ABX
	(n=14)	(n=17)	(n=9)	(n=11)
Body weight (g)	35.09 ± 1.07	34.31 ± 1.32	32.06 ± 0.88	30.15 ± 0.70
Cecum (g)	0.69 ± 0.03	1.03 ± 0.15	0.64 ± 0.03	1.53 ± 0.16 #
Liver (g)	1.63 ± 0.04	1.75 ± 0.08	1.60 ± 0.03	1.50 ± 0.05
Kidney (g)	0.22 ± 0.09	0.21 ± 0.01	0.22 ± 0.01	0.21 ± 0.02
Spleen (g)	0.091 ± 0.003	0.087 ± 0.004	0.034 ± 0.002 *	0.049 ± 0.004 *

Table 4.1 General mouse body parameters assessed at 4-week post-ABX.

Values represent mean ± standard error

$^{\#}$ $p < 0.05$ with respect to non-treated control

*$p < 0.05$ with respect to WT

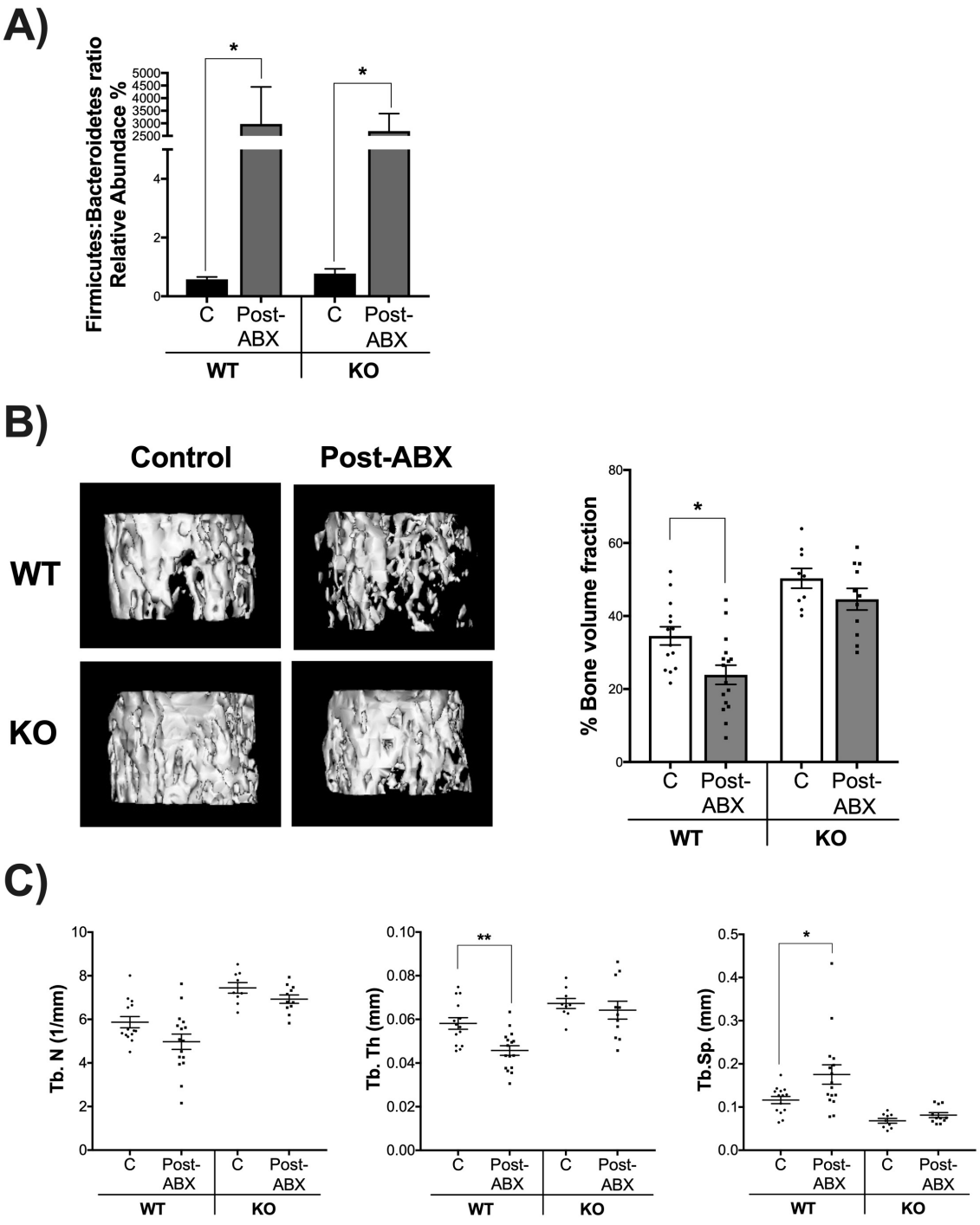

Figure 4.2. Gut microbiota repopulation effects on femoral trabecular bone density require the T and B lymphocytes.

12-week-old C57BL/6 and Rag-KO male mice were treated with water or antibiotics (ABX) for 2-weeks followed by 4 weeks of no treatment (repopulation).

Figure 4.2. (cont'd)

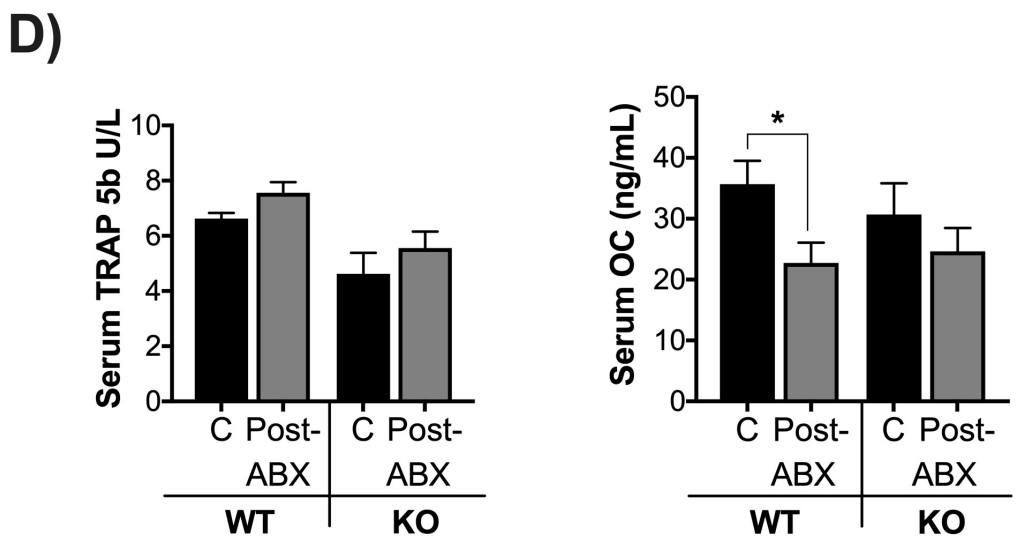

Colonic fecal samples were collected from these mice and analyzed by 16S RNA assay. A) Relative abundance of Firmicutes:Bacteroidetes ratio. B) Representative micro-computed tomography isosurface images by uCT and percentage of femoral bone volume fraction (%BVF); n=9-17 per group. C) Trabecular number (Tb. N (1/mm)), trabecular thickness (Tb. Th (mm)), and trabecular space (Tb. Sp (mm)). D) Serum tartrate- resistance acid phosphatase levels (TRAP 5b(U/L)) and serum osteocalcin levels (OC (mg/mL)); n=5-17 per group. Values represent mean ± standard error. Statistical analysis performed by 1-way ANOVA with Tukey post-test. ****$p<0.0001$, **$p<0.01$, *$p<0.05$. C: control, Post-ABX: antibiotic treated for 2 weeks followed by 4 weeks of no treatment. WT: wild type, KO: Rag-KO. Outliers removed by the ROUT test (Q:0.1%): Serum OC; one in the KO-C and one in the KO-Post ABX. Serum TRAP; one in the WT-C. None of the outliers removed affected the significance of the results.

	Femoral Bone Parameters				
	WT			KO	
Parameter	C	Post-ABX	Post-ABX LR	C	Post-ABX
Femur trabecular	(n=14)	(n=17)	(n=22)	(n=9)	(n=11)
BV/TV	34.42 ± 2.49	25.25 ± 2.85 *	30.91 ± 2.22 (^0.09)	50.21 ± 2.72 *	44.47 ± 2.97
BMD (mg/mL)	286.7 ± 11.07	243.1 ± 13.15 *	277.5 ± 11.02	311.1 ± 15.59	326.4 ± 15.26
BMC (mg)	0.9532 ± 0.045	0.7936 ± 0.043	0.8895 ± 0.045	1.00 ± 0.077	1.046 ± 0.056
Tb. Th. (mm)	0.058 ± 0.002	0.047 ± 0.002 *	0.051 ± 0.002	0.067 ± 0.002	0.064 ± 0.004
Tb. N.(1/mm)	5.87 ± 0.25	5.06 ± 0.34	5.89 ± 0.23 ^	7.44 ± 0.24 *	6.92 ± 0.19
Tb. Sp. (mm)	0.112 ± 0.008	0.1698 ± 0.005 *	0.117 ± 0.007 ^	0.068 ± 0.005	0.081 ± 0.005
Femur Cortical					
Ct.Ar (mm^2)	1.01 ± 0.01	0.94 ± 0.02	0.97 ± 0.02	0.96 ± 0.05	1.00 ± 0.03
Ct.Th (mm)	0.23 ± 0.005	0.22 ± 0.004	0.22 ± 0.004	0.23 ± 0.006	0.23 ± 0.009
Ma.Ar (mm^2)	1.07 ± 0.04	1.08 ± 0.03	1.05 ± 0.03	1.03 ± 0.05	1.02 ± 0.04
Tt.Ar (mm^2)	2.09 ± 0.04	2.03 ± 0.03	2.02 ± 0.04	2.00 ± 0.09	2.02 ± 0.07
Inner perimeter (mm)	3.93 ± 0.080	3.99 ± 0.06	3.91 ± 0.06	3.83 ± 0.12	3.80 ± 0.09
Outer perimeter (mm)	5.39 ± 0.05	5.42 ± 0.11	5.30 ± 0.05	5.25 ± 0.14	5.34 ± 0.14
BMD (mg/cc)	964.8 ± 18.37	931.2 ± 18.57	930 ± 11.17	928.6 ± 21.47	965.4 ± 25.24
BMC (mg)	0.019 ± 0.0004	0.017 ± 0.0005	0.018 ± 0.0005	0.018 ± 0.001	0.019 ± 0.001

Table 4.2 General bone parameters.

Values represent mean ± standard error

Abbreviations: BV/TV, bone volume/total volume; BMD, bone mineral density; BMC, bone mineral content, Tb.Th., trabecular thickness; Tb. N., trabecular number; Tb.Sp., trabecular space. Ct.Ar., cortical area; Ct.Th., cortical thickness; Ma.Ar., marrow area; Tt.Ar., total area.

* $p < 0.05$ with respect to WT-C

^ $p < 0.05$ with respect to WT- Post-ABX

4.4.3 Gut dysbiosis does not alter mechanical bone properties

Gut microbiota manipulations can lead to changes in structural and tissue levels properties. Therefore, we investigated whether 4-week post-antibiotic WT and KO mice display differences in tibia bone mechanical properties. Comparisons across all the groups showed no significant changes in structural (Figure 4.3A) and tissue level mechanical properties (Figure 4.3B). These results suggest that natural repopulation after ABX does not affect the overall strength and tissue properties of the cortical bone in C57BL/6 male mice.

4.4.4 Antibiotic-induced dysbiosis leads to differential abundance of bacteria class in WT and KO mice

To further examine if differences in microbiota between WT and KO mice can explain part of the mechanisms underlying the different phenotype, we analyzed bacterial DNA from colonic fecal samples. We analyzed specific bacterial OTUs at the phylum, class, order, and family levels, to assess differences between the various groups/treatments (Figure 4.4). While the trends were similar, the post-ABX induced OUT shift, in terms of the relative abundance of several bacteria, was significantly different between the WT versus the KO groups. At the phylum level our data show a significant decrease in the relative abundance of Bacteroidetes in WT-ABX groups (Figure 4.4A, $p<0.001$) that was further decreased to almost undetectable levels in the KO-ABX group (Figure 4.4A, $p<0.0001$). This pattern was seen for bacteria in the class (Bacteroidia, 4.4B), order (Bacteroidales, 4.4C) and family (Porphyrormonadaceae, 4.4D). The other commonly altered phylum, Firmicutes, showed no changes after ABX treatment in any of the groups (Figure 4.4A), however, the KO-ABX group showed dramatic increases in bacteria in the class (Bacilli, $p<0.0001$, 4.4B) and order (Lactobacillales, $p<0.0001$, 4.4C). Additionally, the relative abundance of Verrumicrobia phylum was higher in WT-ABX treated groups and further higher in the KO-ABX mice (Figure 4.4A, $p<0.0001$), with bacteria in the class (Verrumicrobiae, 4.4B), order

(Verrucomicrobiales, 4.4C), and family (Verrucomicrobiaceae, 4.4D) following this pattern. The phylum Actinobacteria composed a small part (<1%) of the total bacteria composition and was decreased by ABX treatment. Together, these data suggest that while we don't see significant changes in broad bacterial community diversity (data not shown), the abundance of several OTUs is different between the WT-ABX and KO-ABX groups.

4.4.5 *Lactobacillus reuteri* administration prevents post-antibiotic dysbiosis-induced bone loss in wild type mice

As indicated in figure 4.4C, the relative abundance of Lactobacillales is markedly increased in the KO-ABX compared to WT-ABX treated mice. To test if this lack of increase in Lactobacillales in WT-ABX group is the reason for the distinct bone responses between the two genotypes, we supplemented WT-ABX mice with *Lactobacillus reuteri* 6475 (or water) for four weeks. As shown in figure 4.2, Post-ABX gut microbiota repopulation decreased bone density in the WT male mice by 31% (Figure 4.5A). Treatment with *L. reuteri* however, prevented this bone loss in WT mice (Figure 4.5A, $p<0.05$). Consistent with BVF results, treatment with *L. reuteri* decreased trabecular space (Figure 4.5B, $p<0.05$) and increased trabecular number (Figure 4.5B, $p<0.05$). An increase in osteocalcin levels in the serum was also evident in the post-ABX *L. reuteri*-treated group (Figure 4.5C, $p<0.05$). We also examined the relative abundance of *L. reuteri* and found a significant increase in the post-ABX *L. reuteri* treated group (Figure 4.5D, $p<0.05$). These data suggest that: 1) changes in post-ABX gut microbiota composition between WT and KO, specifically an increase in *Lactobacillales* in the KO-ABX group, can contribute to the difference in bone response, and 2) four weeks of post-antibiotic treatment with *L. reuteri* prevents bone loss in C57Bl/6 strain, similar to BALB/c (30).

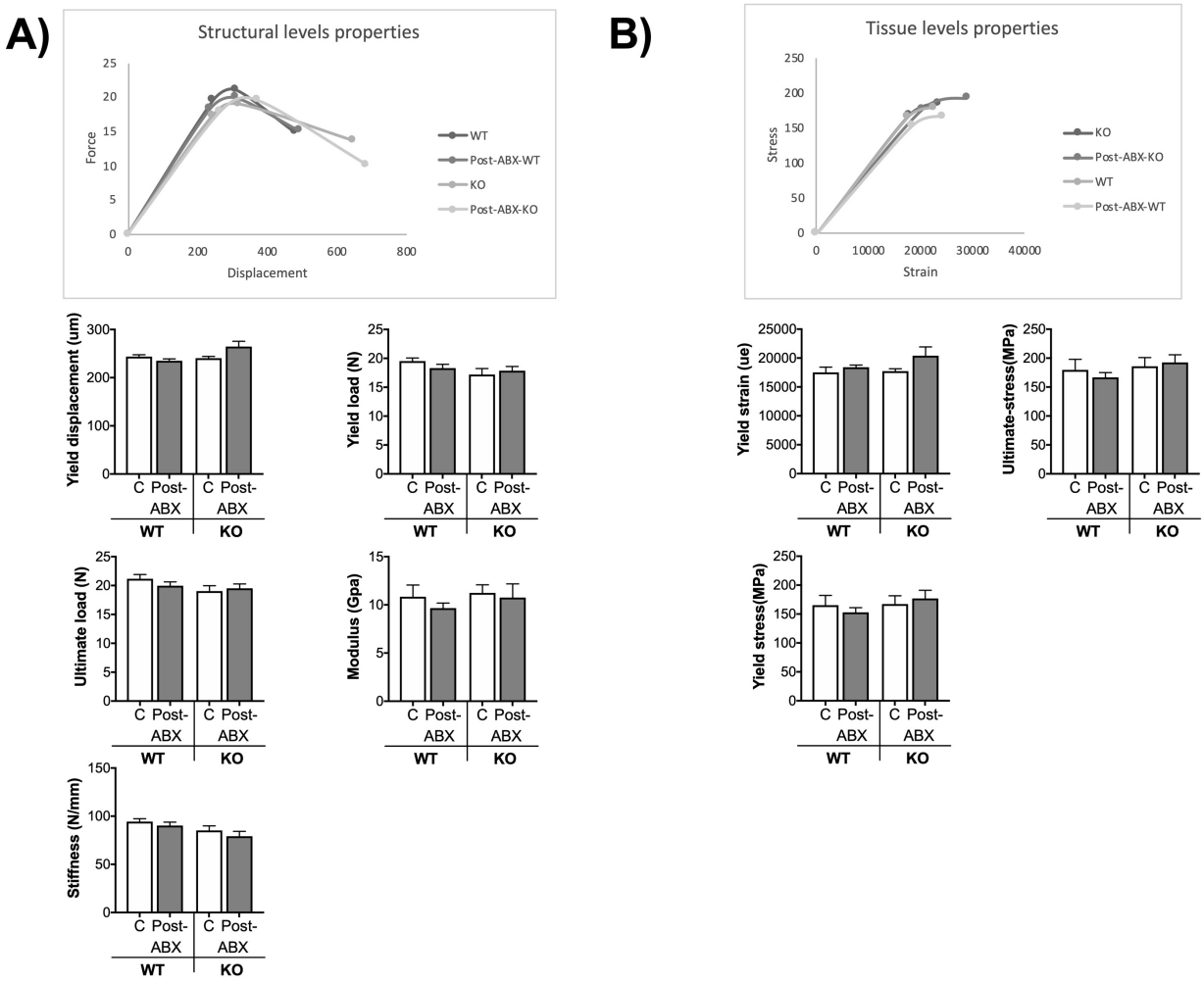

Figure 4.3. Microbial manipulation does not alter mechanical bone properties.

Analysis of tibia mechanical properties from mice described in figure 2 were performed by four-point bending test. A) Structural levels properties. B) Tissue level properties. Values represent mean ± standard error. n= 12-18 per group. C: control, Post-ABX: antibiotic treated for 2 weeks followed by 4 weeks of no treatment. WT: wild type, KO: Rag-KO.

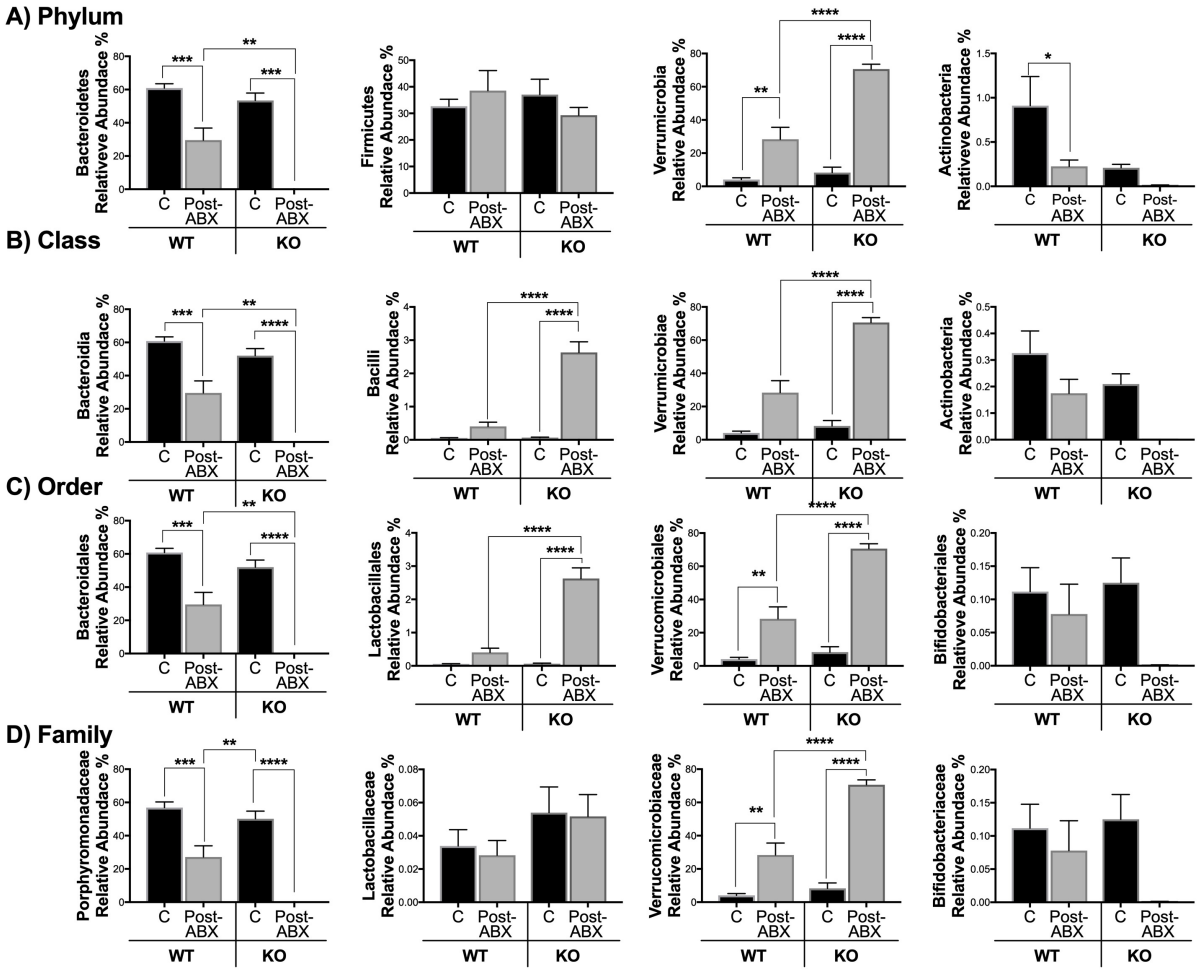

Figure 4.4. Relative abundance of specific bacteria post-antibiotic treatment.

Colon fecal samples from C57BL/6 and Rag-KO treated mice (ABX for 2 weeks and repopulation for 4 weeks) were collected and analyzed. A) Analysis of operational taxonomic units (OTUs) classified to the phylum, B) class, C) order, and D) genus level. Values represent mean ± standard error. n > 7 per group. Statistical analysis performed by 1-way ANOVA with Tukey post-test. ****p<0.0001, **p<0.01, *p<0.05. C: control, Post-ABX: antibiotic treated for 2 weeks followed by 4 weeks of no treatment. WT: wild type, KO: Rag-KO. Outliers removed by the ROUT test (Q:0.1%): Class Actinobacteria; three in the WT:C, one in the WT-Post-Abx and one in the KO-Post-ABX. Order Lactobacillales; one in the WT-C and three in the WT-Post-Abx. Family Lactobacillaceae; one in the WT-C, three in the WT-Post-Abx and one in the KO-Post-ABX.

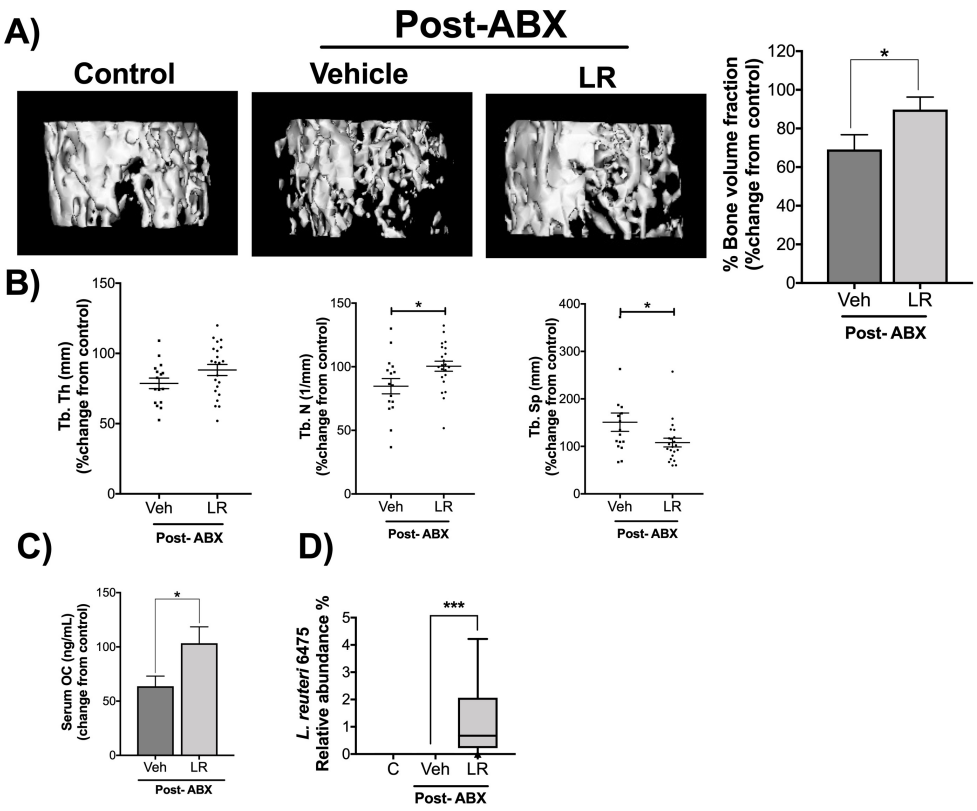

Figure 4.5. Supplementation with *Lactobacillus reuteri* 6475 prevents bone loss in post-antibiotic treated C57BL/6 male mice.

After treatment with ABX for two weeks WT male mice were untreated (natural repopulation) or treated with *L. reuteri* 6475 for four weeks. A) Representative micro-computed tomography isosurface images by uCT. Percentage bone volume fraction expressed as percentage change from control (%BVF). B) Trabecular thickness (Tb. Th (mm)), trabecular number (Tb. N (1/mm)), and trabecular space (Tb. Sp (mm)) expressed as percentage change from control. C) Serum osteocalcin levels (OC (mg/mL)) expressed as percentage change from control. D) Analysis of operational taxonomic units (OTUs) of *L. reuteri* 6475. Values represent mean ± standard error. n > 7 per group. Statistical analysis performed by T-test or 1-way ANOVA with Tukey post-test. ****p<0.0001, **p<0.01, *p<0.05. C: control, Post-ABX: antibiotic treated for 2 weeks followed by 4 weeks of no treatment., LR: *L. reuteri* 6475 treated for 4 weeks after 2 weeks of ABX treatment.

4.5 Discussion

Antibiotics are widely prescribed for the treatment and prevention of bacterial infections. Several studies have shown that antibiotics can also deplete the commensal flora in the host, leading to bacterial disturbances and long-term changes that can have sustained negative impact on the host (53–58). We recently demonstrated that gut microbiota repopulation for 4 weeks following 2-weeks of antibiotic treatment (post-ABX) led to microbial dysbiosis and significantly decreased femoral trabecular bone density in BALB/c male mice (30). Our model to assess the role of the gut microbiota on bone density uses the antibiotics ampicillin and neomycin. These antibiotics were chosen because they are poorly absorbed in the rodent intestine (50–52) and they can also deplete the intestinal microbiota (39,40). Importantly, our lab has shown that two weeks treatment with these antibiotics does not significantly affect trabecular bone density (30), suggesting that these antibiotics do not have direct effects on bone density. In the present study we identify lymphocytes as one of the key players involved in post-ABX dysbiosis-induced bone loss in C57BL/6 male mice. We also identify supplementation with *Lactobacillus* as a possible approach for preventing adverse bone effects following ABX-induced gut dysbiosis. Our studies in C57BL/6 strain also confirm previous findings in BALB/c strain, suggesting that gut dysbiosis-induced bone loss may not be mouse strain-specific.

The effect of T and B lymphocytes and their cytokines on bone density is well known. These cells regulate bone density through the secretion of cytokines or direct cell-cell contact with osteoblasts or osteoclasts (59–61). Cytokines such as IFN-γ, TNF-α, and interleukin 17 (IL-17) are mostly associated with bone loss, mainly by their effect on promoting osteoclastogenesis and preventing osteoblast differentiation (62–66). In contrast, T regulatory cells (Treg) and interleukin 10 (IL-10) modulate bone density by regulating osteoblast gene expression and inhibiting osteoclast differentiation (67–69). We and others have demonstrated that different probiotic

bacteria can regulate the immune system which is associated with beneficial effects on bone. For example, *in vivo*, the probiotic *L. reuteri* decreases TNFα gene expression in the jejunum and ileum, and $CD4^+$ T cells in the bone marrow and these effects are associated with increased bone density (15,17). Intriguingly, in female mice *L. reuteri* requires an elevated inflammatory status to enhance bone density (18). Other probiotics such *Lactobacillus rhamnosus* (LGG) and VSL#3 can decrease intestinal and bone marrow inflammation and can also enhance bone density (14). Interestingly, in a recent study LGG effects on bone density were demonstrated to be mediated by the Treg cells (36). An increase in Treg by LGG was shown to enhance $CD8^+$ T cells which promote bone formation via the Wnt pathway (36). A study by Dar et. al. suggests that the effect of *Lactobacillus acidophilus* (LA) in increasing bone density in OVX mice is via regulation of Treg-Th17 cell balance by inhibiting osteoclastogenic Th17 cells and promoting anti-osteoclastogenic Treg cells (38). Owing to the fact that different bacteria can regulate the immune system with associated benefits on bone, in this study we were interested to see if the negative effects on post-ABX dysbiosis on bone density were mediated by lymphocytes. Our studies clearly demonstrate that absence of T and B lymphocytes inhibits post-ABX dysbiosis-induced bone loss.

Antibiotics have been used previously to study their effects on bone in different animal models. However, unlike our model, these studies were mainly done in young mice and used chronic antibiotic treatment. Cho et al showed that female mice (C57BL/6J) treated chronically with antibiotics for three weeks exhibited a significant increase in BMD, while long term use of the antibiotics (7 weeks) did not have any effect (31). Other studies have also shown that chronic treatment (20 weeks) with low dose of penicillin at birth or at weaning in C57BL/6J female mice increases BMD. Intriguingly, male mice treated with the same low dose of penicillin presented a decrease in bone mineral content when the treatment began at birth (32). Guss et al showed that male mice (C57BL/6J) treated with ampicillin and neomycin from weaning until skeletal maturity

(16 weeks old) exhibit a decrease in femoral cortical area, thickness, and bone bending strength (33). In contrast, 2-month old female BALB/c mice treated with antibiotic for one month showed an increase in bone density (26). Together, these studies suggest that antibiotic use can have an effect on bone density and this effect is variable depending on several factors such as class of antibiotic, dose, treatment duration, sex, age, and strain of the animal. While our model utilized antibiotics to deplete gut bacteria, the effect on bone density was observed in response to changes in gut repopulation, rather than direct effect of antibiotics *per se*. Because we examined bone responses 4 weeks following cessation of ABX treatment, our results likely rule out direct effect of ABX on bone.

Several studies have shown that antibiotic use can lead to changes in gut microbiota composition (dysbiosis), which in some cases can take years to revert to the original configuration (70–73). Previously, using the same model but different strain of mice we found that antibiotic treatment leads to microbial dysbiosis (30). In this study using a different strain of mice, treatment with ABX led to microbial dysbiosis that appeared similar (based on Firmicutes:Bacteriodetes ratio) between WT and Rag-KO mice. Interestingly, by Bray-Curtis analysis we did not see significant differences in gut microbial composition between the WT and KO group after ABX treatment (data not shown). However, when we looked at specific OTUs, the relative abundance of several bacteria was expressed differentially between the WT and KO mice following post-ABX repopulation. This data is consistent with other studies that have shown that different bacteria are present in the WT and KO mice (74,75). One result that should be underscored was the increase in the relative abundance of Lactobacillales in the KO-ABX treated group. Lactobacillales belongs to the Firmicutes phylum which compromise one of the most common phylum of bacteria in the gut. In addition, several studies from our group and other have shown beneficial effects on bone density by treatment with different species of Lactobacillales (14,17,18,30,76,77). Indeed, when

we treated WT mice with *L. reuteri* 6475 for four weeks after antibiotic treatment we were able to prevent the decrease in bone density induced by gut microbiota repopulation. These results suggest that Lactobacillales repopulation in the KO ABX group might be protective and could explain the lack of bone loss in the KO mice. It should however be noted that the relative abundance of other bacteria also changed between the groups and further extensive studies are needed to confirm the contribution of each one of these bacteria in protecting against bone loss in the wild type mice.

Previous studies in germ free mice suggest that gut microbiota can influence bone health. However, the specifics of the regulation is dependent on the source of microbiota for conventionalization as well as the strain, sex and age of the mice. Interestingly, conventionalization of female C57BL/6 germ-free mice with microbiota resulted in loss of femoral trabecular and cortical bone and this was associated with an increase in osteoclastogenic $CD4^{+}$T cells in the bone marrow, suggesting a link between microbiota, immune system and bone (14). In our studies here, we provide further demonstrative evidence using knockout mice that lymphocytes are critical in mediating microbiota effects on bone. Although our studies are consistent with these studies in germ-free mice, comparing our results with the studies in germ-free mice should be done with caution as germ-free mice do not have a fully mature immune system and these differences can directly affect bone formation (14,78).

In summary, in this study we demonstrate a role for lymphocytes in mediating microbiota effects on bone density following ABX-induced dysbiosis. How microbiota repopulation is influenced by the immune system, especially the lymphocytes and the specific cell types involved in this process will be the subject of future studies.

REFERENCES

REFERENCES

1. Kanis JA, Glüer CC. An update on the diagnosis and assessment of osteoporosis with densitometry. Committee of Scientific Advisors, International Osteoporosis Foundation. Osteoporos Int. 2000;11(3):192–202.

2. Reginster JY, Burlet N. Osteoporosis: A still increasing prevalence. Bone. 2006;38(2 SUPPL. 1):1998–2003.

3. Burge R, Dawson-Hughes B, Solomon DH, Wong JB, King A, Tosteson A. Incidence and economic burden of osteoporosis-related fractures in the United States, 2005-2025. J Bone Miner Res. 2007;22(3):465–75.

4. Burge R, Dawson-Hughes B, Solomon DH, Wong JB, King A, Tosteson A. Incidence and Economic Burden of Osteoporosis-Related Fractures in the United States, 2005-2025. J Bone Miner Res. 2006;22(3):465–75.

5. Sahni S, Mangano KM, McLean RR, Hannan MT, Kiel DP. Dietary approaches for bone health: lessons from the Framingham Osteoporosis Study. Curr Osteoporos. 2015;(4):368–79.

6. Demontiero O, Vidal C, Duque G. Aging and bone loss: new insights for the clinician. Ther Adv Musculoskelet Dis. 2012 Apr;4(2):61–76.

7. Ibanez L, Rouleau M, Wakkach A, Blin-Wakkach C. Gut microbiome and bone. Jt Bone Spine. 2017;000(2017):1–6.

8. Hernandez CJ, Guss JD, Luna M, Goldring SR. Links Between the Microbiome and Bone. J Bone Miner Res. 2016 Sep;31(9):1638–46.

9. Pacifici R. Bone Remodeling and the Microbiome. Cold Spring Harb Perspect Med. 2017;1–20.

10. Huttenhower C, Gevers D, Knight R, Abubucker S, Badger JH, Chinwalla AT, et al. Structure, function and diversity of the healthy human microbiome. Nature. 2012 Jun 13;486(7402):207–14.

11. Parvaneh K, Ebrahimi M, Sabran MR, Karimi G, Hwei ANM, Abdul-Majeed S, et al. Probiotics (*Bifidobacterium longum*) Increase Bone Mass Density and Upregulate *Sparc* and *Bmp-2* Genes in Rats with Bone Loss Resulting from Ovariectomy. Biomed Res Int. 2015;2015:1–10.

12. Parvaneh K, Jamaluddin R, Karimi G, Erfani R. Effect of probiotics supplementation on bone mineral content and bone mass density. Sci World J. 2014;2014:1–6.

13. Scholz-Ahrens KE, Adolphi B, Rochat F, Barclay D V., de Vrese M, Açil Y, et al. Effects of probiotics, prebiotics, and synbiotics on mineral metabolism in ovariectomized rats - impact of bacterial mass, intestinal absorptive area and reduction of bone turn-over. NFS J. 2016 Aug;3:41–50.

14. Li JY, Chassaing B, Tyagi AM, Vaccaro C, Luo T, Adams J, et al. Sex steroid deficiency-associated bone loss is microbiota dependent and prevented by probiotics. J Clin Invest. 2016 Apr;126(6):2049–63.

15. McCabe LR, Irwin R, Schaefer L, Britton RA. Probiotic use decreases intestinal inflammation and increases bone density in healthy male but not female mice. J Cell Physiol. 2013 Aug;228(8):1793–8.

16. Zhang J, Motyl KJ, Irwin R, MacDougald OA, Britton RA, McCabe LR. Loss of bone and Wnt10b expression in male type 1 diabetic mice is blocked by the probiotic Lactobacillus reuteri. Endocrinology. 2015;156(9):3169–82.

17. Britton RA, Irwin R, Quach D, Schaefer L, Zhang J, Lee T, et al. Probiotic L. reuteri Treatment Prevents Bone Loss in a Menopausal Ovariectomized Mouse Model. J Cell Physiol. 2014 Nov;229(11):1822–30.

18. Collins FL, Irwin R, Bierhalter H, Schepper J, Britton RA, Parameswaran N, et al. Lactobacillus reuteri 6475 increases bone density in intact females only under an inflammatory setting. PLoS One. 2016;11(4).

19. Irwin R, Lee T, Young VB, Parameswaran N, McCabe LR. Colitis-induced bone loss is gender dependent and associated with increased inflammation. Inflamm Bowel Dis. 2013;19(8):1586–97.

20. Jafarnejad S, Djafarian K, Fazeli MR, Yekaninejad MS, Rostamian A, Keshavarz SA. Effects of a Multispecies Probiotic Supplement on Bone Health in Osteopenic Postmenopausal Women: A Randomized, Double-blind, Controlled Trial. J Am Coll Nutr. 2017;36(7):497–506.

21. Nilsson AG, Sundh D, Bäckhed F, Lorentzon M. *Lactobacillus reuteri* reduces bone loss in older women with low bone mineral density - a randomized, placebo-controlled, double-blind, clinical trial. J Intern Med. 2018;0–3.

22. Laird E, Molloy AM, McNulty H, Ward M, McCarroll K, Hoey L, et al. Greater yogurt consumption is associated with increased bone mineral density and physical function in older adults. Osteoporos Int. 2017;28(8):2409–19.

23. Baothman OA, Zamzami MA, Taher I, Abubaker J, Abu-Farha M. The role of Gut Microbiota in the development of obesity and Diabetes. Vol. 15, Lipids in Health and Disease. BioMed Central; 2016. p. 108.

24. Blandino G, Inturri R, Lazzara F, Di Rosa M, Malaguarnera L. Impact of gut microbiota on diabetes mellitus. Vol. 42, Diabetes and Metabolism. Elsevier Masson; 2016. p. 303–15.

25. Sjögren K, Engdahl C, Henning P, Lerner UH, Tremaroli V, Lagerquist MK, et al. The gut microbiota regulates bone mass in mice. J Bone Miner Res. 2012 Jun;27(6):1357–67.

26. Yan J, Herzog JW, Tsang K, Brennan CA, Bower MA, Garrett WS, et al. Gut microbiota induce IGF-1 and promote bone formation and growth. Proc Natl Acad Sci. 2016 Nov 22;E(47):E7554–63.

27. Novince CM, Whittow CR, Aartun JD, Hathaway JD, Poulides N, Chavez MB, et al. Commensal Gut Microbiota Immunomodulatory Actions in Bone Marrow and Liver have Catabolic Effects on Skeletal Homeostasis in Health. Sci Rep. 2017;7(1):5747.

28. Quach D, Collins F, Parameswaran N, McCabe L, Britton RA, Bidwell J, et al. Microbiota Reconstitution Does Not Cause Bone Loss in Germ-Free Mice. mSphere. 2018;3(1):e00545-17.

29. Schwarzer M, Makki K, Storelli G, Machuca-Gayet I, Srutkova D, Hermanova P, et al. Lactobacillus plantarum strain maintains growth of infant mice during chronic undernutrition. Science (80-). 2016;351(6275).

30. Schepper JD, Collins FL, Rios-Arce ND, Raehtz S, Schaefer L, Gardinier JD, et al. Probiotic Lactobacillus reuteri Prevents Postantibiotic Bone Loss by Reducing Intestinal Dysbiosis and Preventing Barrier Disruption. J Bone Miner Res. 2019;1–18.

31. Cho I, Yamanishi S, Cox L, Methé BA, Zavadil J, Li K, et al. Antibiotics in early life alter the murine colonic microbiome and adiposity. Nature. 2012 Aug;488(7413):621–6.

32. Cox LM, Yamanishi S, Sohn J, Alekseyenko A V, Leung JM, Cho I, et al. Altering the intestinal microbiota during a critical developmental window has lasting metabolic consequences. Cell. 2014;158(4):705–21.

33. Guss JD, Horsfield MW, Fontenele FF, Sandoval TN, Luna M, Apoorva F, et al. Alterations to the Gut Microbiome Impair Bone Strength and Tissue Material Properties. J Bone Miner Res. 2017;32(6):1343–53.

34. Rodrigues FC, Castro ASB, Rodrigues VC, Fernandes SA, Fontes EAF, de Oliveira TT, et al. Yacon Flour and *Bifidobacterium longum* Modulate Bone Health in Rats. J Med Food. 2012;15(7):664–70.

35. Ohlsson C, Nigro G, Boneca IG, Bäckhed F, Sansonetti P, Sjögren K. Regulation of bone mass by the gut microbiota is dependent on NOD1 and NOD2 signaling. Cell Immunol. 2017;317:55–8.

36. Tyagi AM, Yu M, Darby TM, Vaccaro C, Li J-Y, Owens JA, et al. The Microbial Metabolite Butyrate Stimulates Bone Formation via T Regulatory Cell-Mediated Regulation of WNT10B Expression. Immunity. 2018;1–16.

37. Katono T, Kawato T, Tanabe N, Suzuki N, Iida T, Morozumi A, et al. Sodium butyrate stimulates mineralized nodule formation and osteoprotegerin expression by human osteoblasts. Arch Oral Biol. 2008;53(10):903–9.

38. Dar HY, Shukla P, Mishra PK, Anupam R, Mondal RK, Tomar GB, et al. Lactobacillus acidophilus inhibits bone loss and increases bone heterogeneity in osteoporotic mice via modulating Treg-Th17 cell balance. Bone Reports. 2018;8(July 2017):46–56.

39. Cani PD, Bibiloni R, Knauf C, Waget A, Neyrinck AM, Delzenne NM, et al. Changes in gut microbiota control metabolic endotoxemia-induced inflammation in high-fat diet-induced obesity and diabetes in mice. Diabetes. 2008 Jun;57(6):1470–81.

40. Ferrier L, Bérard F, Debrauwer L, Chabo C, Langella P, Buéno L, et al. Impairment of the intestinal barrier by ethanol involves enteric microflora and mast cell activation in rodents. Am J Pathol. 2006 Apr;168(4):1148–54.

41. Collins J, Auchtung JM, Schaefer L, Eaton KA, Britton RA. Humanized microbiota mice as a model of recurrent Clostridium difficile disease. Microbiome. 2015 Aug;3:35.

42. Kozich JJ, Westcott SL, Baxter NT, Highlander SK, Schloss PD. Development of a dual-index sequencing strategy and curation pipeline for analyzing amplicon sequence data on the MiSeq Illumina sequencing platform. Appl Environ Microbiol. 2013 Sep;79(17):5112–20.

43. Team RC. R: a language and environment for statistical computing. R Froundation for Statistical Computing, Vienna, Austria. 2017.

44. McMurdie PJ, Holmes S. phyloseq: An R Package for Reproducible Interactive Analysis and Graphics of Microbiome Census Data. Watson M, editor. PLoS One. 2013 Apr;8(4):e61217.

45. Gardinier JD, Rostami N, Juliano L, Zhang C. Bone adaptation in response to treadmill exercise in young and adult mice. Bone reports. 2018 Jun;8:29–37.

46. Turner CH, Burr DB. Basic biomechanical measurements of bone: A tutorial. Bone. 1993 Jul;14(4):595–608.

47. Shi Y, Zhao X, Zhao J, Zhang H, Zhai Q, Narbad A, et al. A mixture of Lactobacillus species isolated from traditional fermented foods promote recovery from antibiotic-induced intestinal disruption in mice. J Appl Microbiol. 2018;124(3):842–54.

48. Perez-Cobas AE, Gosalbes MJ, Friedrichs A, Knecht H, Artacho A, Eismann K, et al. Gut

microbiota disturbance during antibiotic therapy: a multi-omic approach. Gut. 2012;62(11):1–11.

49. Langdon A, Crook N, Dantas G. The effects of antibiotics on the microbiome throughout development and alternative approaches for therapeutic modulation. Genome Med. 2016;8(1):39.

50. Kimura T, Endo H, Yoshikawa M, Muranishi S, Sezaki H. Carrier-mediated transport systems for aminopenicillins in rat small intestine. J Pharmacobiodyn. 1978;1(4):262–7.

51. Tsuji A, Nakashima E, Kagami I, Yamana T. Intestinal Absorption Mechanism of Amphoteric P-Lactam Antibiotics I: Comparative Absorption and Evidence for In Situ Rat Small Intestine. 1981;70(7).

52. Van Der Waaij D, Berghuis-de Vries JM, Korthals Altes C. Oral dose and faecal concentration of antibiotics during antibiotic decontamination in mice and in a patient. J Hyg (Lond). 1974;73(2):197–203.

53. Mann ER, Andersen P, Alcon-giner C, Leclaire C, Caim S, Wessel H, et al. Antibiotics induce sustained dysregulation of intestinal T-cell immunity by perturbing macrophage homeostasis. :1–16.

54. Zarrinpar A, Chaix A, Xu ZZ, Chang MW, Marotz CA, Saghatelian A, et al. Antibiotic-induced microbiome depletion alters metabolic homeostasis by affecting gut signaling and colonic metabolism. Nat Commun. 2018;9(1):2872.

55. Ge X, Ding C, Zhao W, Xu L, Tian H, Gong J, et al. Antibiotics-induced depletion of mice microbiota induces changes in host serotonin biosynthesis and intestinal motility. J Transl Med. 2017;15(1):1–9.

56. Ubeda C, Pamer EG. Antibiotics, microbiota, and immune defense. Vol. 33, Trends in Immunology. 2012. p. 459–66.

57. Jin Y, Wu Y, Zeng Z, Jin C, Wu S, Wang Y, et al. Exposure to Oral Antibiotics Induces Gut Microbiota Dysbiosis Associated with Lipid Metabolism Dysfunction and Low-Grade Inflammation in Mice.

58. Francino MP, Moya A. Effects of Antibiotic Use on the Microbiota of the Gut and Associated Alterations of Immunity and Metabolism. EMJ Gastroenterol. 2013;1(December):74–80.

59. Klausen B, Hougen HP, Fiehn N -E. Increased periodontal bone loss in temporarily B lymphocyte-deficient rats. J Periodontal Res. 1989;24(6):384–90.

60. Li Y, Toraldo G, Li A, Yang X, Zhang H, Qian WP, et al. B cells and T cells are critical for the preservation of bone homeostasis and attainment of peak bone mass in vivo. Blood.

2007;109(9):3839–48.

61. Sun W, Meednu N, Rosenberg A, Rangel-Moreno J, Wang V, Glanzman J, et al. B cells inhibit bone formation in rheumatoid arthritis by suppressing osteoblast differentiation. Nat Commun. 2018;9(1):5127.

62. Zhang YH, Heulsmann A, Tondravi MM, Mukherjee A, Abu-Amer Y. Tumor necrosis factor-α (TNF) stimulates RANKL-induced osteoclastogenesis via coupling of TNF type 1 receptor and RANK signaling pathways. J Biol Chem. 2001 Jan 5;276(1):563–8.

63. Wang LM, Zhao N, Zhang J, Sun QF, Yang CZ, Yang PS. Tumor necrosis factor-alpha inhibits osteogenic differentiation of pre-osteoblasts by downregulation of EphB4 signaling via activated nuclear factor-kappaB signaling pathway. J Periodontal Res. 2018;53(1):66–72.

64. Kim JW, Lee MS, Lee CH, Kim HY, Chae SU, Kwak HB, et al. Effect of interferon- γ on the fusion of mononuclear osteoclasts into bone-resorbing osteoclasts. BMB Rep. 2012;

65. Gao Y, Grassi F, Ryan MR, Terauchi M, Page K, Yang X, et al. IFN-gamma stimulates osteoclast formation and bone loss in vivo via antigen-driven T cell activation. J Clin Invest. 2007;117(1):122–32.

66. Adamopoulos IE, Chao C chi, Geissler R, Laface D, Blumenschein W, Iwakura Y, et al. Interleukin-17A upregulates receptor activator of NF-κB on osteoclast precursors. Arthritis Res Ther. 2010;12(1):1–11.

67. Xu LX, Kukita T, Kukita A, Otsuka T, Niho Y, Iijima T. Interleukin-10 selectively inhibits osteoclastogenesis by inhibiting differentiation of osteoclast progenitors into preosteoclast-like cells in rat bone marrow culture system. J Cell Physiol. 1995;165(3):624–9.

68. Mohamed SGK, Sugiyama E, Shinoda K, Taki H, Hounoki H, Abdel-Aziz HO, et al. Interleukin-10 inhibits RANKL-mediated expression of NFATc1 in part via suppression of c-Fos and c-Jun in RAW264.7 cells and mouse bone marrow cells. Bone. 2007;41(4):592–602.

69. Zaiss MM, Axmann R, Zwerina J, Polzer K, Gückel E, Skapenko A, et al. Treg cells suppress osteoclast formation: A new link between the immune system and bone. Arthritis Rheum. 2007;56(12):4104–12.

70. Jakobsson HE, Jernberg C, Andersson AAF, Sjölund-Karlsson M, Jansson JJK, Engstrand L, et al. Short-Term Antibiotic Treatment Has Differing Long-Term Impacts on the Human Throat and Gut Microbiome. Ratner AJ, editor. PLoS One. 2010 Mar;5(3):e9836.

71. Jernberg C, Löfmark S, Edlund C, Jansson JK. Long-term ecological impacts of antibiotic administration on the human intestinal microbiota. ISME J. 2007 May;1(1):56–66.

72. Miyoshi J, Bobe AM, Miyoshi S, Huang Y, Hubert N, Delmont TO, et al. Peripartum Antibiotics Promote Gut Dysbiosis, Loss of Immune Tolerance, and Inflammatory Bowel Disease in Genetically Prone Offspring. Cell Rep. 2017 Jul;20(2):491–504.

73. Becattini S, Taur Y, Pamer EG. Antibiotic-Induced Changes in the Intestinal Microbiota and Disease. Vol. 22, Trends in Molecular Medicine. 2016. p. 458–78.

74. Gálvez EJC, Iljazovic A, Gronow A, Flavell R, Strowig T. Shaping of Intestinal Microbiota in Nlrp6- and Rag2-Deficient Mice Depends on Community Structure. Cell Rep. 2017;21(13):3914–26.

75. Zhang H, Sparks JB, Karyala S V., Settlage R, Luo XM. Host adaptive immunity alters gut microbiota. ISME J. 2015;9(3):770–81.

76. Chiang S-S, Pan T-M. Antiosteoporotic effects of Lactobacillus -fermented soy skim milk on bone mineral density and the microstructure of femoral bone in ovariectomized mice. J Agric Food Chem. 2011;59(14):7734–42.

77. Kim JG, Lee E, Kim SH, Whang KY, Oh S, Imm JY. Effects of a Lactobacillus casei 393 fermented milk product on bone metabolism in ovariectomised rats. Int Dairy J. 2009;19(11):690–5.

78. Winter S, Ratner A, Nelson A, Weiser J, Benoist C, Mathis D. Deciphering the tête-à-tête between the microbiota and the immune system. Nature. 2014 Oct;467(7314):426–9.

Chapter 5. Key findings, study limitations and future directions

5.1 Specific aims and novel findings

As described in Chapter 1, bone remodeling is a highly dynamic process that is regulated by several systems and factors. Extensive studies have demonstrated immune system regulation of bone density, yet there is still a lack of understanding of the mechanisms involved in this communication. The overall objective of my thesis work was to understand the role of the immune system, especially lymphocytes and cytokines in the regulation of bone health in multiple models of bone loss. I hypothesized that in our models, the immune system would play a crucial role in the regulation of bone density. In Chapter 2, we demonstrated that interleukin 10 (IL-10) regulates early type 1 diabetes (T1D)-induced trabecular and cortical bone loss. We also identified the mechanism by which IL-10 can regulate osteoblasts during diabetic conditions. In Chapter 3 and 4, we demonstrated the role of T and B lymphocytes in *L. reuteri* beneficial effects on bone density and in the regulation of dysbiosis-induced bone loss. The work performed in this dissertation offers mechanistic insight into how the immune system and its cytokines are involved in the modulation of bone health in different models. A summary of the research objectives and the novel findings are presented below:

Objective 1: To identify the role of the cytokine IL-10 in type 1 diabetes-induced bone loss *in vivo* and to determine its regulatory effects on osteoblasts under high glucose conditions (Chapter 2).

Key findings:

1. IL-10 deficiency enhances early T1D-induced trabecular and cortical bone loss.

2. Long term effects of T1D on bone density are not affected by IL-10 deficiency.

3. Absence of IL-10 exacerbates T1D decrease in osterix gene expression.

4. *In vitro*, IL-10 regulates osterix gene expression in osteoblasts via MAPK pathway.

Objective 2: To characterize the role of lymphocytes in mediating the beneficial effects of *L. reuteri* on bone density in healthy male mice and to determine the mechanisms behind these effects (Chapter 3).

Key findings:

1. *L. reuteri* requires T and B lymphocytes to exert a beneficial effect on bone density in healthy male mice.

2. *Ex* vivo, *L. reuteri* and *L. reuteri* conditioned media regulate the expression of several cytokines (IL-10, TGFβ, IFNγ, and IL-17A) in mesenteric lymph nodes (MLNs) and in isolated $CD3^+$ T-cells, indicating that *L. reuteri* directly affects T-lymphocytes cytokine expression.

3. $CD4^+$ T cells stimulated with *L. reuteri* conditioned media promoted osteogenesis in a T-cell-osteoblast co-culture system.

Objective 3: To identify the role of lymphocytes in post-antibiotic dysbiosis-induced bone loss (Chapter 4).

Key findings:

1. Antibiotic treatment followed by natural repopulation leads to gut dysbiosis and bone loss in male mice.

2. Post-antibiotic dysbiosis-induced bone loss is dependent on lymphocytes as demonstrated using Rag knockout mice.

3. Post-antibiotic treated wild type and lymphocyte deficient mice express different microbiota profiles, characterized by low levels of Lactobacillales in wild type compared to Rag knockout mice.

4. Administration of a *Lactobacillu*s probiotic to wild type mice prevents post-antibiotic dysbiosis-induced bone loss.

5.2 Study outcomes

My research investigated the role of the immune system and cytokines in the regulation of bone density in different mouse models. The data presented in this dissertation demonstrates a link between cytokines, T and B lymphocytes, and gut microbiota in the regulation of bone density in male mice. Although further studies are needed to understand this communication entirely, I have demonstrated that these factors play a key role in the regulation of bone density in three different conditions: type 1 diabetes, probiotic treatment, and dysbiosis. Taken together, the studies described here support the overall hypothesis that the immune system contributes to the regulation of bone density in healthy and pathological conditions.

The first aim was designed to assess the role played by the anti-inflammatory cytokine IL-10 in bone loss induced by T1D in male mice (Chapter 2). IL-10 levels are markedly decreased in T1D mouse models (1) and in T1D patients (2). IL-10 also directly regulates both osteoblasts and osteoclasts (3–6). Despite these findings, no studies have assessed the role of IL-10 in T1D-mediated bone pathology. Our study is the first to demonstrate that IL-10 regulates femoral bone density in male mice during T1D. Using genetically modified mice (IL-10 knockout) and a pharmacological approach to induce diabetes, we observed that in the absence of IL-10, bone loss was exacerbated during early stages of T1D. Interestingly, at a later time point (12 weeks post T1D induction), absence of IL-10 did not further enhance bone loss, suggesting that IL-10 likely inhibits bone loss during early T1D pathogenesis. These differences in kinetic response may be explained by an exacerbated response in the T1D IL-10 knockout group vs T1D wild type group at 4 weeks, as suggested by changes in body weight at 4 weeks but not 12 weeks. This data provides new insight in the understanding of how dysregulation of IL-10 during diabetes can affect bone density.

Our studies further show that absence of IL-10, during early stage of T1D, results in the negative regulation of osteoblasts by suppressing osterix gene expression. We also show that IL-

10 does not influence osteoclasts. These findings are consistent with previous studies from our lab and others showing that T1D bone loss is associated with suppression of osteoblast activity without changes in osteoclast (7,8). Importantly, the exacerbated bone loss in the T1D IL-10 deficient group was independent of local changes in other cytokines. Specifically, gene expression analysis of several pro-inflammatory cytokines in the bone did not show significant changes. It is however, possible that other cytokines could be potentially dysregulated at earlier time points.

In vitro, we show that high glucose decreases osterix gene expression in osteoblasts and treatment with IL-10 reversed this effect. Upon further investigation, we were able to identify a potential pathway that is involved in IL-10 effects on osteoblasts and bone density. Our data revealed that high glucose conditions decreased ERK phosphorylation and IL-10 prevented this effect. Previous studies have shown that osterix gene expression can be regulated by ERK phosphorylation (9), suggesting that ERK phosphorylation by IL-10 is the mechanism by which IL-10 prevents decrease in osterix expression in high glucose conditions. Other MAP-kinase pathways associated with osterix regulation such as JNK and p38 were not affected by IL-10 treatment. ***Our data not only highlights the importance of IL-10 in bone regulation during diabetes in vivo but also elucidates the mechanism behind IL-10 effects on osteoblasts and bone density regulation.***

The second aim was designed to investigate and understand the mechanisms by which *L. reuteri* increases bone density in healthy male mice (Chapter 3). In the past decade, many studies have demonstrated the beneficial effects of probiotics in the regulation of bone health (10–16). However, as the consumption of probiotic increases, understanding the mechanisms involved in mediating their beneficial effects is crucial to further validate their therapeutic potential. Here, we assessed the role of the T and B lymphocytes in *L. reuteri* enhancement on bone density by using Rag-KO mice deficient in mature T and B lymphocytes. Our data show that in the absence of T

and B lymphocytes the beneficial effects of *L. reuteri* on bone are ablated, demonstrating that lymphocytes are important for bone responsiveness to *L. reuteri.* Further studies demonstrate that *L. reuteri* and *L. reuteri* conditioned media enhance the expression of cytokines known to regulate bone remodeling and bone density in MLNs. Lastly, we found that factors secreted from T-cells isolated from MLNs treated with *L. reuteri* conditioned media regulate osteoblast gene expression. This demonstrates that regulation of T-cell cytokine production by *L. reuteri* secreted factors is a potential mechanism by which *L. reuteri* enhances bone density *in vivo*. ***The work performed in this aim offers a mechanistic insight into how the probiotic L. reuteri is beneficial for bone health and suggests that T-lymphocytes play an important role in mediating its beneficial bone effects.***

Lastly, the third aim explored the role of T and B lymphocytes in bone loss induced by gut dysbiosis after antibiotic treatment (Chapter 4). Previously, our lab reported that gut microbiota repopulation after antibiotic treatment induces dysbiosis and bone loss (17). Therefore, this aim was designed to determine whether lymphocytes are also important in this model of bone loss. Through these studies we observed that in the absence of T and B lymphocytes, bone density was not affected by dysbiotic gut microbiota, suggesting the requirement of lymphocytes for bone loss in this model. Moreover, we also show that repopulation of the gut microbiota in the Rag knockout group is characterized by higher levels of Lactobacillales when compared to wild type mice, suggesting a protective effect of this bacteria. Indeed, treatment with *L. reuteri* prevented bone loss induced by dysbiosis in the wild type mice. ***These data suggest that not only the T and B lymphocytes can be beneficial to the bone, but they can also have an adverse effect on bone density in response to gut microbiota changes after antibiotic use***.

5.3 Limitations of the study

Although these studies provide many important insights, some limitations of the models must be acknowledged:

1. The dose of streptozotocin used in this experiment was higher compared to other studies, including several from our lab. However, the proper controls (same streptozotocin dose in the WT group) were used and previous studies from our lab have demonstrated comparable bone loss with both low and high doses of streptozotocin (18,19).

2. Insulin injections were given to T1D IL-10 knockout mice due to the rapid decrease in body weight. Insulin is known to benefit bone density (section 1.3.4.3). However, we don't see correlations between insulin injections and bone effects, which suggest that insulin injections did not affect our results. In addition, this is the group with more bone loss. In fact, our lab and others use insulin injections to prevent further weight loss and distress to the mice (19).

3. The mice used in the IL-10 studies were 7-8 weeks old, at this stage they have not developed a mature bone, and therefore early changes in bone density can be affected by bone modeling (growth) versus remodeling (adult skeleton). However, we did not observe any major differences in bone growth as determined by bone length.

4. *In vitro* work was done using the pre-osteoblast cell line MC3T3E1. These cells are commonly used in the bone field, however, as these cells are not a primary cell line and have been transformed, they can potentially react differently and do not completely reflect the *in vivo* environment.

5. In the antibiotic dysbiosis model we used a cocktail of the antibiotic ampicillin and neomycin. These broad-spectrum antibiotics are not commonly prescribed together in humans. However, this study was designed to induce microbiota depletion and allow repopulation to yield dysbiotic microbiota. This was done to understand the role of gut dysbiosis on bone and not to

assess the direct effects of antibiotics *per se* on bone health. In fact, these antibiotics are poorly absorbed (20–22), limiting their effects to the gut. In addition, we examined the bone four weeks after cessation of antibiotic treatment.

5.4 Future directions

The current studies offer insight into the role of IL-10 as well as T and B lymphocytes in the regulation of bone density in different mouse models. These studies will guide future research that aims to further validate and understand the role of the immune system as a potential target to prevent bone loss.

Our results suggest IL-10 as a possible target for the prevention of bone loss induced by diabetes (Chapter 2). It will be important to next identify the cells that are responsible for the secretion of IL-10 and how these cells are affected during diabetes. These studies will give us a better insight into how IL-10 is regulated during diabetes and bone loss. Macrophages, B cells, T cells, and epithelial cells are some of the cells that can secrete IL-10 (23). We can isolate the immune cells from lymphoid organs such as the spleen, mesenteric lymph nodes and bone marrow in diabetic conditions and look at the expression of IL-10 by flow cytometry. Treatment to increase IL-10 levels in T1D conditions can be used to test the benefits of IL-10 in reducing T1D induced bone loss. Administration of adeno-associated virus (AAV) encoding IL-10 increased the levels of circulating IL-10 in mice (24). This treatment has been shown to be effective in preventing the development of rheumatoid arthritis in the collagen induced arthritis mouse model as well as to reduce the development of colitis (24,25). However, gene therapy strategies associated with IL-10 supplementation have not been approved for clinical trial due to side effects associated with pre-anemic condition (23). Intragastric administration of IL-10–secreting genetically engineered bacterium (*Lactococcus lactis*) into T1D IL-10 deficient mice can also be used (26). Lastly, our *in vitro* data show that IL-10 enhances osterix gene expression in high glucose conditions. However, we do not know what an increase in osterix by IL-10 means to the cell. For example, osterix expression is essential for osteoblast differentiation (27). Therefore, experiments designed to look

at osteoblast differentiation *in vitro* during IL-10 treatment can be done to further understand the role of osterix regulation by IL-10.

Our experiments identified T and B lymphocytes as an important component in the regulation of bone density. We found that T and B lymphocytes are not only involved in promoting bone density by *L. reuteri,* but their absence can prevent bone loss induced by post-antibiotic gut dysbiosis. However, the relative individual contributions of T and B cells in driving these bone effects in both models remains unclear. Therefore, future experiments will need to identify which one of these cells is mediating the bone effect. T and B cell specific knockout mouse models could be utilized to provide insight into their respective contributions to the regulation of bone density by *L. reuteri* and by post-antibiotic dysbiosis. After determining which lymphocytes (T or B) are involved, we can use more specific knockouts such as $CD4^+$ T cell knockout mice to further characterize the specific cell population involved in these effects. In Chapter 3 we only focused on understanding the role of *L. reuteri* on T cells *in vitro*. We decided to focus on T cells due to our previous data that show changes in $CD4^+$ T cells by *L. reuteri* (28). However, it will also be interesting to assess if B cells, isolated from the spleen and mesenteric lymph nodes, can respond similarly to *L. reuteri* treatment *in vitro*. Our *in vitro* data also shows that *L. reuteri* conditioned media can regulate $CD3^+$ T cells similarly to live bacteria. However, our knowledge in terms of the molecule that is responsible for this effect is limited. Therefore, future studies designed to identify these molecules (e.g. by HPLC) will contribute to our knowledge in terms of the mechanism by which *L. reuteri* conditioned media can benefit the bone. Furthermore, the impact of *L. reuteri* conditioned media *in vivo* is unclear. New experiments need to be designed to identify the dose and mode of delivery of *L. reuteri* conditioned media in our different models, i.e. is gut delivery important for the observed effects.

In the post-antibiotic dysbiosis model (Chapter 4) a significant increase in the relative abundance of the order Lactobacillales in the lymphocytes deficient mice was noted. To test the hypothesis that an increase in Lactobacillales contribute to the prevention of bone loss in this group, we treated wild type mice with *L. reuteri*. Our findings show that *L. reuteri* treatment can prevent post-antibiotic dysbiosis-induced bone loss. However, other studies can be done to further confirm if Lactobacillales in general are protective against dysbiosis-induced bone loss. This can be addressed in several ways: 1) different species of probiotics, one that belongs to the Lactobacillales order (e.g. *Lactobacillus acidophilus*) and one that is not derived from Lactobacillales (e.g. *Bifidobacterium longum*), can be used to repopulate the microbiota for four weeks (as we did with *L. reuteri*). By doing this we can determine if the effect that we see in the bone is specific to *L. reuteri* or if other Lactobacillales or bacteria from a different order can have the same effect; 2) repopulation of the gut microbiota with the gut microbiota from post-antibiotic lymphocyte deficient mice (increased Lactobacillales) by doing fecal microbiota transplant will also help understand the contribution of Lactobacillales together with other bacteria; 3) promote the repopulation of only Lactobacillales by using antibiotics such as vancomycin that will prevent the growth of other bacteria, as some lactobacillus species are resistant to vancomycin (29). Interestingly, in our studies the expression of other bacteria also changed between the groups, therefore new studies need to assess the contribution of each one of these bacterial species in protecting against bone loss in the wild type mice. Our preliminary data (data not shown) also demonstrated that post-antibiotic dysbiosis-induced bone loss is sex-specific since antibiotic treated female mice did not lose bone. Therefore, future studies should focus on identifying why female mice are protected against post-antibiotic treatment induced bone loss.

Our studies demonstrate that changes in microbiota composition after antibiotic treatment induces bone loss. However, we have not identified how these changes in microbiota contribute to

bone loss. For example, are these bacteria secreting specific metabolites that can be driving the bone effect? To test this, we could perform fecal and serum metabolomic analysis from four weeks post-antibiotic treated mice to further determine how these changes in bacteria affect bone loss. After identifying possible metabolites, *in vitro* and *in vivo* studies should be done to determine their role in bone regulation. *In vivo* studies can include the use of germ-free mice to identify the role of specific metabolites in bone density without the contribution of gut bacteria. After identifying the mechanism by which these metabolites regulate bone cells *in vitro*, inhibition of those specific pathways *in vivo* can further determine their role in bone density regulation.

5.5 Conclusions

Osteoporosis is a growing public health issue. Worldwide, this disease is estimated to affect more than 200 million people and in the US it accounts for over 2 million bone fractures (30,31). Current treatments for osteoporosis have side effects and reduced patient compliance. Therefore, it is important to identify additional novel therapeutic targets with fewer side effects. The immune system has been known for decades to influence bone health, however, we still have a lot to learn. Many studies have demonstrated the beneficial effects of probiotic consumption on the immune system and bone health in humans and animal models. However, the mechanisms of these effects are not completely understood. Our data shows key role for probiotics and lymphocytes in the regulation of bone density. In addition to their direct effects on bone, *L. reuteri* also regulates immune cells to impact bone indirectly. In summary, my thesis work has uncovered the mechanisms linking the immune system and probiotic effects to bone health. These studies identify therapeutic strategies to treat osteoporosis specifically by regulation of the immune system.

REFERENCES

REFERENCES

1. Schloot NC, Hanifi-Moghaddam P, Goebel C, Shatavi S V, Flohe S, Kolb H, et al. Serum IFN-gamma and IL-10 levels are associated with disease progression in non-obese diabetic mice. Diabetes Metab Res Rev. 2002;18(1):64–70.

2. Van Exel E, Gussekloo J, De Craen AJM, Frölich M, Wiel AB Van Der, Westendorp RGJ. Low production capacity of interleukin-10 associates with the metabolic syndrome and type 2 diabetes: The Leiden 85-plus study. Diabetes. 2002;

3. Evans KE, Fox SW. Interleukin-10 inhibits osteoclastogenesis by reducing NFATc1 expression and preventing its translocation to the nucleus. BMC Cell Biol. 2007;8:4.

4. Hong MH, Williams H, Jin CH, Pike JW. The Inhibitory Effect of Interleukin-10 on Mouse Osteoclast Formation Involves Novel Tyrosine-Phosphorylated Proteins. J Bone Miner Res. 2000 Feb 18;15(5):911–8.

5. Xu LX, Kukita T, Kukita A, Otsuka T, Niho Y, Iijima T. Interleukin-10 selectively inhibits osteoclastogenesis by inhibiting differentiation of osteoclast progenitors into preosteoclast-like cells in rat bone marrow culture system. J Cell Physiol. 1995;165(3):624–9.

6. Dresner-Pollak R, Gelb N, Rachmilewitz D, Karmeli F, Weinreb M. Interleukin 10-deficient mice develop osteopenia, decreased bone formation, and mechanical fragility of long bones. Gastroenterology. 2004;127(3):792–801.

7. Botolin S, McCabe LR. Bone loss and increased bone adiposity in spontaneous and pharmacologically induced diabetic mice. Endocrinology. 2007 Jan;148(1):198–205.

8. Zhang J, Motyl KJ, Irwin R, MacDougald OA, Britton RA, McCabe LR. Loss of bone and Wnt10b expression in male type 1 diabetic mice is blocked by the probiotic Lactobacillus reuteri. Endocrinology. 2015;156(9):3169–82.

9. Lu X, Gilbert L, He X, Rubin J, Nanes MS. Transcriptional regulation of the osterix (Osx, Sp7) promoter by tumor necrosis factor identifies disparate effects of mitogen-activated protein kinase and NFKB pathways. J Biol Chem. 2006;281(10):6297–306.

10. McCabe LR, Irwin R, Schaefer L, Britton RA. Probiotic use decreases intestinal inflammation and increases bone density in healthy male but not female mice. J Cell Physiol. 2013 Aug;228(8):1793–8.

11. Collins FL, Irwin R, Bierhalter H, Schepper J, Britton RA, Parameswaran N, et al. Lactobacillus reuteri 6475 increases bone density in intact females only under an inflammatory setting. PLoS One. 2016;11(4).

12. Rodrigues FC, Castro ASB, Rodrigues VC, Fernandes SA, Fontes EAF, de Oliveira TT, et al. Yacon Flour and *Bifidobacterium longum* Modulate Bone Health in Rats. J Med Food. 2012;15(7):664–70.

13. Li JY, Chassaing B, Tyagi AM, Vaccaro C, Luo T, Adams J, et al. Sex steroid deficiency-associated bone loss is microbiota dependent and prevented by probiotics. J Clin Invest. 2016 Apr;126(6):2049–63.

14. Ohlsson C, Engdahl C, Fak F, Andersson A, Windahl SH, Farman HH, et al. Probiotics protect mice from ovariectomy-induced cortical bone loss. PLoS One. 2014 Jan;9(3):e92368.

15. Nilsson AG, Sundh D, Bäckhed F, Lorentzon M. *Lactobacillus reuteri* reduces bone loss in older women with low bone mineral density - a randomized, placebo-controlled, double-blind, clinical trial. J Intern Med. 2018;0–3.

16. Parvaneh K, Ebrahimi M, Sabran MR, Karimi G, Hwei ANM, Abdul-Majeed S, et al. Probiotics (*Bifidobacterium longum*) Increase Bone Mass Density and Upregulate *Sparc* and *Bmp-2* Genes in Rats with Bone Loss Resulting from Ovariectomy. Biomed Res Int. 2015;2015:1–10.

17. Schepper JD, Collins FL, Rios-Arce ND, Raehtz S, Schaefer L, Gardinier JD, et al. Probiotic Lactobacillus reuteri Prevents Postantibiotic Bone Loss by Reducing Intestinal Dysbiosis and Preventing Barrier Disruption. J Bone Miner Res. 2019;1–18.

18. Motyl K, McCabe LR. Streptozotocin, type 1 diabetes severity and bone. Biol Proced Online. 2009 Mar 6;11(1):296–315.

19. Raehtz S, Bierhalter H, Schoenherr D, Parameswaran N, McCabe LR. Estrogen Deficiency Exacerbates Type 1 Diabetes Induced Bone TNFα expression and Osteoporosis in Female Mice. Endocrinology. 2017 Apr 14;

20. Kimura T, Endo H, Yoshikawa M, Muranishi S, Sezaki H. Carrier-mediated transport systems for aminopenicillins in rat small intestine. J Pharmacobiodyn. 1978;1(4):262–7.

21. Tsuji A, Nakashima E, Kagami I, Yamana T. Intestinal Absorption Mechanism of Amphoteric P-Lactam Antibiotics I: Comparative Absorption and Evidence for In Situ Rat Small Intestine. 1981;70(7).

22. Van Der Waaij D, Berghuis-de Vries JM, Korthals Altes C. Oral dose and faecal concentration of antibiotics during antibiotic decontamination in mice and in a patient. J Hyg (Lond). 1974;73(2):197–203.

23. Bijjiga E, Martino AT. Interleukin 10 (IL-10) Regulatory Cytokine and its Clinical Consequences. J Clin Cell Immunol. 2013;1–6.

24. Goudy K, Song S, Wasserfall C, Zhang YC, Kapturczak M, Muir A, et al. Adeno-associated virus vector-mediated IL-10 gene delivery prevents type 1 diabetes in NOD mice. PN. 2001;98(24):13913–8.

25. Henningsson L, Eneljung T, Jirholt P, Tengvall S, Lidberg U, van den Berg WB, et al. Disease-Dependent Local IL-10 Production Ameliorates Collagen Induced Arthritis in Mice. PLoS One. 2012;7(11):1–8.

26. Steidler L, Hans W, Schotte L, Fiers W, Remaut E. Treatment of Murine Colitis by Lactococcus lactis Secreting Interleukin-10. Science (80-). 2000;289.

27. Nakashima K, Zhou X, Kunkel G, Zhang Z, Deng JM, Behringer RR, et al. The Novel Zinc Finger-Containing Transcription Factor Osterix Is Required for Osteoblast Differentiation and Bone Formation. Cell. 2002;108(1):17–29.

28. Britton RA, Irwin R, Quach D, Schaefer L, Zhang J, Lee T, et al. Probiotic L. reuteri Treatment Prevents Bone Loss in a Menopausal Ovariectomized Mouse Model. J Cell Physiol. 2014 Nov;229(11):1822–30.

29. Russell SL, Gold MJ, Hartmann M, Willing BP, Thorson L, Wlodarska M, et al. Early life antibiotic-driven changes in microbiota enhance susceptibility to allergic asthma. EMBO Rep. 2012;13(5):440–7.

30. Reginster JY, Burlet N. Osteoporosis: A still increasing prevalence. Bone. 2006;38(2 SUPPL. 1):1998–2003.

31. Burge R, Dawson-Hughes B, Solomon DH, Wong JB, King A, Tosteson A. Incidence and economic burden of osteoporosis-related fractures in the United States, 2005-2025. J Bone Miner Res. 2007;22(3):465–75.